University of Alberta

CYCLIC TESTS OF SHEAR WALLS CONFINED WITH DOUBLE HEAD STUDS

by

Syed Salman Mobeen

A thesis submitted to the Faculty of Graduate Studies and Research in partial fulfillment of the

requirements for the degree of MASTER OF SCIENCE

In
Structural Engineering

Department of

Civil and Environmental Engineering

Edmonton, Alberta
Fall 2002

National Library of Canada
Acquisitions and Bibliographic Services
395 Wellington Street
Ottawa ON K1A 0N4
Canada

Bibliothèque nationale du Canada
Acquisitions et services bibliographiques
395, rue Wellington
Ottawa ON K1A 0N4
Canada

Your file Votre référence

Our file Notre référence

The author has granted a non-exclusive licence allowing the National Library of Canada to reproduce, loan, distribute or sell copies of this thesis in microform, paper or electronic formats.

L'auteur a accordé une licence non exclusive permettant à la Bibliothèque nationale du Canada de reproduire, prêter, distribuer ou vendre des copies de cette thèse sous la forme de microfiche/film, de reproduction sur papier ou sur format électronique.

The author retains ownership of the copyright in this thesis. Neither the thesis nor substantial extracts from it may be printed or otherwise reproduced without the author's permission.

L'auteur conserve la propriété du droit d'auteur qui protège cette thèse. Ni la thèse ni des extraits substantiels de celle-ci ne doivent être imprimés ou autrement reproduits sans son autorisation.

0-612-81446-7

Canada

University of Alberta

Library Release Form

Name of Author: Syed Salman Mobeen

Title of Thesis: Cyclic Tests of Shear Walls Confined with Double Head Studs

Degree: Master of Science in Structural Engineering

Year this Degree Granted: 2002

Permission is hereby granted to the University of Alberta Library to reproduce single copies of this thesis and to lend or sell such copies for private, scholarly or scientific research purposes only.

The author reserves all other publication and other rights in association with the copyright in the thesis, and except as herein before provided, neither the thesis nor any substantial portion thereof may be printed or otherwise reproduced in any material form whatever without the author's prior written permission.

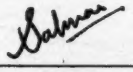

Syed Salman Mobeen

Apt#1013 Newton Place
8515-112 Street
Edmonton T6G1K7, Alberta
Canada

Submission *Date* Sept. 5, 2002

University of Alberta

Faculty of Graduate Studies and Research

The undersigned certify that they have read, and recommend to the Faculty of Graduate Studies and Research for acceptance, a thesis entitled Cyclic Tests of Shear walls Confined with Double Head Studs submitted by Syed Salman Mobeen in partial fulfillment of the requirements for the degree of Master of Science in Structural Engineering.

Dr. A.E. Elwi, Thesis Supervisor

Dr. Amin Ghali, Co-Supervisor

Dr. R. Driver

Dr. W. Moussa

Sept 5, 2002
Dated

ABSTRACT

Reinforced concrete shear walls are integral structural elements provided in tall buildings to resist lateral forces arising from wind or earthquakes. Earthquake-resistant shear walls should possess adequate ductility in addition to strength and stiffness. Ductility demand in reinforced concrete shear walls can be fulfilled by properly detailed confinement reinforcement in their boundary elements.

Double head studs were recently introduced as efficient confinement reinforcement in reinforced concrete columns. They are intended to replace conventional single-legged crossties with 90-135 degrees hooks, which were observed to open in previous tests and therefore loose efficiency.

This thesis reports a study of confinement effectiveness of double head studs in the boundary elements of reinforced concrete shear walls compared to the confinement provided by the conventional crossties. Three full-scale concrete shear walls (h/w = 3) were tested which were confined either with; 10M conventional crossties, 9.5 mm Ø double head studs and 12.7 mm Ø double head studs respectively in their boundary elements, keeping identical confinement volumetric ratio. The tests were performed under fully reversible, quasi-static cyclic action in a displacement control mode.

Improvement in displacement ductility of walls confined with studs is observed to be significant compared to their strength gain. Energy absorption of walls with double head studs was also found to be better than the wall confined with conventional crossties.

Comparison of the current tests with previous shear wall tested in other research programs showed that walls with identical axial load ratio, shear force ratio and cross-section shape, the displacement ductility ratio (μ_Δ) increases with the increase in confinement reinforcement ratio (ρ_s).

ACKNOWLEDGEMENTS

The author would like to express his sincere gratitude and appreciation to his research supervisor, Professor A. E. Elwi for his consistent guidance, interest and encouragement throughout this study. The author would also like to appreciate the guidance of his co-supervisor, Professor Amin Ghali for his interest and advices during the thesis.

The author would like to appreciate "Decon Canada", for supplying at no cost Double Head Studs and for being industrial financer in this study and also to Natural Sciences and Engineering Research Council of Canada for providing further financial support.

The author also appreciate the technical assistance of laboratory technicians L. Burden and R. Helfrich of I.F. Morrison Structural Engineering Laboratory at the University of Alberta, Canada.

Lastly the author would like to appreciate helps of all friends and family members in assisting and encouraging the author.

Table of Contents

Chapter			Page
1.	INTRODUCTION		
	1.1	Introduction and Background	1
	1.2	Main Features of Reinforced Concrete Shear Wall	2
	1.3	Conventional Confinement Reinforcement	3
	1.4	Draw Backs of The Conventional Crossties	4
	1.5	Introduction of Double Head Studs as Good Confinement	4
	1.6	Scope and Objectives	6
	1.7	Organization of the Thesis	6
2.	LITERATURE REVIEW		
	2.1	Introduction	9
	2.2	Design Strategy of Concrete Shear Wall	9
	2.3	Capacity Design	10
	2.4	Literature Survey	11
		2.4.1 Dazio A., Wenk T., and Bachmann H. (1999) (German)	12
		2.4.2 Oesterle R.G, Fiorato A.E. and Corley W.G (1980)	14
		2.4.3 ACI Code, 318-2002 , American Concrete Institute	17
		2.4.4 Ozcebe G. and Saatcioglu M. (1987)	19
		2.4.5 Sheikh S.A. and Uzumeri S.M (1980)	20
		2.4.6 Moehle J.P., ASCE A.M. and Cavanagh T. (1985)	21
		2.4.7 Dilger W.H. and Ghali A. (1997)	23
	2.5	Role of confinement in the light of previous research	25
3.	EXPERIMENTAL PROGRAM		
	3.1	Introduction	39
	3.2	Prototype Structure	39

3.3 Specimen Design 40
3.3.1 Specimens Detail..... 41

3.4 Material 44
3.4.1 Concrete 44
3.4.2 Reinforcement..... 45
3.5 Fabrication Procedure..... 46
3.6 Test Set-Up 47
3.6.1 Base Fixing System 47
3.6.2 Lateral Load Assembly and Its Reaction System 48
3.6.3 Vertical Loading Assembly 49
3.6.4 Lateral Bracing System 51
3.7 Instrumentation 52
3.7.1 Load and Reaction Measurements 52
3.7.2 Strain Gauges 53
3.7.3 Deflection Measurements 53
3.7.4 Rotation Measurement 54
3.8 Procedures 55
3.8.1 Set-Up Sequence 55
3.8.2 Troubleshooting 56
3.8.3 Loading Procedure 56

4. TEST RESULTS AND OBSERVATIONS
4.1 Introduction 99
4.2 Loading Procedure 99
4.2.1 Application of Vertical loads 99
4.2.2 Application of Lateral loads 99
4.3 Test Observations 101
4.3.1 Wall W-1 101
4.3.2 Wall W-2 103
4.3.3 Wall W-3 105

4.4 Cracking and Crack Width 107

5. A COMPARATIVE EXPERIMENTAL RESULTS ANALYSIS

5.1 Introduction 142

5.2 Nominal strength capacities prediction 143

5.3 Comparison of the three walls of the current testing program 144

5.3.1 Lateral load versus tip displacement response 144

5.3.2 Strength comparison 146

5.3.3 Ductility comparison 147

5.3.4 Energy absorption 148

5.4 Comparison of the current tests with previous tests in different research programs 148

5.4.1 Analysis of results of the comparative study 151

5.4.2 Discussion of the results involving the strength parameters 152

5.4.3 Role of confinement in affecting displacement ductility ($\mu\Delta$) 156

6. SUMMARY, CONCLUSIONS AND FUTURE RECOMMENDATIONS

6.1 Summary 187

6.2 Conclusions 190

6.3 Future recommendations 190

LIST OF REFERENCES 193

LIST OF TABLES

Table		Page No.
Table 2.1	Specimens Description (after Dazio A., Wenk T. and Bachmann H.)	27
Table 2.2	Yield and Ultimate tensile strengths of the reinforcing bar (after Dazio A., Wenk T. and Bachmann H.)	27
Table 3.1	Concrete Properties	98
Table 3.2	Properties of Reinforcing Steel	98
Table 5.1(a)	Test Details	182
Table 5.1(b)	Concrete Dimensions	183
Table 5.1(c)	Reinforcement Ratios	184
Table 5.1(d)	Applied Load and Capacity	185
Table 5.1(e)	Material Properties	186

LIST OF FIGURES

Figure		Page No.
1.1	Typical cross-section of shear wall	8
1.2	Reinforcement congestion due to hooks of crossties	8
2.1	Reinforcement details of WSH1 (after Dazio, et al., 1999)	28
2.2	Reinforcement details of WSH2 (after Dazio, et al., 1999)	28
2.3	Reinforcement details of WSH3 (after Dazio, et al., 1999)	29
2.4	Reinforcement details of WSH4 (after Dazio, et al, 1999)	29
2.5	Reinforcement details of WSH5 (after Dazio, et al, 1999)	30
2.6	Reinforcement details of WSH6 (after Dazio, et al, 1999)	30
2.7	Load Tip-displacement responses of six walls (after Dazio, et al., 1999)	31
2.8	Specimen and their Reinforcement details (after Oesterle, et al., 1999)	32
2.9	Detailing requirements in ACI 318-2002 Sec 21.4.4	33
2.10	Column and ties detail (after Ozcebe G.and Saatcioglu M., 1987)	33
2.11	Columns details of. Sheikh S. A. and Uzumeri S.M, (1980)	34
2.12	Test results showing effect of reinforcement configuration (after Sheikh S. A. and Uzumeri S.M., 1980)	35
2.13	Test results showing effect of spacing and volumetric ratio (after Sheikh S. A. and Uzumeri S.M., 1980)	35
2.14	Test results showing effect of steel configuration, amount and tie spacing (after Sheikh S. A. and Uzumeri S.M., 1980)	36
2.15	Test results showing effect of steel configuration and tie spacing (after Sheikh S. A. and Uzumeri S.M., 1980)	36
2.16	Specimen and their Reinforcement details (after Moehle J. P.and Cavanagh T., 1985)	37

2.17	Specimen and their Reinforcement details (after Dilger W. H.and Ghali A.,1997)	37
2.18	Configurations of Double Head Studs used in the tests (after.Dilger W. H and Ghali A.,1997)	38
2.19	Figure 2.19 Results of test showing the effectiveness of Double Head Studs (Dilger W.H.and Ghali A., 1997)	38
3.1	Typical specimen detail of present research	57
3.2 (a)	W-1 reinforcement details in elevation	58
3.2 (b)	W-1 Reinforcement detail in cross-section	59
3.3	Plate inserts and end zone in wall W-1	60
3.4	Cages of wall W-1 and W-2, ready for concreting	60
3.5	Specified dimensions of double head studs	61
3.6	Photograph of double head studs	62
3.7 (a)	W-2 Reinforcement details in elevation	63
3.7 (b)	W-2 Reinforcement details in cross-section	64
3.8	Cage of wall W-2	65
3.9 (a)	W-3 Reinforcement details in elevation	66
3.9 (b)	W-3 Reinforcement details in cross-section	67
3.10	Cage of wall W-3	68
3.11	Double head studs in wall W-3	68
3.12 (a)	stress-strain curve of 15 M deformed rebars	69
3.12 (b)	stress-strain curve of 10 M deformed rebars	69
3.13 (a)	stress-strain curve of 12.7 mm Ø double head studs	70
3.13 (b)	stress-strain curve of 9.5 mm Ø double head studs	70
3.14	Typical base formwork	71
3.15	Base cages and formwork of W-1 and W-2	72
3.16	Base Pre-stressing set-up	73
3.17	Lateral loading jack, yoke and load arm	74
3.18	Plan of lateral loading assembly	75
3.19	Elevation of lateral loading assembly	76
3.20	Lateral pulling assembly and vertical load cells	77

3.21	Test frame elevation	78
3.22	Test frame section A-A	79
3.23	Lateral load-reaction frame	80
3.24	Vertical load distribution beam and watt braces	80
3.25	Leveling of two vertical load points on the boundary elements	81
3.26	Top distribution beam resting on the two vertical load points	81
3.27	Tension ties top connection, leveling rod is also visible	82
3.28	Tension ties connected to top distribution beam and Vertical Jacks, gravity load simulators also visible	82
3.29	Typical lateral braces on each side of wall	83
3.30	LVDTs, RVDTs and Load cells layout. Typical for W-1, W-2 and W-3	84
3.31 (a)	W-1 Strain gauges layout on main bars-east elevation	85
3.31 (b)	W-1 Strain gauges layout on main bars-west elevation	86
3.31 (c)	W-1 Strain gauges layout in cross-section	87
3.32 (a)	W-2 Strain gauges layout on main bars-east elevation	88
3.32 (b)	W-2 Strain gauges layout on main bars-west elevation	89
3.32 (c)	W-2 Strain gauges layout in cross-section	90
3.32 (d)	Photograph of strain gauges on double head studs	91
3.33 (a)	W-3 Strain gauges layout on main bars-east elevation	92
3.33 (b)	W-3 Strain gauges layout on main bars-west elevation	93
3.33 (c)	W-3 Strain gauges layout in cross-section	94
3.34	Top and mid-height LVDTs for measurement of lateral displacements	95
3.35	North side vertical displacement measuring LVDT	95
3.36	South side vertical displacement measuring LVDT	96
3.37	Rotation meter at yoke, in lateral loading assembly	96
3.38	Rotation meter at top distribution beam	97
4.1	Hysteresis response of wall W-1	109

4.2	Wall W-1 loading history	110
4.3 (a)	Strain in vertical bars of W-1	111
4.3 (b)	Strain in vertical bars of W-1-continued	112
4.4 (a)	Strain in stirrups of W-1	113
4.4 (b)	Strain in stirrups of W-1-continued	114
4.5 (a)	Strain in crossties of W-1	115
4.5 (b)	Strain in crossties of W-1-continued	116
4.6	W-1, Four stages of response with summary of events occurred during test	117
4.7	Hysteresis response of wall W-2	118
4.8	Wall W-2 loading history	119
4.9 (a)	Strain in vertical bars of W-2	120
4.9 (b)	Strain in vertical bars of W-2-continued	121
4.10 (a)	Strain in stirrups of W-2	122
4.10 (b)	Strain in stirrups of W-2-continued	123
4.11 (a)	Strain in crossties of W-2	124
4.11 (b)	Strain in crossties of W-2-continued	125
4.12	W-2, Four stages of response with summary of events occurred during test	126
4.13	Hysteresis response of wall W-3	127
4.14	Wall W-3 loading history	128
4.15 (a)	Strain in vertical bars of W-3	129
4.15 (b)	Strain in vertical bars of W-3-continued	130
4.16 (a)	Strain in stirrups of W-3	131
4.16 (b)	Strain in stirrups of W-3-continued	132
4.17 (a)	Strain in double head studs of W-3	133
4.17 (b)	Strain in double head studs of W-3-continued	134
4.18	W-3, Four stages of response with summary of events occurred during test	135
4.19	West side view of W-1, after test, with broken bar visible	136
4.20	East side view of W-1, after test, with buckled bar visible	136

4.21	South side view of W-1, after test, with broken bar visible	137
4.22	North side view of W-1, after test, with buckled bars	137
4.23	West side view of W-2, after test, with broken bar and double head studs visible	138
4.24	East side view of W-2, after test, with broken bar and double head studs visible	138
4.25	Broken bars visible at south side of W-2 after test	139
4.26	Broken bars visible at north side of W-2 after test	139
4.27	East side view of W-3, after test, with broken bar and double head studs visible	140
4.28	West side view of W-3, after test, with broken bar and double head studs visible	140
4.29	Broken bars visible at south face of W-3 after test	141
4.30	Broken bars visible at north side of W-3 after test	141
5.1	W-1, Four stages of response with summary of events occurred during test	161
5.2	W-2, Four stages of response with summary of events occurred during test	162
5.3	W-3, Four stages of response with summary of events occurred during test	163
5.4	Load-tip displacement envelops of three walls specimens (Up to 78 mm tip displacement)	164
5.5	Load-tip displacement response of three walls specimens (Up to 78 mm tip deflection)	165
5.6	Four stages of load-displacement response of three walls	166
5.7	Non-dimensionalized moment ratio Vs displacement ductility	167
5.8	Non-dimensionalized shear ratio Vs displacement ductility	167
5.9	Moment ratio Vs displacement ductility ratio	168
5.10	Variation of displacement ductility ratio with number	168

of inelastic cycles

5.11	W-1, Energy absorbed Vs tip displacement (Total response-south)	169
5.12	W-2, Energy absorbed Vs tip displacement (Total response-south)	170
5.13	W-3, Energy absorbed Vs tip displacement (Total response-south)	171
5.14	Energy absorbed Vs tip displacement of three walls (Total response-south)	172
5.15	Energy absorbed Vs tip displacement (Up to 78 mm tip deflection-south)	173
5.16	Energy absorbed in each cycle in three walls	174
5.17	Energy absorbed with number of cycles	175
5.18	Energy absorbed Vs tip displacement (Total response-north)	176
5.19	Variation of moment ratio with confinement reinforcement content	177
5.20	Moment ratio VS confinement ratio for walls with close moment capacities	177
5.21	Variation of shear force ratio with confinement reinforcement content	178
5.22	Variation of displacement ductility ratio with confinement reinforcement content	178
5.23	Effect of axial load on displacement ductility ratio	179
5.24	Effect of axial load on displacement ductility ratio (selected walls)	179
5.25	Effect of confinement reinforcement content on displacement ductility ratio	180

5.26	Effect of shear force ratio on displacement ductility ratio	180
5.27	Effect of number of inelastic cycles on displacement ductility ratio	181

LIST OF NOTATIONS

A_{cp}	Area of concrete section resisting shear
A_{cv}	Net area of concrete section bounded by web thickness and length of section in the direction of shear force
$A_{end\ zone}$	Gross cross-sectional concrete area of boundary element
A_g	Gross cross-sectional concrete area of shear wall
A_{st}	Total area of horizontal shear reinforcement
Cyc.	Cyclic
DHS	Double head studs
E_c	Modulus of elasticity of concrete
E_s	Modulus of elasticity of steel
f'_c	Compressive strength of concrete
f_y	Yield strength of steel reinforcement
f_u	Ultimate tensile strength of steel reinforcement
h	Clear height of wall above the base
h/w	Aspect ratio of wall
h_f	height of wall above the base to the point of application of lateral load
Int.	Intermediate
Mono.	Monotonic
M_{cyc}	Modified cyclic
M_{max}	Maximum bending moment observed in the test (V_u x h_f)
M_n	Nominal flexural capacity of the wall cross-section under a constant applied axial load
NC	Number of cycles
NIC	Number of inelastic cycles
NSC	Number of stable cycles
P_{max}	Maximum axial load applied in the test
P_n	Nominal axial load carrying capacity of wall without considering bending moment according to Equation **10-2 ACI 318-2002**
Rect.	Rectangular

V_{max}	Maximum shear force applied in the test
V_n	Nominal shear capacity of wall according to Equation **21-7 ACI 318-2002**
w	width of shear wall (overall outside longer dimension of wall cross-section)
Δ_y	Wall top displacement at first yield in flexural reinforcement
Δ_u	Maximum wall top displacement in test
Ø	Nominal diameter of steel reinforcement and double head studs
ρ	Ratio of area of vertical reinforcement to the column cross-sectional area
ρ_f	Ratio of total area of flexural reinforcement in boundary elements to the gross area of the boundary element
ρ_h	Ratio of area of horizontal shear reinforcement to the web cross-sectional area of shear wall in a vertical plane
ρ_n	Ratio of total area of vertical web reinforcement to the cross-sectional area of wall in a horizontal plane
ρ_s	Ratio of volume of confinement reinforcement to the volume of concrete core (out-to-out of confinement) having that confinement
$\rho_{s(ties)}$	Ratio of volume of crossties reinforcement to the volume of concrete
ρ_t	Ratio of total area of vertical reinforcement to the total cross-sectional area of shear wall in a horizontal plane
μ_Δ	Displacement ductility ratio (Δ_u / Δ_y)
μ_ϕ	Curvature ductility ratio (ϕ_u / ϕ_y)

CHAPTER 1

INTRODUCTION

1.1 Introduction and background

Reinforced concrete shear walls are provided in tall buildings as integral structural elements to resist lateral forces arising from wind and earthquake. The name "Shear Wall" generally reflects the idea that the "shear force" governs the design of shear walls, but most of the time, it is not true. The load transfer mechanism in shear walls leads to large flexural stresses in the wall extremities and hence the design requirements for these end zones become the dominant feature in the design of shear walls. These end zones are referred to as boundary elements.

The design of shear walls follows similar strategies for the two load cases, namely wind and earthquake. In the design for wind, the behavior of the structure and of the shear wall is restricted to remain elastic and the wall is thus proportioned to provide adequate strength and stiffness. But, the design for earthquake has been a special field of study, as it requires the additional property of "Ductility" in the structure, in addition to the strength and stiffness. Ductility can be defined as the ability of a structure or its components or of material, to offer resistance in the inelastic range without undergoing much degradation.

Although there is a class of buildings and structures designed to withstand major earthquake induced forces and remain functional. It is because of their functional importance that ideally they are supposed to be serviceable even after a severe event. This class includes hospitals, telecommunication towers, offices of the law-enforcing agencies, stand-by power plants etc.

Apart from this important building category, other structures are usually designed for much smaller earthquake forces. The reduction of forces imposes ductility requirements on the structure that allow large plastic deformations and thus considerable energy absorption ability. The scope of the discussion will be limited to the design of those buildings and structures in which the seismic forces, adjusted for potential ductility capacity, control the strength requirements of the structure.

The ideal ductile structure absorbs energy, while responding to the seismic actions in its inelastic range, and dissipates it through the plastic hinges formed at critically yielded locations. The mechanism of absorbing and dissipating seismic energy could be sustained or prolonged, without much loss of strength, only if the plastic hinges are able to permit rotations successfully throughout the seismic actions. Certain factors can affect the ideal response of a structure and change the desired behavior of the structure into severe disaster and undesirable modes of failure (Refer to Chapter 2). The risk that a structure fails in undesirable modes of failure can be minimized by applying the so-called " Principle of Capacity Design". The philosophy of the capacity design will be discussed in chapter 2.

1.2 Main features of reinforced concrete shear wall

Reinforced concrete shear walls are the extreme cases of wide rectangular columns. They have been proven to be one of the most efficient bracing systems against lateral forces. Shear walls in a building may be provided as up-standing cantilevers, or, if required by the design, two or more shear walls may be coupled with each other through coupling beams (which is called as Coupled Shear Wall system). Cantilever shear walls are suited for low-to medium-rise buildings.

Shear walls are subjected to compressive axial forces as well as reversible in plane bending moments and accompanying shear forces. Axial (longitudinal) stresses originate from the combined action of gravity loads and bending moments caused by the lateral forces.

The load transfer mechanism in shear walls allows the concentration of high normal stresses in the end zones (referred to as the boundary elements). The flexural reinforcement is usually provided with higher concentrations in these end zones. Figure 1.1 shows a typical cross-section of a shear wall with boundary elements. During seismic events, the concentration of high compressive and tensile stresses in the boundary elements causes yielding of flexural steel reinforcement and formation of plastic hinges.

Because of the lateral support provided by the floors, Building Code Requirements for Reinforced Concrete (ACI 318-2002) recommends the design of the end zones to satisfy the adequacy criteria applicable to the short columns. ACI 318-2002 recommends the extension of the end zones from the region where the compressive stress exceeds 0.2 f_c' to the point where it becomes less than 0.15 f_c'. Since shear walls are designed to resist earthquake forces in addition to other lateral loads, the requirement of ductility also arises in the boundary elements where the plastic hinges are expected to form.

The ductility demand in reinforced concrete structures is fulfilled by providing properly detailed steel confinement within the expected plastic hinges in the form of closed hoops and single-legged crossties. This has been reflected in the design recommendations of ACI 318-2002, Sec 21.7.6.4 for structures subjected to high and moderate seismic risks. The confinement reinforcement prevents the vertical bars from buckling in addition to providing confinement to concrete.

1.3 Conventional confinement reinforcement

The traditional confinement reinforcement in compression members, as recommended by ACI 318-2002, is in the form of closed stirrups and single-legged crossties. The cross ties, as recommended by the ACI 318-2002, tie the reinforcing bars lying on opposite faces of reinforced concrete compression members (refer to Figure 1.1). A cross tie has a 90 degrees hook at one end and a 135 degrees hook at the other end, to allow for easy installation on site.

1.4 Draw backs of the conventional crossties

The crossties work well in compression members but some research work has shown that the crossties become less effective under high compressive cyclic loading (Refer to chapter 2). The main problem with crossties is anchorage slippage because of the crushing of concrete within the bends and hooks (Dilger and Ghali,1997). The crushing of concrete occurs as a result of high radial stresses in concrete developed to equilibrate the tensile force in the crosstie. The slippage occurs even before reaching the yield strength of the crosstie. In some experiments the opening of 90° hooks was also observed (Moehle and Cavanagh, 1985), causing the spalling of concrete cover and premature failure of the specimen.

In addition to the above drawbacks, the problem of reinforcement congestion in the areas of the closely spaced vertical bars and crossties (like the end zones of shear wall) has also been observed on site (Refer to Figure 1.2). To avoid this congestion, sometimes the concrete dimensions are increased and hence the free floor space of buildings is reduced.

1.5 Introduction of Double Head Studs as good confinement

Several researchers have studied the effective role of confinement in the plastic zones of reinforced concrete shear walls and columns (Refer to chapter No. 2). The key factors that are found to be effective in improving the response of the member, in terms of strength and ductility, are the volumetric ratio of the confinement reinforcement, its distribution in the cross-section, the geometric configuration and the end conditions for anchorage. Further research has been done to optimize these factors and also to explore the circumstances in which those factors might not be efficient.

Recently, Dilger and Ghali (1997) studied the effectiveness of anchorage of the confinement reinforcement and also its impact on the overall strength and ductility of the columns.

They introduced a form of confinement called " Double Head Studs", by its geometry, which solved some of the basic problems with conventional crossties. They compared the effectiveness of the conventional single-legged crossties with that of the double head studs and argued that the introduction of the double head studs in compression members enhances the strength and the ductility. The main reason of the improvement in behavior was effective mechanical anchorage of the double head studs that originates as a result of their geometrical configuration. The double head studs is simply a rod, with two round heads welded or forged at its two ends (Refer to Figures 3.5 and 3.6), and is placed in the concrete member in such a way that its two ends lie close to the exterior concrete surface, just like a cross tie lying in concrete column or shear wall through the thickness of the member.

Double head studs are a modified form of the single head shear studs but their function and use is totally different. Single head shear studs were introduced to increase the shear capacity of relatively thin reinforced concrete flexural members like flat slabs and spread footings but the double head studs were introduced in the reinforced concrete compression members to enhance the confinement behavior and hence their ductility capacity. The double head studs work in tension and the two heads mechanically confine the concrete between them and thus prevent the bulging-out of the concrete under high compressive stresses. The problem of anchorage slippage due to crushing of the concrete inside the bends of the conventional cross ties has also been solved in the case of double head studs. The heads of the double head studs should be larger and thick enough to bear safely on concrete surface and at the same time develop sufficient force required to yield the stem of the studs. The double head studs can be assumed fully effective and anchored just behind their heads.

1.6 Scope and objectives

The objective of this experimental program, in a broad view, is to study the effect of varying confinement parameters in the boundary regions of reinforced concrete shear walls on the overall wall strength and ductility. Specifically, the effectiveness of the Double Head Studs as a confinement reinforcement in the boundary regions of reinforced concrete shear walls will be studied under in-plane cyclic lateral loads and constant vertical loads. The effect of varying the double head studs distribution in the cross section as well as along the height of shear wall, on the strength, ductility and failure modes, will also be studied.

Another aspect of the experimental program is to compare the behavior of the shear walls built with conventional single-legged crossties in their boundary elements with the walls built with the recently introduced double head studs (as confinement reinforcement) under fully reversible in-plane cyclic loads and constant vertical load.

One beneficial outcome of the provision of double head studs compared to the conventional crossties is the removal of excessive reinforcement congestion due to hooks and bends of crossties in the areas of closely spaced bars in reinforced concrete members, such as the boundary elements of shear walls.

The scope of the current research involved testing three full-scale reinforced concrete shear walls; one confined with conventional cross-ties and the other two with double head studs in their boundary elements.

1.7 Organization of the Thesis

This section provides an outline of the organization of the thesis with brief description of the contents of each chapter

Chapter 2 presents a literature survey of the research work, reported to date, on the study of confinement behaviour in shear walls and concrete columns, specifically, those involving double head studs as confinement reinforcement.

Chapter 3 describes the experimental phase of the thesis in detail. It includes the fabrication procedure of the designed test specimens. It also describes the erection and working of loading assemblies and load frames together with instrumentation and testing procedures (in brief).

Chapter 4 describes the testing procedures in detail and it also presents the test results, observations and the specimens behaviour during the test.

In chapter 5, analysis of the current test results is presented together with a comprehensive study and comparison of previous shear wall tests in different other research works.

Finally in chapter 6, summary and conclusions of the current research work are given along with the recommendations for further work in this area.

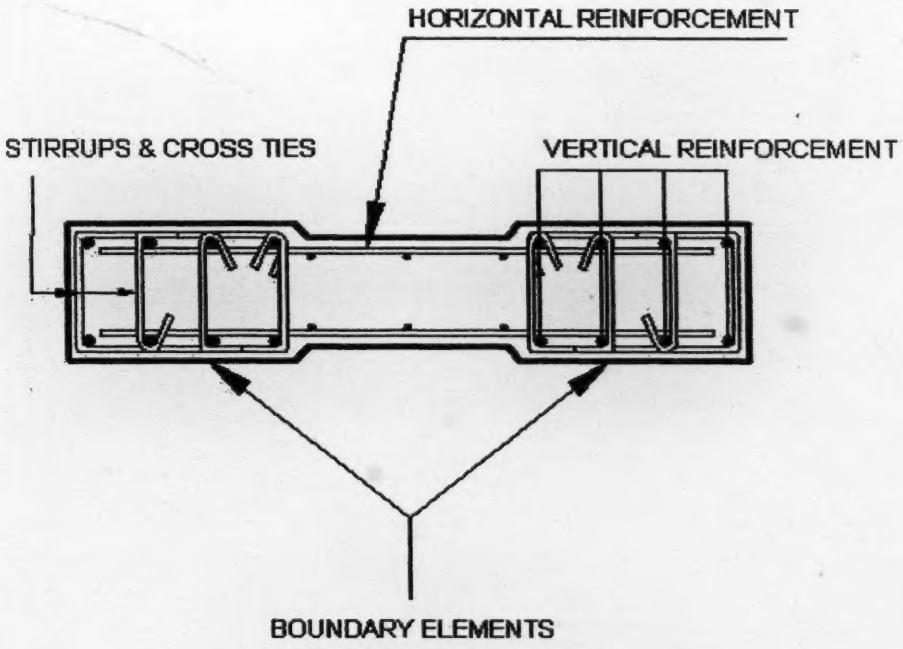

Figure 1.1 Typical cross-section of a shear wall

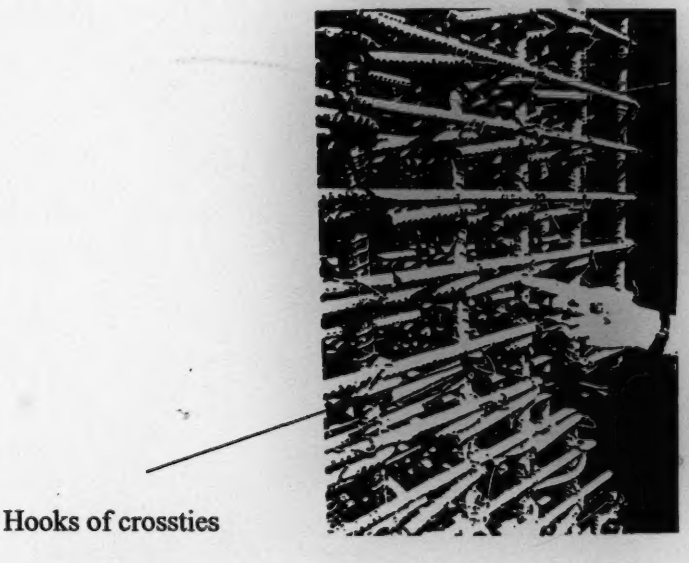

Figure 1.2 Reinforcement congestion due to hooks of crossties and rings

CHAPTER 2

LITERATURE REVIEW

2.1 Introduction

This chapter will mainly present a survey of research work that is carried out to explore factors and conditions influencing confinement behavior in reinforced concrete columns and in end zones (boundary elements) of Reinforced Concrete Shear Walls, which in turn affect the over all strength and ductility. It also presents the design recommendations for structural walls in ACI 318-2002 for the structures vulnerable to high seismic risk with a brief review of the Capacity design. In the end conclusions will be derived from the previous research work and need for the current testing program will also be discussed in light of the conclusion.

2.2 Design strategy of concrete shear wall

As already discussed in Chapter 1, the design of concrete shear walls for earthquake loads requires proper fulfillment of ductility requirements in the expected potential plastic hinges to maintain structural integrity under large inelastic deformations during seismic events. The load transfer mechanism in shear walls leads to the concentration of large flexural (axial) stresses in the end zones (or the Boundary elements). The adequacy and design of these end zones are important factors in the overall wall design. Research showed that concrete shear walls, with properly confined boundary elements, exhibited far better and ductile response compared to the response of walls without boundary elements (Naeim, F., 1989). This is because confined boundary elements not only delay vertical bar buckling but also enhance the shear capacity of the wall through the dowel action. Similarly, moment to shear ratio (M_p/V) at the base of wall was found to play an important role in affecting the behavior of shear walls. Research

work showed that shear capacity at the base of shear walls is higher than that predicted from the recommended standard procedures (Naeim, F., 1989). The ideal ductile behavior of structural walls could be severely affected by unavoidable shear deformations at the wall base. Shear failure is the most undesirable failure mode for any structural member. Although shear deformations are unavoidable, they could be minimized in seismic design by applying the principles of "Capacity Design". It is discussed in detail in the next section.

2.3 Capacity design

The definition or the aim of capacity design, in its simplest form is " To design the structure in such a way as to fail in a desirable mode". The most desirable response of a structure during a severe earthquake is the one that exhibits more ductility. A traditional analogy to illustrate the concept of the capacity design is that of a chain failing in a ductile mode, having only one weak (ductile) link in it with remaining links brittle (Paulay and Priestley, 1992). The behavior of this chain is shown to be ductile due to the presence of the ductile link in it, provided the strength of all the other brittle links is greater than the maximum feasible strength of the weak link. In this analogy, the ductile link represents the lateral load resisting system such as a shear wall (or the hinging zone of the shear wall) while the remaining brittle links represent the other elements or the remaining part of the structure that desires to remain elastic throughout a seismic event.

The ideal ductile behavior of the shear wall could be achieved by prohibiting any source of undesirable modes of failure. Shear deformation at the base of a shear wall is the most undesirable factor that affects the ideal ductile response. The adverse effect of high shears, acting along with the yield moment, has been observed on the deformation capacity of the plastic hinges at the base of shear walls. Anchorage slippage of the longitudinal reinforcement may also ignite the undesirable deformations, as shown by some experimental results as will be discussed in section 2.4.2.

Capacity design requires distinct elements of the lateral load resisting system (such as a shear wall) to be designed and detailed to dissipate energy under severe earthquake imposed deformations. The energy dissipation occurs at plastic hinge locations within these elements, such as the bottom portion of a cantilever shear walls or the joint of the coupling beams in a coupled-shear wall system. Plastic rotations, without much stiffness degradation in the plastic hinges, are ensured by providing special confinement to both concrete and the flexural reinforcements in these zones, in the form of anchored hoops and transverse reinforcements. All other structural elements are then protected against actions that could cause brittle failure by providing them strengths greater than that corresponding to the maximum strength in those plastic hinges (Paulay and Priestley, 1992).

The only uncertainty in the response of capacity-designed structures lies in the level of inelastic deformations that may occur during strong ground motion. However, properly detailed and confined plastic regions could accommodate significant variations in the ductility demands from the expected values without much loss of resistance to the lateral forces. In other words, structures designed by using the principles of capacity design are more tolerant to the imposed seismic deformations (Paulay and Priestley, 1992).

2.4 Literature survey

The literature survey is mainly focused on research work highlighting the effect of confinement on the strength and ductility of reinforced concrete shear walls. As obvious from the background and design strategy of shear walls, the main components to be designed with precision are the boundary elements at the wall extremities. Behavior and design of these boundary elements follow and include the behavior and design rules for short columns, (ACI Code, 318-2002) therefore the survey also includes some research work carried out to explore the factors affecting confinement behavior in reinforced concrete columns. In some research work, the testing phase includes short column tests under axial and reversible lateral loads with varying confinement parameters while the

results of tested columns are used to develop analytical model that describes the behavior of confined concrete in the boundary elements of Shear walls, (Sheikh S.A and Uzumeri S.M., 1980).

2.4.1 Dazio, A., Wenk, T., and Bachmann, H. (1999) (German)

Dazio et al. tested six concrete shear walls under quasi-static cyclic lateral load and constant vertical load. WSH1 to WSH6 walls were 4950 mm high and 150 mm x 2000 mm in cross-section, with height to width (h/w) ratio of approximately 2.5. The test was carried out at the Institute of Structural Engineering (IBK), Zurich. The main objective of the test was to adapt proven design rules for central Europe with moderate seismicity pertaining to structural walls found in the countries with high seismicity. All the specimens were designed according to Eurocode.

The test parameters were the ductility of reinforcing steel, vertical and horizontal steel reinforcement ratios (ρ_f and ρ_h), axial load and the design methods. The reason of vertical load being a parameter is to simulate exterior and interior wall loadings. Vertical reinforcement in the web region consisted of either 6 mm or 8 mm ø with horizontal spacing of 125 mm or 140 mm. The horizontal web reinforcement consisted of 6 mm ø bars at a vertical spacing of 150 mm in all the test specimens. Vertical reinforcement in the boundary region was provided with six bars of diameter ranging from 8 mm to 12 mm. All the vertical bars of end zone were stabilized against buckling by closed hoops or single-legged ties except specimen WSH4. Average f'_c for the six test specimens was 45 MPa. Figures 2.1 through 2.6 show the cross-section and the reinforcement details of the six wall specimens. The reinforcement detail provided in the test specimens clearly indicates the variation of confinement parameter (in addition to other parameters) by varying the content and configuration of confinement reinforcement. A summary of the description of test specimens is provided in Table 1.1, while tensile properties of reinforcing bars are given in Table 1.2. Flexural reinforcement used in WSH1, WSH2 and WSH5 had comparatively less deformation capacity as mentioned in the coupon tests

results, 10 mm ø bar of WSH1 reached ultimate strain of 6 % while 12 mm ø bar of WSH4 reached approximately 8.5 % strain at ultimate.

The test started with two forced-control cycles up to 75% of the designed bending strength of the corresponding test specimen to determine idealized yield displacement (Δ_y) and the displacement ductility ratio, $\mu_\Delta = 1$. In the subsequent cycles, the displacement ductility was increased in steps of 1, beginning with $\mu_\Delta = 2$, till the failure of the specimen.

Load-tip displacement response of all the test specimens is shown in Figure 2.7. Test observations and some conclusions are summarized as follows:

i) While comparing WSH1 and WSH2, the effect of increasing confinement content becomes obvious. Vertical steel reinforcement as well as the confinement reinforcement configuration and spacing in the end zones of the two specimens were identical. The difference was only in the diameter of crossties in the boundary elements (Refer to Figures 2.1 and 2.2) and also in the strain hardening properties of the vertical reinforcing steel in the boundary elements. WSH2 showed better response than WSH1 in terms of strength and ductility. The volumetric ratio of confinement reinforcement in the end zones of the two specimens differed by 2.5 % but gain in axial load capacity was approximately 7.2 %. On the other hand, regarding ductility, WSH1 showed less ductile behavior than WSH2. The lateral load in WSH1 was dropped by 14 % at $\mu_\Delta = 3$, while WSH2 showed a stable and ductile behavior even at $\mu_\Delta = 3$ and the drop in lateral load was 2.5 % after $\mu_\Delta = 3$.

ii) The effect of confining the vertical reinforcement in the end zones is visible by comparing the hysteresis loops of WSH3 and WSH4. WSH3 had closed hoops and cross ties in the boundary elements while WSH4 had only a U-shaped end hook at the extreme edges of wall. The amount and distribution of vertical reinforcement was identical in the two walls. Gain in lateral load capacity was

observed to be 2.5 % but gain in the ductility is more obvious from the hysteresis loops of the two walls as WSH3 reached $\mu_\Delta = 6$ and showed stable loops while WSH4 reached $\mu_\Delta = 5$ but showed stable hoops only up to $\mu_\Delta = 4$.

iii) Walls WSH1, WSH2, WSH3 and WSH5 failed by fracture of the vertical reinforcement in the end zones while WSH4 was failed in concrete compression crushing due to wider reinforcement spacing. WSH6 was failed by a sudden collapse of the concrete compression zone after fracture of several ties of the confinement reinforcement.

iv) All specimens had similar energy dissipation capacity except WSH5 which had smaller capacity because of heavily pinched hysteresis loops due to the presence of high axial load and having low reinforcement ratio (ρ_f).

v) Stiffness of the cracked specimen, but mainly uncracked, was approximately 75 to 80 % of the uncracked stiffness.

vi) Steel reinforcement with insufficient strain hardening capability, which is used in WSH1, WSH2 and WSH5, resulted in an insufficient deformation capacity in WSH1 and unsatisfactory deformation capacity in WSH2 and WSH5.

2.4.2 Oesterle, R.G., Fiorato, A.E. and Coreley, W.G (1980)

Oesterle et al. tested several reinforced concrete shear walls with and without boundary elements, but only four tests were published in the literature considered. The main objective of test was to investigate the reinforcement details in the structural walls as recommended by the ACI Building Code 1977 and the Uniform Building Code 1976. The walls were tested under fully reversible, quasi-static lateral load, without axial load. These tests were mainly focused on the detailing of transverse reinforcement in the

boundary elements and anchorage of the horizontal wall reinforcement within hinging regions of structural walls.

The test specimens were 15 ft high and 6 ft 3 inch wide, resulting in the height to width ratio (h/w) of 2.4, with square boundary elements of 12 inches x 12 inches and web thickness of 4 inches. Figure 2.8 shows view of a typical test specimen together with the reinforcement details of four walls; B1, B2, B3, B5.

Walls B1 and B3 had identical reinforcement except for the transverse reinforcement in the boundary elements. Vertical reinforcement content in the boundary elements of B1 and B3 corresponded to 1.1 % of the boundary element area. Transverse reinforcement in the boundary elements of B1 was designed according to sec 7.10, ACI 318-77 and the resulting ties spacing was 8 inches (203 mm), which also corresponded to 16 times the vertical bar diameter. Wall B3 had transverse reinforcement of the boundary elements designed according to A.6.5 of ACI 318-77. The resulting spacing of the transverse hoops and ties was 1.33 inches (34 mm), which also corresponded to 2.7 times the vertical bar diameter. This detail was provided only within the lower 6 ft (1.83 m) of the wall while the remaining upper portion of the wall had ordinary column ties.

Similarly, wall specimens B2 and B5 had nominally identical reinforcement except for the transverse reinforcement in the boundary elements. Both walls had 3.7 % vertical reinforcement content in the boundary regions. Specimen B2 was reinforced with ordinary column ties at a spacing of 8 inches (203 mm) in the boundary elements, which also corresponded to 10.7 times the vertical bar diameters, while wall specimen B5 had hoops and ties spaced at 1.33 inches (34 mm) or 1.8 times the vertical bar diameters in the boundary elements. This special detail in B5 was provided within the lower 6 ft (1.83 m) of the wall while ordinary column ties were provided over the remaining height.

Test observations and conclusions are summarized as follows:

i) There was little difference in the hysteretic response of specimens B1 and B3 up to 30th cycle, after which strength decay was more observed in specimen B1 than in B3.

ii) Deterioration in strength and stiffness of B1 was caused by damage to the boundary elements due to alternate tension and compression followed by the buckling of the main vertical bars.

iii) Specimen B3 did not show significant increase in strength as compared to B1, although the transverse reinforcement ratio in the boundary elements of B3 was approximately double that of B1. However improvement in the ductility was observed in B3 and the increased confinement reinforcement maintained integrity of the boundary elements by delaying bar buckling and containing the concrete core. B3 reached a tip displacement of 8 inches (203 mm) compared to 6 inches (152 mm) tip displacement of B1.

iv) Deterioration was less observed in B3 compared to B1

v) The capacity of wall specimens B2 and B5 were limited by web crushing. Specimen B2 reached a capacity corresponded to nominal shear stress of $0.6\sqrt{f'_c}$ (MPa) while the specimen B5 reached shear capacity of $0.73\sqrt{f'_c}$ (MPa).

vi) In specimen B2, the boundary elements were severely deteriorated prior to the web crushing. Due to increased transverse reinforcement spacing in B2, several vertical bars buckled and concrete was lost in load reversal, while in B5 the closely spaced transverse hoops delayed bar buckling. The lateral shear was carried by the boundary elements even after the web crushing, because of the increased strength of B5.

vii) The special transverse reinforcement arrangement in specimen B5 resulted in enhanced shear capacity to form a plastic hinge at the lower ends of the boundary elements.

2.4.3 ACI 318-2002 (2002), Building Code Requirements for Structural Concrete, American Concrete Institute

ACI Code 2002, committee 318 provides special design requirements for the walls in areas of high seismic risk in Chapter 21, " *Special provisions for walls in areas of high seismic risk*" Section 21.7, supplemented by Chapters 10, 11 and 14 (if applicable) for the design requirements of walls subjected to axial force, shear force and bending moment.

Section 21.7 requires that the minimum reinforcement ratio for structural walls should not be less than 0.0025, along both longitudinal and transverse axes and requires at least two curtains of reinforcement if the factored in-plane shear force exceeds $2A_{cv}\sqrt{f'_c}$.

Section 21.7.6 discusses the requirements of the boundary elements or the end zones of structural walls. It requires provision of boundary elements at boundaries and at edges around openings of structural walls when the extreme-fiber stress, corresponding to factored forces including earthquake effect, exceeds $0.2\ f'_c$ unless the entire wall is reinforced with transverse reinforcement conforming to the confinement provisions for columns. The extent of boundary elements inside the wall cross-section and along the wall height is required up to the point where the calculated compressive stress is less than $0.15\ f'_c$.

The same section requires that the boundary elements should be adequate enough to carry all the factored axial forces in the plane of the wall (diaphragm) resulting from the combined effect of axial and flexural loads. The cross-section of boundary elements

must have adequate strength (determined as an axially loaded short column with appropriate strength reduction factors) to resist the factored axial compressive force at the critical section. Similarly, the boundary element must have adequate reinforcement to resist the tensile force developing because of the bending moment at the section. The design axial load strength is provided in Section 10.3.6.2, Equation 10-2, for non-prestressed tied compression members, as:

$$\emptyset P_n = 0.8 \emptyset (0.85 f'_c (A_g - A_{st}) + f_y A_{st}) \qquad \textbf{(ACI Eq. 10-2)}$$

Where Ø is the strength reduction factor= .7 for tied columns in compression

Transverse reinforcement in the boundary elements is required to fulfill the confinement requirements of Section 21.4.4.1 through Section 21.4.4.4 for columns. Figure 2.9 shows the detailing requirements of transverse reinforcement for column cross-section as required by Section 21.4.4, which is also applicable on the boundary elements. Vertical spacing of transverse reinforcement is required not to exceed one-quarter of the minimum member dimension or 4 inches. (100 mm).

The shear strength requirements for structural walls are described in Section 21.7.4. Equation 21-7, Section 21.7.4 provides the shear strength requirement for structural walls and diaphragms with height to width (h/w) ratio greater than or equal to 2, as:

$$V_n = A_{cv} (2 \sqrt{f'_c} + \rho_n f_y) \qquad \textbf{(ACI Eq. 21-7)}$$

The upper bound on the above equation for shear strength is given in Section 21.7.4.4 for individual wall pier (wall segment), as:

$$V_n \leq 10 A_{cp} \sqrt{f'_c}$$

2.4.4 Ozcebe, G. and Saatcioglu, M. (1987)

The main objective of the work was to study experimentally the confinement in reinforced concrete columns under constant axial load and reversible cyclic lateral load that produces a peak shear stress of approximately $0.5\sqrt{f'_c}$ MPa. The testing program consisted of four 1-meter high 350 x 350 mm square columns with f'_c ranging from 32 MPa to 39 MPa. Vertical steel reinforcement was provided with eight 25.2 mm (1.0 inch) diameter bars (ρ = 3.27 %), one at each corner and at each mid-side. The reinforcement ratio (ρ) was kept identical in the four test specimens. Four types and configurations of transverse reinforcement were used for four specimens. Two specimens were reinforced transversely with 11.3 mm diameter closed stirrups but with different vertical spacing, while the remaining two specimens were reinforced with 6.4 mm diameter single legged crossties in addition to 6.4 mm diameter closed stirrups (with identical vertical spacing). Volumetric ratio of the transverse reinforcement (ρ_s) was identical in the last two test specimens and is also approximately equal to one of the previous two specimens with closed stirrups only. The only difference in the last two specimens was the configuration of the crossties, one had crossties with 135 degree hooks at both ends while the other had crossties with a 135 degree hook at one end and a 90 degree hook at the other end. Layout of reinforcement and details of the test specimens are shown in Figure 2.10; the first test specimen conformed to the design requirements of ACI 318-83.

All the test specimens were first loaded vertically with 600 kN load, which was kept constant throughout the test, and then displaced laterally back and forth with increments of one yield displacement (Δ_y) between successive displacement levels. The constant vertical compressive stress corresponded to 12 % of the nominal column capacity or 20 % of the column design strength.

The test showed that the first specimen which was designed according to the provisions of ACI 318-83 for the regions of high seismic risk, exhibited rapid degradation in strength and stiffness when it was subjected to lateral load reversals. The strength loss was approximately 20 % at a displacement level of $3\Delta_y$. The second specimen that was

reinforced with 50 % more transverse reinforcement as compared to the first specimen, showed better response and lost 30 % of the strength at a displacement level of $4\Delta_y$. The last two specimens, that were reinforced with crossties and closed stirrups, showed ductile response with very little or no degradation in strength and stiffness. The behavior of the last two specimens, in terms of strength and stiffness, was approximately identical although the difference was only in the end configurations of the crossties.

The test observations and conclusions from analysis of the test result are summarized as:

i) Proper confinement significantly improves the behavior of concrete columns subjected to cyclic loading.

ii) The amount of transverse reinforcement required by ACI 318-83 is adequate to insure ductile behavior, but, the detailing requirements for confinement reinforcement are not adequate for columns with unsupported longitudinal bars.

iii) Unsupported longitudinal bars, not engaged by the hooks of crosstie or closed stirrups, are not capable of providing the necessary confinement required in hinging regions.

iv) Performance of crossties with 135 degree hook at both ends was as satisfactory as the crossties with a 135 degree at one end and a 90 degree hook at the other end.

v) Refined plane-section analysis, with a confined concrete stress-strain model and steel stress-strain relationship with strain hardening, produces satisfactory predictions of moment capacities.

2.4.5 Sheikh, S.A. and Uzumeri, S.M (1980)

This work examined the impact of various confinement parameters on the behavior of tied columns in terms of strength and ductility, under monotonic concentric axial load. The main parameters were the distribution and the configuration of vertical and transverse reinforcements. Sheikh and Uzumeri performed 24 tests on 1960 mm high 305 mm square columns with four sets of transverse and longitudinal reinforcement

configurations. Further subdivision of the parameters was carried out by varying the transverse steel reinforcement ratio (ρ_s) and also by introducing heat-treated transverse reinforcement to have a flat yield plateau. The four major steel configurations are shown in Figure 2.11. Compressive strength of concrete varied between 31.31 MPa (4.54 ksi) to 40.9 MPa (5.93 ksi). Tests were carried out in Load-control mode, but the unloading branch of the load-axial deformation was traced out approximately by manually controlling the load.

Figures 2.12 through 2.15 compares the graphical test results

Test observations and conclusions are summarized as follows:

i) Strength gain up to 70% was observed as a result of increased concrete confinement in the form of transverse rectangular hoops and well distributed longitudinal reinforcement.

ii) Reducing the tie spacing results in higher concrete strength and ductility even though the stiffness of ties was reduced in order to maintain the same volumetric ratio.

iii) The amount of transverse reinforcement has a very significant effect on the behavior of confined core. However, the change in transverse steel content results in a less than proportional change in the strength and ductility of the confined concrete.

2.4.6 Moehle, J.P., and Cavanagh T. (1985)

This research studied the effectiveness of two types of crossties compared to intermediate hoops. The first type had 180^0 hooks at both ends (as permitted by Uniform building code 1982, for ductile frames in regions of high seismic risk) that engages the perimeter hoop and is tied against the longitudinal bar. The second type of crosstie had a 90 degree hook at one end and a 135 degree hook at the other end (as permitted by the ACI, Committee 318-83, to simplify fabrication on-site).

Ten, 914 mm (36 in.) high, 305 mm x 305 mm square columns were tested under monotonically increasing axial compression. Vertical steel reinforcement ratio (ρ) was identical in eight columns and was achieved by providing 8- No. 6 Grade 60 bars (nominal area 284 mm^2) symmetrically arranged, one at each corner and one at each mid-side. Transverse reinforcement provided in all the test specimens was No. 2 Grade 60 (nominal area of 31.6 mm^2). Two columns employed intermediate hoops with the peripheral hoops, two had crossties with 180 degree hooks at both ends (in addition to the peripheral hoops), two had crossties with a 90 degree hook at one end and 135 degree hook at the other end (in addition to the peripheral hoops), two columns had only closed hoops without any intermediate hoop or crosstie, and the last two columns were plain cement concrete. The mean strength of concrete cylinders was 38 MPa. The test was performed in load-control mode. Figure 2.16 shows the cross-sections of the four specimen types.

Results of the test and some conclusions are summarized as follows:

i) Columns with intermediate hoops (in addition to the peripheral hoops) developed highest strength and showed nearly plastic load-deformation response beyond the peak load. This was caused by higher transverse reinforcement ratios compared to columns with crossties.

ii) Columns with crossties having 180 degree hooks at both ends showed slightly better behavior than columns with crossties having a 90 degree hook and a 135 degree hook.

iii) Columns without crossties showed the least response among the four types, although fulfilling the requirements of ACI 318-83 provisions for high seismic risk to tie every alternate vertical bar. Hence, the importance of engaging unsupported vertical bars became obvious in their test.

iv) Columns having 135 degree and 90 degree hooked crossties were slightly less ductile than those having 180 degree hooks, which were in turn slightly less ductile then columns with intermediate hoops.

v) 90 degree hooks of some crossties eventually opened and pulled out of the concrete leading to partial loss of effectiveness of the crossties.

vi) Crossties having 180 degree hooks and engaging perimeter hoops resulted in the fracture of the hoops at the crosstie locations.

2.4.7 Dilger W.H. and Ghali A. (1997)

Dilger and Ghali studied the effectiveness of anchorage of the confinement reinforcement and its impact on the overall strength and ductility of columns. Dilger and Ghali introduced a form of confinement, " Double Head Stud", in reference to its configuration, which solved some of the basic problems with the conventional crossties. They compared the effectiveness of the conventional single-legged crossties with that of the Double Head Studs and showed that the introduction of the Double Head Studs in compression members enhances their strength and ductility.

The testing program consisted of five short walls (or wide columns) 500 mm x 150 mm in cross-section and 800 mm high with central test zone of 400 mm, tested under axial compression. Figure 2.17 shows specimens and their reinforcement details. Specimen 1 had no reinforcement, intended to produce results for unconfined concrete. Specimen 2 had no longitudinal (vertical) reinforcement in the test region and it was provided transversely with 15 conventional crossties (each 5.7 mm diameter) normal to the wall surface in the test zone. The crossties had 180^0 and 90^0 hooks at the two ends with a cross-sectional area of 25 mm^2, spaced at 75 mm on center, representing 0.29 % of the wall area within the test zone. The crossties were placed on 5.7 mm diameter closed hoops. Specimen 2 was intended to determine the effect of confinement provided by the

crossties only, in the absence of longitudinal bars. Specimen 3 was identical to specimen 2 except that the conventional crossties were replaced by double head studs of the same diameter and material quality. The number and spacing of all the reinforcement of specimen 2 was identical to those of specimen 3. Specimen 4 was reinforced longitudinally with ten-10M bars, with total cross-sectional area of 1000 mm^2, representing 1.33 % of the horizontal cross-section. Transverse reinforcement in the test zone of specimen 4 was provided with 15 conventional crossties (having 180^0 and 90^0 hooks at the two ends) and 10M closed hoops at 75 mm on center. Similarly, specimen 5 was identical to specimen 4, only the crossties of the transverse reinforcement were replaced by Double head studs of the same cross-sectional area. The compressive strength f'_c ranged between 20.0 MPa to 21.6 MPa. The mean yield strength of 10 M bars was 410 MPa while the yield strength of crossties and Double head studs was 595 MPa. The test observations and conclusions are summarized as:

i) Columns (or walls), reinforced with double head studs as the transverse reinforcement, exhibited more ductile behavior and higher ultimate strength compared to columns (or walls) reinforced with conventional crossties. Specimen 5 showed 10 % greater strength than specimen 4 and was also more ductile.

ii) Specimen 3 showed more ductility than specimen 4, although specimen 3 had no vertical reinforcement and showed little lower strength than specimen 4.

iii) Anchorage of the crossties having a 180 degree hook and a 90 degree bend is not sufficient to develop yield stress in the ties in spite of the anchorage enhancement by the vertical bars lodged in the hooks and bends.

iv) Double head studs exhibited large strains beyond the yield at failure load of the column.

v) Close inspection of the tested specimens showed that the concrete was intact behind the heads of studs showing the adequacy of the heads in yielding the studs.

The main reason of the improvement in behavior is the effective mechanical anchorage of the double head studs, which is a result of their geometric configuration. Double head stud is simply a rod, having two round heads welded or forged at its two ends (Refer to Figure 2.18), and is placed in the concrete member in such a way that its two ends lie close to the exterior concrete surface.

Double Head Studs are a modified form of the Single Head Shear Studs but their function and use is totally different. Single Head Shear Studs were introduced to increase the shear capacity of relatively thin Reinforced concrete flexural members such as flat slabs and spread footings but double head studs were introduced in compression members to enhance the confinement behavior and hence the ductility capacity. Double head studs work in tension and the two heads mechanically confine the concrete between them and thus prevent the bulging-out of concrete under high compressive stresses. The problem of anchorage slippage due to crushing of the concrete inside the bends of the conventional cross ties has also been solved in the case of double head studs The heads of the double head studs are big and strong enough to bear safely on confined concrete and at the same time develop sufficient force required to yield the stem of the studs. The double head studs can be assumed fully effective and anchored just behind their heads.

2.5 Role of confinement in the light of previous research

Based on the above review, it can be concluded that properly detailed and confined plastic zones are essential to achieving satisfactory inelastic responses of earthquake-resistant structural components.

Nearly all researches concluded that the effective confinement to both concrete and flexural steel in the plastic zones is the most prominent factor that enhances the rotation capacity within the plastic hinges (or improves the ductility of reinforced concrete members). Not only the ductility increases but also gain in the load carrying capacity is observed as a result of confining the critical plastic zones. Factors that can improve confinement include the configuration, volumetric ratio and the distribution of the confinement reinforcement. Anchorage of the longitudinal and transverse reinforcement in shear walls was also found to be of significance while sustaining vertical and lateral cyclic loads. Summarizing the two important factors, it could be concluded that the proper confinement to the critically yielded plastic zones together with good anchorage to the longitudinal and transverse reinforcement, can significantly improve the behavior of reinforced concrete shear walls and columns in terms of increased ductility and strength.

The effectiveness of Double head studs as confinement reinforcement has been proved in the research work by Dilger and Ghali (Reference 2.4.7), but the testing was carried out on short elements resembling wide columns or walls under monotonic concentric axial loads. So, it is now the intention of the current thesis to test the effectiveness of Double head studs in the boundary elements of Reinforced Concrete Shear Walls.

Table 2.1 Specimens description (after Dazio A., Wenk T. and Bachmann H.)

Specimen	ρ_s Web (%)	ρ_s End (%)	ρ_s Total (%)	ρ_v Hor. Web (%)	End Confinement Config. , Dia. & vertical spacing	$N / (A_g f_c)$
WSH1	0.3	1.32	0.54	0.25	Ø 6 Hoop, Ø 3.5 Tie @ 75 mm o/c	0.05
WSH2	0.3	1.32	0.54	0.25	Ø 6 Hoop, Ø 4.2 Tie @ 75 mm o/c	0.05
WSH3	0.54	1.54	0.82	0.25	Ø 6 Hoop, Ø 4.2 Tie @ 75 mm o/c	0.05
WSH4	0.54	1.54	0.82	0.25	Ø 6 U at end only @ 150 mm o/c	0.05
WSH5	0.27	0.67	0.39	0.25	Ø 4.2, two Hoops @ 50 mm o/c	0.11
WSH6	0.54	1.54	0.82	0.25	Ø 6 & Ø 4.2 Hoops @ 50 mm o/c	0.11

Table 2.2 Yield and Ultimate tensile strengths of the reinforcing bar (after Dazio A., Wenk T. and Bachmann H.)

Wall	f_y(MPa)				f_u (MPa)			
	12mmØ	10mmØ	8mmØ	6mmØ	12mmØ	10mmØ	8mmØ	6mmØ
WSH1	-	549	-	584	-	620	-	602
WSH2	-	578	-	486	-	750	-	540
WSH3	578	-	578	486	750	-	750	-
WSH4	583	-	525	486	-	-	-	-
WSH5	-	-	525	486	-	-	683	540
WSH6	535	-	546	486	660	-	705	-

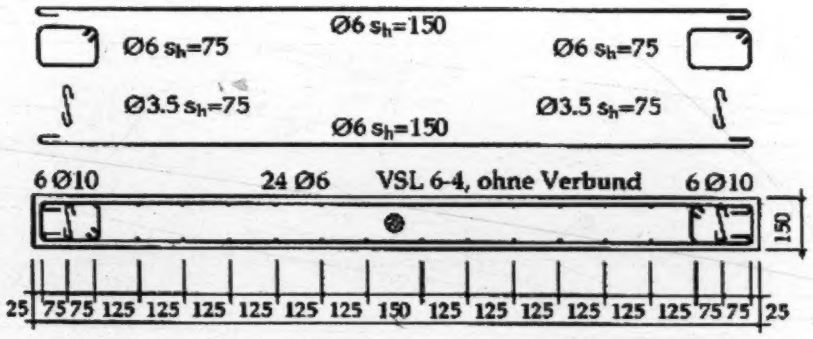

Figure 2.1 Reinforcement details of WSH1 (after Dazio et al. 1999)

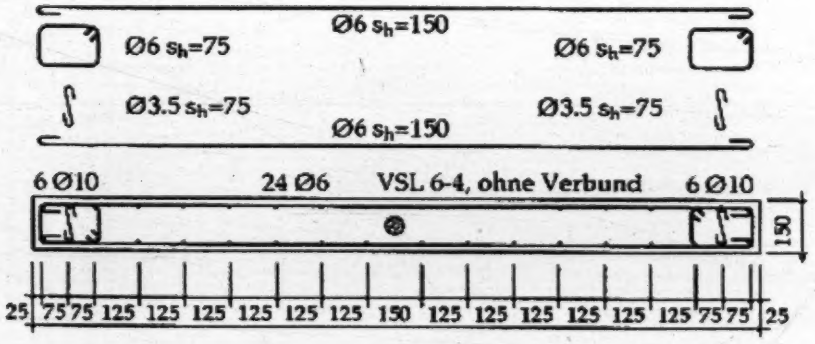

Figure 2.2 Reinforcement details of WSH2 (after Dazio et al. 1999)

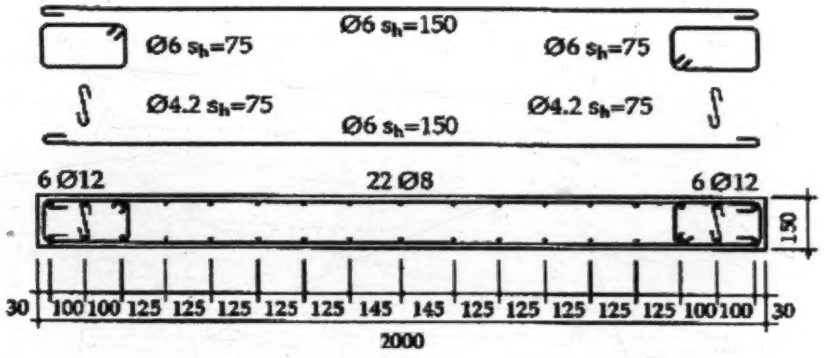

Figure 2.3 Reinforcement details of WSH3 (after Dazio et al., 1999)

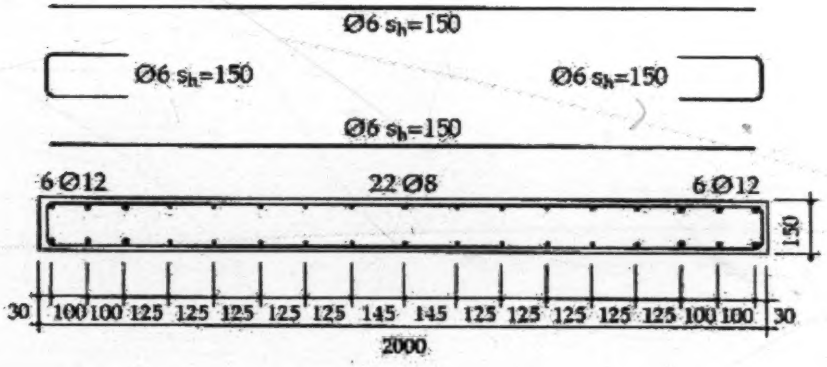

Figure 2.4 Reinforcement details of WSH14 (after Dazio et al., 1999)

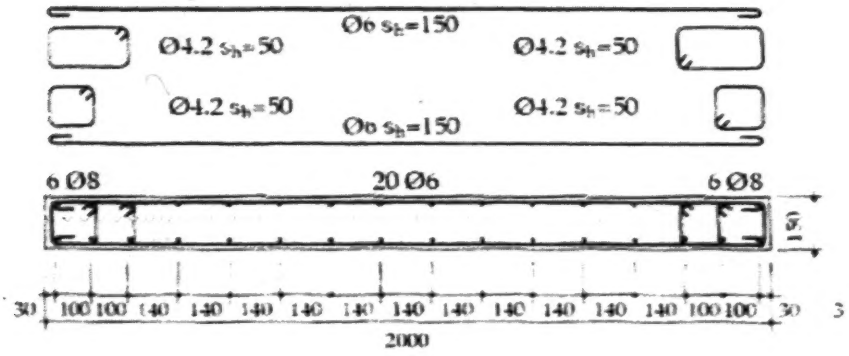

Figure 2.5 Reinforcement details of WSH5 (after Dazio et al., 1999)

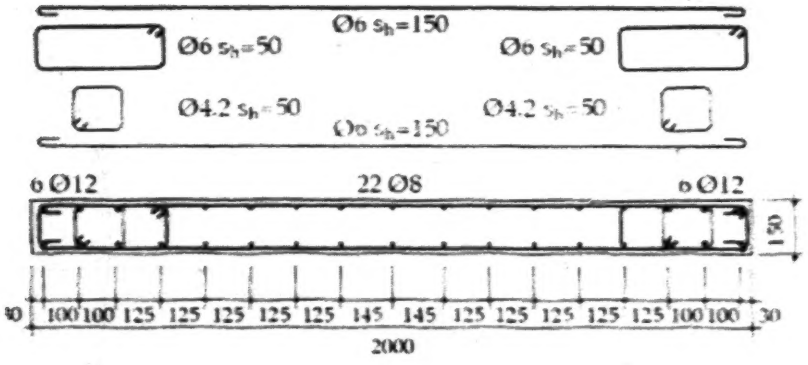

Figure 2.6 Reinforcement details of WSH6 (after Dazio et al., 1999)

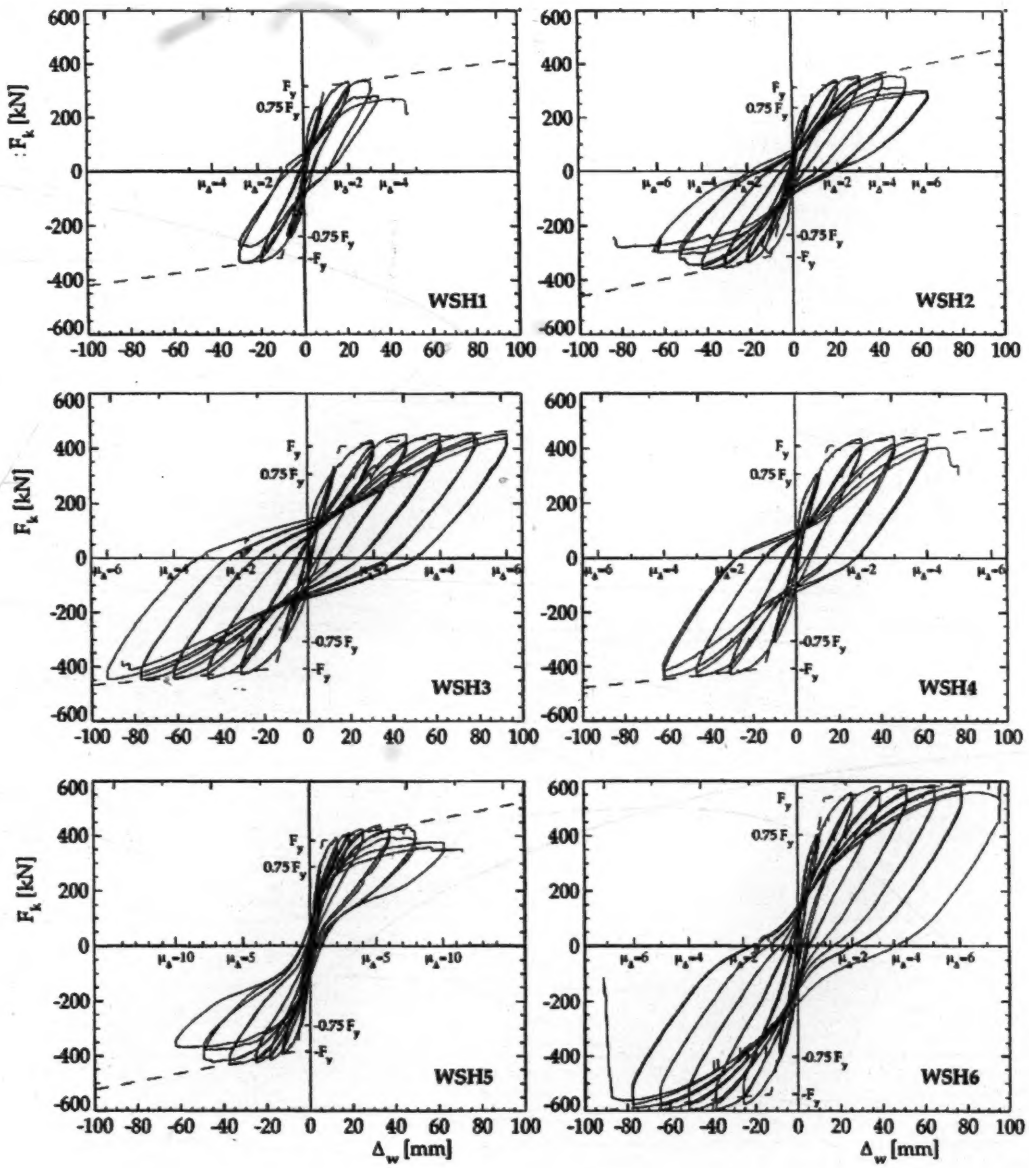

Figure 2.7 Load Tip-displacement responses of six walls (after Dazio et al., 1999)

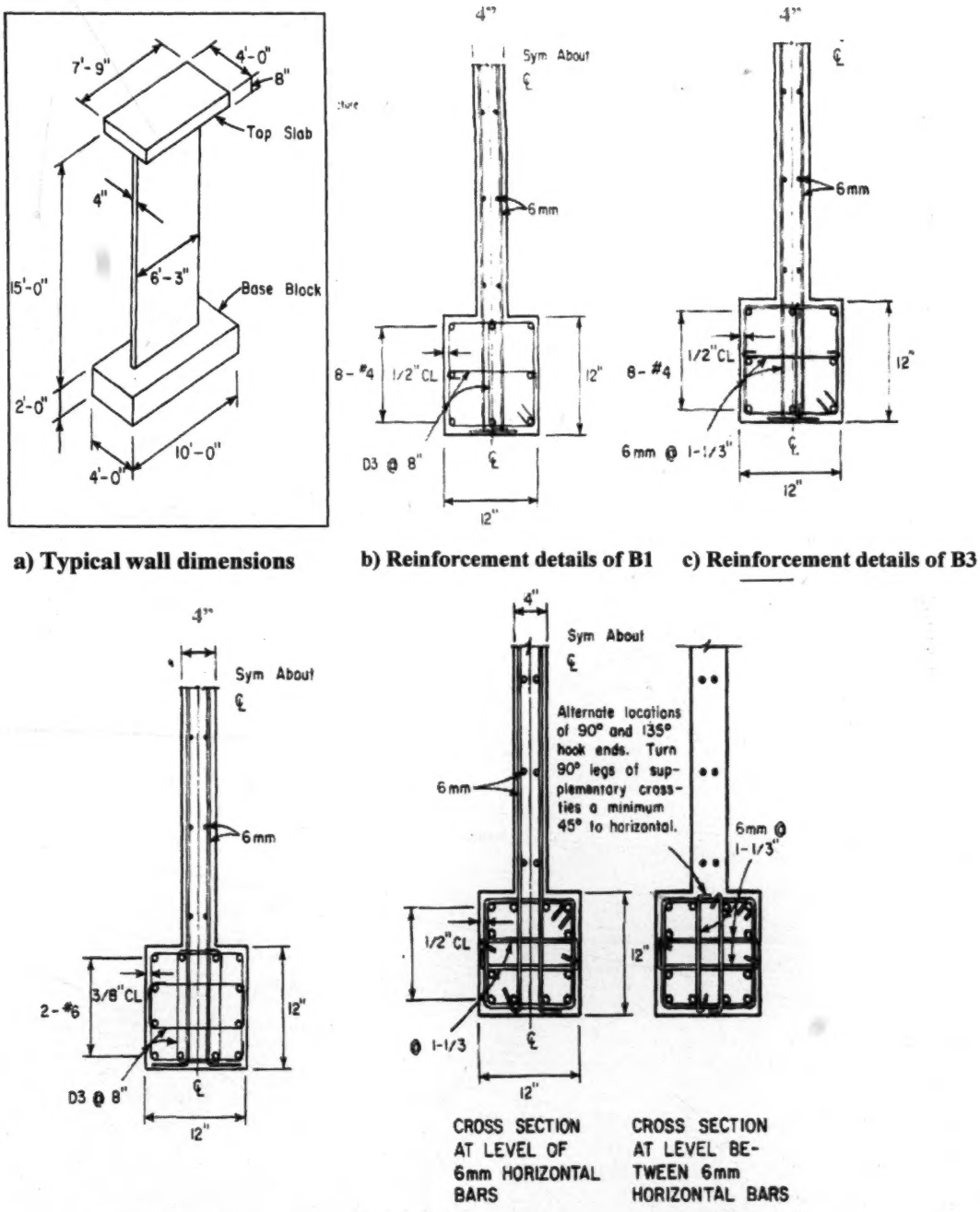

a) Typical wall dimensions **b) Reinforcement details of B1** **c) Reinforcement details of B3**

d) Reinforcement details of B2 **e) Reinforcement details of B5**

Figure 2.8 Specimen and their Reinforcement details (after Oesterle, et al.)

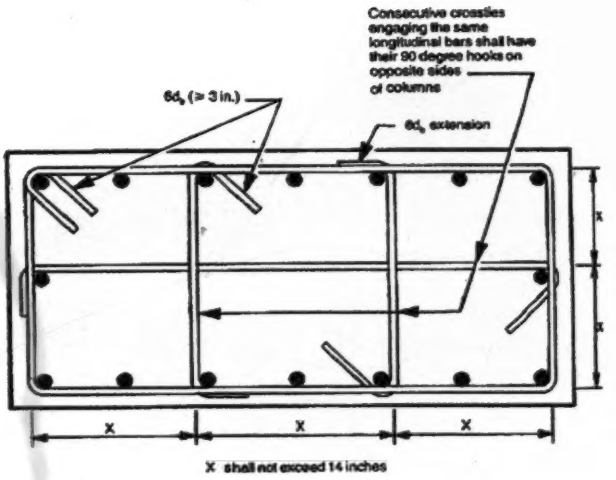
Consecutive crossties engaging the same longitudinal bars shall have their 90 degree hooks on opposite sides of columns
$6d_b$ ($\geq$ 3 in.)
$6d_b$ extension
X
X
X
X
X shall not exceed 14 inches

Figure 2.9 Detailing requirements in ACI 318-2002 Sec. 21.4.4

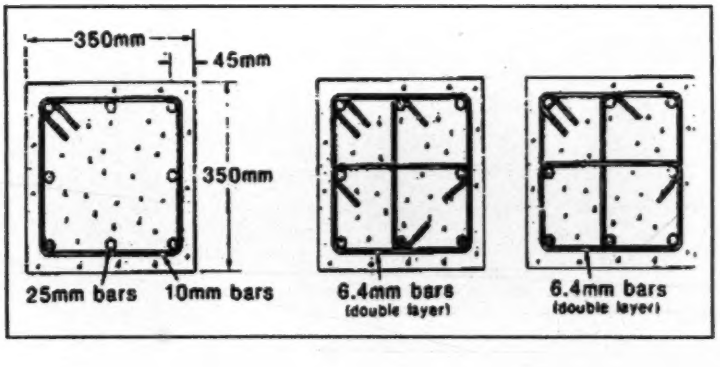

Figure 2.10 Column and ties detail (after Ozcebe and Saatcioglu 1987)

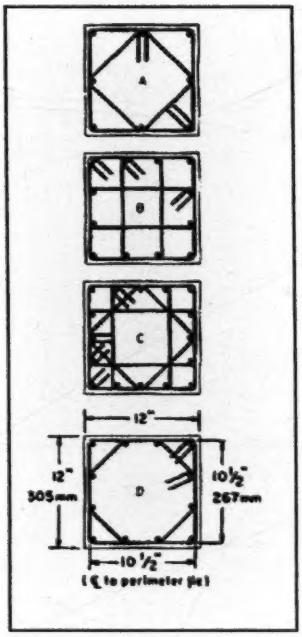

Figure 2.11 Columns details (after Sheikh and Uzumeri 1980)

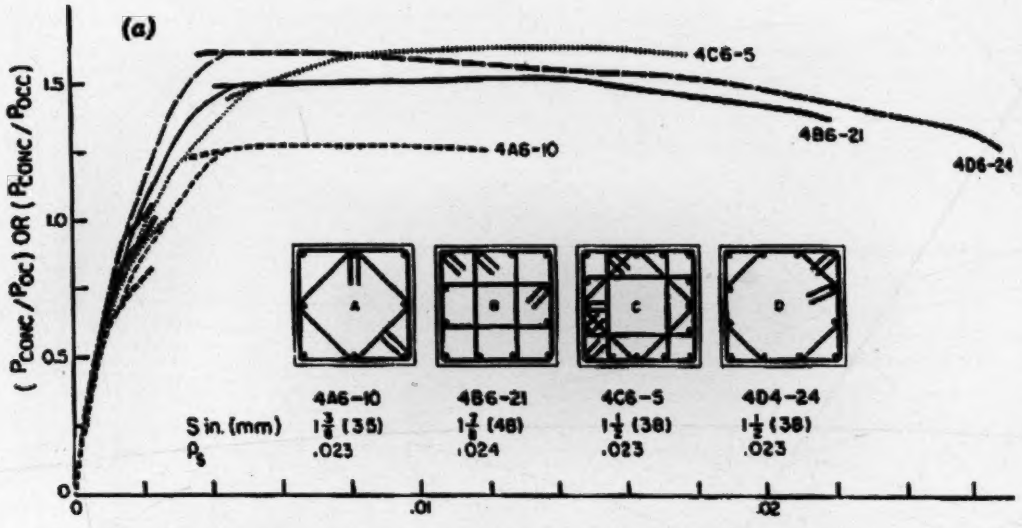

Figure 2.12 Test results showing effect of reinforcement configuration (after Sheikh and Uzumeri 1980)

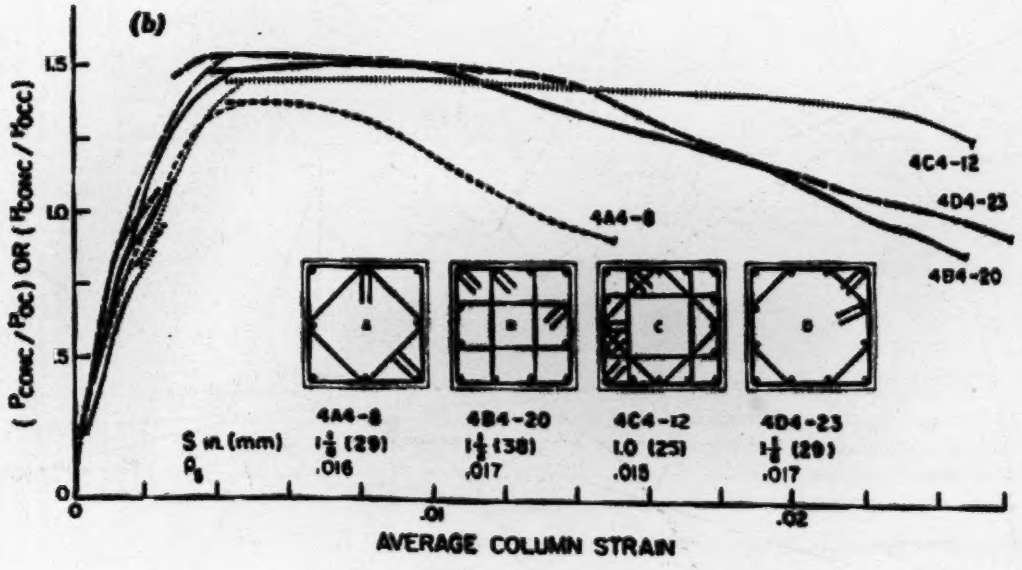

Figure 2.13 Test results showing effect of spacing and volumetric ratio (after Sheikh and Uzumeri 1980)

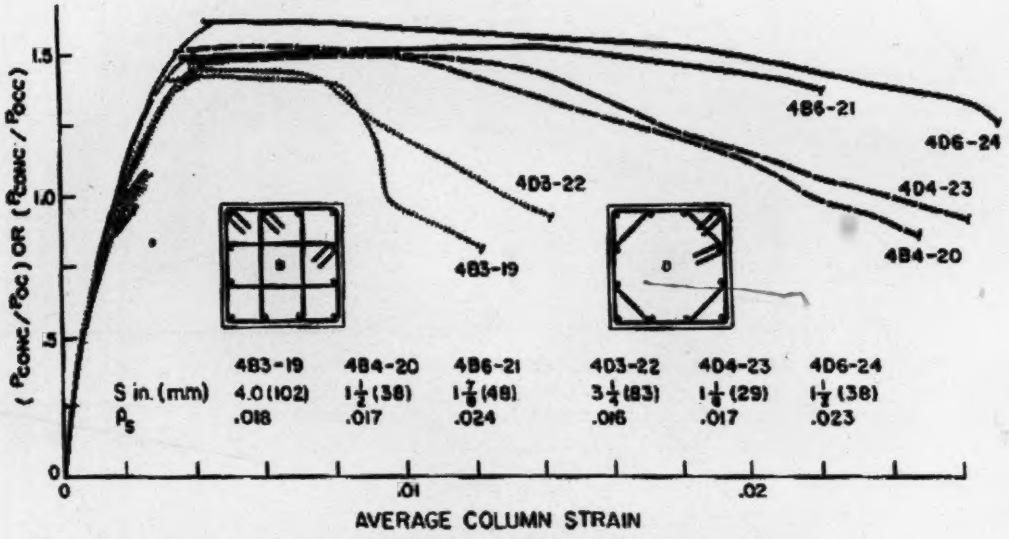

Figure 2.14 Test results showing effect of steel configuration, amount and tie spacing (after Sheikh and Uzumeri 1980)

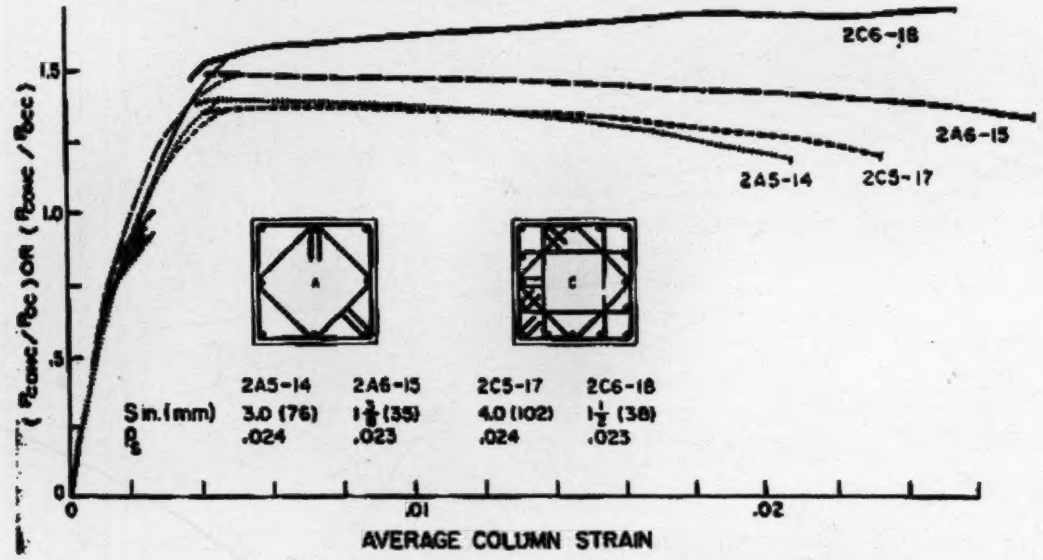

Figure 2.15 Test results showing effect of steel configuration and tie spacing (after Sheikh and Uzumeri 1980)

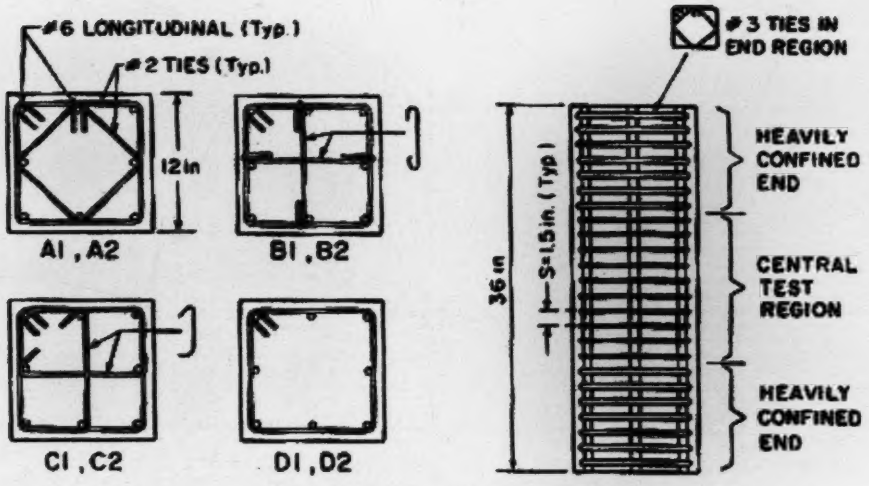

Figure 2.16 Specimen and their Reinforcement details (after Moehle and Cavanagh 1985)

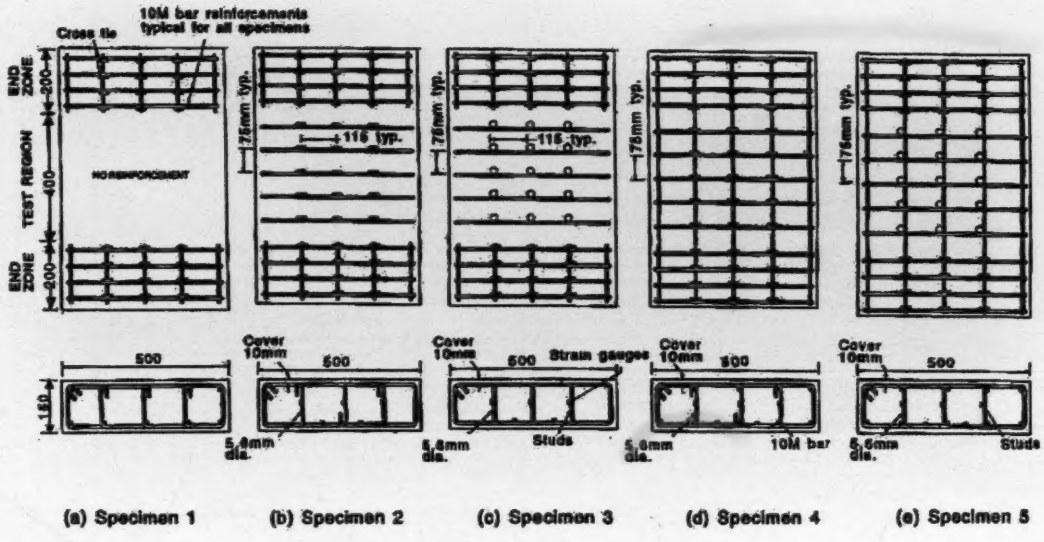

Figure 2.17 Specimen and their Reinforcement details (after Dilger and Ghali 1997)

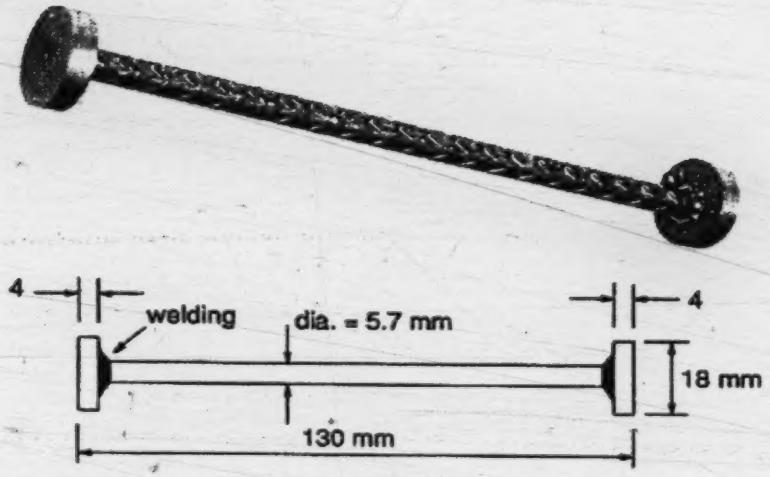

Figure 2.18 Configurations of Double Head Studs used in the tests (after Dilger and Ghali 1997)

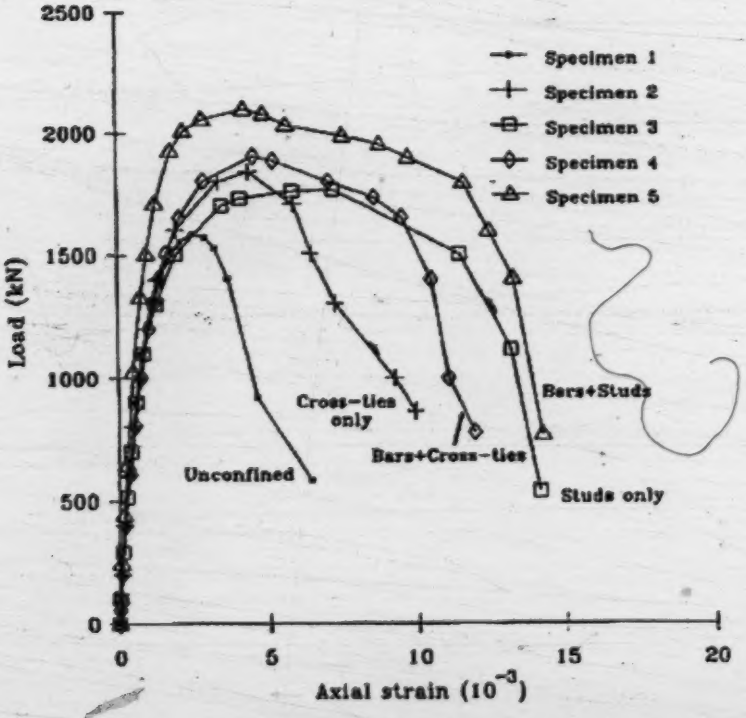

Figure 2.19 Results of test showing the effectiveness of Double Head Studs (after Dilger and Ghali 1997)

CHAPTER 3

EXPERIMENTAL PROGRAM

3.1 Introduction

Experimental phase of the thesis mainly involved the design and preparation of the test specimens and the reaction frames as well as carrying-out of the tests. The reaction frames were sub-assemblies of steel members, designed to resist and transmit the applied forces to the floor, within a reasonable safety limit. The design of the test specimens will be discussed in detail in Sec. 3.3 while Sec. 3.6 describes in detail the design basis and functioning of the reaction frames. Testing and loading procedures used in the experimental program conformed to globally accepted and practiced testing procedures intended to closely simulate real life situations. The testing procedure will be discussed in detail in Sec. 3.8.

3.2 Prototype structure

The prototype structure, on which design of the test specimens was based, represents the lower portion of a typical exterior shear wall of a six-story residential building, having five bays of 6 m each, in each direction in plan. The testing method was planned to be quasi-static-cyclic, which corresponds to the static design approach used in the design of test specimens. For testing purposes, the resultant of lateral seismic forces, acting at different floor levels, was concentrated at the top level of the test specimen, i-e at about 3.3 m above the base level. Location of the prototype building was assumed to lie in seismic zone IV of the Uniform Building Code 1997 and the detailing requirements be conformed to ACI 318-2002, Chapter 21 "Special Provisions for Seismic Design".

3.3 Specimen design

The main objective of the experimental program was to study confinement behavior in the boundary regions of concrete shear walls. Another aspect of the experimental work was to compare the behavior of the conventional single-legged crossties with the recently introduced Double Head Studs in the boundary elements of the shear walls. The traditional confinement reinforcement in compression members, as recommended by ACI 318-2002, is in the form of closed stirrups and single-legged crossties. The cross ties, as permitted by the ACI 318-2002, have a 90 degrees hook at one end and a 135 degrees hook at the other end, to allow for easy installation at site. Crossties are used to tie the reinforcing bars lying on the opposite faces of the reinforced concrete compression members. Cross ties not only provide confinement to the concrete but also anchor the vertical bars and prevent them from buckling after the spalling-off of the concrete cover. The cross ties work well in compression members but some research work has showed that the cross ties become less effective under high compression and bending moments in the presence of heavy shear forces or under cyclic loading (Refer to Chapter 2 " Literature Review").

Double head studs have already been tested and proved to be efficient means of confinement in reinforced concrete columns under concentric compression (Dilger and Ghali 1997) but their behavior under cyclic shear loading is studied only in ongoing research work at the University of Alberta. Therefore, the design of test specimens for the present experimental program constitutes an aspect of comparative study as well as an aspect of the parametric study. For comparative study, wall W-1 was designed which is confined with conventional crossties in its boundary elements and it will be treated as the reference wall. For parametric study, specimens W-2 and W-3 were designed, although these would also be included in the comparative study. The varying parameters between W-2 and W-3 were the cross-sectional area of double head studs and their distribution in wall cross-section while keeping the total volumetric ratio of confinement reinforcement constant in the three walls. The adjustment in the vertical spacing of studs was made in W-2 and W-3, where the cross-sectional area of double

head studs was not identical to the crossties in W-1. The adjustments were required in order to maintain identical volumetric ratio of the confinement reinforcement in the three wall specimens.

3.3.1 Specimens detail

Three specimens W-1, W-2 and W-3 were designed to achieve the research objectives. These specimens were designed by considering two main factors; one was the capacity of the available testing resources and second was the experience gained from a previous testing performed at University of Alberta, in 1999.

The gross geometric properties of the three wall specimens were identical. The overall height of a typical specimen was 4.2 m including 0.6 m thick concrete base (Refer to Figure 3.1 for the concrete dimensions of a typical wall specimen). The base was used to fix the specimen to the lab floor (Often referred to as Strong floor). Overall depth of the wall cross-section was 1.2 m including two 0.4 m wide boundary elements at each end.

The specimens were designed according to the provisions of Chapter 16, Sec. IV, Uniform Building Code UBC 1997 and Chapter 21, ACI-318-2002, "Special Provisions for Seismic Design". The predicted lateral load carrying capacity of the wall specimens under a constant axial load was computed by using computer software PCA-COL, developed by the Portland cement association (Refer to Table 5.1 for load and moment capacities). PCA-COL basically formulates the load-moment interaction diagram of reinforced concrete columns while fulfilling the design requirements of ACI 318-2002. It does not include the effect of strain hardening of steel reinforcement and the increased concrete compressive strength f'_c due to confinement. Axial load was applied as to cause a compressive stress of 0.15 f'_c on the wall.

The area of study was mainly focused on the confinement behavior. Therefore, there was no variation in the geometric properties and the amount of vertical steel

reinforcement of the three wall specimens. The varying parameters were then selected so as to highlight the effect of varying confinement parameters.

Wall W-1

Wall W-1 was treated as a reference specimen in the current testing program, as it closely resembled the most commonly practiced reinforcement detailing allowed by the current standards. It was provided with eight 15M vertical bars in each boundary element and six 10 M vertical bars in the web. Transverse reinforcement in the boundary regions was provided in the form of 10M closed rings. 10M conventional cross ties were also provided in the boundary regions to prevent the buckling of vertical bars after spalling of the concrete cover. The crossties had a standard 90 degree hook at one end and a 135° hook at the other end, representing the most commonly used reinforcement type in columns & boundary elements of shear wall. A total of four crossties were provided at any particular level of wall, two in each boundary element. The transverse reinforcement including crossties was spaced vertically at 100 mm on center. It is important to mention here that according to Clause 21.4.4.2, Chapter 21 of ACI 318-2002, the minimum spacing of the transverse reinforcement was specified to be the minimum of (a) one-quarter the minimum cross-section dimension, (b) six times the diameter of longitudinal reinforcement and (c) s_x, which is according to Equation 21-5 ACI 318-2002 (s_x shall not be more then 152 mm and shall not be less than 100 mm). Therefore, it was decided to place the transverse reinforcement at 100 mm on center. The shear capacity of wall was achieved by using 10 M straight horizontal bars spaced vertically at 100 mm on center. These bars were extended to the end of boundary elements so as to develop proper anchorage. Figure 3.2 shows the complete reinforcement detail of wall W-1. Figure 3.3 shows a close-up of the reinforcement in the end zone. All specimens were cast on their sides and then lifted to the vertical position. Figure 3.4 shows a general view of the casting position of wall specimens.

Wall W-2

Wall specimens W-2 and W-3 were designed mainly by replacing the conventional crossties in the boundary region of W-1 with two types of double head studs, one for each wall specimen. Figures 3.5 and 3.6 show the shape and geometric properties of two types of the studs. The studs in W-2 and W-3 were provided only up to half wall height, 1.8 m from the base, since that region was considered to be the test region or the study region. The remaining upper portions of wall specimens W-2 and W-3 were provided with the conventional cross ties in the boundary regions similar to wall W-1 For the comparative study of the confinement behavior in the three wall specimens, the volumetric ratio of the confinement reinforcement to the volume of concrete was selected to be a constant parameter. Since the cross-sectional area of the studs was not identical to those of conventional crossties, the vertical spacing of the transverse reinforcement including studs was adjusted in specimens W-2 and W-3 in order to maintain a constant volumetric ratio of confinement reinforcement

Wall specimen W-2 was provided with 9.5mm Ø in place of 10 M conventional cross ties in the boundary regions. Two double head studs were provided in each boundary element at any level of the lower test region of wall W-2, similar to the crossties in wall W-1. In order to achieve a volumetric ratio of the transverse reinforcement identical to that in W-1, the vertical spacing of studs together with closed stirrups was calculated and provided at 90 mm as compared to the spacing of 100 mm for the cross ties in wall W-1. Figure 3.7 shows the reinforcement details of wall W-2, and Figure 3.8 shows installed double head studs.

Wall W-3

Wall specimen W-3 was provided with 12.7 mm (1/2 inch) ø double head studs. However, since the provision of two 12.7 mm Ø studs in each boundary element would have resulted in a vertical spacing greater than 100 mm, which was specified to be

maximum according to Sec. 21.4.4.2, A.C.I 318-2002, only one 12.7 mm Ø stud was provided in each boundary element at a particular level. The resulting vertical spacing of transverse reinforcement, including 12.7 mm Ø double head studs, was 88 mm that made the volumetric ratio of transverse reinforcement of W-3 equal to the W-1 and W-2. Complete reinforcement details of W-3, are shown in Figures 3.9 through 3.11. The main purpose of selecting two different types of studs in W-2 and W-3 was to compare the effect of varying cross-sectional and head area as well as the distribution of double head studs, on the compression carrying capacity of the boundary elements. The heads of studs were supposed to provide a means of confinement to the concrete of the boundary elements.

3.4 Materials

3.4.1 Concrete

Normal density concrete was used in the three wall specimens. It was obtained from a local ready mix supplier. The mix design provided by the supplier showed the following ratios and contents.

Slump	100 mm
Unit weight	2333 kg / m^3
Max. aggregate size	20 mm
Cement type	10
Cement content	207 kg / m^3
Sand content	48.3% mass
Fly ash	23 kg / m^3
W/c ratio	0.66
Admixture (water reducer) (Master Builder's Pozz 322)	621 ml / m^3

Five concrete cylinders (150 mm x 300 mm) were cast for each wall specimen to determine the compressive strength of concrete. Cylinder tests were carried out at two different stages for each wall, one at an early stage and another at the time of testing of the respective wall specimen. The results of early stage testing showed sufficient strength gain that allowed lifting up the wall specimens as they were cast in a horizontal position (Refer to Sec. 3.8, " Procedures" for casting details). The cylinder test results are shown in Table 3.1.

3.4.2 Reinforcement

Reinforcing bars

Since the reinforcement for the three walls was ordered in a single lot and came from the same heat, the coupon tests were needed only for each size of reinforcing bars and not for every wall specimen. There were mainly two sizes of rebar used in the three wall specimens; 10 M and 15 M. Three coupon-tests were performed for each size. The coupon test results are shown in Table 3.2. Stress-strain curves are also plotted and shown in Figure 3.12.

Double Head Studs

Double head studs were manufactured and supplied by "Decon Canada", designer and producer of Stud rails. The Stud rail is a series of single head studs welded on a single metal strip at some desired spacing in single or multi rows. Stud rails have been used globally in reinforced concrete design to increase the shear capacity of flat slabs and shallow foundations. The double head studs were manufactured by welding a second head to the other end of single head shear studs. Two different types of studs were used in the current testing program; 9.5 mm Ø in wall W-2 and 12.7 mm ø in W-3. Table 3.2 shows the geometric and material properties provided by the supplier. Three coupon tests were performed for each size of stud. These tests were performed in MTS-1000 kN machine after removing the two heads of studs. The results of coupon tests are shown in

Table 3.2. Stress-strain curves are also plotted and shown in Fig. 3.13. The plots show that the stud shaft is cold drawn with no evident yield plateau.

3.5 Fabrication procedure

Casting of the wall specimens was carried out in a controlled environment inside the I.F Morrison Structural Engineering Laboratory, University of Alberta. Each specimen was cast in two phases. Phase I involved the casting of concrete wall bases and Phase II involved the casting of the wall itself.

In Phase I, the formwork for wall bases was fabricated by using 20 mm thick plywood stiffened by 2 inches x 6 inches wooden counter-forts to prevent the bulging of plywood (Refer to Figure 3.14). Eight hollow PVC conduits, each 0.6 m long and having internal diameter of 76 mm, were positioned in a typical base cage to leave holes in the concrete base for the 2 inches Ø anchor bolts. These bolts were then used to fix the wall specimen with the strong floor (Refer to Sec. 3.8 "Procedures" for details). The position of these PVC conduits was carefully selected such that they would became aligned with the holes in the strong floor and at the same time these conduits were aligned symmetrically around the wall cage (Refer to Figure 3.15). It is important to mention here that the vertical reinforcement of the wall was not lap spliced at the base level, instead, all the vertical reinforcement of the wall was itself positioned and tied to the base cages at the time of casting of the concrete bases.

Phase II involved the casting of 3.6 m high walls above the concrete bases. Due to limited lab resources for placing and vibrating concrete from a height of 3.6 m, it was planned to cast the walls in a horizontal plane just like a slab. Bottom formwork was prepared by using 20 mm thick plywood, stiffened with 2 inches x 6 inches wooden beams supported on 2 inches x 6 inches wooden props (Refer to Figure 3.4). Wooden wedges and filler plywood were fixed in the web region of the formwork to achieve the desired reduced wall thickness in the web region. A simple and efficient formwork for the top surface was also prepared which would cover only the entire web region of the

wall. It was placed over the concrete surface immediately after the concrete pouring and tapped with a rubber hammer in order to achieve the required concrete shape of the wall in cross-section.

Curing of the walls was done by wrapping polythene around the exposed wall surface immediately after the initial setting of concrete to avoid the loss of moisture by evaporation. The wall surface was kept wet inside the polythene throughout the curing period. After curing for two weeks, one phase of cylinder testing was performed to check the concrete strength and compare it with the stresses expected during lifting of the wall. The wall specimens were then lifted up to a vertical position and again wrapped with polythene all around. Curing of the wall specimens was performed for a period of one month.

3.6 Test set-up

The test set-up used for testing of wall specimens consisted of four prominent features:

1. Base fixing system.
2. Lateral loading assembly and its reaction system.
3. Vertical loading assembly and its reaction system.
4. Out-of-plane bracing system.

3.6.1 Base fixing system

To avoid slippage of the wall specimens under high lateral loads the specimens were rigidly fixed to the laboratory floor (also referred to as Strong floor) by pre-stressing the bases against the strong floor. Eight-65 mm Ø, 2 m long high strength bolts were used for that. These bolts were passed through the holes of the concrete bases and coinciding holes of the strong floor. These bolts were then pre-stressed in two stages to a total force of 700 kN each (approximately 70% of the bolt yield strength). The prestressing was

done in two stages with a three days interval to allow for the settlement of base leveling material (plaster of Paris) under high compression. Figure 3.16 shows the pre-stressing set-up

3.6.2 Lateral load assembly and reaction system

Lateral Load Assembly

The lateral load was applied to the test specimens through two dual acting jacks, each having 500 kN capacity. The jacks were mounted adjacent to each other at the same elevation. These jacks were jointly connected to the reaction frame through a pin-connection assembly, "Clevis". The two jacks were connected to a common oil pumping valve/manifold so that they could be operated simultaneously and under the same fluid pressure. To obtain a single force output from the two jacks that could be applied to the test specimen, a W-section beam was connected to the tips of two jacks through a "Yoke" assembly (which is a Y-shaped solid steel part used to connect two components coming from one side to a single component on the other side (Figure 3.17). The jacks were connected to the Yoke by a pin mechanism to permit free rotation in a vertical plane. This pin was connected to a short, horizontally mounted W-sec, acting as a "Lateral Load Arm", which had a welded end plate 400 x 400 x 30 mm thick at its other end that was bearing directly on the wall face. Since the load arm was expected to rotate with the wall face due to bending and deflection of the wall, the internal pin at the Yoke was required in order to relieve the jacks from any bending stresses. A load cell was also sandwiched between the Yoke and loading arm to measure the single force output that was applied perpendicular to the wall face. Figure 3.17 shows a photograph of the lateral loading assembly while figures 3.18 and 3.19 show schematic diagrams of lateral loading and pulling assemblies.

The mechanism described above was designed to work in pushing the wall, but it couldn't work in pulling the wall, therefore, a pulling assembly was additionally attached with the lateral pushing assembly. The pulling assembly consisted of two channels 200 mm deep, running along the 1200 mm long faces of wall. These channels were bolted to

the projected portion of bearing plate of the lateral load arm at one end, while their opposite ends were bolted to another bearing plate provided at the opposite face of the wall. To prevent this assembly from slipping down, a hat shaped steel component was mounted on top of the wall with its two wings connected to top flanges of the channels of the pulling assembly. Figure 3.20 shows a view of the components and arrangement of the lateral pulling assembly.

Lateral Load-Reaction System

Since there was no existing strong wall available in the I.F. Morrison Structural Engineering laboratory at the time of testing, a lateral load-reaction frame was designed and fabricated. The reaction frame was a two-storied steel frame. It was approximately 4 meter high and was square in plan-view with a side dimension of 2.43 meters (8 feet). It consisted of steel W-Section columns forming the corners of the square. In between these columns, diagonal braces were introduced both in vertical and horizontal planes to control the lateral movement of the frame. Bracing in the horizontal plane was provided only at the level of the lateral load to transfer the lateral forces by truss action to the columns and thus minimize the local deflection of the beam at which the jacks were mounted. Cross braces in the vertical planes were also provided at two levels in the two side bays of the reaction frame. These bays were parallel to the direction of lateral loads. The main purpose of the provision of these braces in the vertical plane was to control and minimize the lateral drift of the reaction frame that in turn helped in saving the stroke of lateral jacks. The reaction frame was designed for a lateral load of 1000 kN applied at 3.8 meters above the floor level. Detailed schematic diagrams and photographs of the reaction frame are shown in Figures 3.21, 3.22 and 3.23. The floor of the laboratory was thoroughly checked for existing capacity to carry the frame reactions.

3.6.3 Vertical loading assembly

Vertical loads, that simulate the gravity load on a structure, were applied to the test specimens through four vertically mounted single-acting jacks, each jack had 350 kN

capacity. The jacks were mounted in a vertical load reaction frame often referred to as "Gravity Load Simulator". Two jacks were placed on each side of the wall (i-e West and East sides). These two jacks on each side of the wall were connected to a common manifold so that they could be operated simultaneously. These jacks were connected to a top vertical load distribution beam through 125 mm wide and 25 mm thick tension ties. The vertical load distribution beam was a cruciform shaped beam fabricated by connecting two 600mm W-Sections perpendicular to each other at their mid length. Figure 3.24 shows a view of the distribution beam. The beam rested on top of the wall at points over the two boundary elements, (Refer to Figures 3.25 and 3.26 for vertical load points), such that its two wings projected freely on each side of the wall (i-e East and West sides). Two tension ties were connected to the bottom of each wing of the distribution beam through a pin assembly as shown in Figure 3.27.

Vertical load distribution beam was braced laterally by the so-called "Watt brace" at the top, to avoid out of wall-plane movement. The Watt brace is a special type of articulating bracing that allows free movement and rotation of the top distribution beam in the direction of lateral loads along with the wall tip (i-e North-South movement), but restricts its out of wall-plane movement (i-e the East - West movement). Figure 3.24 shows a view of the Watt brace.

As mentioned above, the bottoms of the tension ties were connected to the top of the four 350 kN jacks. These jacks were in turn connected to a "Gravity Load Simulator" reaction system that was tied to the strong floor. As the name implies, the "Gravity Load Simulator", maintains the verticality of the gravity simulation throughout the lateral movement of wall. Its function is to make the vertical loading jacks move as a rigid body with the wall tip under the application of lateral loads. The rigid body motion of the jacks was provided by the sway of the articulating gravity load simulators. Since the jacks were connected to the top distribution beam through tension ties, they were compelled to move with the wall tip by the tension ties. The jacks moved as a rigid body along with the wall tip because they were connected to the gravity load simulators at their bottom end and the simulators can translate north and south easily.

A gravity load simulator is a simple linkage assembly composed of two articulating inclined members, a bottom distribution beam and a jack holding triangular truss. The jack holding triangular portion of the simulator was hung in between the two articulating diagonal members just like a swing (See Figure 3.28). All the main joints of the simulator were pin joints so that bending moments were not restrained and all joints can rotate freely including the two bottom joints where the inclined members connected to the bottom distribution beam. As a result, the simulator can translate easily in plane, along with the tip of wall when it moves laterally. The only stationary member of the simulator was its bottom distribution beam, which was fixed to the strong floor through two supports at its two ends. The vertical load carrying capacity of the "Gravity Load Simulator" was 400 kN and its maximum one-way translation about the mean position was 915 mm. The two 610 mm long supports of simulators were also small built-up assemblies that consisted of 150 mm deep channels 610 mm long, rigidly connected to the strong floor through two 2 inches Ø Dewidag high strength rods. The simulators were connected to the supports by bolting their bottom chords with the top flanges of the support channels.

3.6.4 Lateral bracing system

In order to avoid any out of plane movement of the wall during the test, an efficient bracing system was provided at about 250 mm below the lateral load application level. It was a rectangular steel frame, 1200 mm long 400 mm wide. It was fabricated by welding 6 mm thick steel plate in between 50 mm deep small channels, 400 mm apart, to form a rectangular assembly. A steel cylinder 50 mm Ø, 300 mm long was attached to one end of the bracing that acted as a roller. Four braces were used in the test, two were provided on each side of the wall (See Figure 3.29). These braces were attached to the frame beams at the far ends with the rollers touching the wall surface. To minimize the friction between steel rollers and concrete surface, two steel channels 1.8 m long and 200 mm deep were mounted on wall, one on each face, such that their flange tips were touching the wall surface and the rollers of bracing rolled on their webs. The two

channels were connected to each other and also snug against the wall surface using 25 mm Ø threaded rods through their webs in their over hanging portions.

3.7 Instrumentation

Instrumentation in the tests consisted of load cells, LVDTs, Rotation meters (RVDTs) and Strain gauges. A complete description follows.

3.7.1 Load and reaction measurements

Vertical and horizontal loads were measured and monitored with load cells provided at the points of application of loads and they were also cross-checked by the load cells readings at reaction points or by fluid pressure-gauges. There was no reaction monitoring point or cross-checking reference available for the applied lateral loads because the specimens were fixed to the strong floor by pre-stressing. Slippage of the wall base was monitored throughout the load history. The lateral load-measuring load cell was provided in between the jacks and the load arm (See Figure 3.17). The capacity of lateral load-monitoring load cell was 1000 kN. It was obvious that the lateral load arm would have rotated in the wall plane relative to the wall face due to bending and deflection of the wall, so that the load monitored by the load cell at the lateral-loading would be the normal component of the lateral force acting on the face of wall.

The vertical load was monitored with 500 kN load cells provided within the four tension ties of the vertical load application assembly. The tension ties were directly connected to the loading jacks. The applied load was cross verified by checking the vertical equilibrium between the load points and the reaction points. Two load cells, each having capacity of 900 kN, were provided at the two reaction points over the two boundary elements. These two points were in fact the two supports of vertical load distribution beam. Figure 3.26 shows a view of the vertical load cells and Figure 3.30 shows a schematic view of the load cell positions.

3.7.2 Strain gauges

Strain gauges were mounted on both vertical and transverse reinforcements of the wall specimens. A total of 36 strain gauges were mounted in each specimen of which 12 were attached to the vertical reinforcement close to the base to monitor their flexural yielding, while the remaining 24 strain gauges were mounted on the transverse reinforcement to study the confinement behavior. Strain gauges on the transverse reinforcement were mounted at mid-height of cross ties and the double head studs. Figure 3.31 shows a view of the strain gauges on the studs while Figures 3.31 through 3.33 shows a complete layout of the strain gauges in the three wall specimens W-1, W-2 and W-3.

3.7.3 Deflection measurements

Vertical and horizontal displacements were measured throughout the test by using eight Linear Variable Deformation Transformers (LVDTs). Figure 3.30 shows a schematic of the LVDT distribution. The laboratory floor, also referred to as "strong floor", was used as the reference for the measurement of vertical displacements. The horizontal displacements (both in-plane and out-of-plane) were measured with reference to two unloaded steel columns attached to the strong floor. The displacements measured included top of wall (tip) displacement, lateral out-of-plane displacement, base slippage and vertical deformation of the wall top due to rotation. Additionally, during the first test, the top deflection and base slippage of the reaction frame were also monitored to verify its stiffness.

In-plane tip displacement of the wall was measured by LVDT LV-1, its range was ± 250 mm. The displacement at mid-height of the wall was measured by LVDT LV-2 having a range of ± 125 mm (Refer to Figure 3.34 for Top and Mid height LVDTs). Lateral out-of-plane displacement was measured by two LVDTs LV-3 and LV-4, with a range of ± 50 mm, connected to the wall top level at the south and north ends. Slippage of

the wall base was also monitored by LVDT LV-5, having a range of ± 12.5 mm, connected at the mid depth of the base at its south end only.

Vertical displacements, including deformation of the wall cross-section, were measured at the top level, both at the north and south ends of wall by LVDTs LV-6 and LV-7 respectively. These LVDTs were placed at the floor level (See figure 3.35 and 3.36 for North and South vertical LVDTs) but their wire extensions were attached to the top vertical load-distribution beam. The range of LV-6 and LV-7 was ± 75 mm.

As mentioned earlier, lateral drift of the reaction frame was measured at its top level in the direction of the lateral loads (North-South). LVDT LV-8 with a range of ± 25 mm was mounted over the East-West beam of the reaction frame at the top level. In addition to all the data-logged instrumentation, two manual dial gauges were placed at the column bases of the reaction frame, to monitor their slippage under lateral loads.

3.7.4 Rotation measurement

Rotation was not measured at any point on the specimen but was monitored at two points on the loading assemblies using Rotation meters (often abbreviated as RVDTs). One RVDT was attached to the lateral loading assembly at the yoke (that also acted as a pin joint between lateral jacks and the load arm) to monitor the combined rotation of lateral loading jacks and wall tip bending under the lateral loads (Refer to Figure 3.37).
A second RVDT was placed over the vertical load distribution beam to monitor its tilting in the East-west plane (Refer to Figure 3.38). Tilting of the top distribution beam was expected as a result of any unequal vertical load application, as the vertical load on wall was applied through the tension ties connecting the vertical-loading jacks and the two wings of top distribution beam.

3.8 Procedures

3.8.1 Set-Up sequence

Initially each test specimen was positioned in the test frame and its alignment with the lateral-loading jacks was accomplished by a floating offset from the loading jacks to both ends of wall using a plumb line. The specimens were then leveled both in-plane and out-of-plane by using shims and steel plates. Steel guide plates were then placed and snugged at three points around the base to define the wall position in the test frame. The wall specimen was then lifted straight up to a height of 1.5 m by the overhead crane and leveling plaster was laid under it. Immediately after laying the plaster, the specimen was dropped to its final position defined by the guide plates and the plaster was allowed to bubble out from the sides of concrete base to ensure a smooth and leveled surface beneath the wall specimen. The specimens were then left undisturbed for 3 days for the leveling plaster to dry out completely.

Eight-50 mm Ø, 2 m long high strength bolts were then passed through the base holes and the coinciding strong floor holes. The bolts were then pre-stressed to a force of 700 kN (70% of their yield strength) in two stages with 24 hours interval (Refer to Figure 3.16 for a pre-stressing set-up). After fixing the specimen to the strong floor, the lateral load application assembly was mounted on the wall specimen and connected to the lateral-loading jacks. Lateral bracings were then placed and snug with the specimen from both sides (i-e from east and west) to control out-of-plane motion of wall. Knife-edge and bearing plates were placed at the two vertical-load points at the top of the wall after applying a layer of plaster there. The vertical load distribution beam was then placed on top of the specimen, resting at the two pre-leveled points over the boundary elements (Refer to figure 3.25 and 3.26 for a view of the top loading points). Tension ties were then placed with one end connected to the vertical load distribution beam while the other end was connected to the vertical-loading jacks. The jacks were already fixed in the "Gravity Load Simulators" on each side of the wall (i-e on east and west sides).

All the strain gauges, load cells, LVDTs and RVDTs were connected to a 60 channels "Fluke" data acquisition system.

3.8.2 Troubleshooting

After connecting load cells, LVDTs and RVDTs to the data logger, initial readings were taken. Troubleshooting was carried out to verify the working of instrumentation by applying small vertical and horizontal loads on the wall specimen. Load cell readings were verified by checking equilibrium at load and reaction points. Functioning of LVDTs and RVDTs was verified by applying known displacements and comparing with the readings shown by the data logger. After verifying the working of all the instrumentation, the wall was brought to its initial position to start the loading procedure.

3.8.3 Loading procedure

The gravity load application was identical in all specimens. To simulate the real loading condition on a shear wall, the vertical load (that resembled gravity loads) was applied and slowly increased to its maximum value, keeping in view the equal load input from both loading sides (i-e from east and west). The vertical load was then maintained at its maximum value throughout the test. The value of vertical load that was applied and maintained throughout the test was approximately 1000 kN with a variation of 5%, this value of vertical load corresponded to a compressive stress of 0.15 f'_c.

Each wall was then loaded laterally in a displacement control mode throughout each test. The loading procedure in each wall will be described in detail in chapter 4.

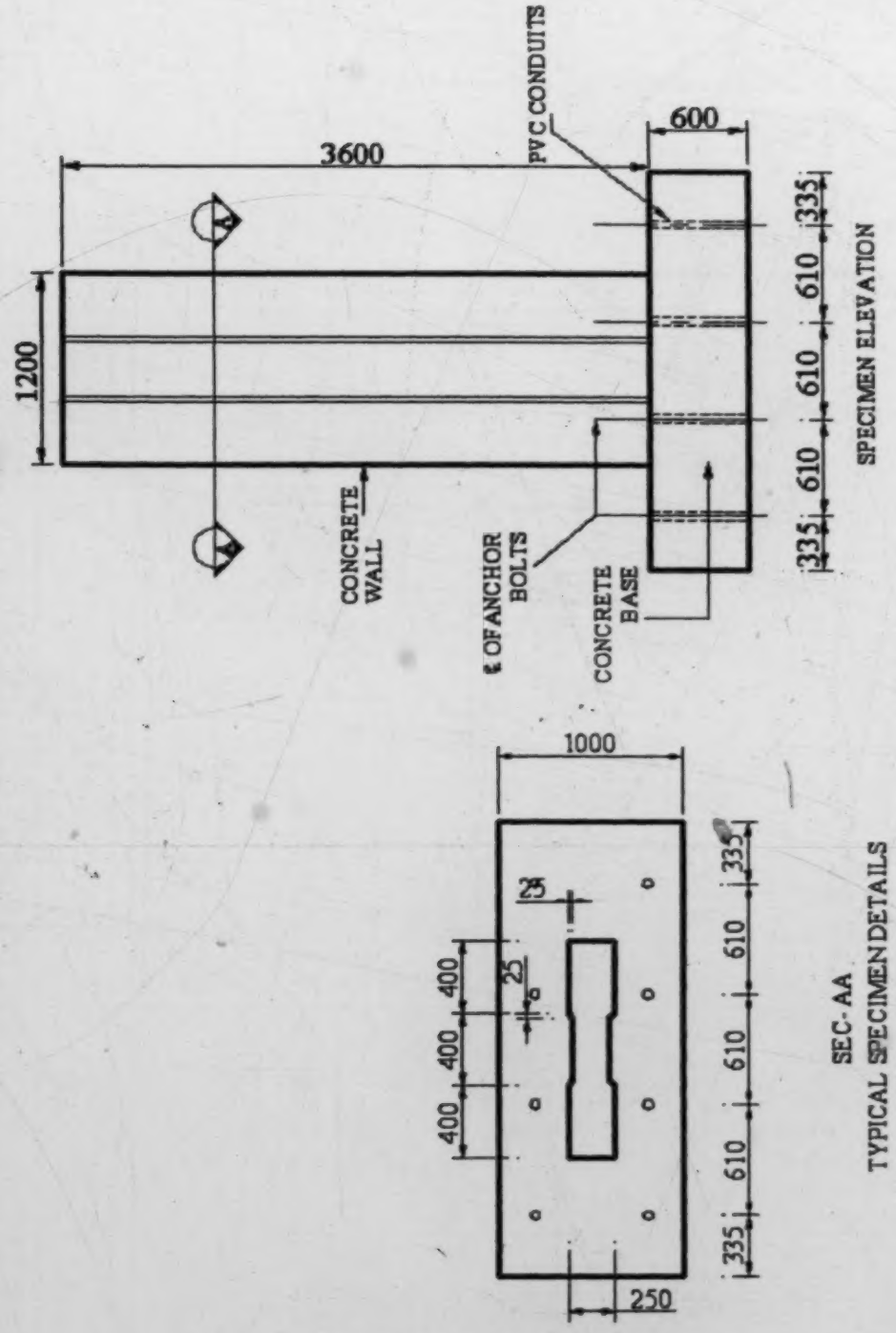

Figure 3.1 Typical specimen detail

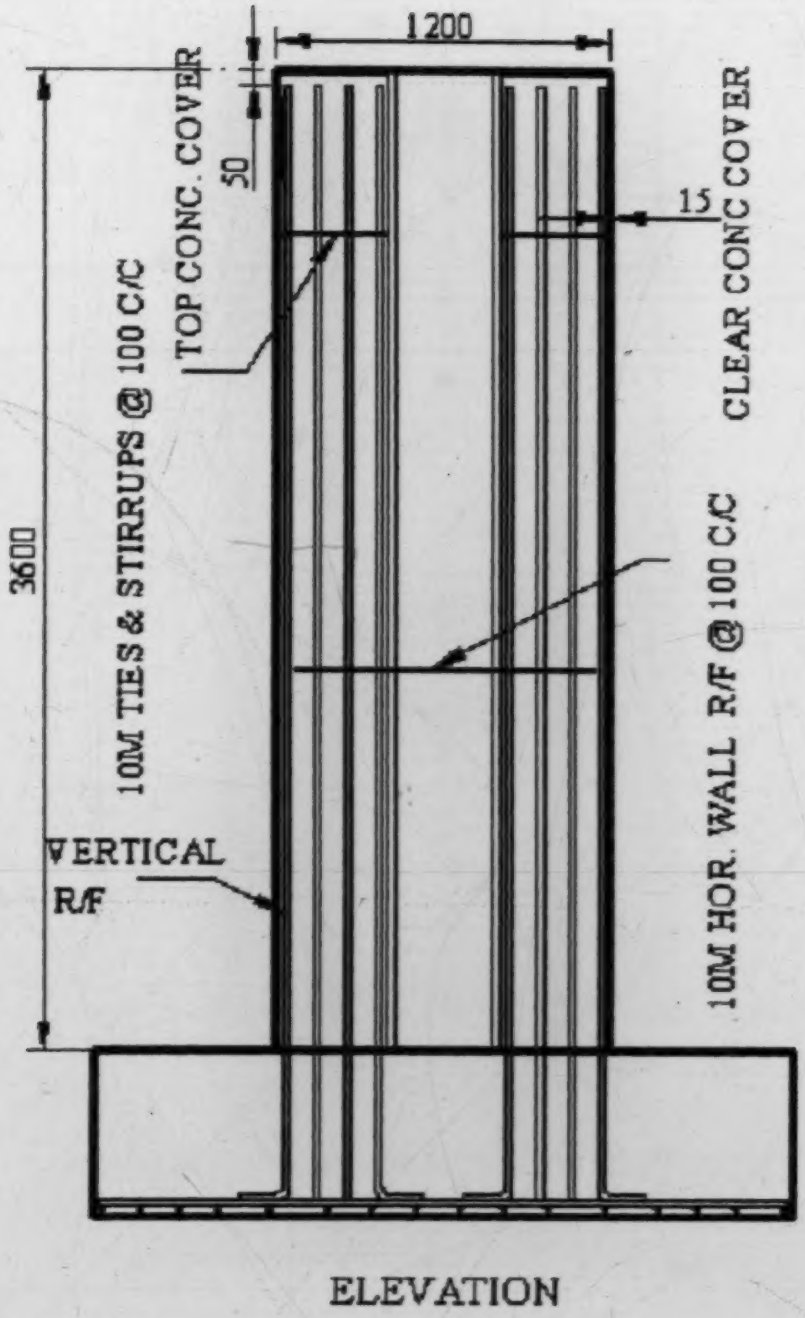

Figure 3.2 (a) W-1 reinforcement details

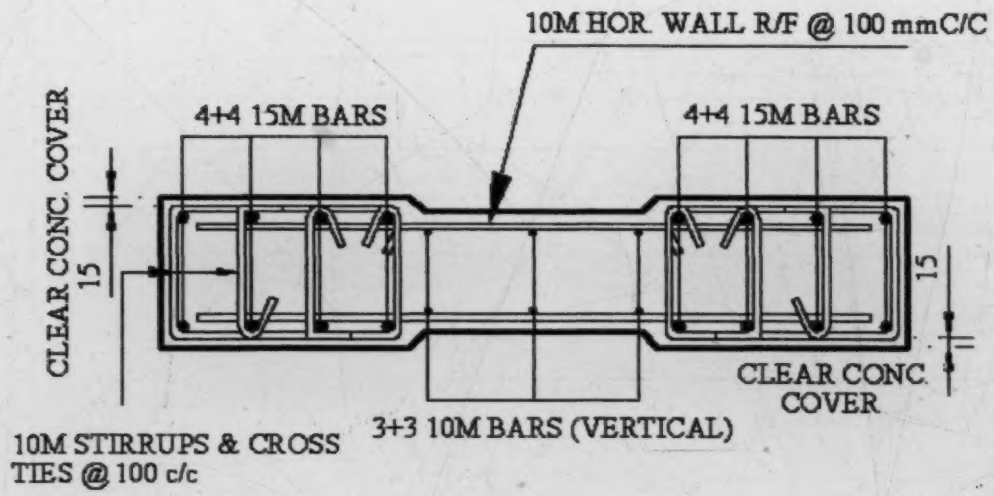

TYP. SEC. OF WALL "W-1"

Figure 3.2 (b) W-1 Reinforcement detail in x-section

Figure 3.3 Plate inserts and end zone in wall W-1

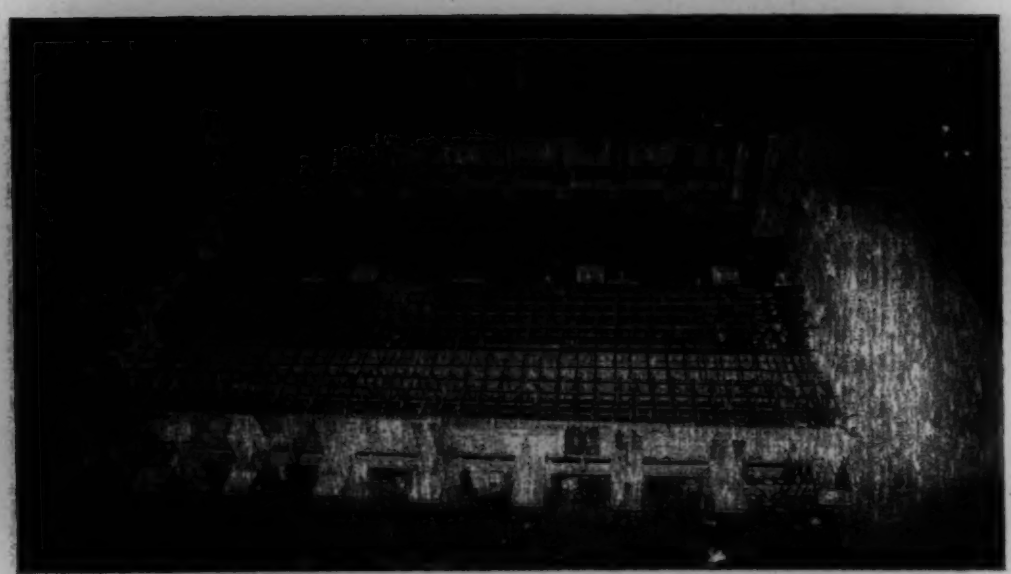

Figure 3.4 Cages of wall W-1 and W-2, ready for concreting

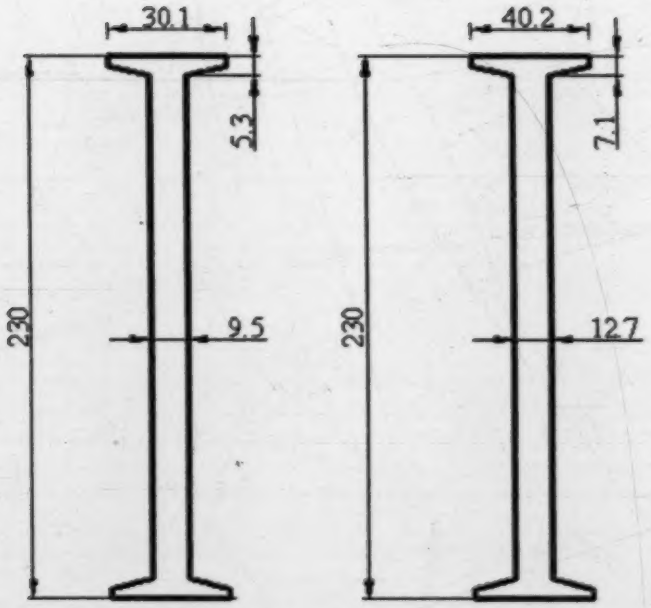

Figure 3.5 Specified dimensions of double head studs

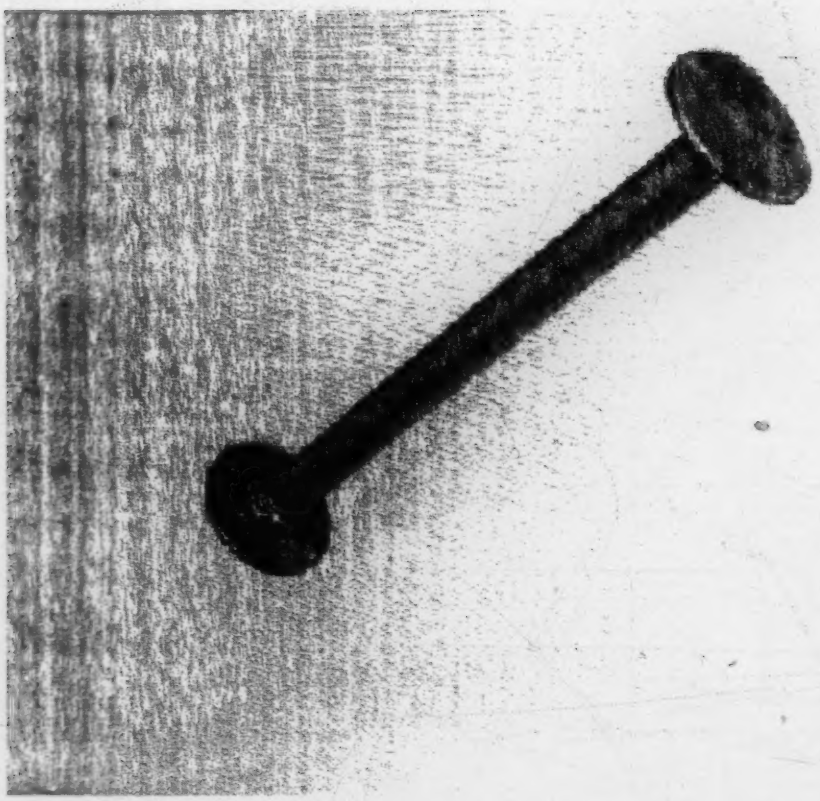

Figure 3.6 Photograph of double head stud

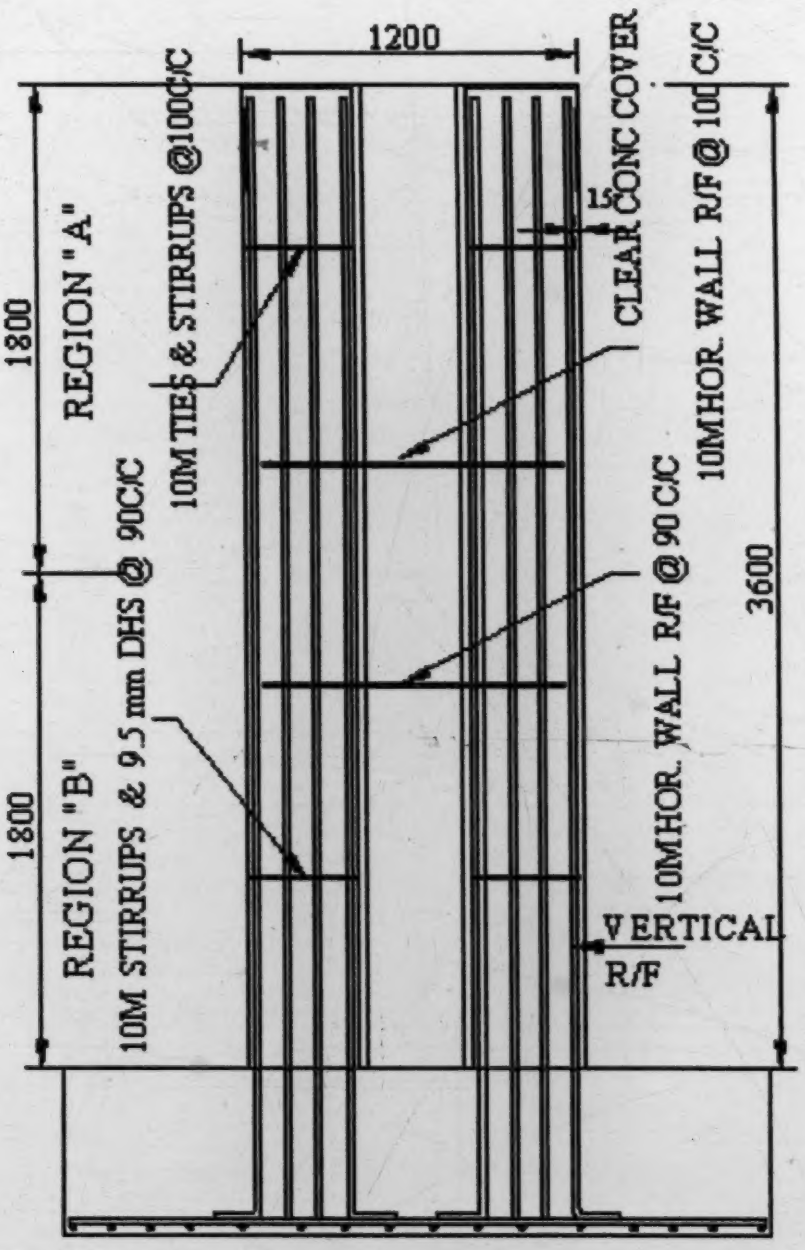

ELEVATION

Figure 3.7 (a) W-2 Reinforcement details

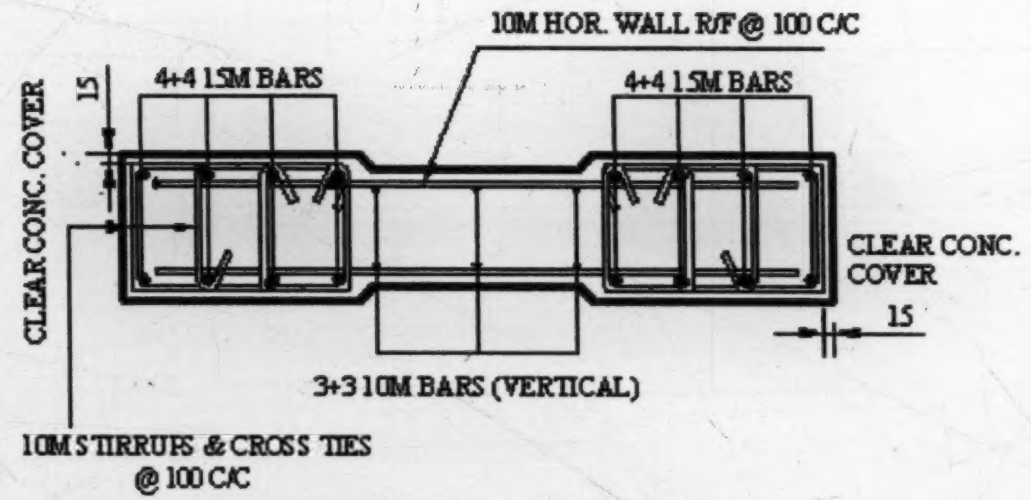

SEC. OF WALL - REGION "A"

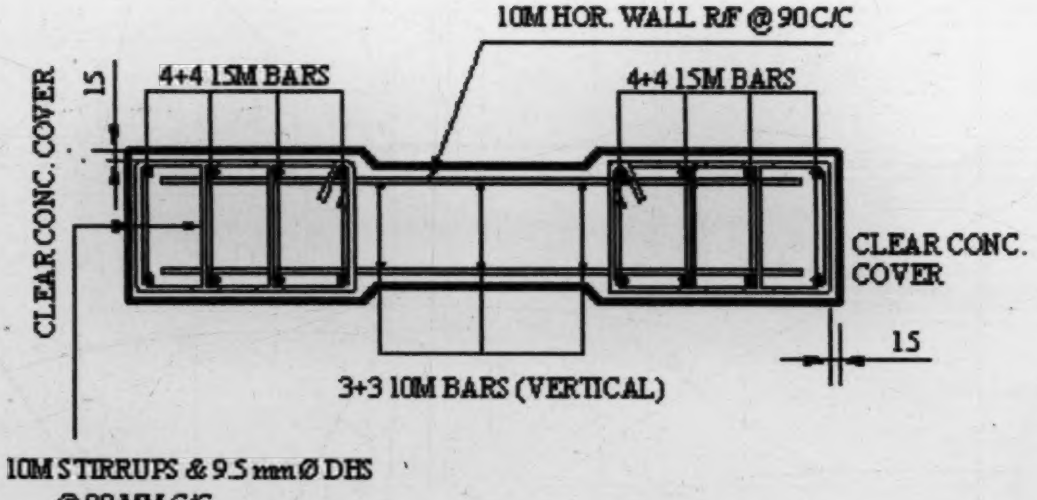

SEC. OF WALL - REGION "B"

Figure 3.7 (b) W-2 Reinforcement detail in x-section

Figure 3.8 Cage of wall W-2, Studs are visible

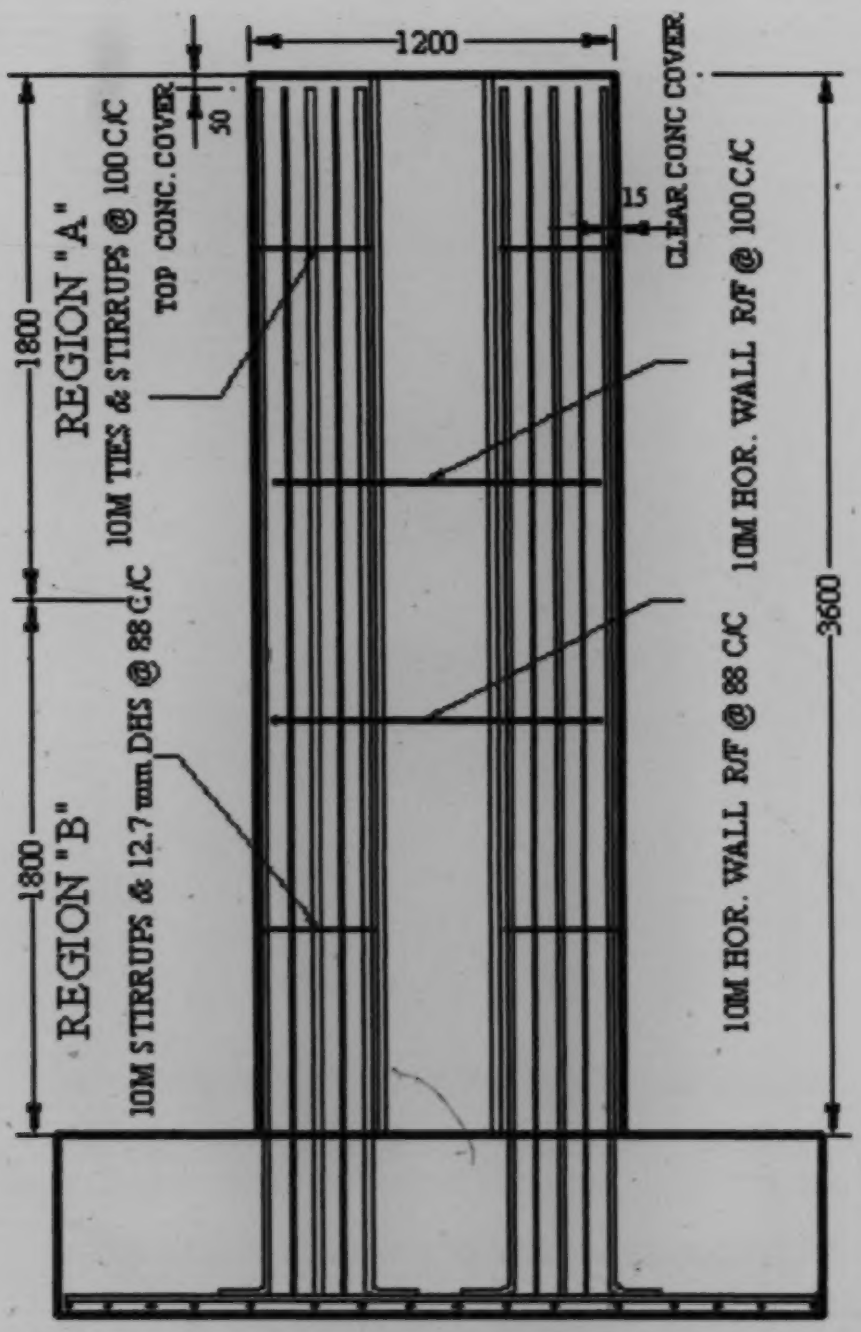

ELEVATION

Figure 3.9 (a) W-3 Reinforcement details

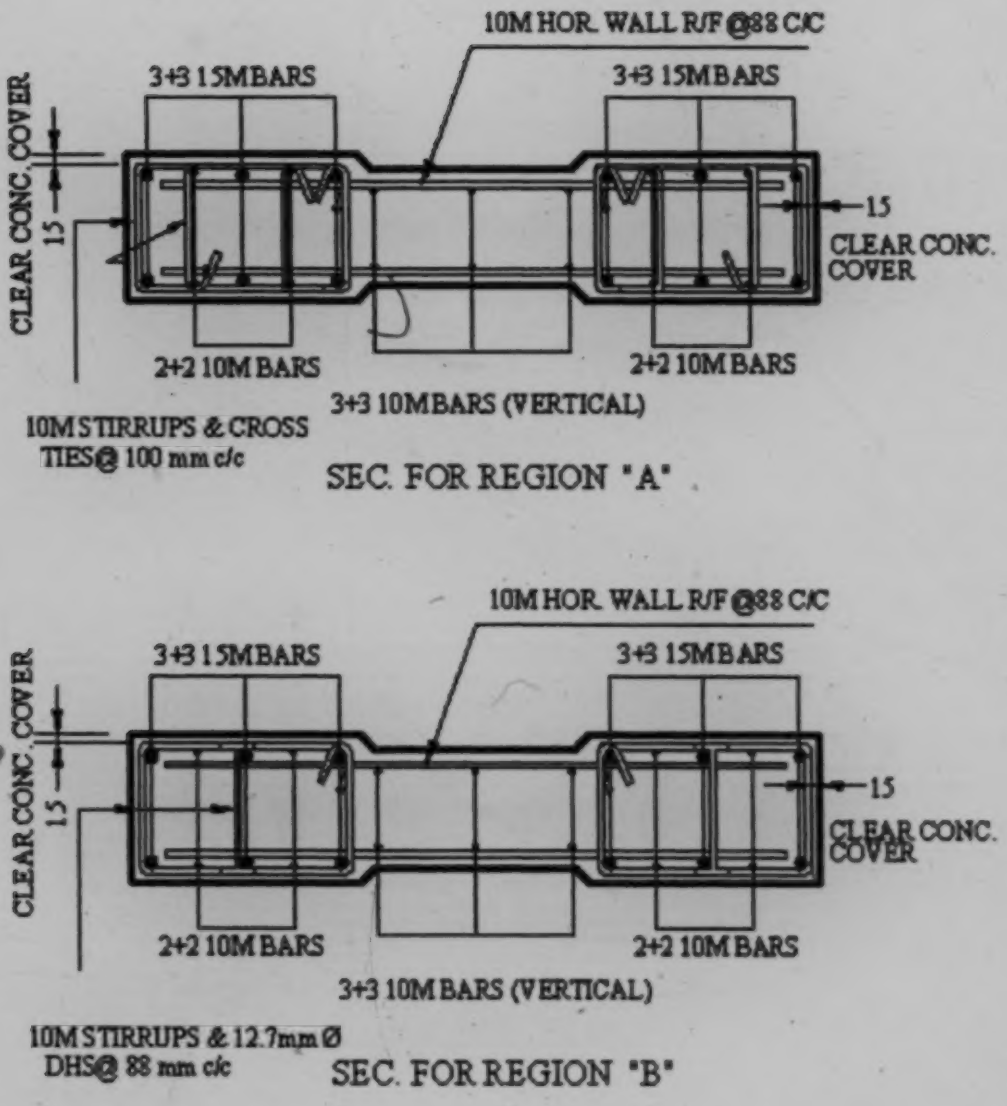

Figure 3.9 (b) W-3 Reinforcement detail in x-section

Figure 3.10 Cage of wall W-3

Figure 3.11 Double Head Studs in wall W-3

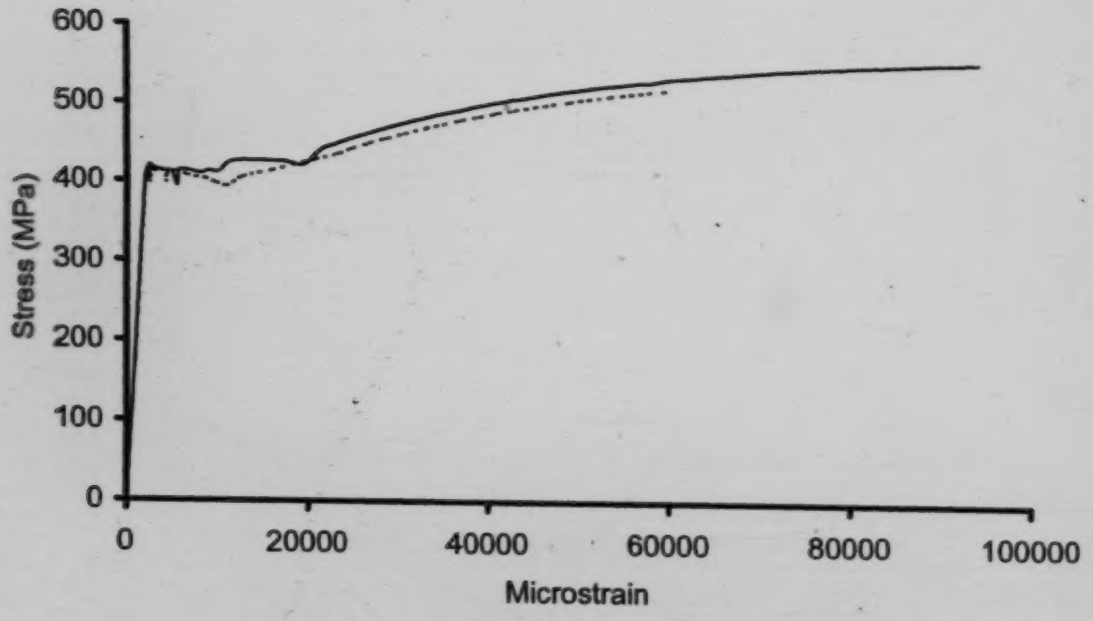

(a) 15M Deformed Rebars with Nominal Area of 200 mm^2

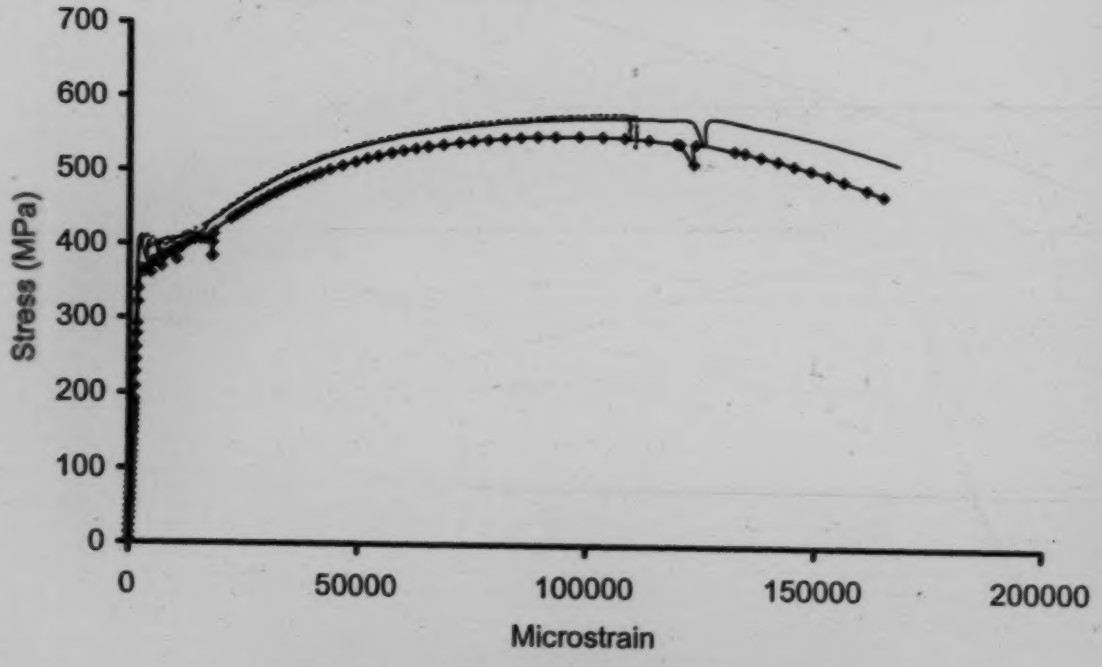

(b) 10M Deformed Rebars with Nominal Area of 100 mm^2

Figure 3.12 Typical Stress-Strain Curves

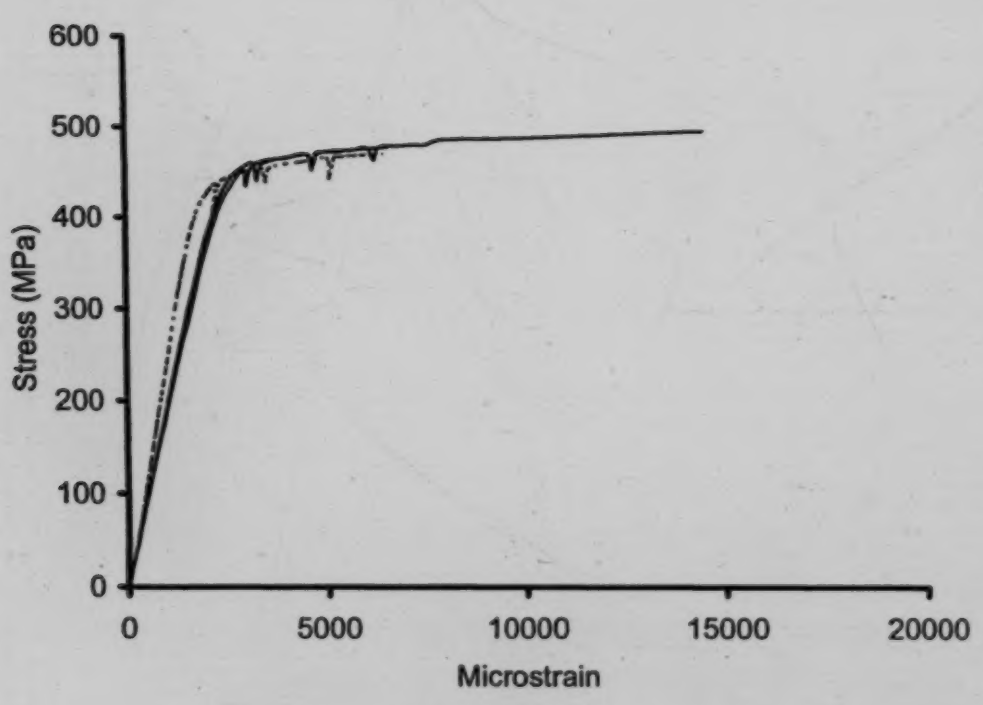

(a) 12mm Dia Double Head Studs with Nominal Area of 127 mm^2

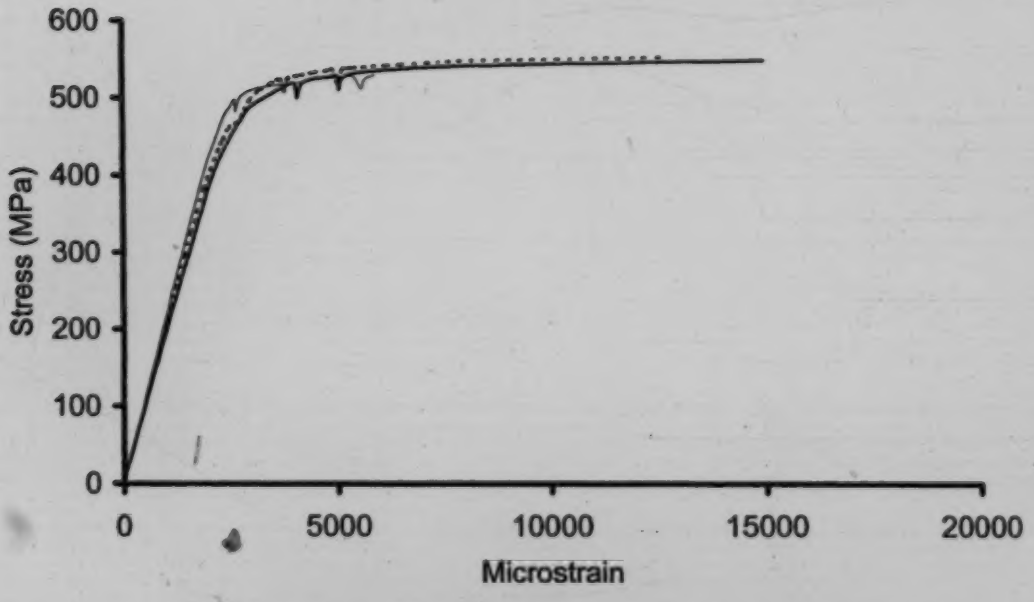

(b) 9mm Dia Double Head Studs with Nominal Area of 71 mm^2

Figure 3.13 Double Head Studs Typical Stress-Strain Curve

Figure 3.14 Typical base form work

Figure 3.15 Base cages and form work of W-1 andW-2

Figure 3.16 Pre-stressing set-up for base fixing system

Figure 3.17 Lateral loading jacks, yoke and load arm

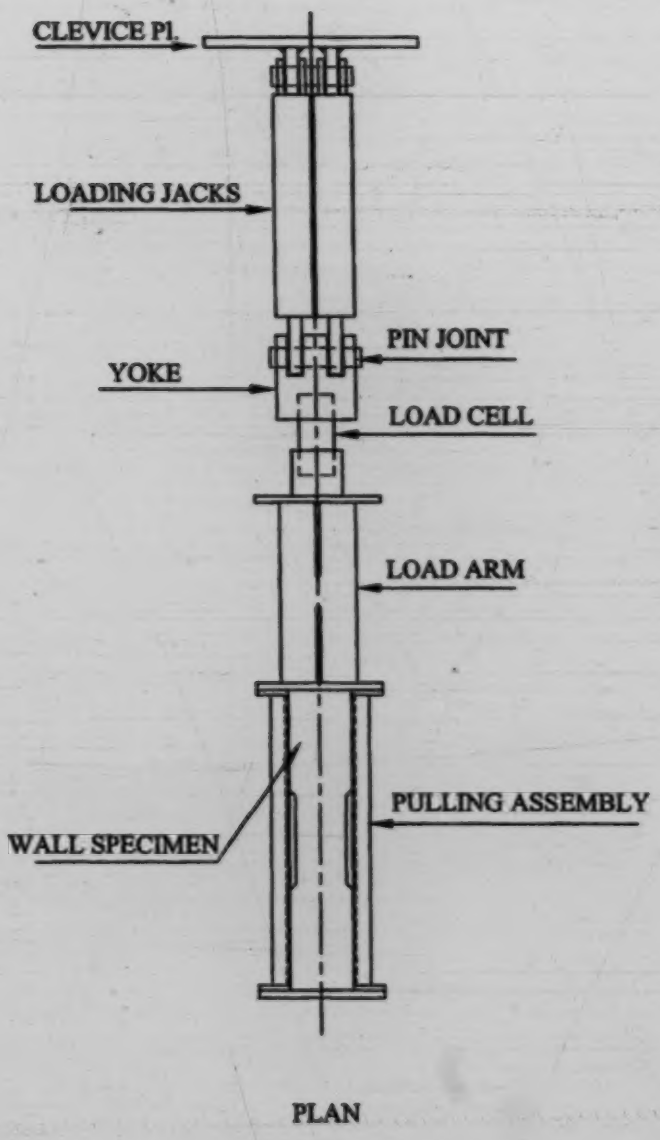

Figure 3.18 Lateral loading assembly

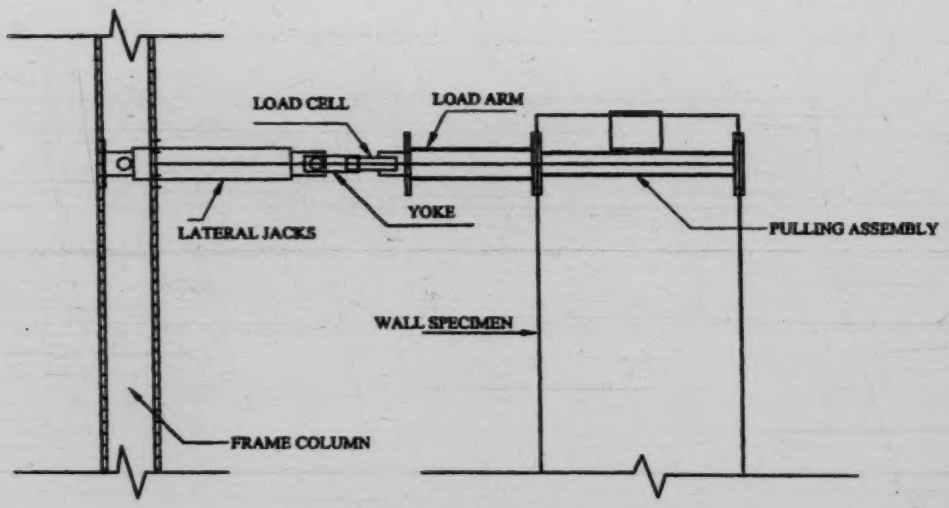

Figure 3.19 Lateral loading assembly

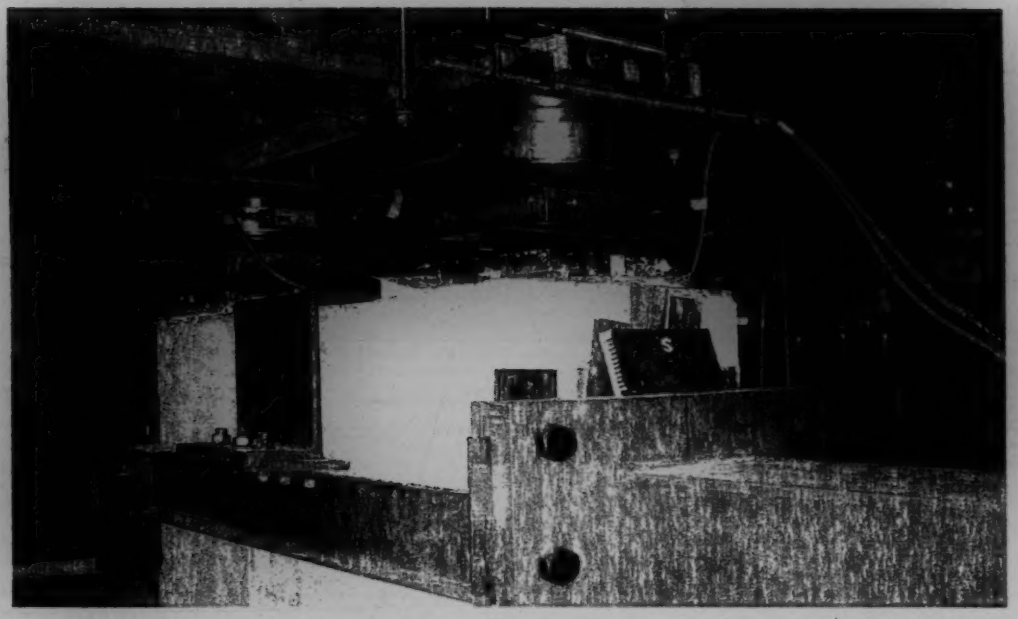

Figure 3.20 Lateral pulling assembly and vertical load cells

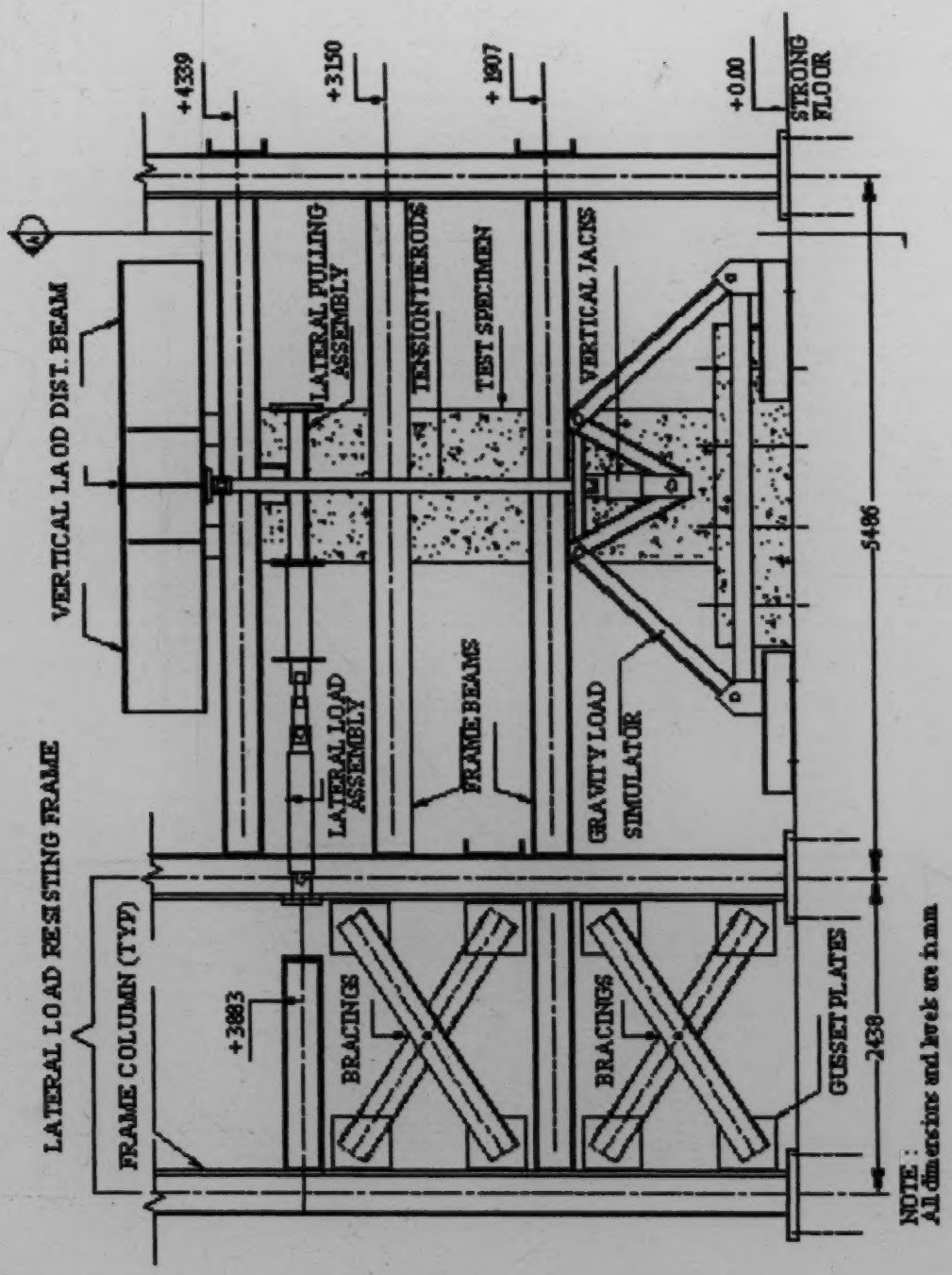

Figure 3.21 Test frame elevation

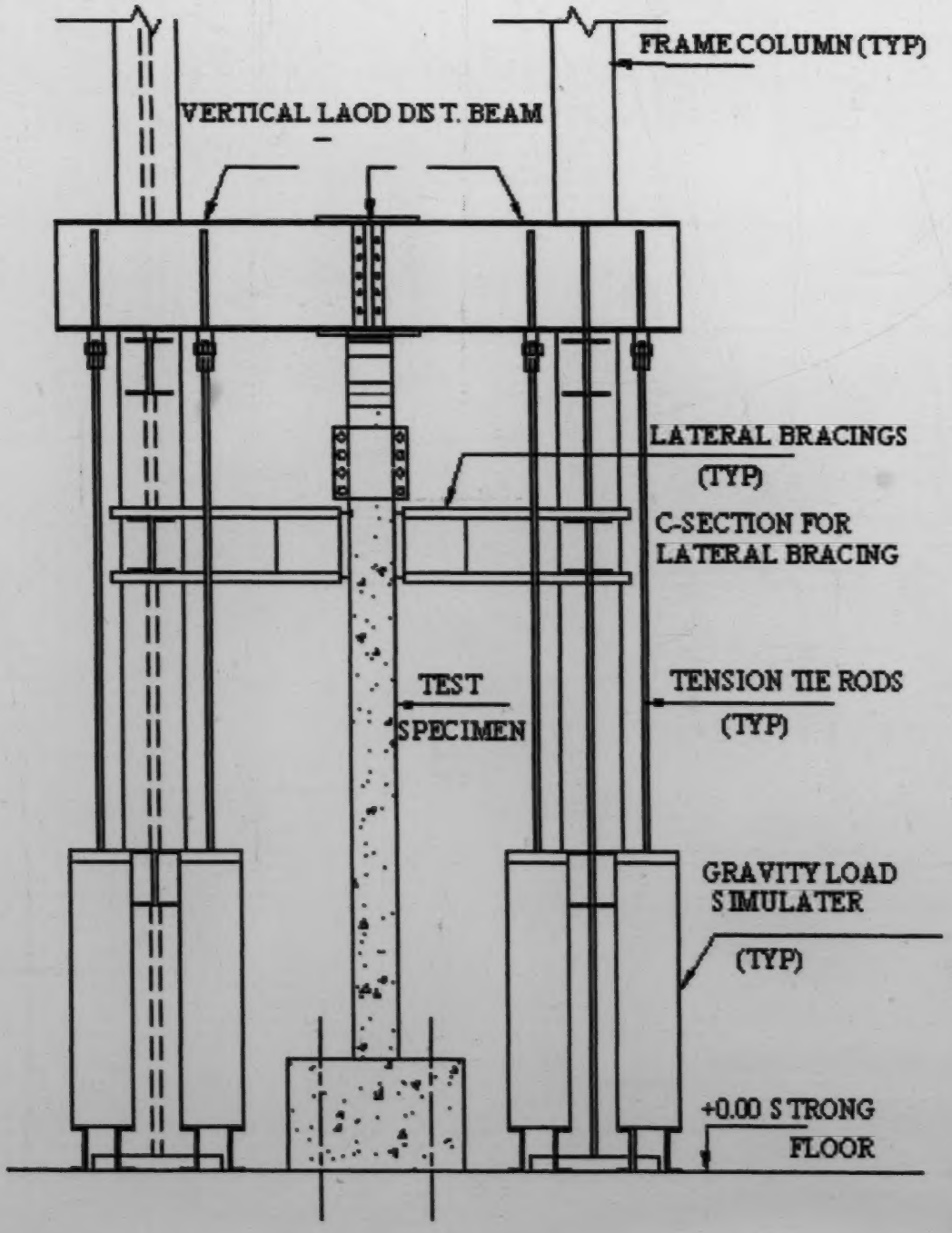

Figure 3.22 Test frame sec A-A

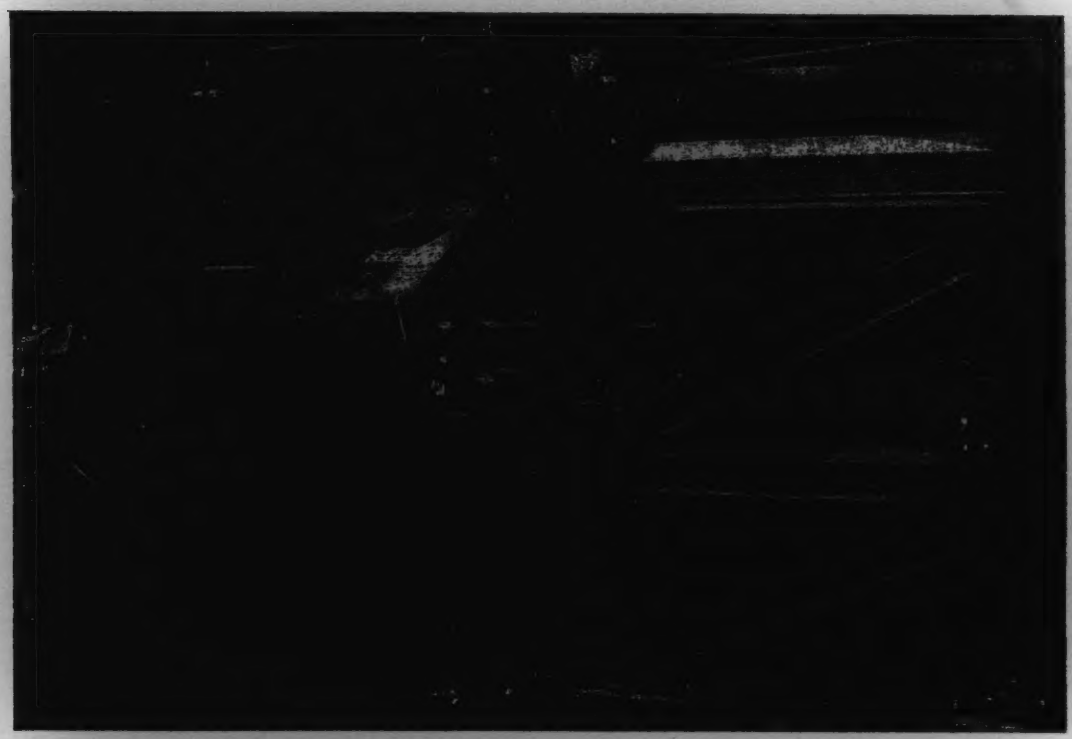

Figure 3.23 Lateral load-reaction frame

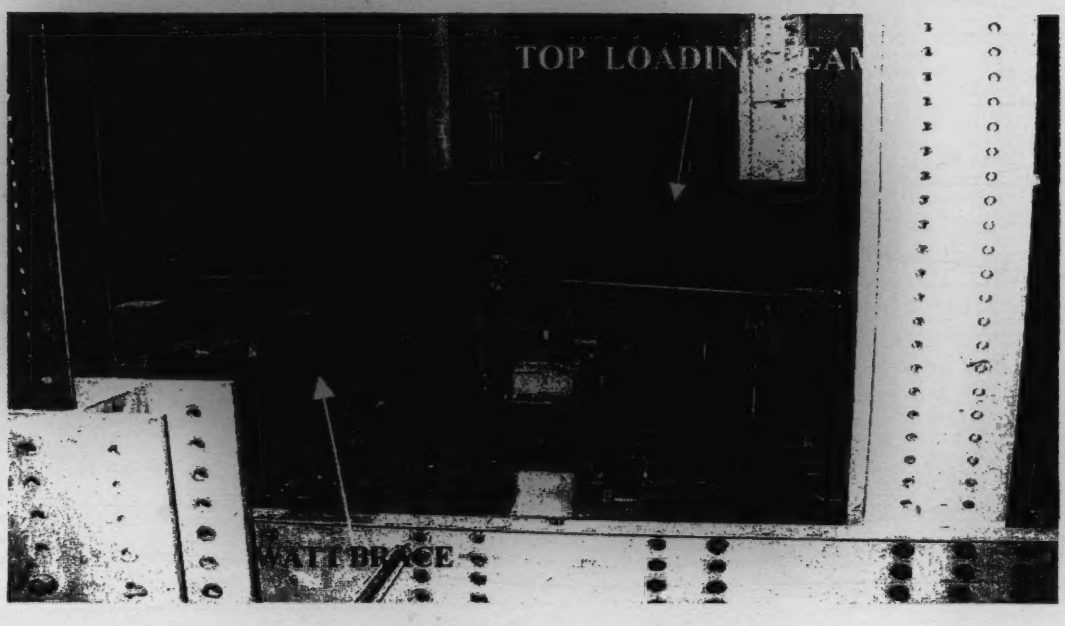

Figure 3.24 Vertical load distribution beam and watt brace

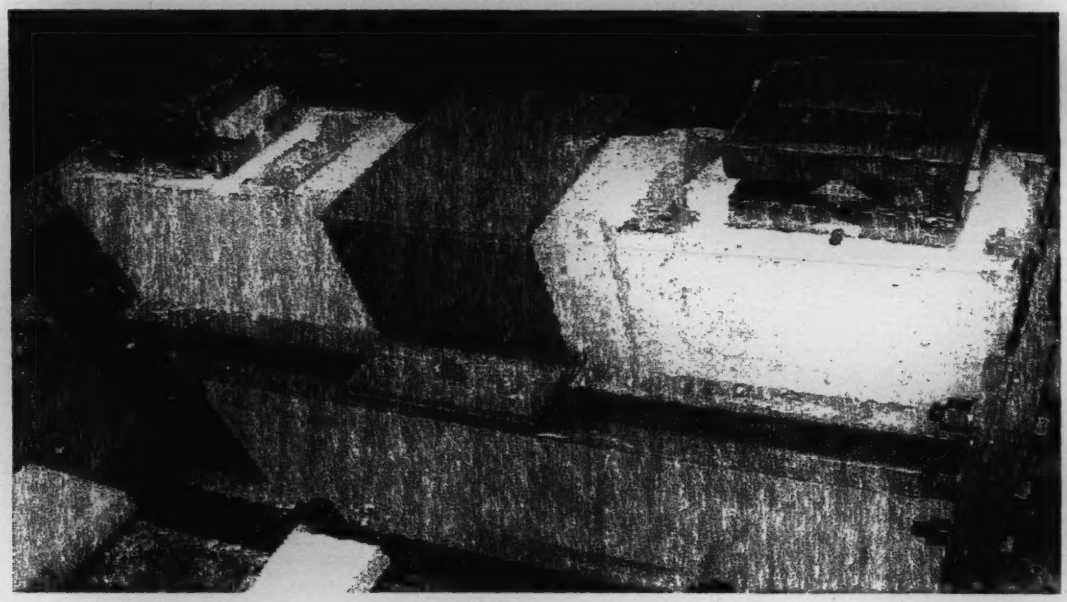

Figure 3.25 Leveling of vertical load points over the boundary elements

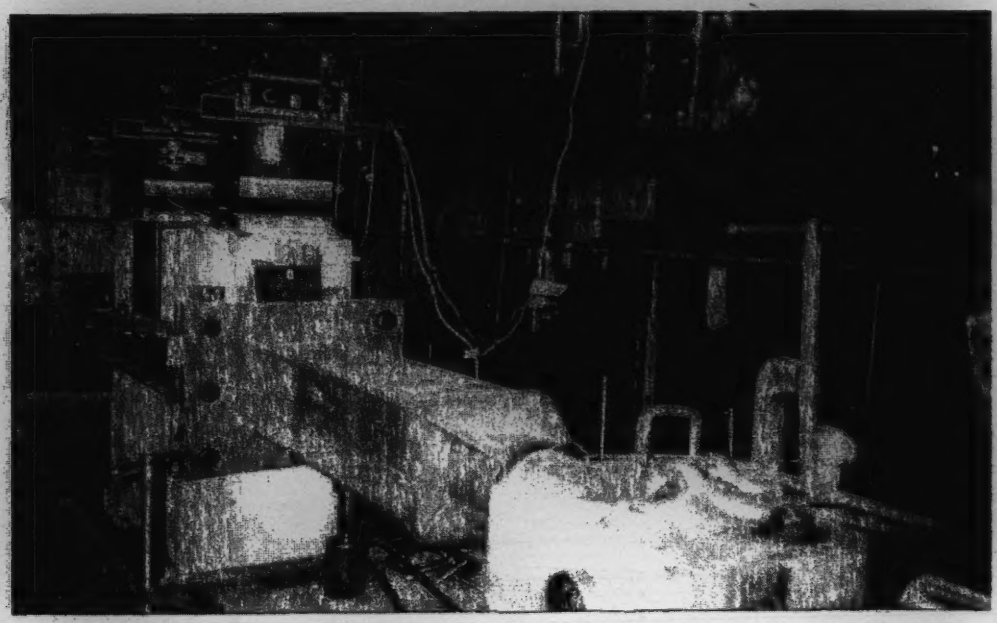

Figure 3.26 Top distribution beam rested over the wall

Figure 3.27 Tension ties connection, leveling rod is also visible

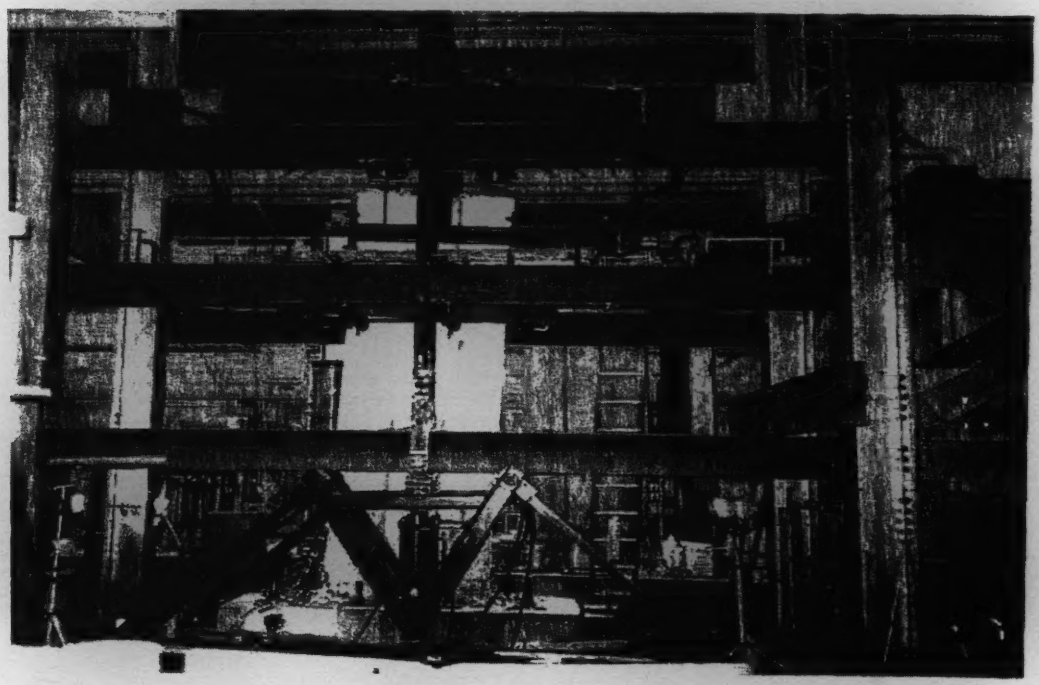

Figure 3.28 Tension ties connected to top distribution beam & vertical jacks, gravity load simulators are also visible

Figure 3.29 Typical lateral braces on each side of wall

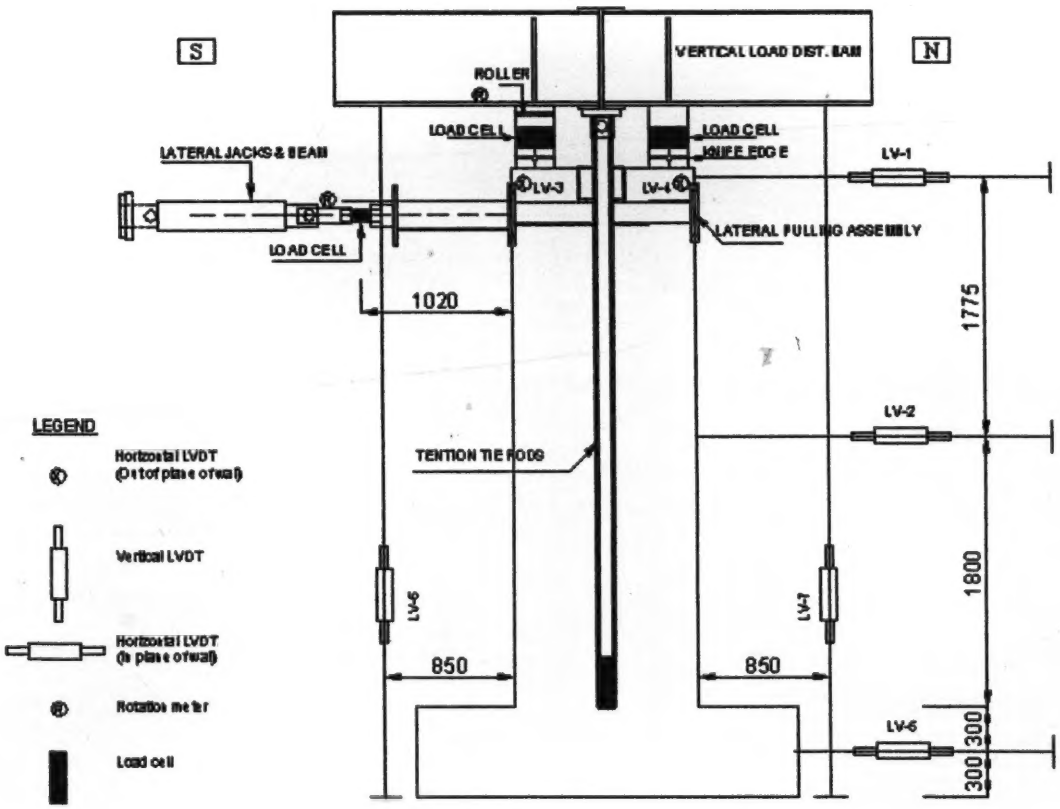

Figure 3.30 LVDTs, RVDTs and Load cells layout Typical for W-1, W-2, W-3

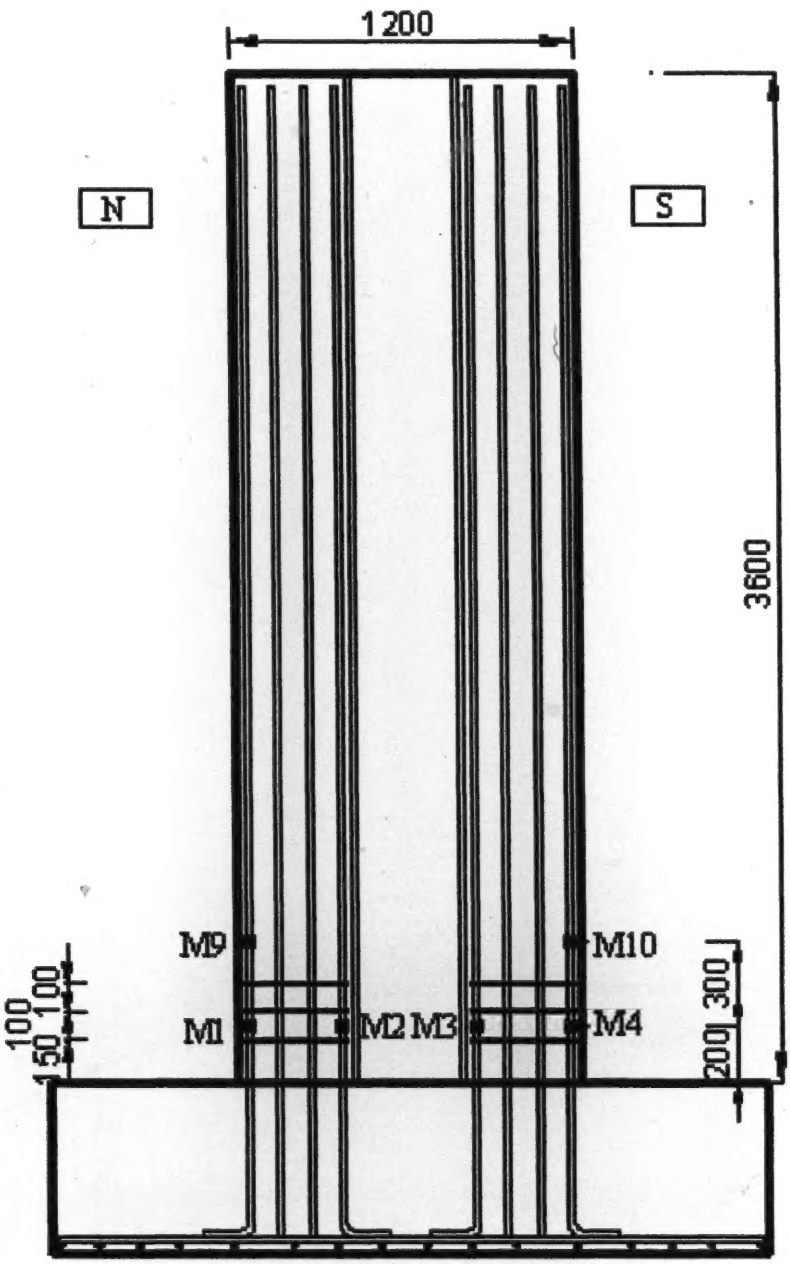

EAST - ELEVATION

Figure 3.31 (a) W-1 Strain gauges layout on main bars

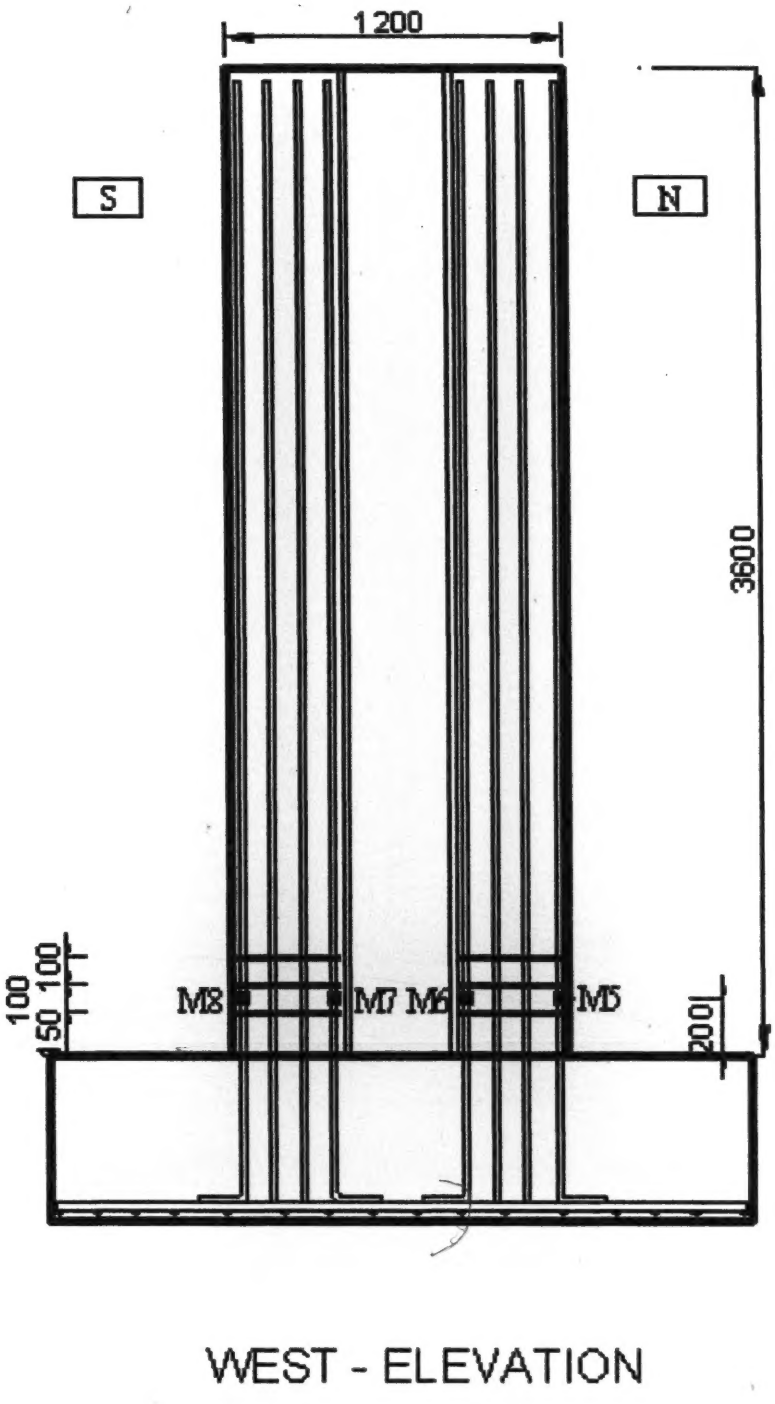

WEST - ELEVATION

Figure 3.31 (b) W-1 Strain gauge layout in west elevation

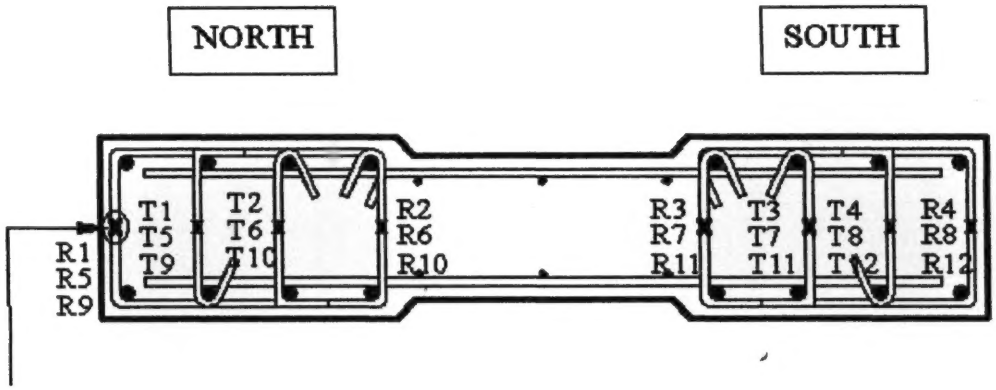

Note :

R1 - R4 & T1 - T4 are at 1st. level from base
R5 - R8 & T5 - T8 are at 2nd. level from base
R9 - R12 & T9 - T12 are at 3rd. level from base

TYP. SEC OF W-1

Figure 3.31 (c) W-1 Strain gauge layout in x-section

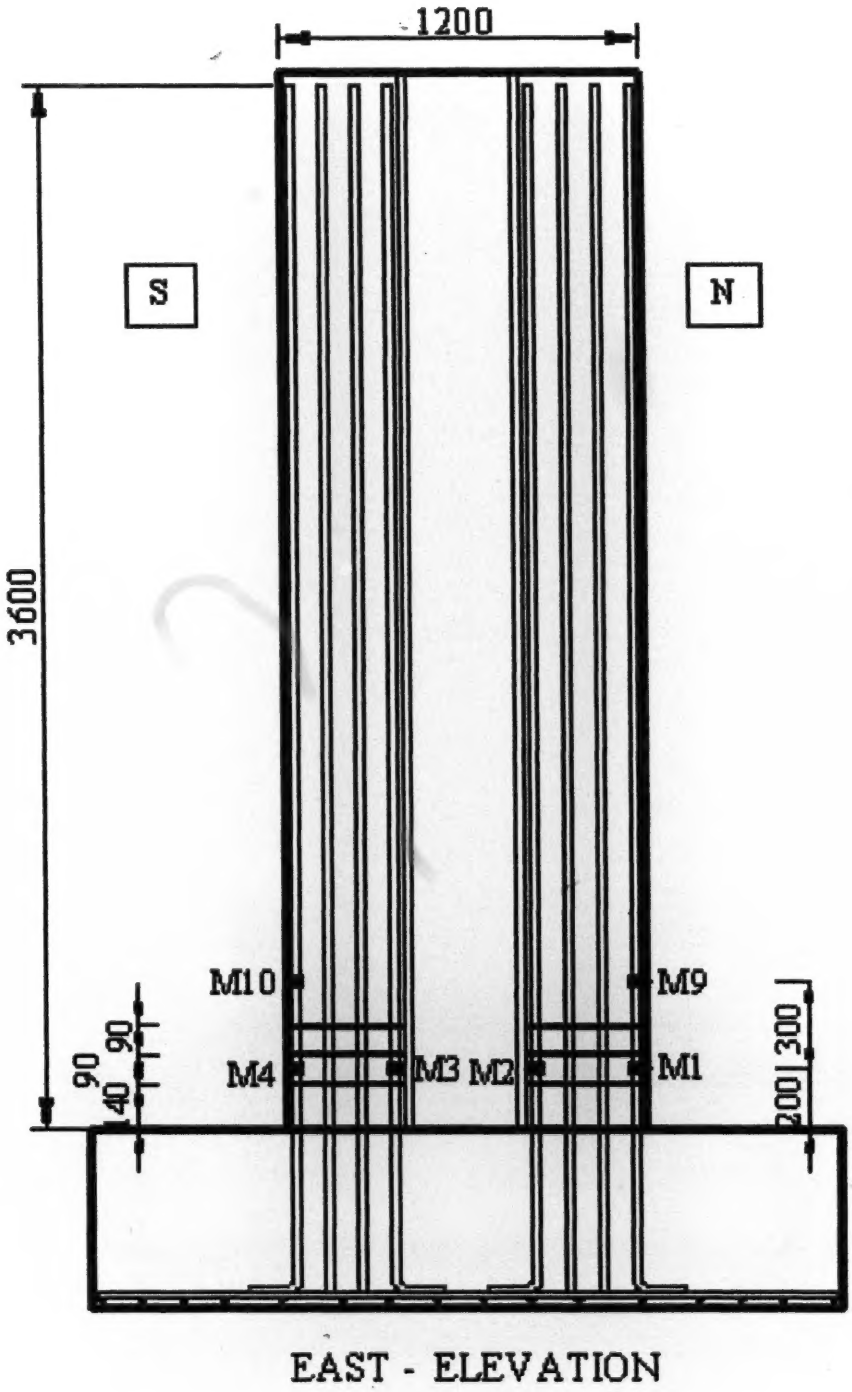

Figure 3.32 (a) W-2 Strain gauge layout in east elevation

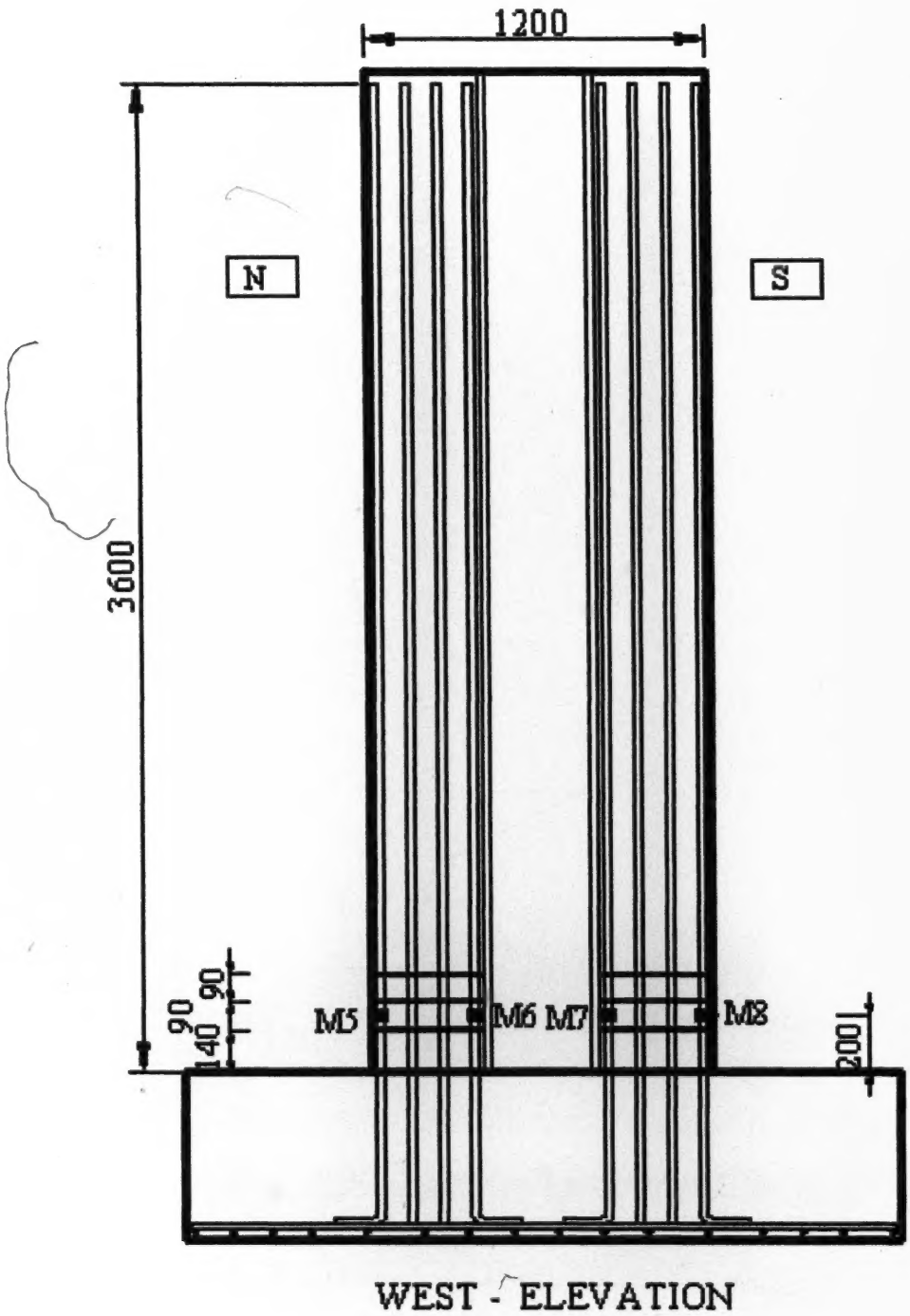

Figure 3.32 (b) W-2 Strain gauge layout in west elevation

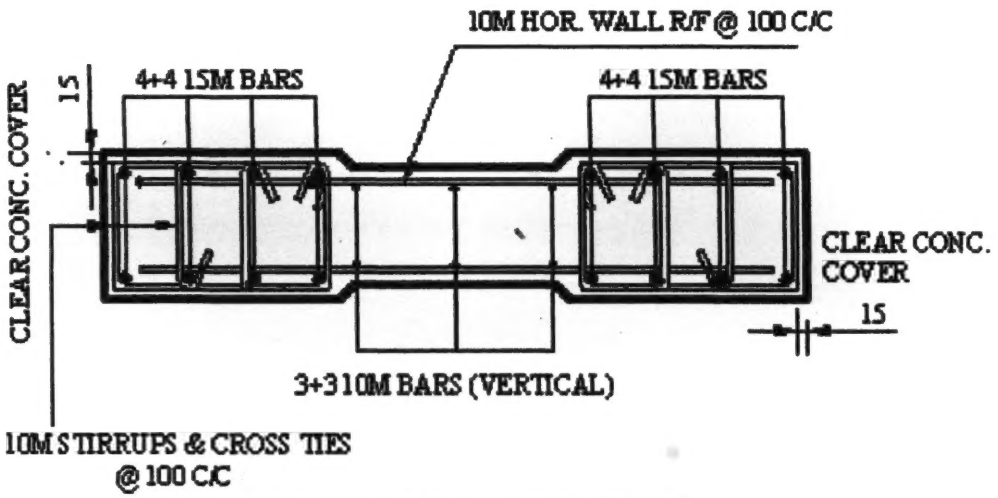

SEC. OF WALL - REGION "A"

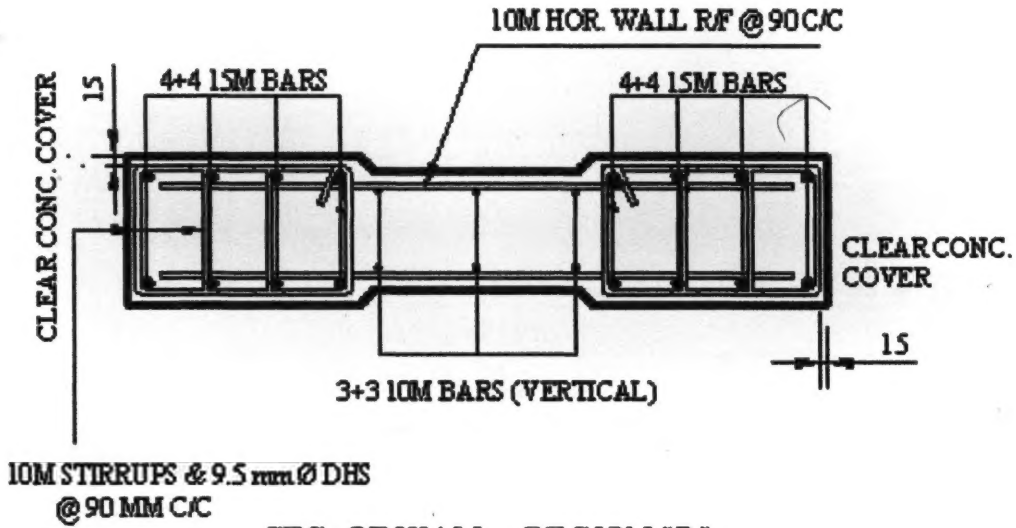

SEC. OF WALL - REGION "B"

Figure 3.32 (c) W-2 Strain gauge layout in x-section

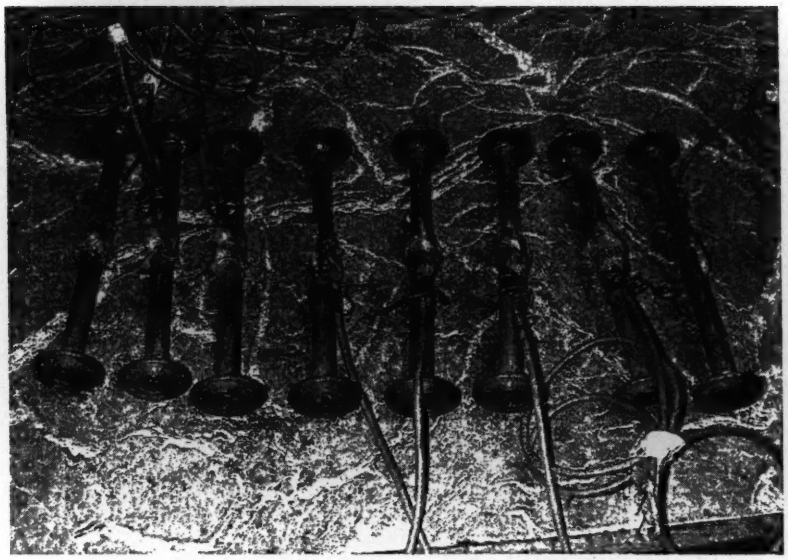

Figure 3.32 (d) Strain gauges on Double Head Studs

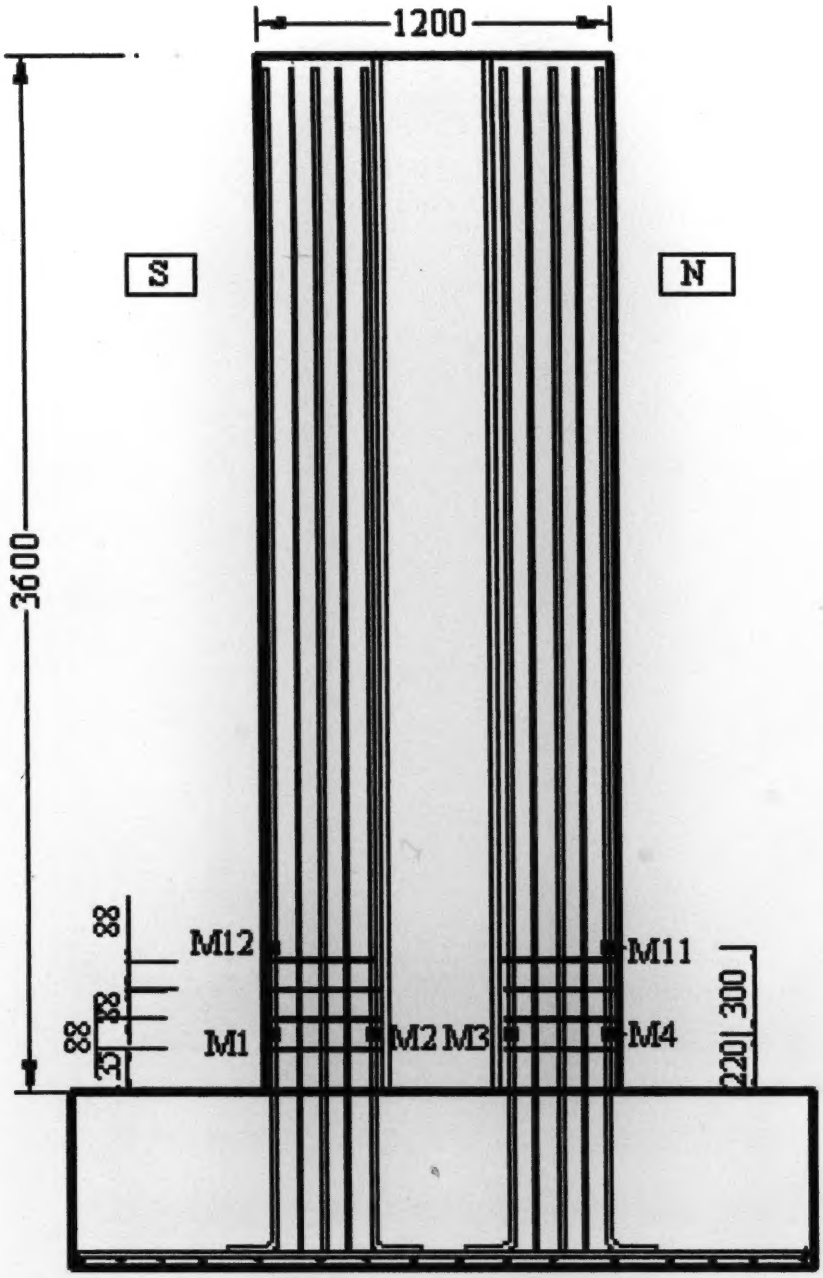

EAST - ELEVATION

Figure 3.33 (a) W-3 Strain gauge layout in east elevation

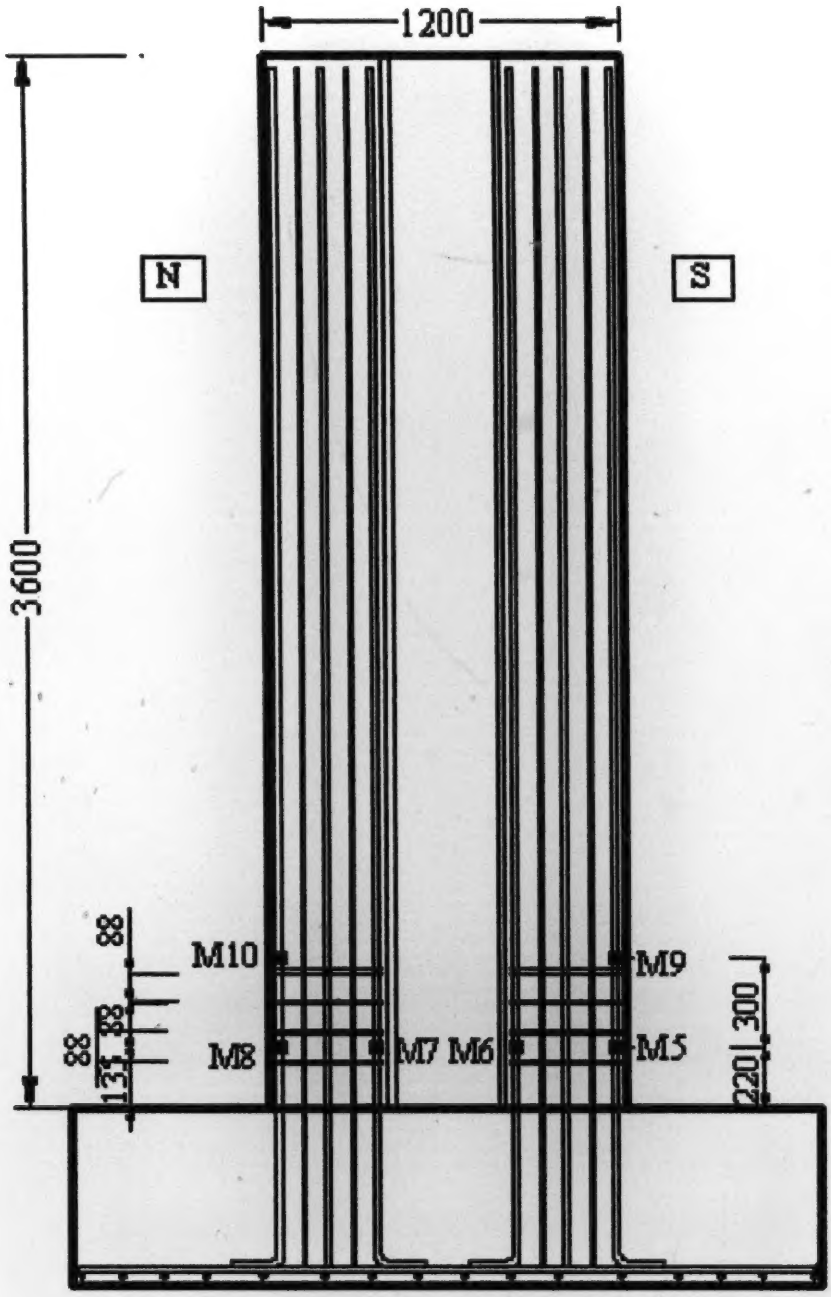

WEST - ELEVATION

Figure 3.33 (b) W-3 Strain gauge layout in west elevation

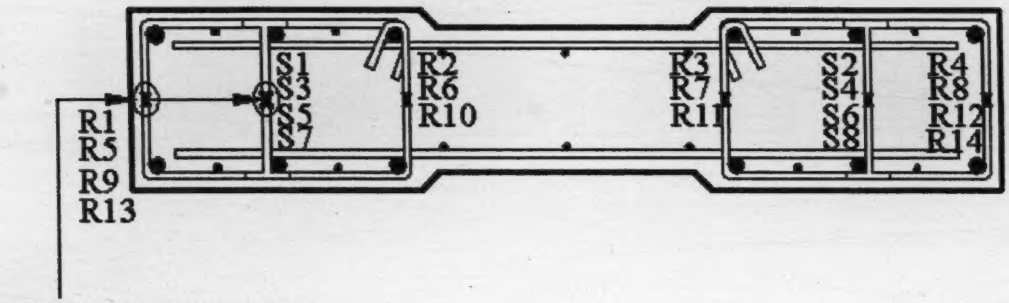

Note :

R1 - R4 & S1 - S2 are at 1st. level from base
R5 - R8 & S3 - S4 are at 2nd. level from base
R9 - R12 & S5 - S6 are at 3rd. level from base
R13 - R14 & S7 - S8 are at 4th. level from base

TYP. SEC OF W-3

Figure 3.33 (c) W-3 Strain gauge layout in the x-section

Figure 3.34 Top and mid-height LVDTs for measurement of lateral displacements

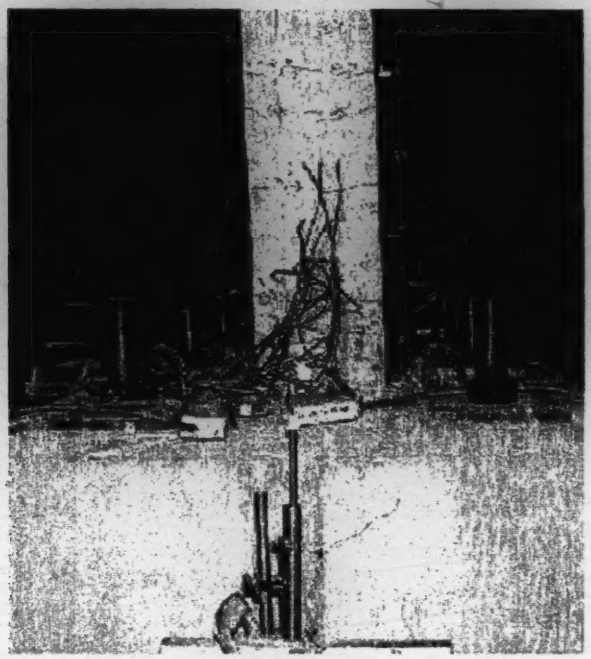

Figure 3.35 vertical LVDT at north face

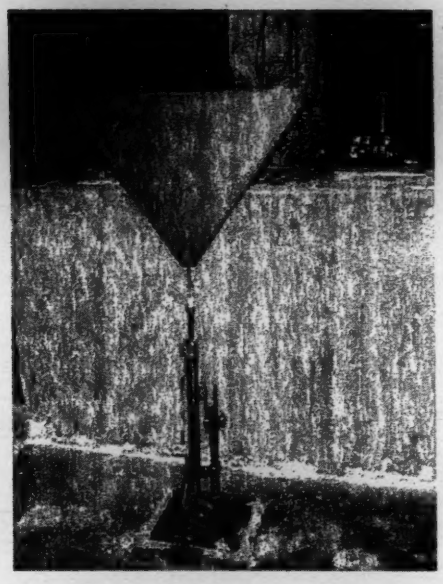

Figure 3.36 vertical LVDT at south face

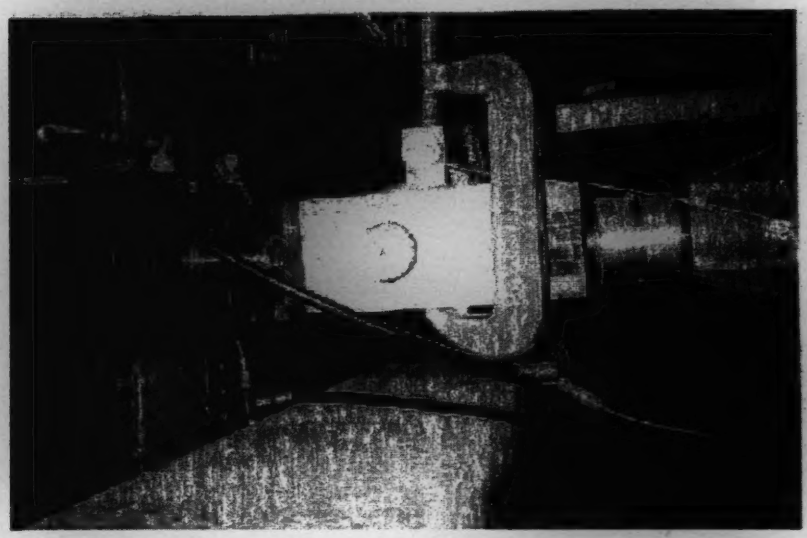

Figure 3.37 Rotation meter over yoke in lateral loading assembly

Figure 3.38 Rotation meter at top distribution beam

Table 3.1 Concrete Properties

Specimen	Age (Days)	Compressive Strength (MPa) (f'_c)	Modulus of Elasticity (MPa) (E_c)
W1	14	15.5	17716
	90	24.0	22045
W2	14	15.5	17716
	130	25.9	22768
W3	7	14.3	17020
	155	27.3	23520

Table 3.2 Properties of Reinforcing Steel

Specimen	Nominal Diameter (mm)	Nominal Area (mm^2)	Yield Stress (MPa)	Ultimate Stress (MPa)	Modulus of Elasticity (MPa)
Rebar	10	100	383.5	517	189000
Rebar	15	200	394.5	514	190000
Double Head Studs	9	71	510.0	528	205000
Double Head Studs	12	127	444.0	497	190000

CHAPTER 4

TEST RESULTS AND OBSERVATIONS

4.1 Introduction

In this chapter, test procedures and results from the test data are presented in detail. In addition to the test results, observations during testing, regarding the response of specimens, are also discussed. The response of the three wall specimens is presented mainly with respect to the lateral load versus wall top deflection relation (also referred to as lateral load versus tip-displacement response or the Hysteresis loops).

4.2 Loading Procedure

4.2.1 Application of Vertical loads

To simulate real loading conditions on a shear wall, the vertical load (that simulated gravity loads) was applied first and it slowly increased to its maximum value. It was then maintained at its maximum value throughout the test. The value of vertical load that was applied and maintained throughout the test was 1000 kN with a variation of 5%, this value of vertical load corresponds to a compressive stress of approximately 0.15 f'_c.

4.2.2 Application of Lateral loads

Each wall was then loaded laterally, back and forth, in a displacement control mode throughout the test. Lateral displacements were started after the vertical load was applied and maintained at the required value (ie. 0.15 stress). At any given lateral displacement level, three cycles were performed, starting with the first displacement level of 3 mm tip displacement towards the south direction. Consecutive displacement levels

were increased by increments of 3 mm over the previous displacement level, and three cycles were performed at each displacement level.

Initially it was planned that 3 mm displacement increments would be maintained between consecutive displacement levels until spalling of the concrete cover and then large displacement cycles would be given to achieve higher displacement levels corresponding to higher displacement ductility ratios (μ_Δ). W-1, which is the reference specimen, was tested first. It was loaded according to the scheduled testing procedure described above and reached the tip displacement of 27 mm but no spalling had been observed, although the wall had cracked markedly. The cyclic response was then changed significantly on reaching a tip displacement of 30 mm and its stiffness was greatly reduced without any spalling of the concrete cover. The initial plan was then changed at that point and large displacement increments were started to achieve higher lateral displacements corresponding to higher ductility ratios before complete collapse of the test specimen. The yield tip displacement (Δ_y) was determined out from the load versus tip displacement response up to 30 mm total tip displacement and it was 12 mm. The wall was then planned to displace with large increments corresponding to its ductility ratio (μ_Δ) between further consecutive displacements i.e. after 30 mm tip displacement the next displacement level corresponded to 42 mm and so on until the failure of the specimen occurred.

At the tip displacement of 78 mm, which also corresponds to the displacement ductility ratio (μ_Δ) of 6.5, the vertical bars of the boundary elements started to break and again the loading plan further changed. After the first bar ruptured, the wall was then displaced by further higher displacement increments corresponded to higher multiples of the displacement ductility ratio in the desirable direction. Further details of the test are discussed in Section 4.4.1. The next two tests were then performed following the same loading sequence in order to have common comparative bases but the large tip displacements (the displacement given to wall W-1 after the fracture of the vertical bars) were applied in the end of each test according to the test situation and which is not same for the three walls.

4.3 Test Observations

4.3.1 Wall W-1

Wall W-1 was tested by following the test procedure and sequence discussed in Section 4.2. Lateral load versus tip displacement response (Hysteresis loops) of W-1 is shown in Figure 4.1. Complete displacement history as a function of the number of cycles is plotted in Figure 4.2. First displacement was given towards the south to create tension in the loading assembly, consecutive load cycles were then followed. First flexural crack was formed in the second cycle of first (1^{st}) displacement level (corresponds to 3 mm tip displacement) on the north face of wall. The lateral load was 152 kN at that instant. The crack was formed at approximately 238 mm above the base, which is approximately equal to the thickness of wall at boundary elements.

In the following cycles, the stiffness reduced as a result of spread of cracking but the lateral load increased. On reaching the fourth (4^{th}) displacement level, corresponding to 12 mm tip displacement, the extreme vertical bars just reached the yield strain. At the tip displacement of 24 mm, nearly all the extreme vertical reinforcement in the boundary elements yielded in both tension and compression. Figures 4.3 through 4.5 show the strains in the vertical bars, stirrups and the crossties respectively for W-1. Much variation in vertical load (approximately 10%) was observed at that level as the wall moves back and forth, so, the vertical load was corrected and maintained during further lateral movement of the wall.

Cracks propagated both in the web and along the height of wall and nearly reached half the wall height at the end of 30 mm tip-displacement cycles. The wall had completed total 30 cycles up to the tip displacement of 30 mm. Spalling of the concrete cover was not observed yet but the stiffness of the wall was much reduced because of the yielding of vertical reinforcement, so, it was decided to displace the wall with large tip displacements corresponding to higher ductility levels. The yield tip-displacement (Δ_y) was worked out to be 12 mm from the lateral load versus tip deflection response at which

the stiffness of the wall seemed to be decreased more as compared to its previous response and the exterior vertical bars of the boundary elements had just reached their yield strain. The wall had already achieved 30 mm tip displacement, which, according to the computed value of Δ_y, corresponded to the displacement ductility ratio (μ_Δ) of 2.5. The wall was then displaced with the increments of one ductility ratio (μ_Δ) between consecutive displacement increments that corresponded to 12 mm tip displacement. Lateral load was not increased much after the wall had achieved the ductility ratio of 2.5 and the wall was moving at the almost ideal yield plateau on lateral load versus tip displacement response showing ductility in the response. Spalling of concrete started at μ_Δ of 3.5 (at a tip displacement of 42 mm). The stirrups at north side of wall, near the base, yielded at μ_Δ of 4.5 (54 mm tip displacement) while the stirrup at south side, near the base, yielded at μ_Δ of 5.5 (66 mm tip displacement). Maximum lateral load was observed to be 375 kN at the μ_Δ of 5.5 (66 mm tip displacement) cracks were also formed in the compression cycles at the same displacement level on the extreme face of the boundary elements at about 250 mm above the base.

Buckled vertical bars were visible in the first cycle at μ_Δ of 5.5 (i.e. at a tip displacement of 66 mm), due to the spalling of large concrete chunks from the corners at about 125 mm above the base level. A tearing crack also formed right at the wall-base connection at the same displacement level. The cross ties were stressed up to 75% of their yield strength at μ_Δ of 6.5 (78 mm tip displacement). In the second cycle at μ_Δ of 6.5, while the wall was moving towards south, southwest corner bar was broken in tension at a tip displacement of 77.7 mm and the lateral load was suddenly dropped by 8%.

Keeping in view the deteriorated condition of the wall the loading sequence was then changed and it was decided to displace the wall with large tip displacement to absorb more energy. The wall was then displaced to by 125 mm (which corresponds to a μ_Δ of approximately 10) towards the south, keeping the broken bar side in compression. The wall then pushed back towards the north to a total tip displacement of 135 mm (μ_Δ of approximately 11). Only one crosstie on each side yielded in these two large

displacement cycles, while strain gauges stopped working on some of the critical cross ties. It was observed that the stirrups close to the base were not yielded which may be because of the restraining effect of the base. The test was then stopped at that level, to avoid damage to the out-of plane lateral supports of the top distribution beam through which the vertical load was applied.

Figure 4.6 showed the variation of maximum lateral load in a cycle with the tip displacement of the wall W-1. Details of important events have also marked on the figure, which include the onset of first yield in the vertical bars, yielding in remaining vertical bars, stirrups, and cross ties. It is obvious from Figure 4.6 that the stirrups close to the base, were yielded at the tip displacement of 54 mm on the north side and at 66 mm on the south side.

4.3.2 Wall W-2

W-2 and W-3 were tested following the same displacement controlled cycles under which W-1 was tested, in order to compare their behavior on equal displacement bases. Lateral load versus tip displacement response (Hysteresis loops) of W-2 is shown in Figure 4.7 and its complete displacement history as a function of number of cycles is plotted in Figure 4.8. First crack was observed at the north face in the third cycle of 3 mm tip-displacement towards south, the lateral load was 165 kN at that point. The crack was formed at approximately 240 mm above the base, which is also approximately equal to the wall thickness there. Similarly, first crack on the south face was then appeared in the third cycle of 3mm tip-displacement towards the north, which was also at approximately the same level as that of the north face.

The stiffness started to reduce as the test proceeded due to the spread of cracking and the extreme vertical bars gradually reached their first yield at a tip displacement of 12 mm (which also corresponds to the yield displacement Δ_y). The response of the W-2 in terms of cracking and stiffness was very much identical to the W-1. All the extreme vertical reinforcement of the boundary elements reached the yield strength both in tension

and compression at the tip displacement of 27 mm. Figures 4.9 through 4.11 show the strain in the vertical bars, stirrups and the double head studs of the boundary elements respectively. After the yielding of vertical reinforcement, there was not much increase in the lateral load in further cycles and the yield plateau started from the tip displacement of 30 mm ($\mu_\Delta = 2.5$). Spalling of the concrete cover started at μ_Δ of 3.5 and the head of a double head stud became visible at about 150 mm above the base. Compression cracks appeared at the same ductility level near the bottom of the wall at about 125 mm above the base.

In the further cycles, spalling increased with the spread of cracking both inwards into the web as well as along the wall height. The wall showed ductile response similar to that of W-1 and the maximum lateral load was observed to be approximately 376.7 kN.

The first buckled vertical bar became visible at μ_Δ of 5.5 (tip displacement of 66 mm) in the extreme north face of the wall. W-2 successfully went through the three cycles at $\mu_\Delta = 6.5$ (corresponds to the tip displacement of 78 mm) and hence it went through one cycle more than W-1 without any bar fracture and it has somewhat longer yield plateau at one side than W-1 which had a vertical bar fracture in the second cycle at $\mu_\Delta = 6.5$. Two stirrups have also yielded at the same displacement ductility ratio, these stirrups were in the third position from the base, i-e the stirrups at the second level were not yielded, that might be because of the restraining effect of the base. Some of the double head studs have also reached 75% of their yield stress.

In the first cycle at $\mu_\Delta = 7.5$ (tip displacement of 90 mm), while the wall was moving towards south, the two extreme north corner bars were broken one by one in tension and the lateral load suddenly dropped by 18%.

The wall was then decided to be subjected to a large tip displacement towards the north by keeping the broken bars side in compression. While displacing towards the north, on reaching the tip displacement of 79 mm, one vertical bar at the south face was broken and after a further increment of 5 mm, another bar at the same face was broken

but the wall continued to be pushed towards north. At $\mu_\Delta = 7.5$ (tip displacement of 90 mm), one double head stud yielded in the north boundary element at about 140 mm above the base and the wall was pushed further to a total tip displacement of 130 mm towards the north ($\mu_\Delta = 11$ approximately). At the maximum tip displacement towards the north one more double head stud reached 80% of the yield strain in the north boundary element. The wall then pushed back towards the south to a total tip displacement of 138 mm (approximately $\mu_\Delta = 11$). During the displacement towards the south, two double head studs yielded in the south boundary element at about 140 mm and 235 respectively above the base while one stud reached 80% of the yield strain. To observe the behavior of confinement, the wall was again pushed towards the north but on reaching 116 mm total tip displacement one more vertical bar at south side was ruptured and the lateral load was dropped significantly. The test was then decided to stopped at that level as the stirrups and double head studs at the bottom level of wall had already yielded and the wall had also reached the tip displacement equal to that wall W-1 had reached in the first test.

Figure 4.12 presents the variation of maximum lateral load in a cycle with the tip displacement of the wall W-2. Details of important events have also marked on the figure, which include the onset of first yield in the vertical bars, yielding in remaining vertical bars, stirrups, and the double head studs.

4.3.3 Wall W-3

W-3 was also tested under the same displacement controlled cycles as W-1 and W-2 were tested. Lateral load versus tip displacement response (Hysteresis loops) of W-3 is shown in Figure 4.13 and complete displacement history of W-3 as a function of number of cycles is plotted in Figure 4.14. First crack was observed at the north face in the second cycle of 3 mm displacement level, the lateral load was 148 kN at that point. The crack was formed at approximately 200 mm above the base (which is close to the thickness of the wall at boundary elements).

In further cycles, the stiffness continuously reduced as a result of spread of cracking and some of the extreme vertical bars reached yield at the tip displacement of 12 mm, which also corresponds to the yield displacement (Δ_y). Figures 4.15 through 4.17 show the strain in the vertical bars, stirrups and the double head studs of the boundary elements respectively.

Cracking pattern was observed to be identical walls W-1 or W-2. Yielding of all vertical bars occurred at $\mu_\Delta = 2.5$ (tip displacement of 30 mm) i-e approximately at the same displacement ductility ratio as it happened in wall W-1 or W-2. W-3 achieved a little higher strength and maximum lateral load was observed to be 394.4 kN.

Cracks in the compression cycle appeared at $\mu_\Delta = 2.5$, i-e at the tip displacement of 30 mm, near the bottom of the wall at about 100 mm above the base. Spalling of concrete from the corners started at $\mu_\Delta = 3.5$, i-e at tip displacement of 42 mm. First buckled vertical bar became visible at $\mu_\Delta = 5.5$ which corresponds to the tip displacement of 66 mm at the extreme south face of the wall. W-3 also went successfully through the three cycles at $\mu_\Delta = 6.5$ (tip displacement of 78 mm). Two stirrups also yielded at this displacement level in the third and fourth position vertically from the base, i-e the stirrups at the second level were not yielded. W-3 also completed one cycle at $\mu_\Delta = 7.5$, which corresponds to the tip displacement of 90 mm and hence achieved the maximum number of cycles before any vertical bar fractured.

During the second cycle at $\mu_\Delta = 7.5$ (tip displacement of 90 mm), the north side inner 10M bar in the boundary element was broken in tension and the lateral load dropped by 15%. The wall was then subjected to a large tip displacement of 130 mm, which corresponds to the $\mu_\Delta = 10$, towards the north by keeping the broken bars side in compression. The wall was then pushed back towards the south to a total tip displacement of 135 mm, which corresponds to the $\mu_\Delta = 11$ approximately. While displacing towards the south one 15M vertical bar at the north face was broken. Yielding in double head studs still was not achieved and thus the wall was pushed towards the north again to a

total tip displacement of 168 mm (μ_Δ = 13.5). During that large tip displacement, only one double head stud yielded in the north boundary element lying at about 217 mm above the base while three studs reached 80% of the yield strain. Keeping in view the danger to the lateral braces of the top distribution beam, the test was then stopped at that level and the wall was returned to zero load position.

Figure 4.18 presents the variation of maximum lateral load in a cycle with the tip displacement of the wall W-2. Details of important events have also marked on the figure, including onset of first yield in the vertical bars, yielding in remaining vertical bars, stirrups, and the double head studs.

4.4 Cracking and Crack Width

Crack width was measured manually at only one level on both the north and south faces of the walls by using a plastic card ruled with lines of different thickness (often referred to as crack detector). The crack measuring level was approximately 500 mm above the base. Crack pattern is almost identical in all three walls, each wall formed crack up to half wall height from the base. First crack in each wall specimen was formed at about 200 mm to 250 mm above the wall base. This is also approximately equal to the thickness of the wall at the ends (i-e 250 mm). The flexural tension cracks propagated approximately horizontally from the extreme faces of wall into the boundary elements and after reaching half the width of the boundary elements the cracks became inclined diagonally towards the base. All cracks propagated diagonally into the web and even some of those reached the opposite boundary element in the last stages of the test. The most affected region of the wall in which the flexural cracks opened and closed during the back and forth displacement of wall was lying in between the level of 250 mm and 750 mm from the base, although the cracks were formed up to 1800 mm above the base. Deterioration of the concrete was initiated mainly with the formation of compression cracks after the yielding of main vertical reinforcement and chunks of concrete spalled off due to the buckling of vertical bars.

In wall W-1, the level of flexural cracks formation above the base increased with the increase in loading cycles up to $\mu_\Delta = 4.5$, which corresponds to the tip displacement of 54 mm), but after the formation of the compression cracks no new flexural crack was formed, instead the existing cracks just opened and closed with some further extension in length and width. Maximum crack width up to the $\mu_\Delta = 1$ (tip displacement of 12 mm) was 0.4 mm that gradually increased to 0.6 mm at $\mu_\Delta = 2$ (tip displacement of 24 mm). The crack width further increased to 1.5 mm at $\mu_\Delta = 3.5$ (tip displacement of 42 mm). The maximum crack opening measured to be approximately 8.5 mm at the extreme faces of wall ends in the last cycles of the test. Figures 4.19 through 4.22 show some photographs of W-1 after the test, from different directions. Figure 4.21 shows the broken bar at south side. The cracking pattern is also obvious from these photos

Wall W-2 showed a similar crack pattern as that of W-1 but the crack widths in the initial load cycles were observed to be little less than W-1 but it became similar in the final load cycles. At $\mu_\Delta = 1$ (tip displacement of 12 mm), maximum crack width was 0.2 mm and it became 0.45 mm at $\mu_\Delta = 2.0$, which corresponds to the tip displacement of 24 mm. At $\mu_\Delta = 3.5$, the crack width became 1.5 mm, which is approximately the same as W-1 had at the same tip displacement. Maximum crack opening was observed to be the same as W-1 exhibited, although the crack width could not be measured with sufficient accuracy when exceeding 1.5 mm. Figures 4.23 through 4.26 show some photographs of W-2 after the test from different directions. Figure 4.25 and 4.26 show the broken bars at south and north sides respectively.

The crack pattern and crack widths, at different displacement levels, of W-3 were quite similar to W-2 (Refer to Figures 4.27 through 4.30). At $\mu_\Delta = 1$ (tip displacement of 12 mm), maximum crack width was 0.25 mm and it became 0.5 mm at $\mu_\Delta = 2.0$. At $\mu_\Delta = 3.5$, the crack width became 1.5 mm and in the last stages of the test, the active cracks opened by 8.0 mm (approximately). Figures 4.29 and 4.30 show views of the broken bars at the south and the north sides.

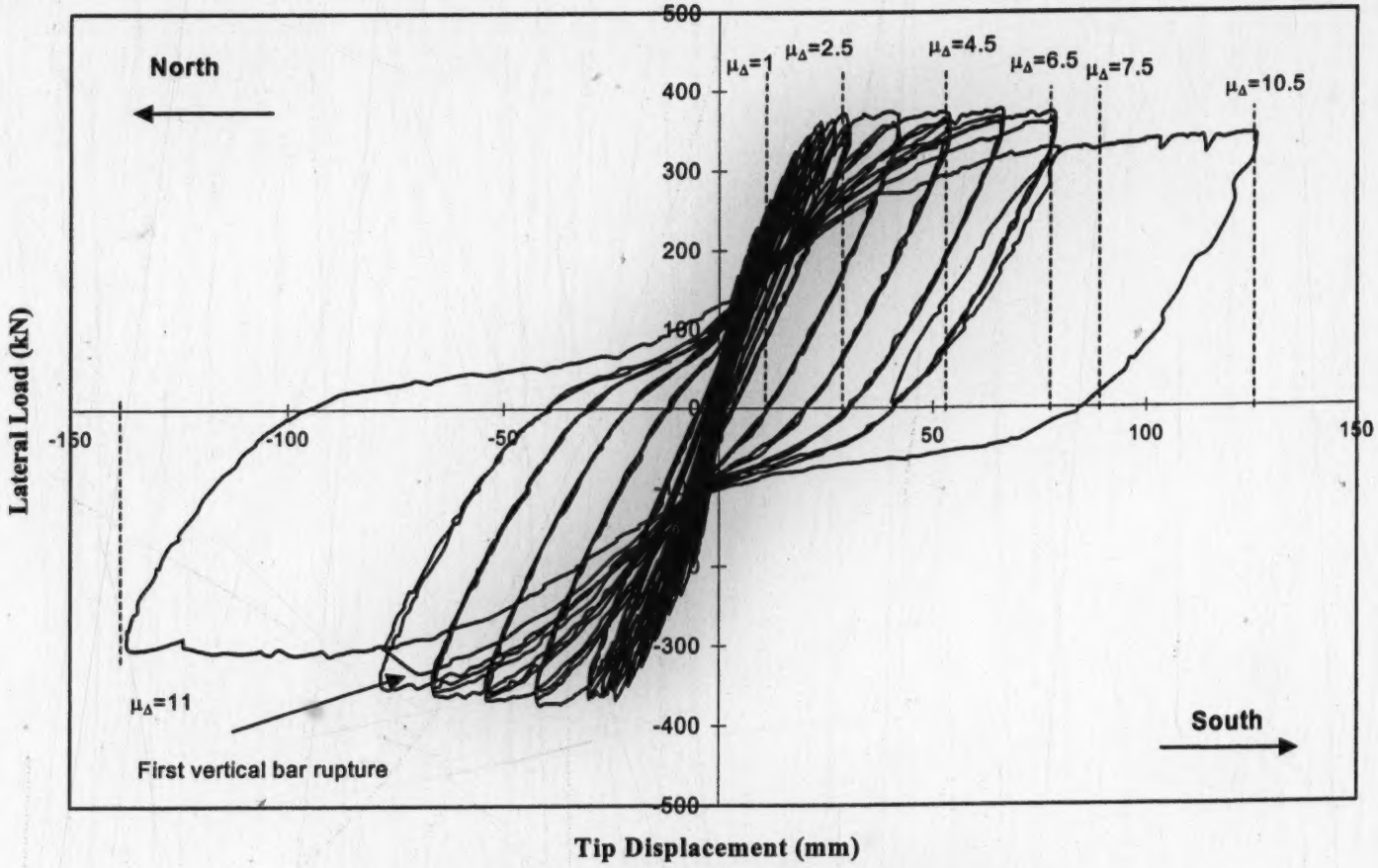

Figure 4.1 Load Vs tip displacement response of wall W-1

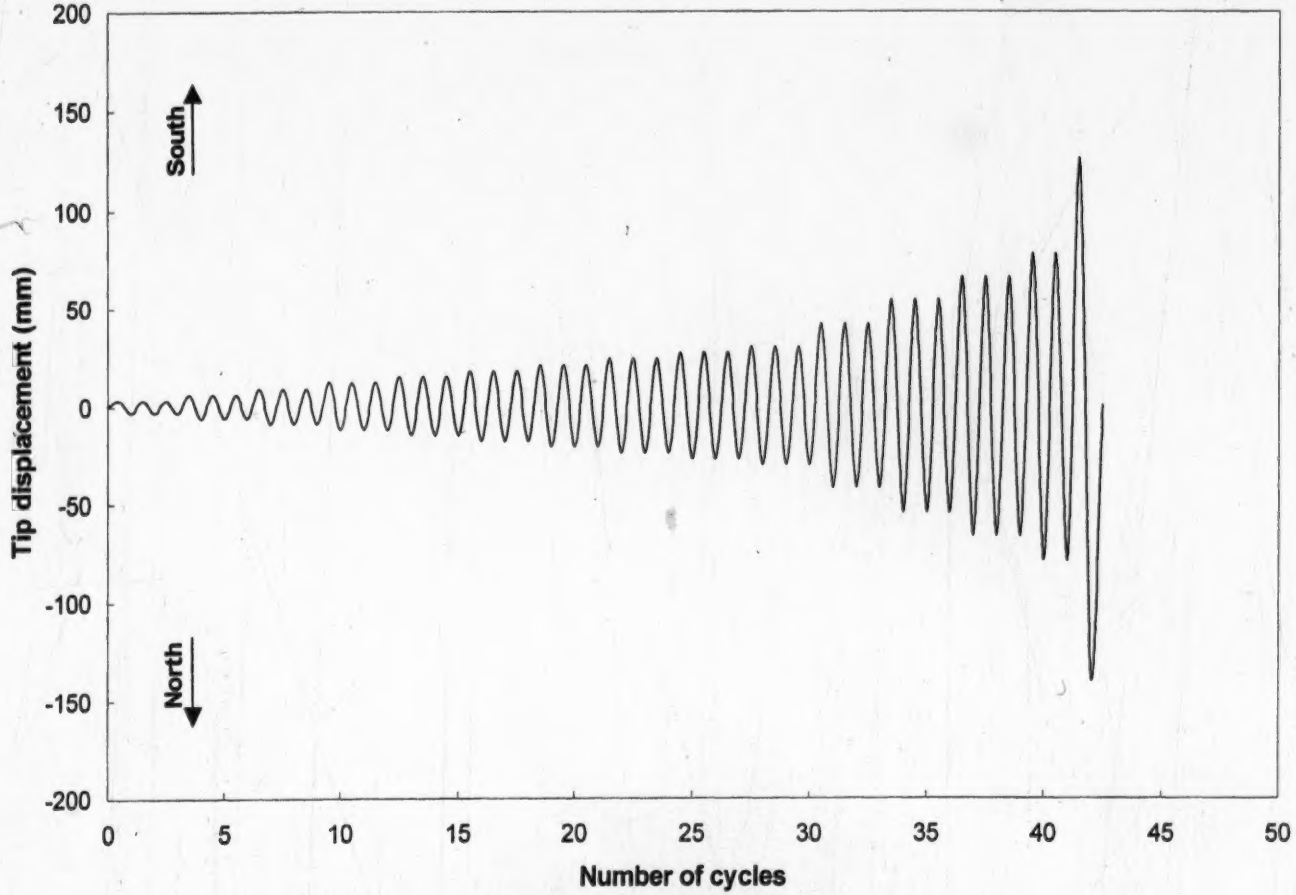

Figure 4.2 W-1 Loading history

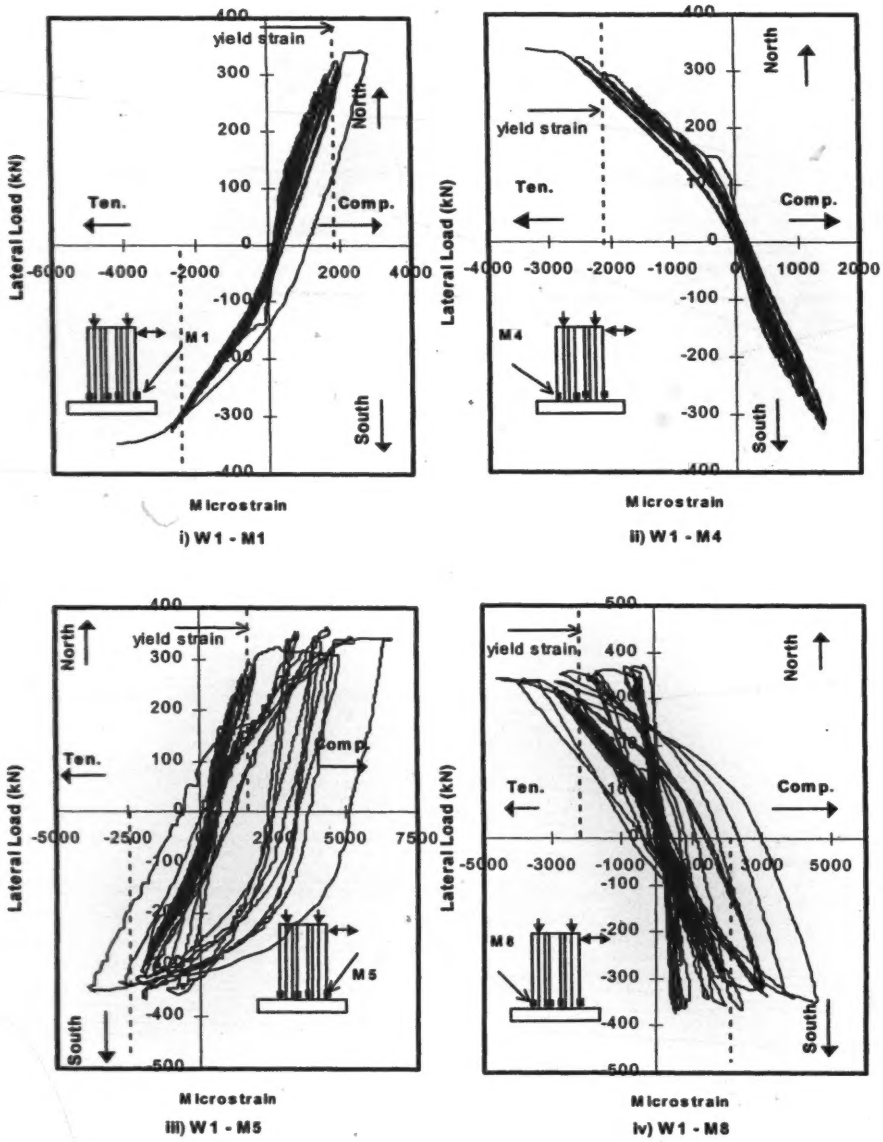

Figure 4.3(a) Strain in the vertical bars of W-1

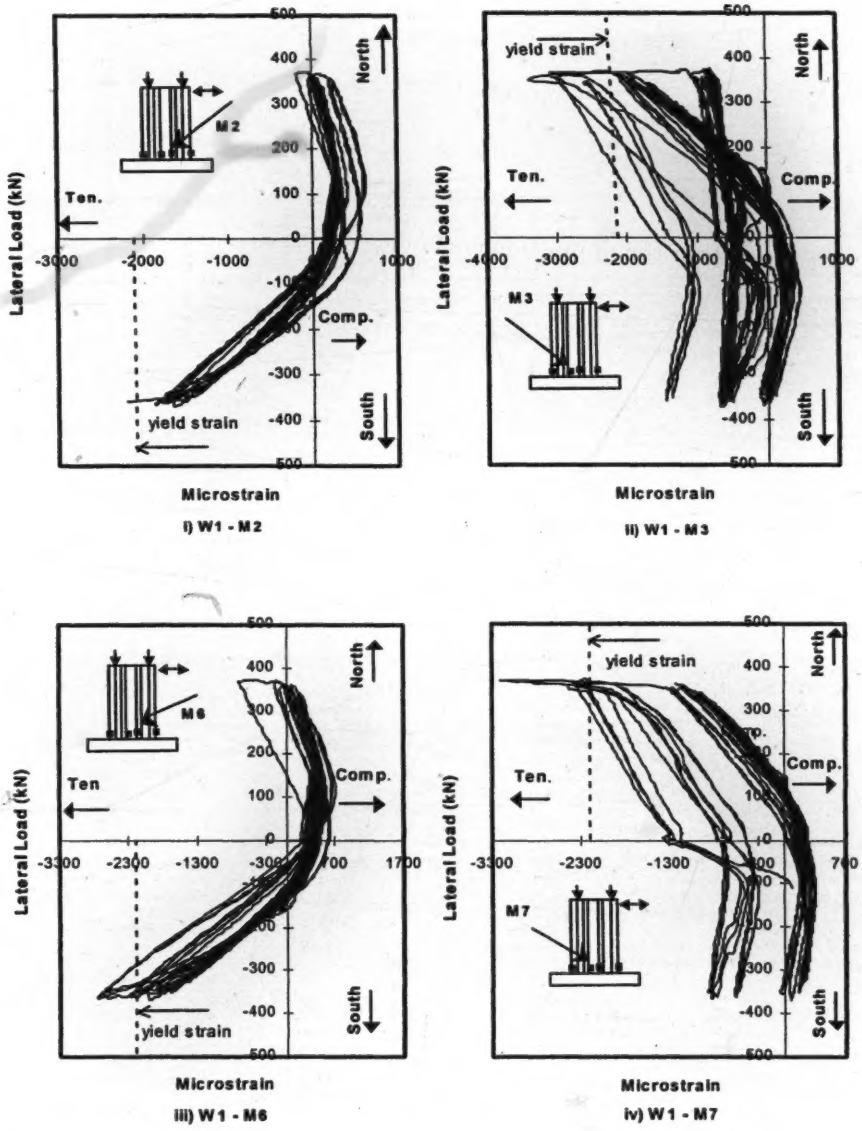

Figure 4.3(b) Strain in the vertical bars of W-1

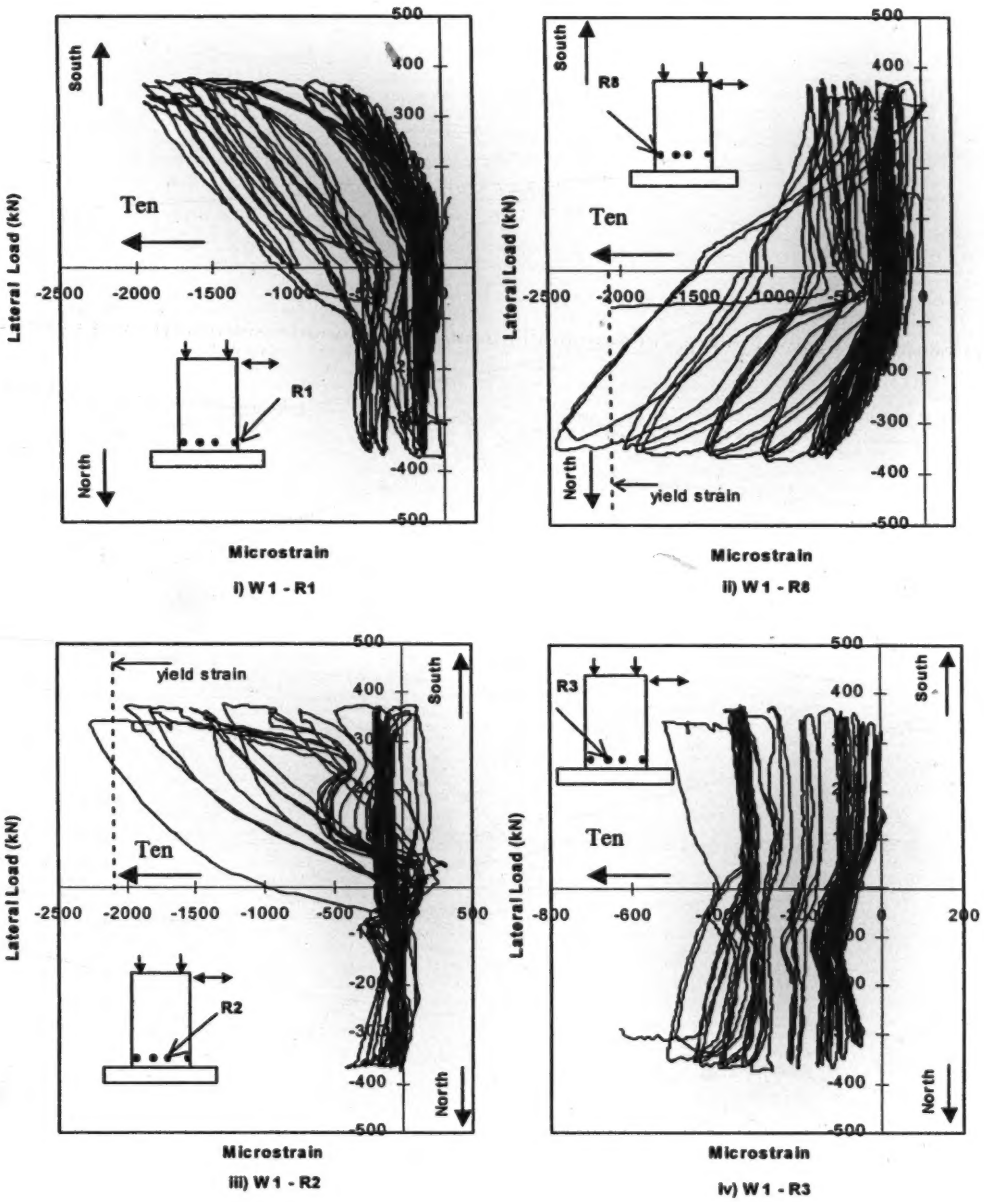

Figure 4.4(a) Strain in the stirrups of W-1

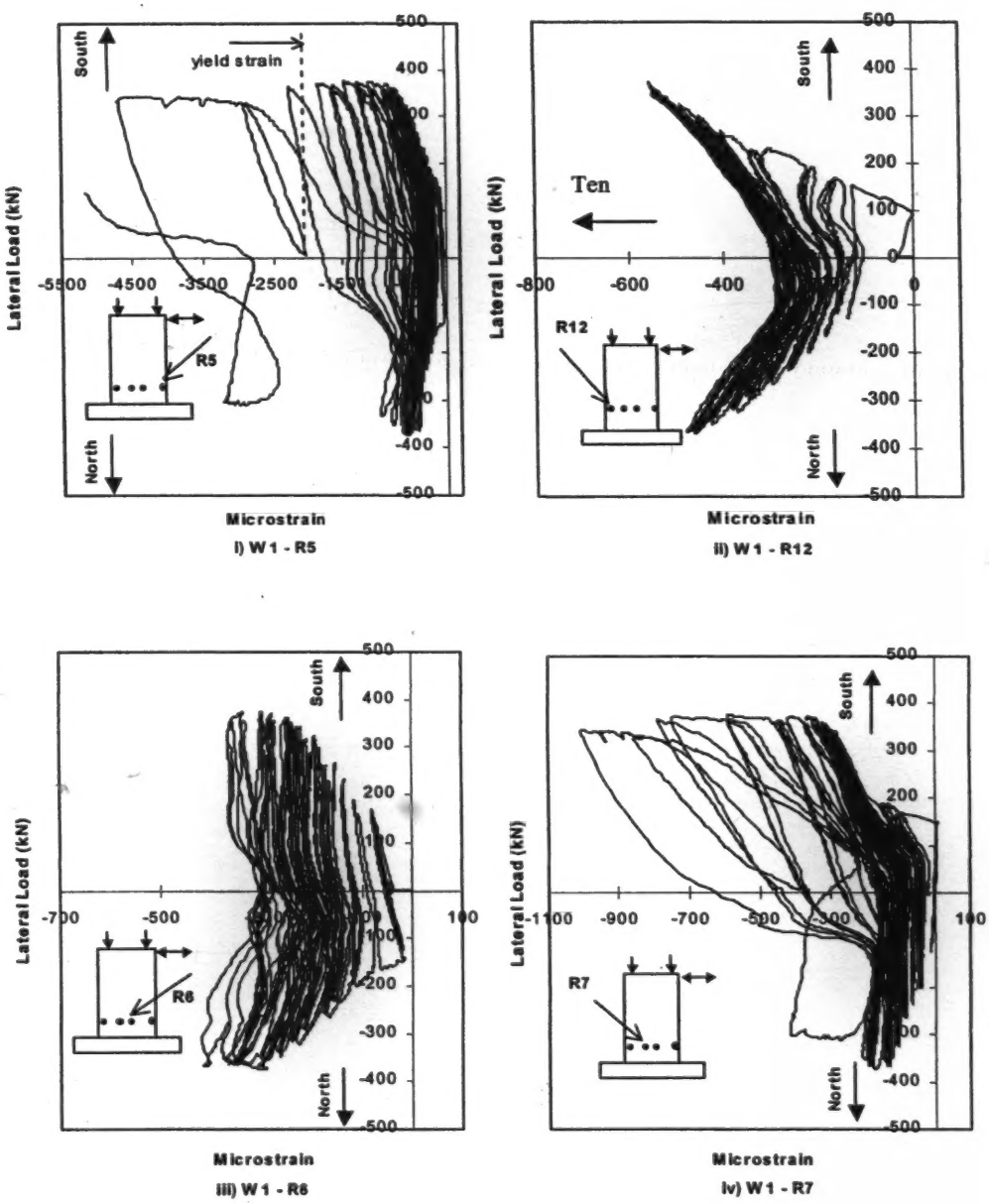

Figure 4.4(b) Strain in the stirrups of W-1

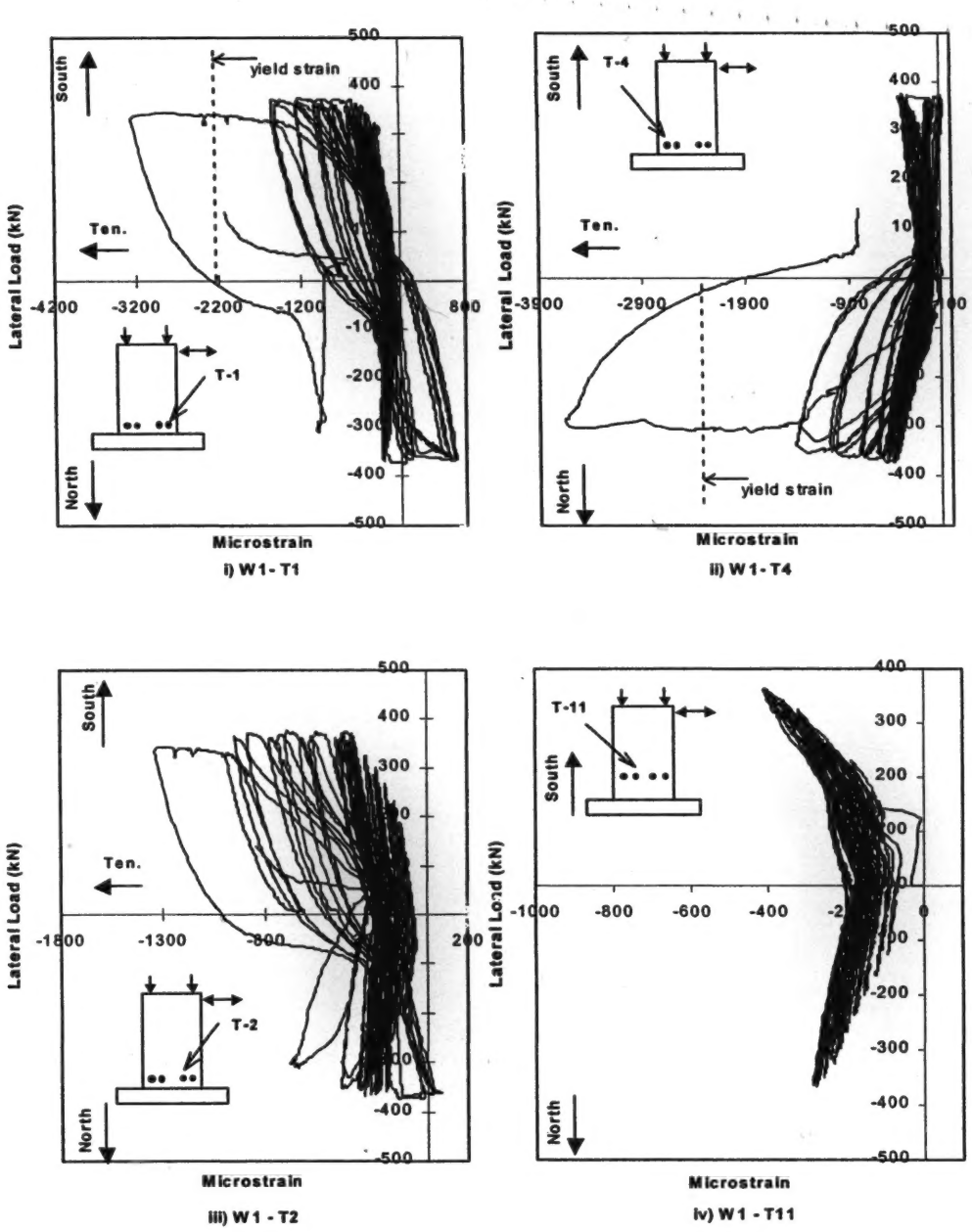

Figure 4.5(a) Strain in the crossties of W-1

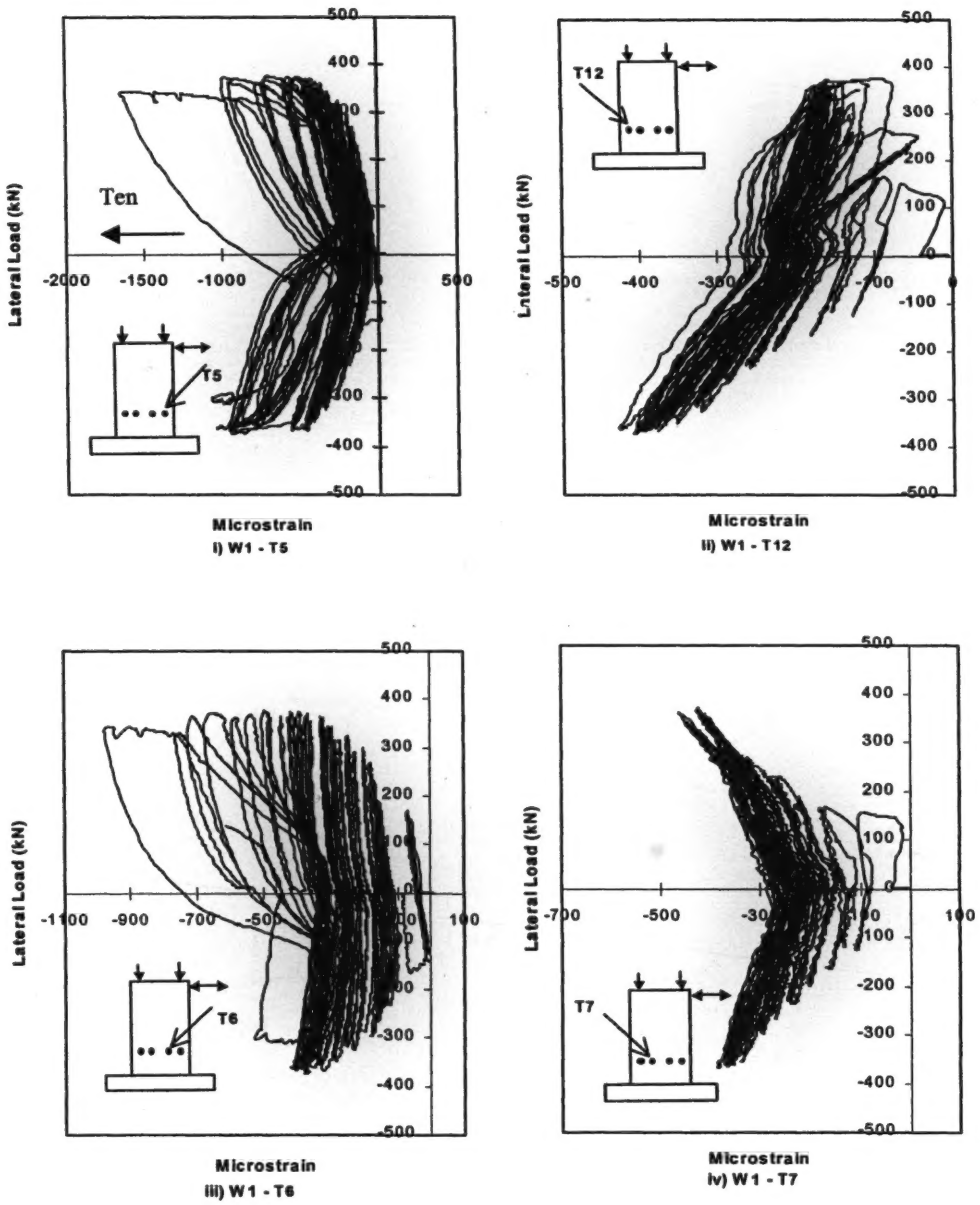

Figure 4.5(b) Strain in the crossties of W-1

Figure 4.6 W-1 four stages of response with events summary

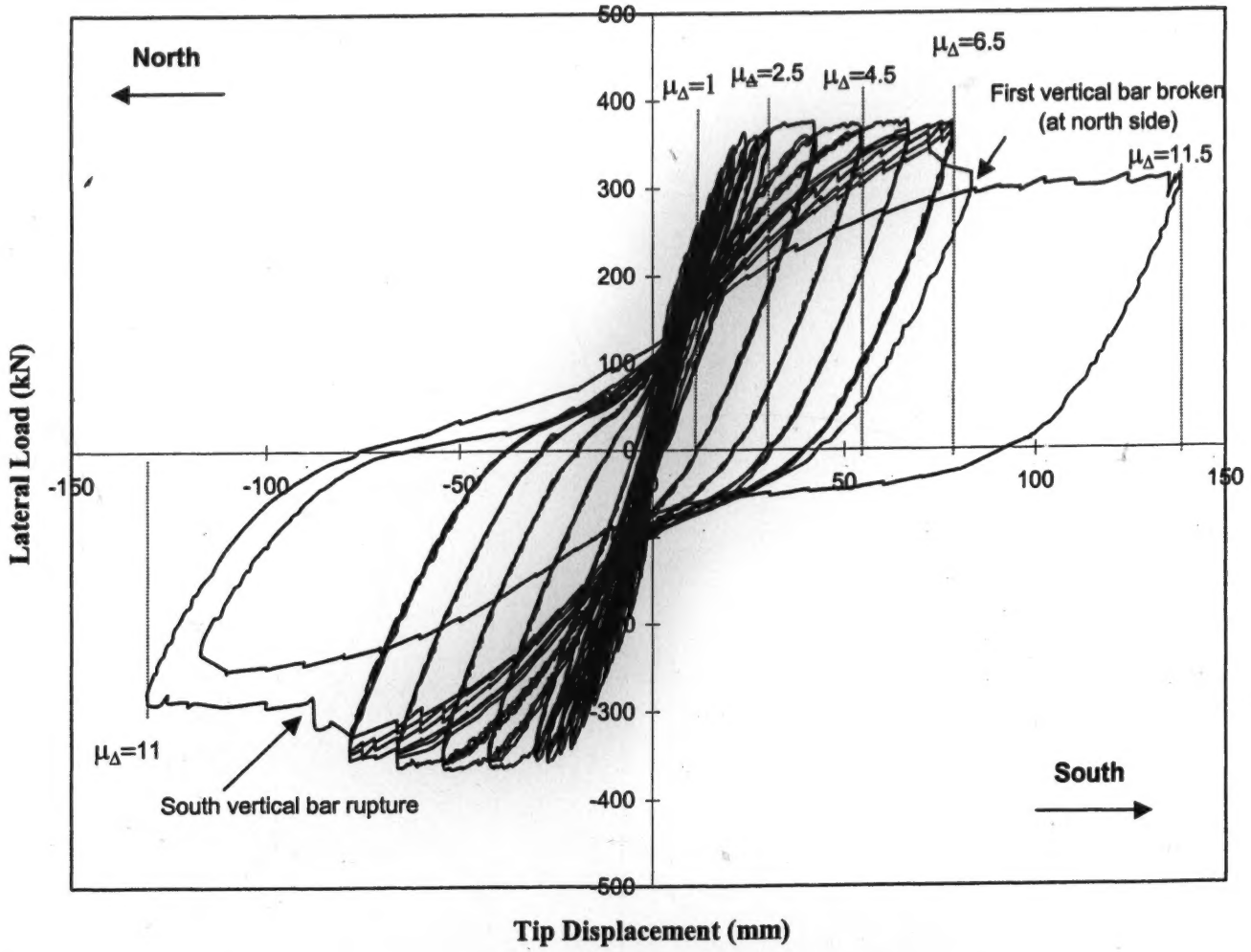

Figure 4.7 Load Vs tip displacement response of W-2

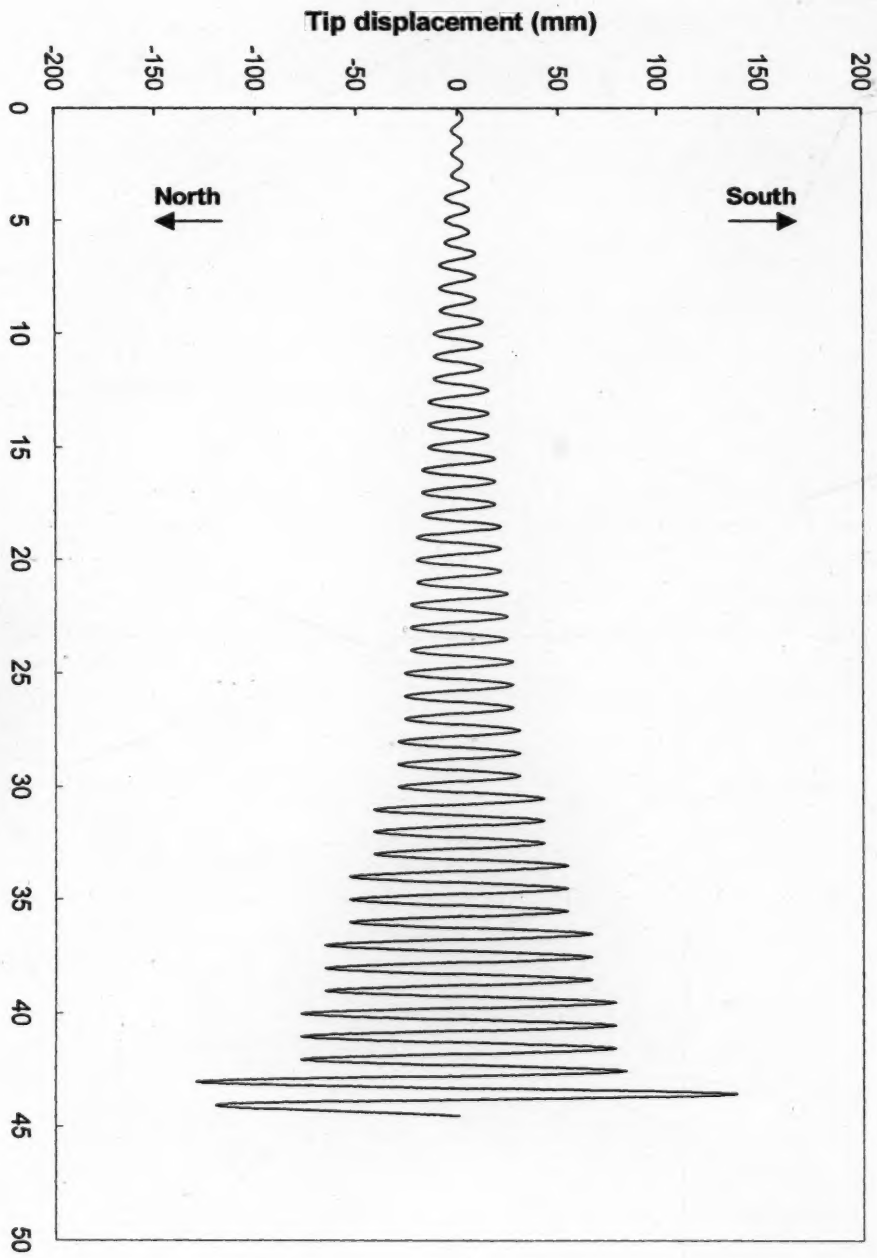

Figure 4.8 W-2 Loading history

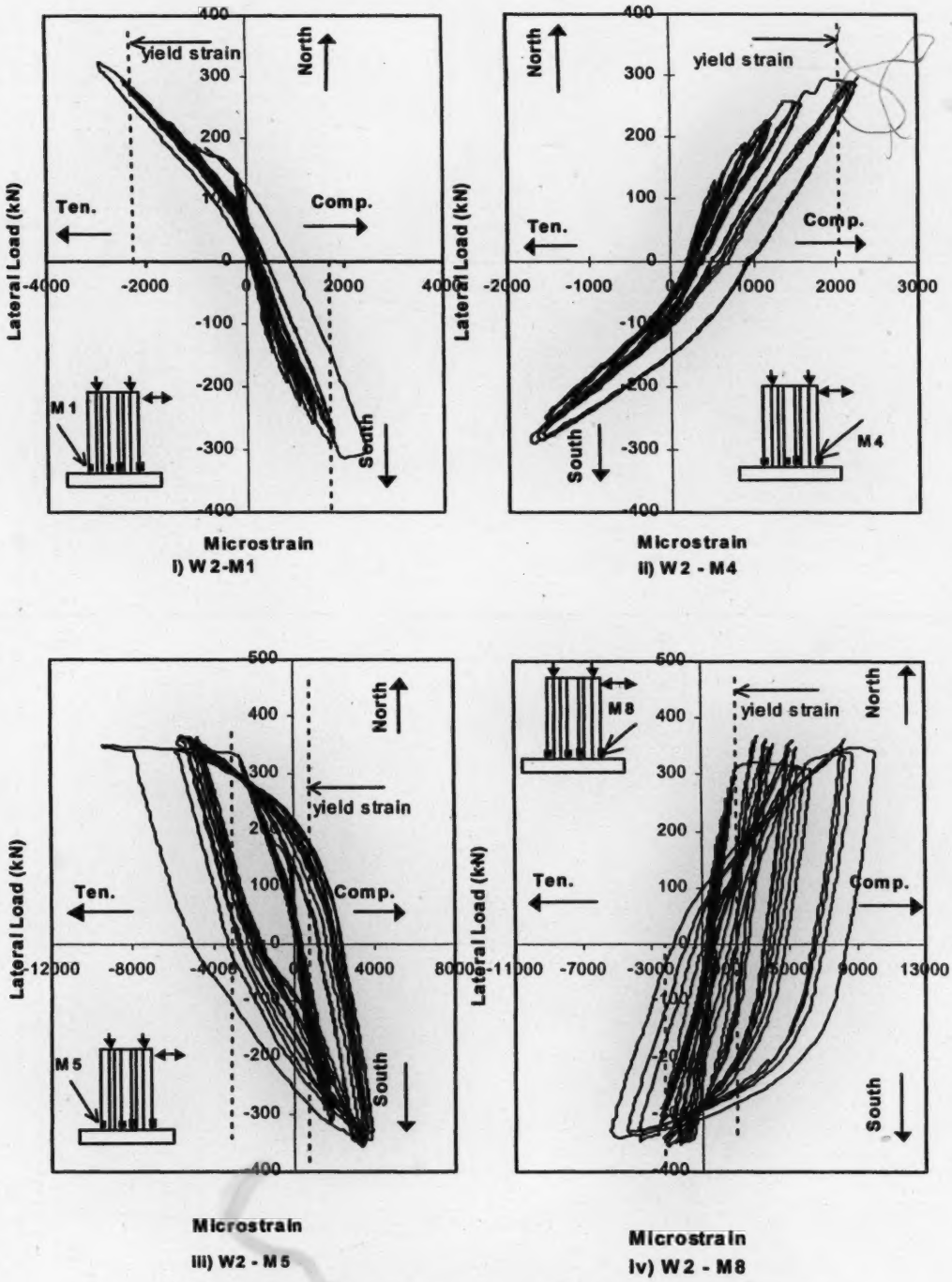

Figure 4.9(a) Strain in the vertical bars of W-2

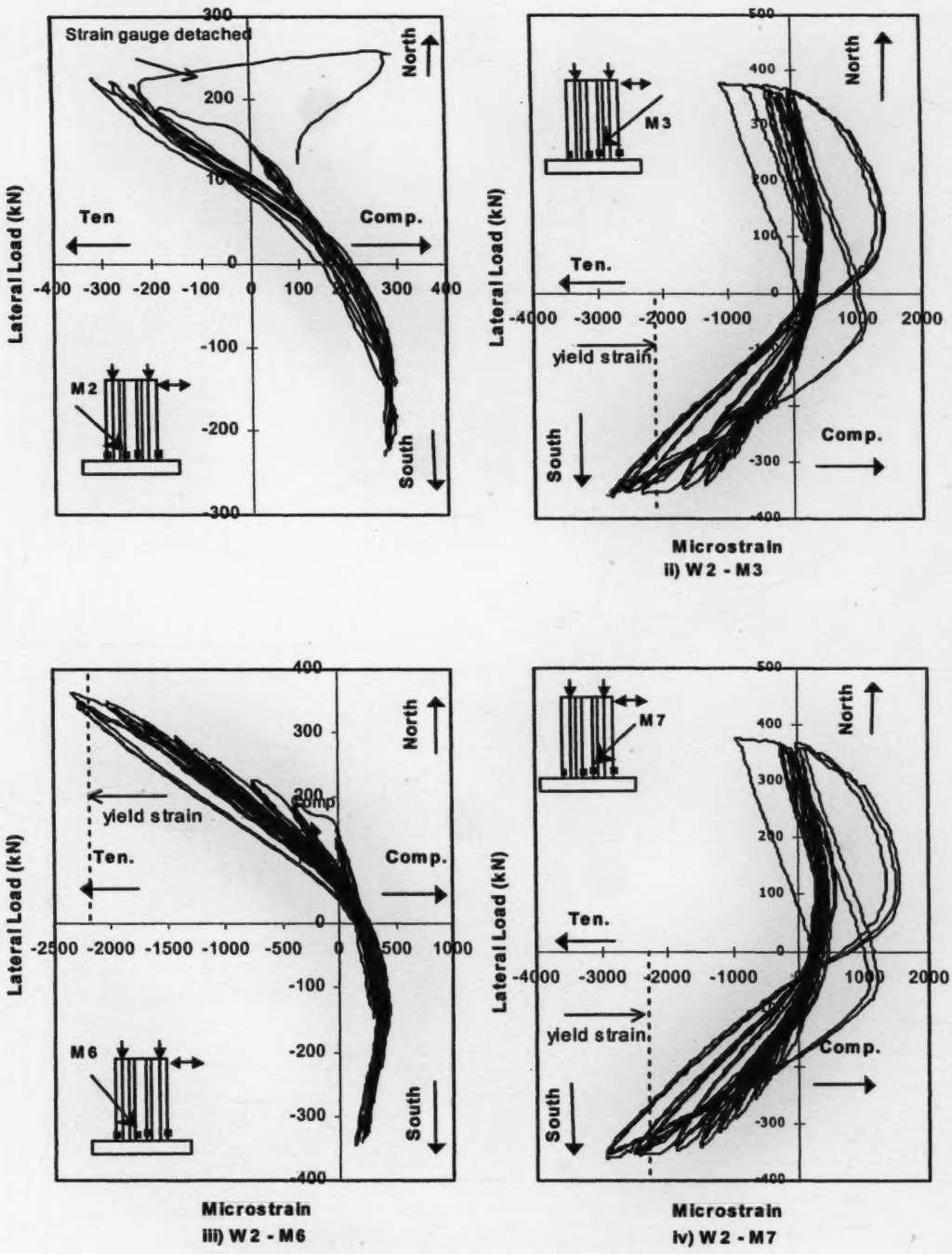

Figure 4.9(b) Strain in the vertical bars of W-2

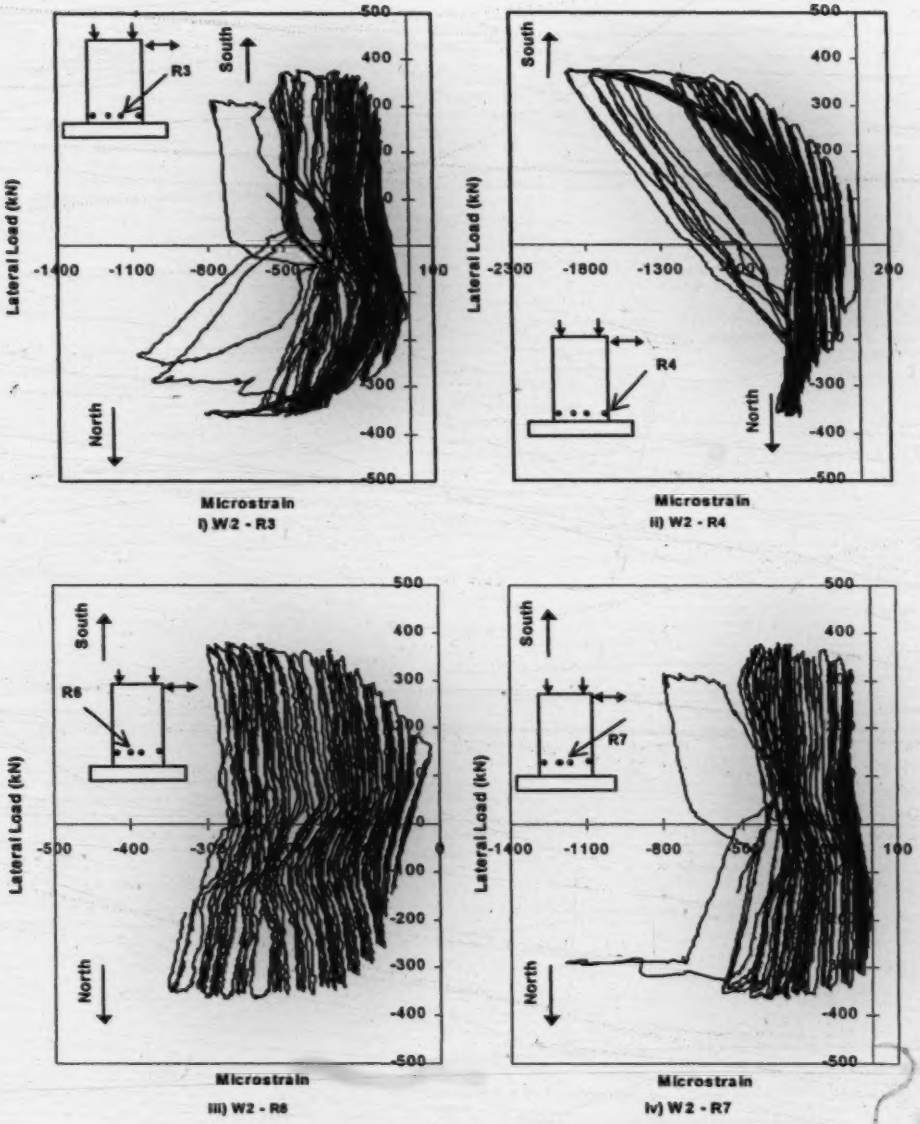

Figure 4.10(a) Strain in the stirrups of W-2

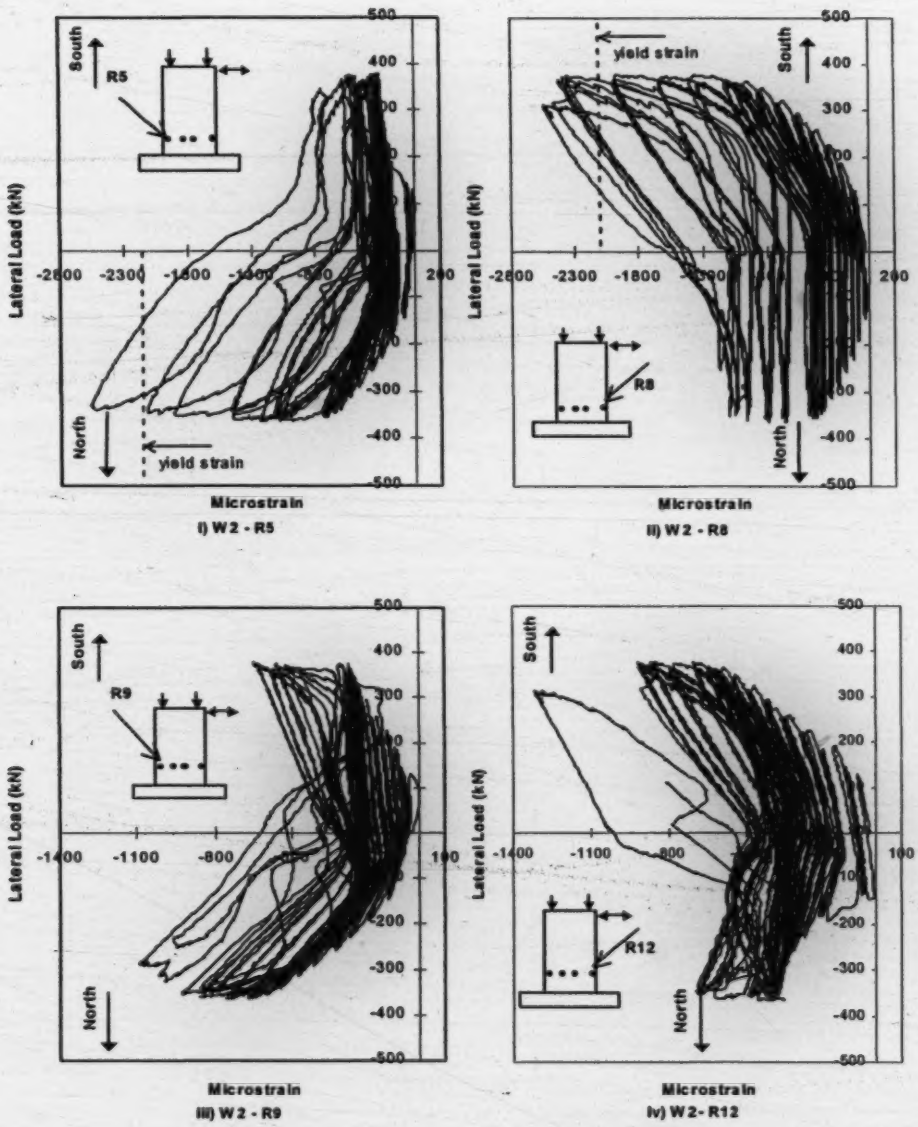

Figure 4.10(b) Strain in the stirrups of W-2

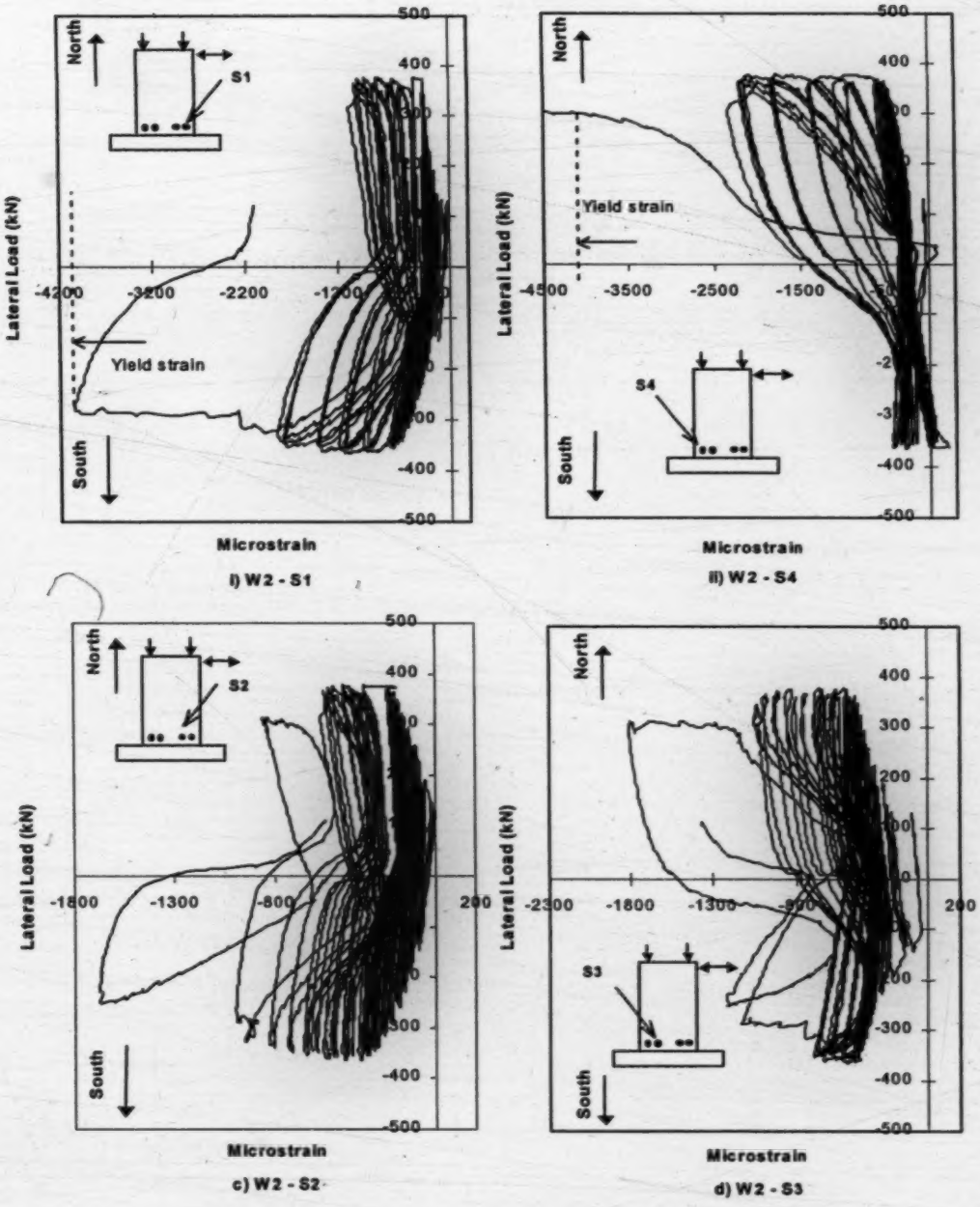

Figure 4.11(a) Strain in the double head studs of W-2

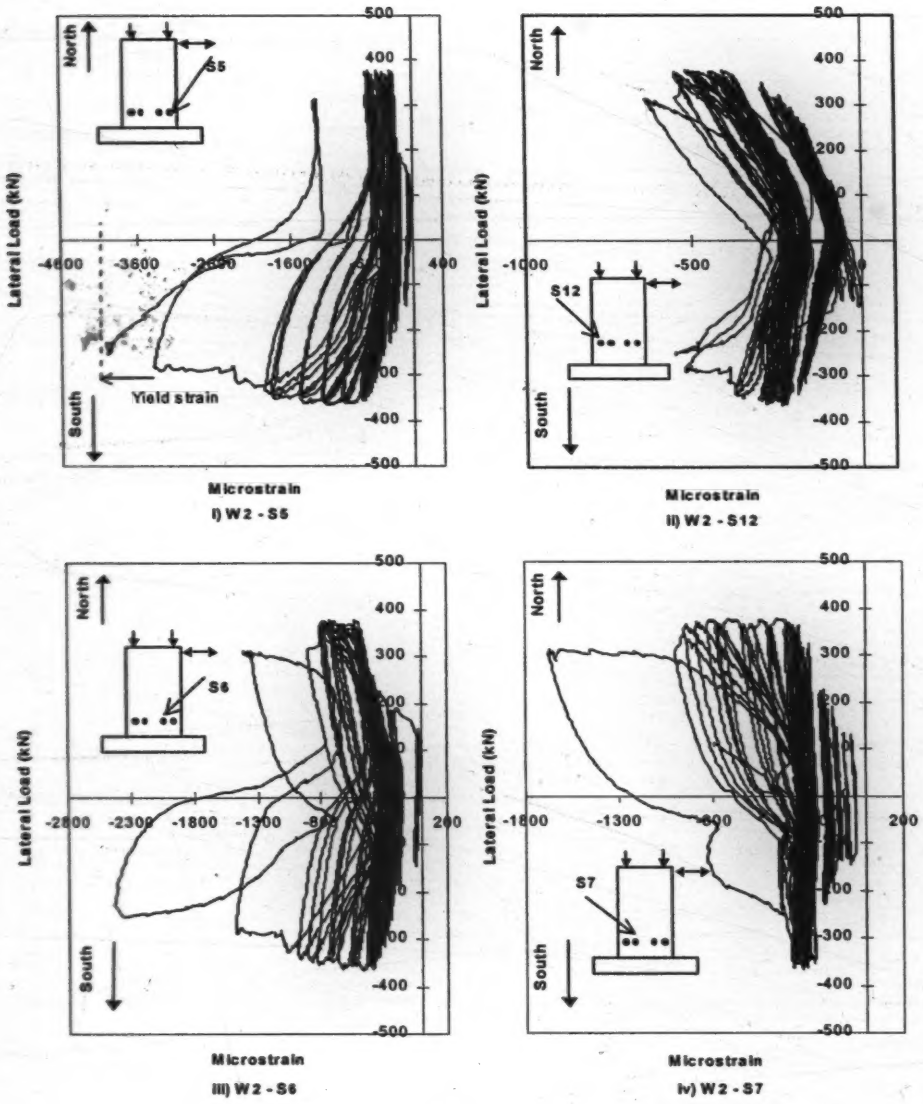

Figure 4.11(b) Strain in the double head studs of W-2

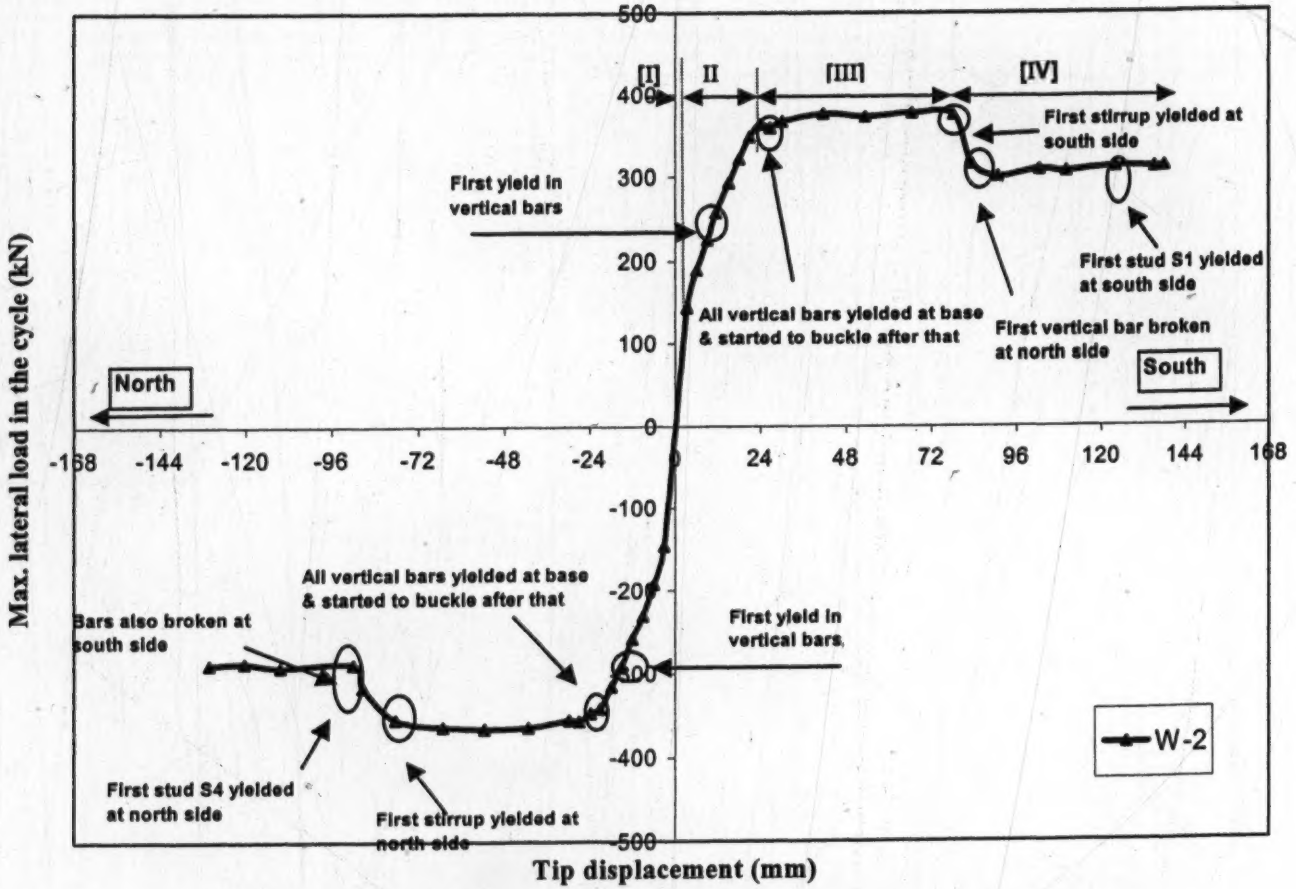
Max. lateral load in the cycle (kN)
Tip displacement (mm)
[I]
II
[III]
[IV]
First yield in vertical bars
First stirrup yielded at south side
First stud S1 yielded at south side
All vertical bars yielded at base & started to buckle after that
First vertical bar broken at north side
North
South
All vertical bars yielded at base & started to buckle after that
Bars also broken at south side
First yield in vertical bars
First stud S4 yielded at north side
First stirrup yielded at north side
W-2

Figure 4.12 W-2 Four stages of response with summary of events occurred during test

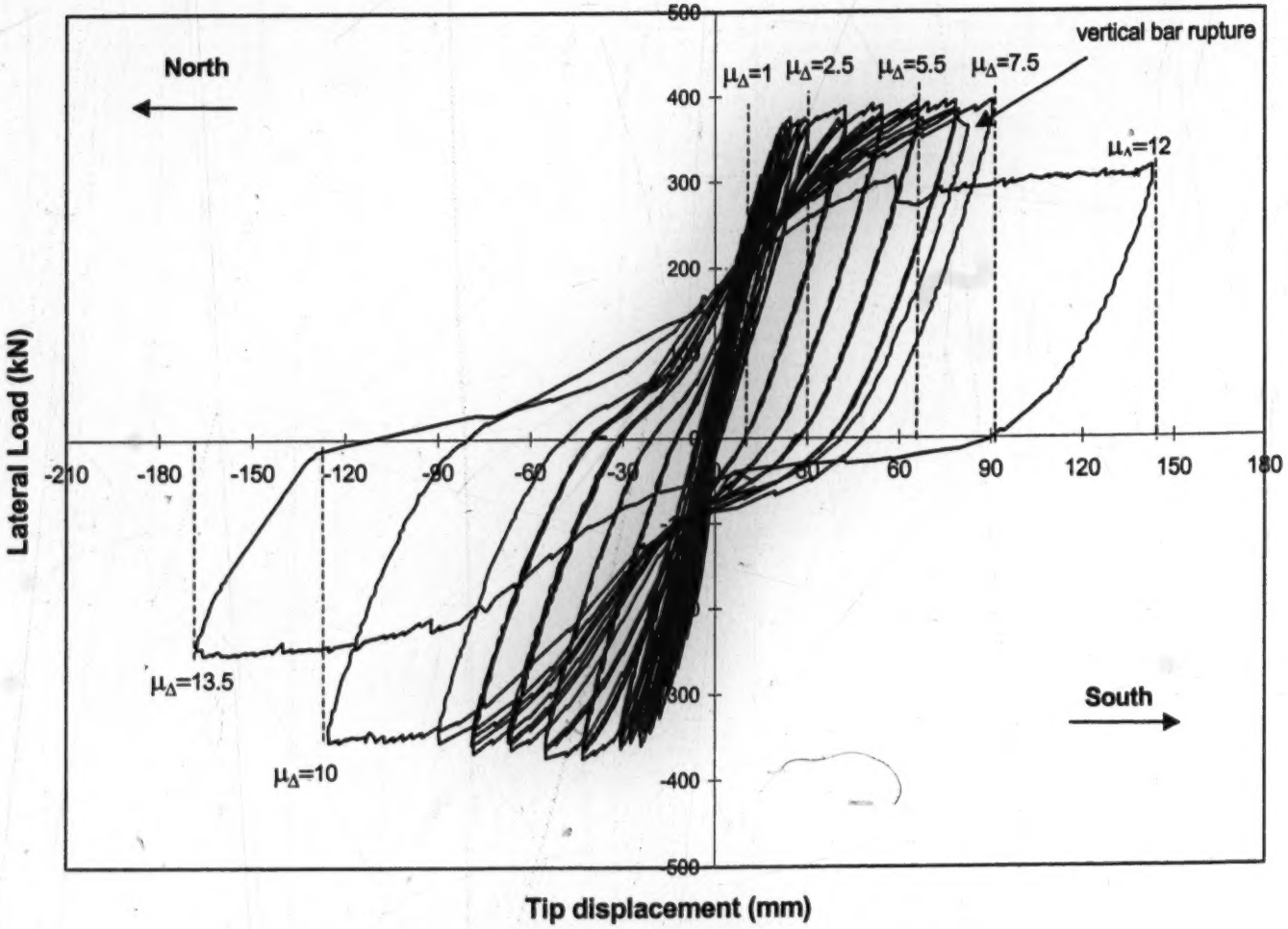

Figure 4.13 Lateral load Vs tip displacement response of W-3

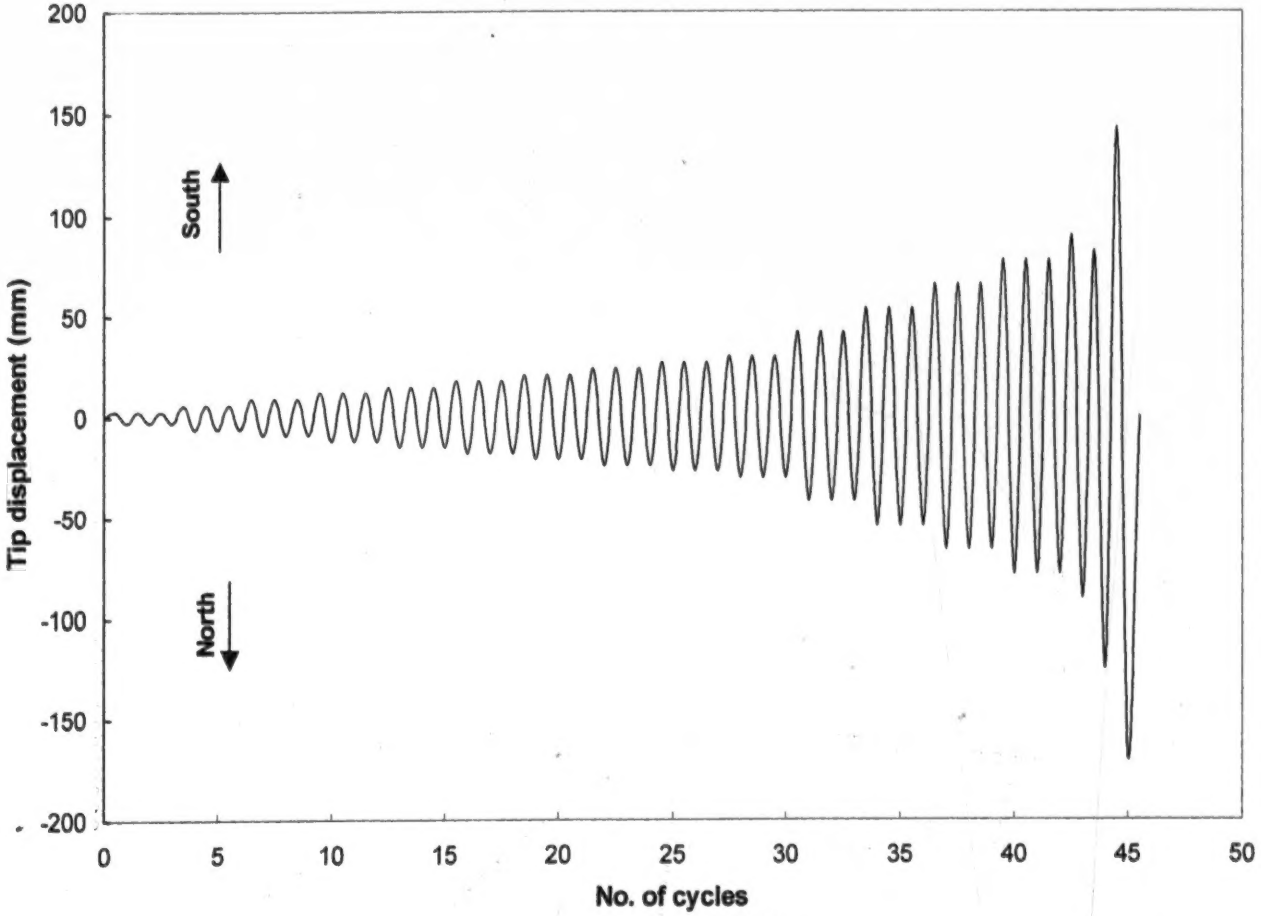

Figure 4.14 W-3 Loading history

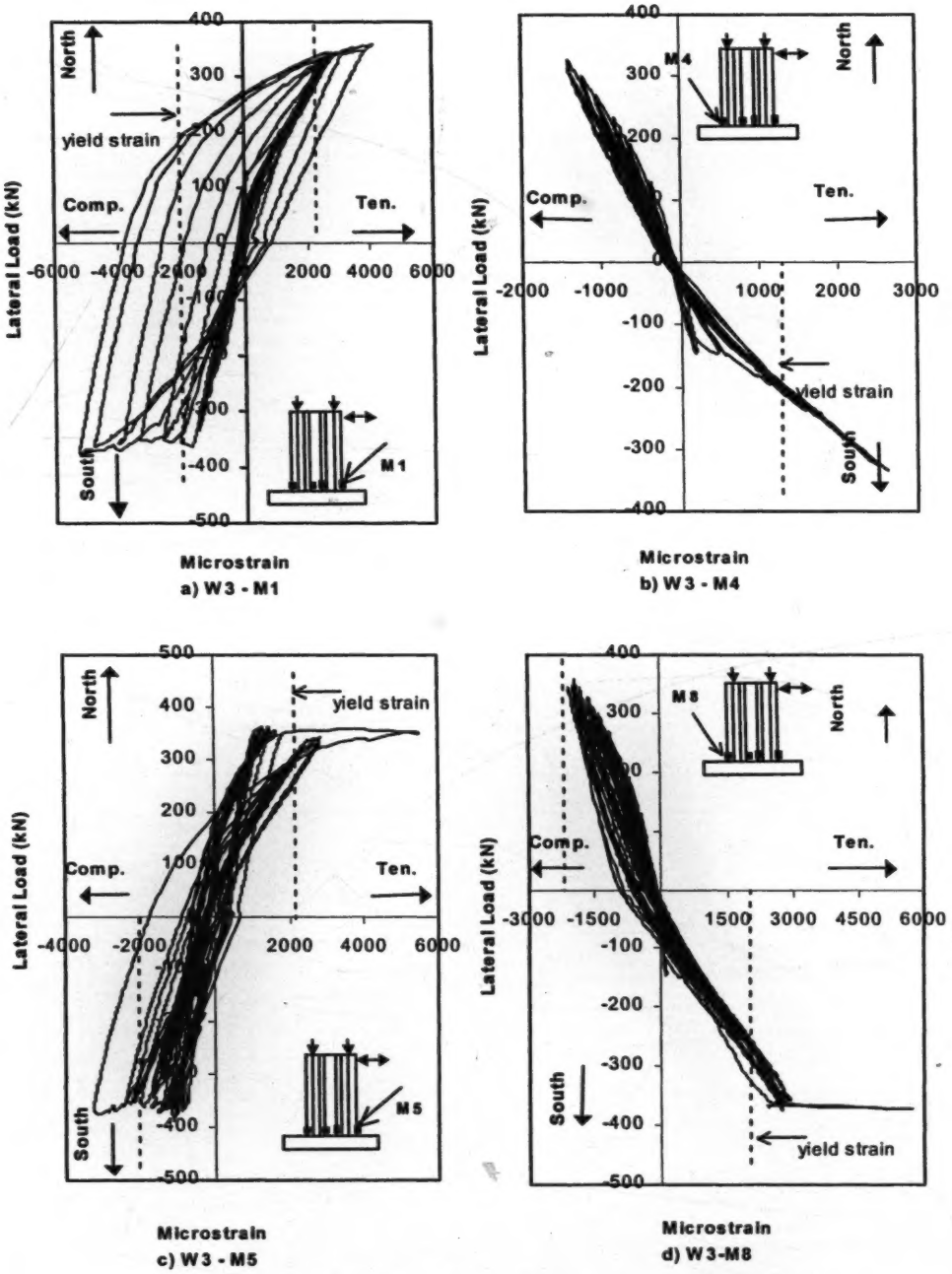

Figure 4.15(a) Strain in the vertical bars of W-3

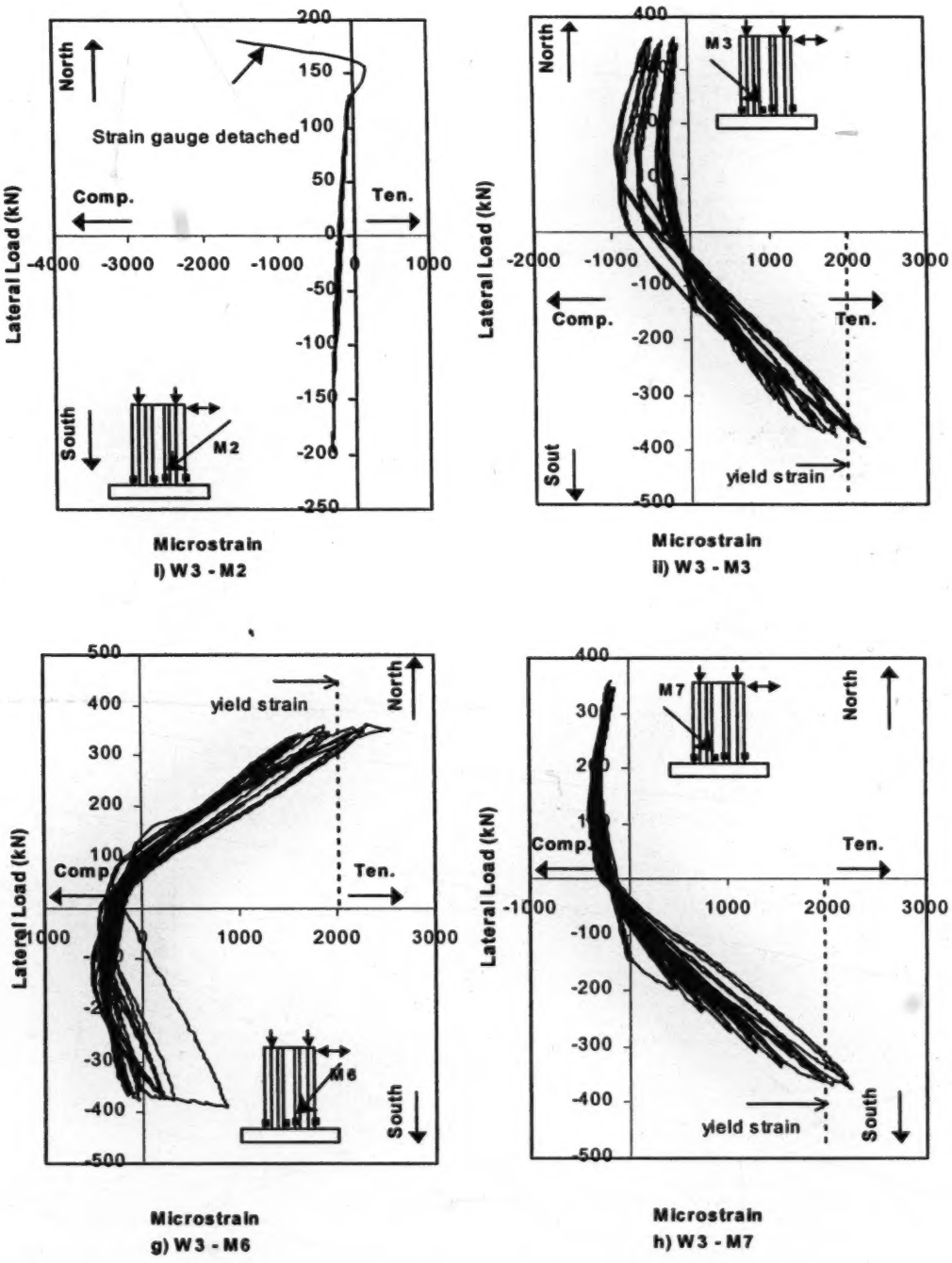

Figure 4.15(b) Strain in the vertical bars of W-3

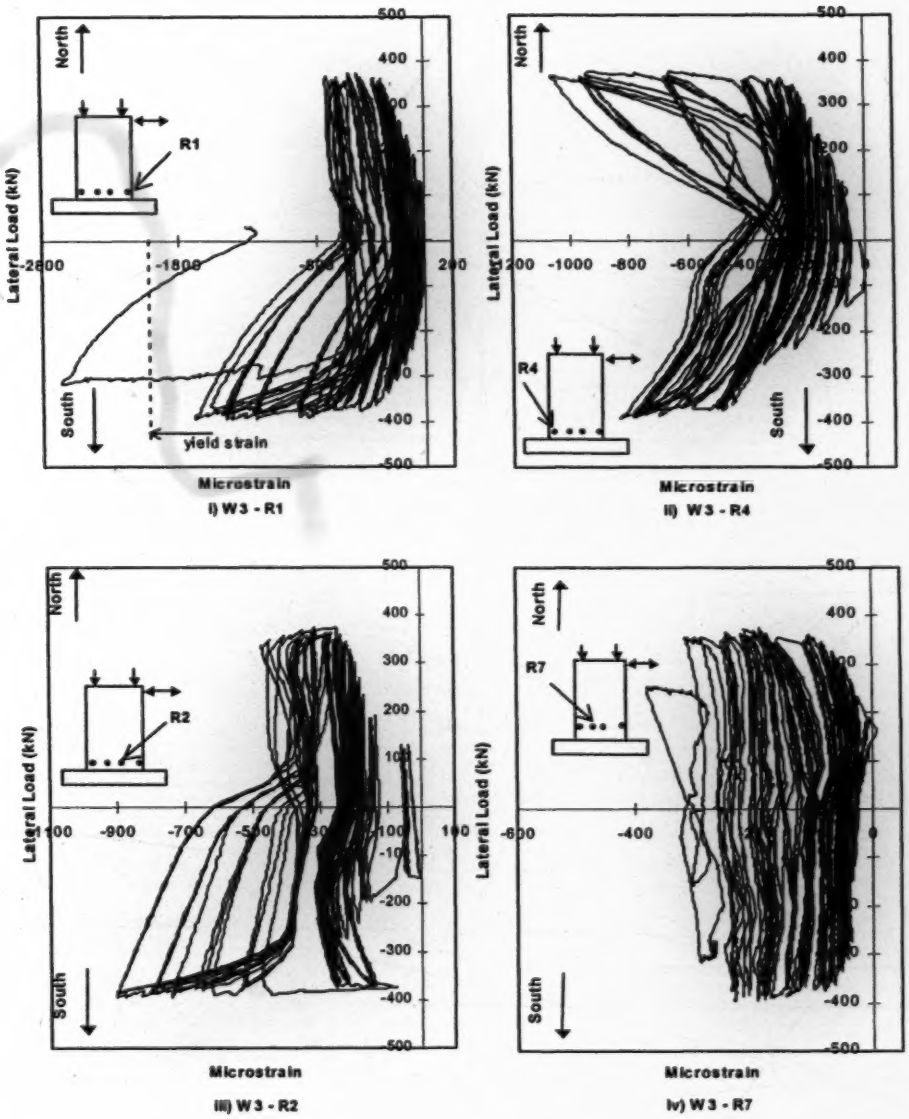

Figure 4.16(a) Strain in the stirrups of W-3

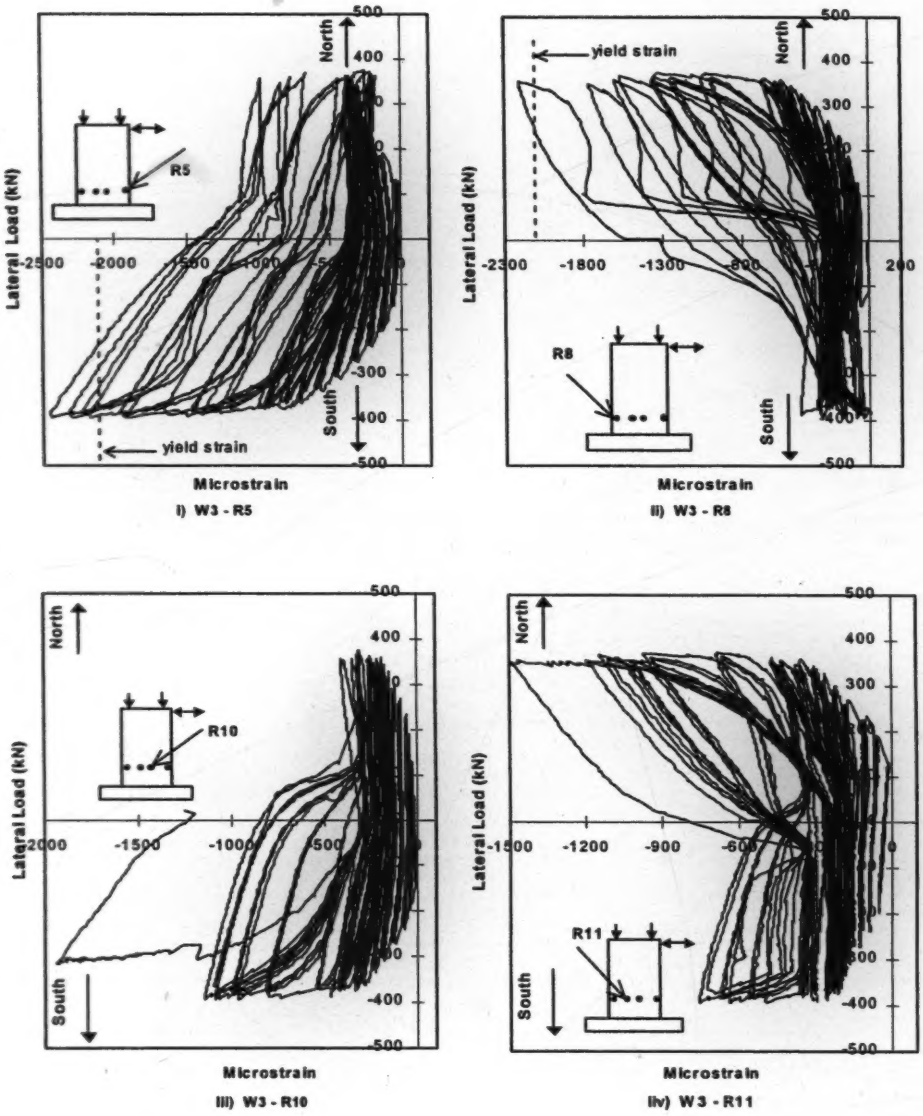

Figure 4.16(b) Strain in the stirrups of W-3

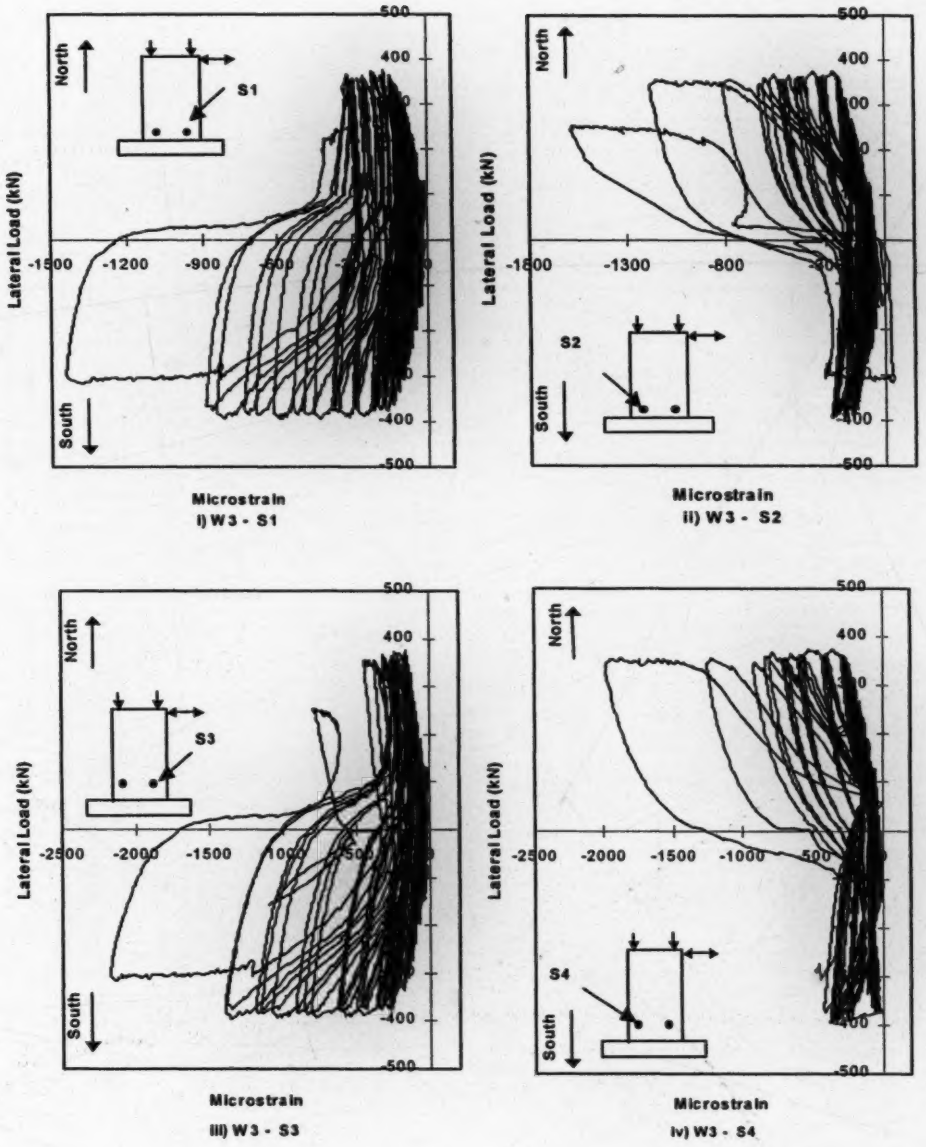

Figure 4.17(a) Strain in the Double Head Studs of W-3

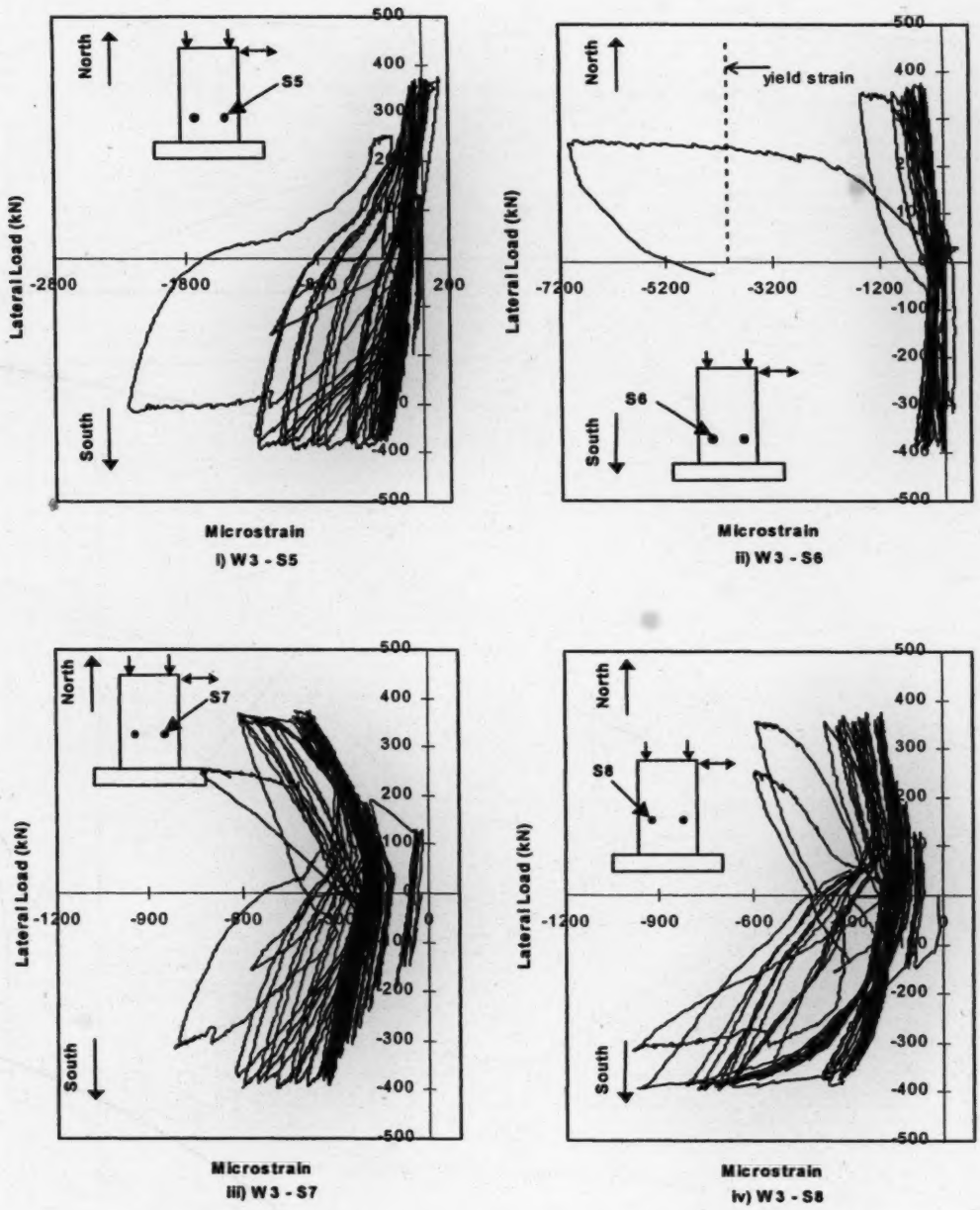

Figure 4.17(b) Strain in the Double Head Studs of W-3

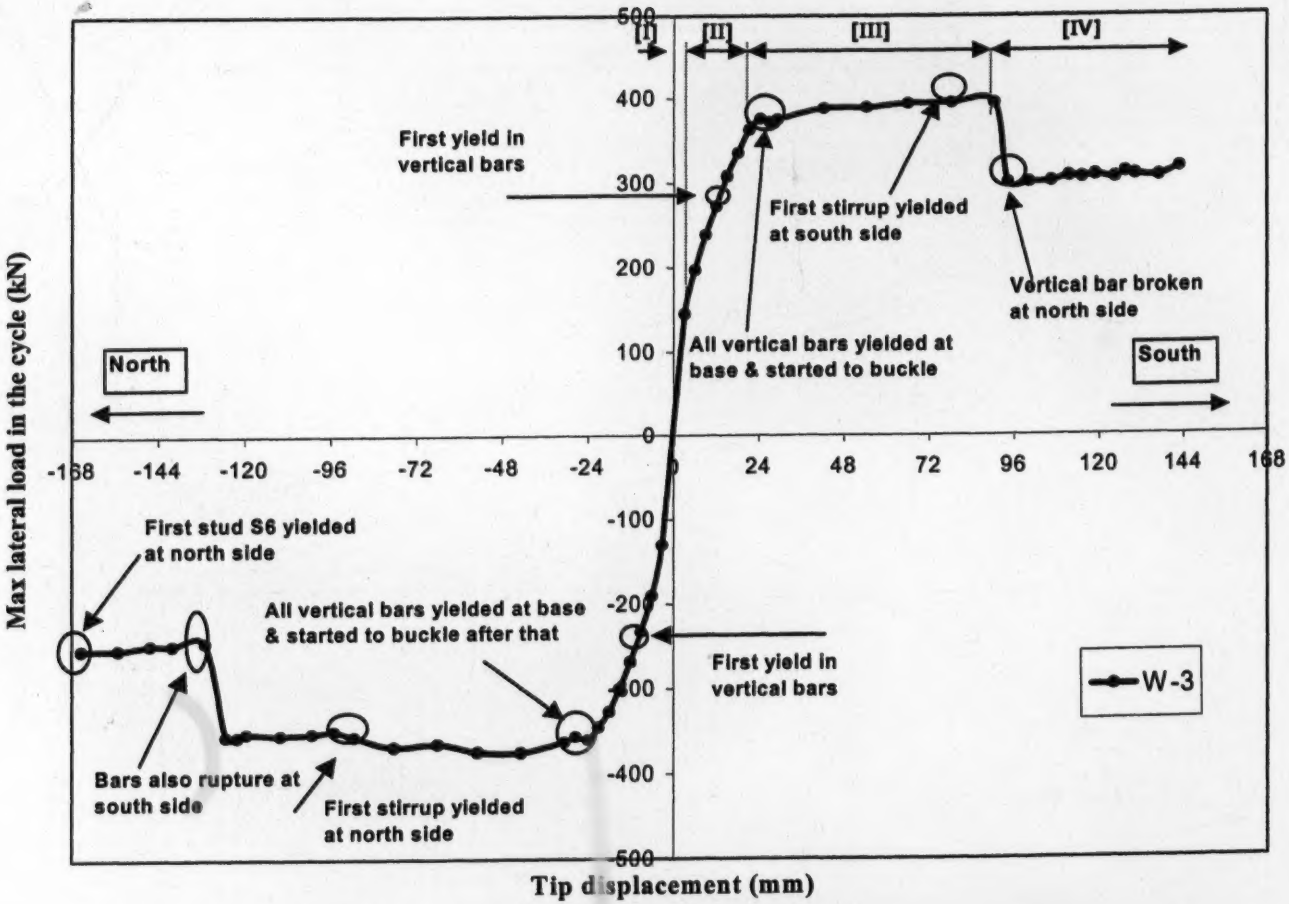

Figure 4.18 W-3 Four stages of response with summary of events occurred during test

Figure 4.19 West side view of W-1 after the test, with broken bar visible

Figure 4.20 East side view of W-1 after the test, with buckled bar visible

Figure 4.21 South side view of W-1 after test with broken bar visible

Figure 4.22 North side view of W-1 after test with buckled bars

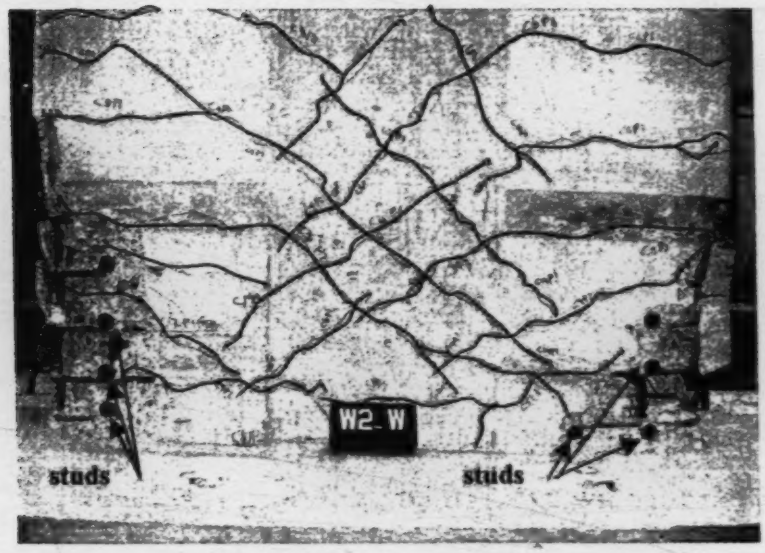

Figure 4.23 West side view of W-2 after test with broken bars & studs visible

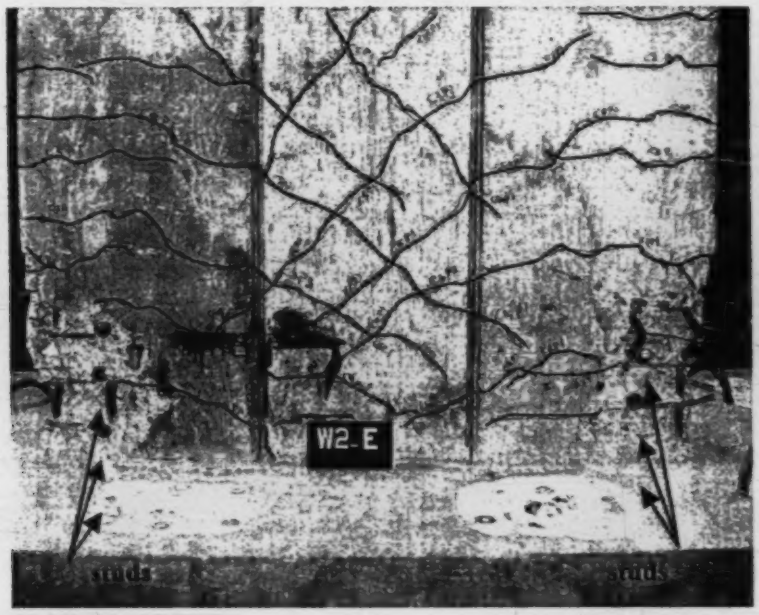

Figure 4.24 East side view of W-2 after test with broken bars & studs visible

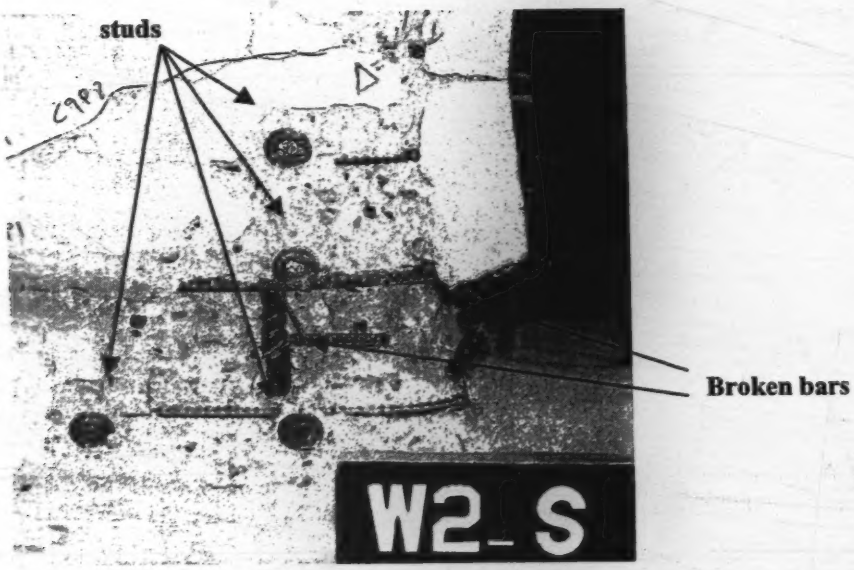

Figure 4.25 Broken bars visible at south side of W-2 after test

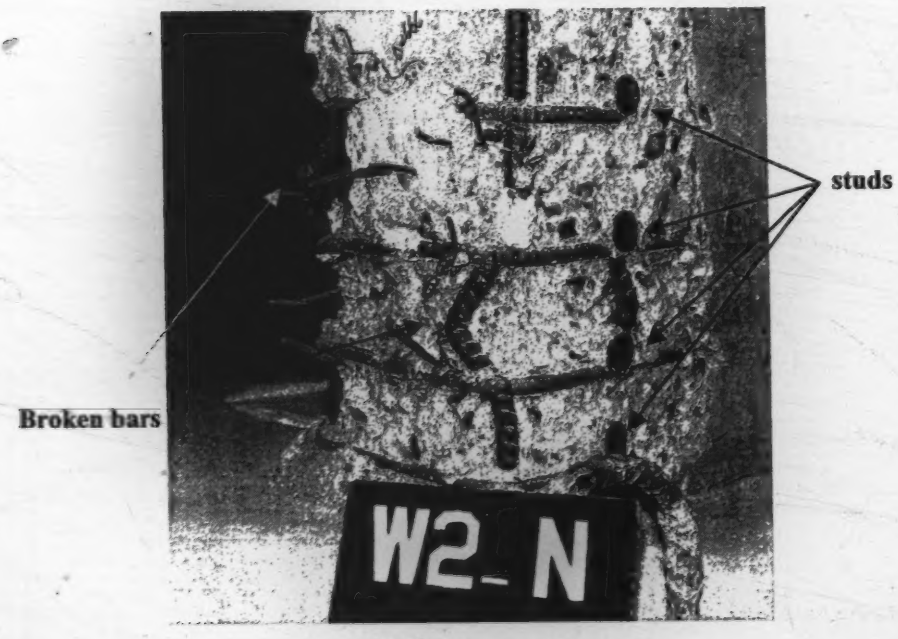

Figure 4.26 Broken bars visible at north side of W-2 after test

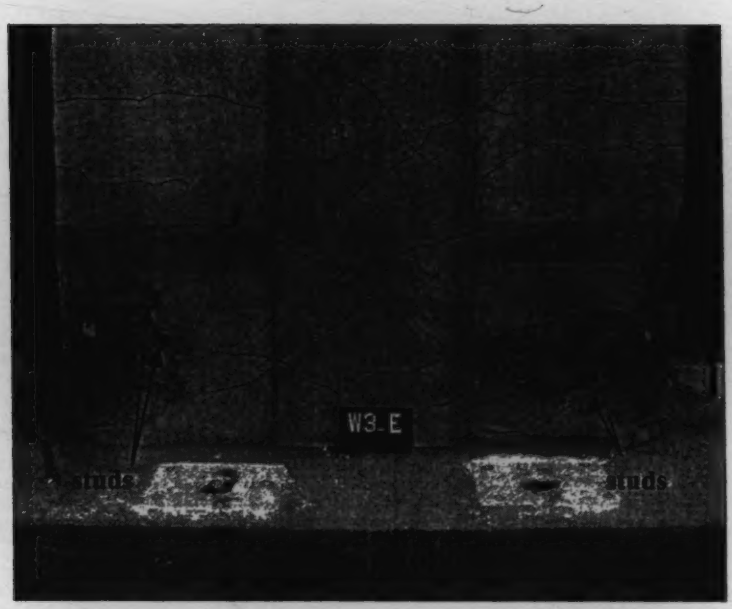

Figure 4.27 East side view of W-3 after test with broken bars & studs visible

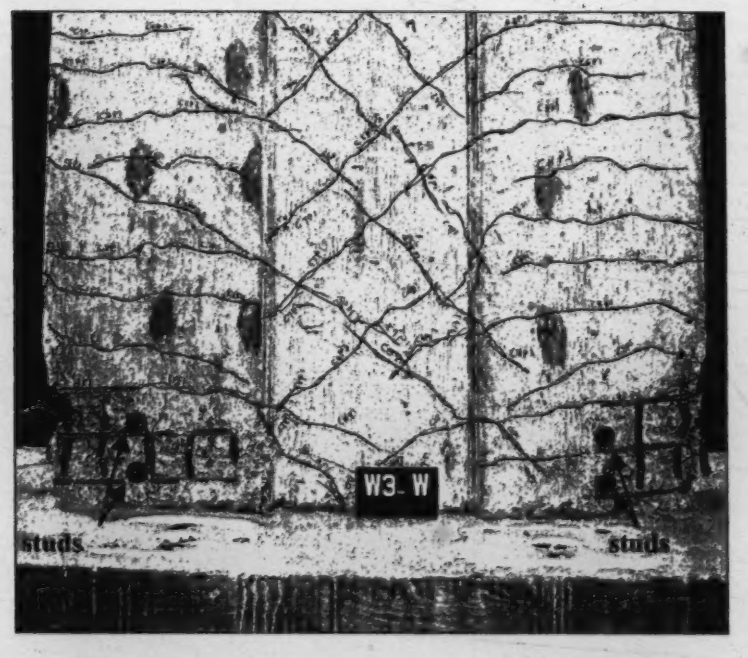

Figure 4.28 West side view of W-3 after test with broken bars & studs visible

Figure 4.29 Broken bars are visible at south face of W-3 after test

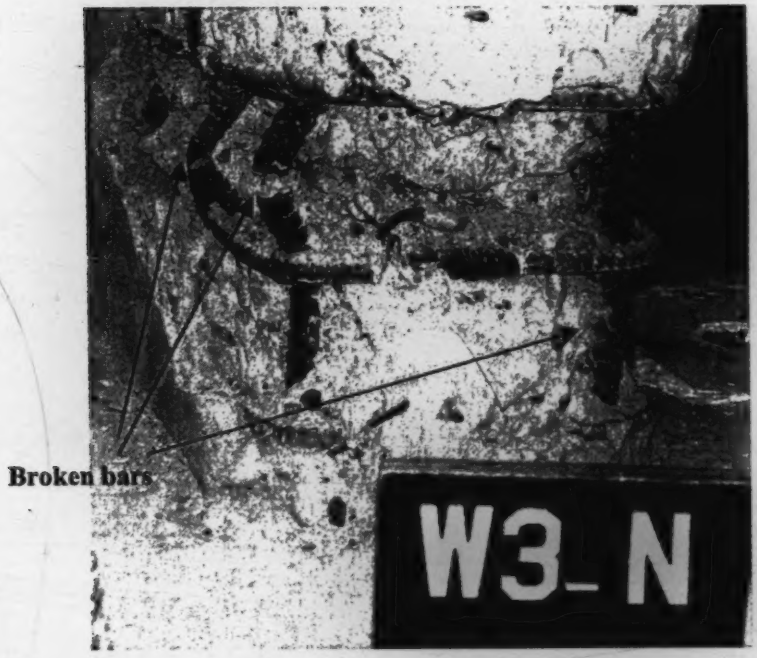

Figure 4.30 Broken bars are visible at north face of W-3 after test

CHAPTER 5

ANALYSIS OF TEST RESULTS

5.1 Introduction

This chapter presents a comprehensive comparative test-results analysis. It includes comparison of shear walls tested in the current testing program as well as in some other previous research work. The comparison is carried out on the basis of different parameters but it is limited to the shear walls falling in an identical behavioral category. Shear walls tested in other literature exhibited different behavior depending upon their aspect ratio (h/w) even after possessing identical nominal flexural capacities. Shear walls having aspect ratio (h/w) less than 1.0 have been categorized as shear dominated walls, as shear deformations dominate in their response, while walls having h/w ratio greater than 2.0 have been categorized as the flexural dominated shear walls, as the flexural deformations dominate in their response under the action of lateral loads. The present comparative study is limited to the tests of shear walls having h/w ratio greater than 2.0 as most of the tall buildings or structures have shear walls with h/w ratio exceeding 2.0.

The chapter mainly presents two comparisons; the first comparison includes the three walls of the current testing program only, while the second comparison extends to walls tested in other research programs. The comparative study is intended to highlight the role of confinement in the boundary elements of reinforced concrete shear walls in affecting their strength and ductility.

5.2 Nominal strength capacities prediction

In a comparative study, it is usually required to normalize the strength parameters with respect to the nominal strength capacities predicted by some recognized and globally accepted tools or standards. In this thesis, the nominal flexural, axial and shear capacities are predicted according to ACI-318-2002 code. Shear walls, with h/w ratio greater than 2.0, behave like a reinforced concrete member under axial compression and bending moment. Therefore, strain compatibility analysis of the wall cross-section under a constant axial load is required for the prediction of nominal moment capacity.

Nominal cross-sectional moment capacity M_n of the selected walls, under a constant axial load (if applied in the test), is calculated by using the computer software PCA-COL and PCA-IRR (1995), developed by the Portland Cement Association. The software PCA-COL and PCA-IRR basically formulates the nominal load-moment interaction diagrams for concrete members in compression and bending by strain compatibility analysis without considering the work hardening of steel reinforcement and the enhanced concrete strength due to the confinement effect. It fulfills the requirements of the ACI 318-2002 code regarding strength reduction factors and upper and lower limits of the nominal strength capacities. It is important to mention that all wall sections are analyzed.

Nominal axial load carrying capacity P_n, without any bending moment acting, is calculated according to Section 10.3.5.2, *flexural and axial loads* (ACI 318-95) as:

$$\phi P_{n\,(max)} = 0.80\,\phi\,[0.85\,f'_c\,(A_g - A_{st}) + f_y\,A_{st}] \qquad \textbf{(ACI Eq.10-2)}$$

Nominal shear strength of the walls V_n is calculated according to Section 21.7.4, *special provisions for seismic design* (ACI 318-2002) for walls with h/w ratio greater than 2.0 as:

$V_n = A_{cv} (2\sqrt{f'_c} + \rho_h f_y)$ (ACI Eq.21-7)

5.3 Comparison of the three walls of the current testing program

Four aspects are considered in the following. These include the lateral response strength, ductility and energy absorption.

5.3.1 Lateral load versus tip displacement response

Hysteresis loops of three wall specimens are already presented in Section 4.35 and are shown in Figures 4.1,4.7 and 4.13. Summaries of the test history of individual walls are also described in detail in Section 4.3.1 through 4.3.3 and also presented in Figures 4.6 and 4.12 and 4.18. For comparison, the summarized test histories are presented again here in Figures 5.1 through 5.3 and the envelope of the response of the three walls up to 78 mm tip deflection is shown in Figure 5.4. The comparison limit for the three walls is set up to the second cycle of 78 mm tip displacement. At that level the first vertical bar of wall, W-1 ruptured, but in W-2 and W-3, none of the vertical bars ruptured before this tip-displacement. Figure 5.5 shows the variation of maximum lateral load in a cycle plotted against the tip deflection, for the three wall-specimens up to tip displacement of 78 mm. The response of the three wall specimens up to the end of test is shown in Figure 5.6. The response of the three walls are similar to each other and can be sub-divided into four idealized stages as shown in Figure 5.6.

Stage I (Initial)

In this stage, the stiffness of each walls specimen matched the uncracked section stiffness. First crack in all three specimens was formed at a tip displacement of 3 mm. After that level the stiffness reduced as a result of cracking in all three walls.

Stage II (cracked walls)

In this stage, the stiffness of the wall specimens continuously reduced because of the spread of cracking including formation of new cracks as well as opening of the previously formed cracks. The extreme vertical reinforcement of the boundary elements also yielded in this stage including some inner bars close to the neutral axis of the section. This stage ended at a tip displacement of approximately 21mm to 24mm, which corresponds to a displacement ductility ratio (μ_Δ) of approximately 2.

Stage III (Maximum lateral load)

This is ideally a constant lateral-load plateau, although there is small variation in the load, but, compared to the previous stages, we can idealize it as constant load stage. Remaining inner vertical bars of the boundary elements also yielded at the start of this stage and cracking in concrete further spread, specially, the diagonal cracks through the web of the wall. Spalling of the concrete also started in this stage after the formation of cracks in the concrete cover during compressive cycle. The length of Stage-III plateau is different in the three wall specimens and it is an indication of ductility capacity of the respective wall. This stage started from the displacement ductility ratio (μ_Δ) of 2.0 for the three walls but it lasted up to $\mu_\Delta = 6.5$ for walls W-1 and W-2 and up to $\mu_\Delta = 7.5$ for W-3, which indicates that W-3 showed more ductility compared to W-1 and W-2.

The other significant difference in the test history of three walls in stage III is the early yielding of stirrups in W-1 compared to the other two walls as indicated in Figures 5.1 through 5.3. The confinement stirrups in W-1, close to the base, started to yield at $\mu_\Delta = 4.5$, while in W-2 and W-3 the stirrup's yielding started at $\mu_\Delta = 6.5$. The early yielding of stirrups in W-1 indicates that the lateral bulging of concrete was resisted more by the stirrups in W-1 compared to W-2 and W-3. Consequently it can be said that in walls W-2 and W-3 double head studs resisted the lateral bulging of concrete better than the conventional cross ties in addition to the resistance offered by the stirrups.

Crossties in wall W-1 and double head studs in wall W-2 and W-3 had reached nearly 50 to 75% of their yield strain at the time when the stirrups yielded. Stage III ends

at the initiation of the fracture of vertical flexural reinforcement of the boundary elements resulting in the drop of lateral-load carrying capacity of walls.

Stage IV (Failure)

This is a load-shedding and failure stage, initiated by the breaking of vertical reinforcing bars, resulting in a sudden drop in lateral load capacity and wall stiffness. The first drop in lateral load was approximately 5-10%. After the first vertical bar broke, the test specimens were subjected to big lateral displacements in the desirable direction to attain higher displacement ductility levels. Lateral load carrying capacity further dropped due to fracture of more vertical rebars in the boundary elements. During subsequent large displacement cycles further confinement reinforcements including stirrups, crossties (in W-1) and double head studs (in W-2 and W-3) yielded.

5.3.2 Strength comparison

Wall W-1 achieved a maximum lateral load of 375.95 kN, W-2 achieved 376.7 kN and W-3 achieved 394.393 kN. The difference in the lateral load level achieved between W-1 and W-2 is negligible but W-3 achieved 4.9 % more lateral load as compared to W-1 and 4.7 % as compared to W-2. The increase in the lateral load capacity of W-3 can be because of 12% higher f'_c compared to W-1 (Refer to Table 3.1) or better confinement. Nominal cross-sectional moment capacities of the three wall specimens are calculated, using their actual measured material properties, under a constant axial load of 1025 kN and are presented in Table 5.1 (d). The table also shows the moment capacity achieved in each wall test relative to the nominal predicted moment capacity. All three walls exceeded their predicted moment capacities by: 41 % for W-1, 39% for W-2, and 43 % for W-3.

5.3.3 Ductility comparison

Ductility in the wall tests is observed and compared by evaluating the displacement ductility ratio (μ_Δ), defined as the ratio of the ultimate tip displacement of wall achieved in the test to the tip displacement at yield (Δ_u/Δ_y). Refer to table 5.1 for the numerical values of the displacement ductility ratio for the three wall specimens. It is obvious from the values that, although the three tests were not proceeded up to the failure of the specimens, W-3 achieved μ_Δ of 13.5 while W-1 and W-2 achieved μ_Δ of 11. Figures 5.7 and 5.8 show and compare the displacement ductility levels achieved by three walls compared to their normalized moment and shear capacities respectively. It is obvious from the figures that W-3 achieved a displacement ductility level higher than W-1 and W-2.

Vertical reinforcement started to rupture in W-1 and W-2 at $\mu_\Delta = 6.5$, which corresponds to the tip displacement of 78 mm but in W-3 the first bar ruptures at $\mu_\Delta = 7.5$, which corresponds to 90 mm tip displacement. W-3 achieved 15 % more μ_Δ at the onset of the first bar ruptured. Similarly W-3 achieved 36 % more ($\Delta_{\text{ultimate load}} / \Delta_y$) ratio as compared to both W-1 and W-2.

Another factor that affects the behavior of structural members in inelastic range is the number of inelastic cycles during the loading history. In reinforced concrete members, under fully reversible cyclic loading, steel reinforcement sometimes fractures because of either low cycle fatigue or because of accumulated excessive plastic strain in consecutive inelastic cycles, including large plastic deformations due to the buckling of bars in compression phase of the cycle. Similarly concrete starts spalling off after being cracked in previous cycles in tension causing a degradation effect on strength and stiffness of the member. Table 5.1 presents the total number of inelastic cycles achieved by each wall and Figure 5.9 shows same in a graphical form relative to the normalized nominal strengths. W-3 completed 10% more inelastic cycles than W-1 and 4.7 % more than to W-2. Figure 5.10 shows the effect of the number of inelastic cycles on the displacement ductility ratio.

5.3.4 Energy absorption

The area enclosed within the lateral load versus tip displacement response (or the hysteresis loop) is a measure of the energy absorbed by the wall specimens. Figures 5.11 through 5.14 show the variation in the energy absorbed by the walls with the increment in tip displacement towards the South. Figure 5.15 shows a comparison of the energy absorbed by the three walls up to the second cycle of the ductility ratio of 6.5 (tip displacement of 78 mm), after that cycle breaking of the vertical bars initiated in W-1. Figure 5.14 shows that W-3, which was confined with larger studs, absorbed 43 % more energy compared to W-1 at the onset of rupture of first vertical bar. Similarly W-2, which was confined with smaller studs showed a 22 % increase in the energy absorption compared to W-1 at the onset of rupture of first vertical bar.

It is obvious from Figure 5.15 that there is a sudden drop in the energy absorption rate in all three wall-specimens after the ductility ratio of 2.5 (tip displacement of 30 mm). The obvious reason is the yielding of all the main flexural reinforcement in all three walls at this ductility level. After the drop, the rate of energy absorption increased in all three walls in an identical manner. Figure 5.16 shows the energy absorption in each cycle while 5.17 shows the variation in cumulative energy absorbed with displacement cycles. Similar energy calculations are carried out for the north side. Figure 5.18 shows the variation in energy absorption with tip displacement towards north. Observing the energy absorption plots of the three walls up to the identical displacement levels, it can be concluded that the W-3 absorbed significantly higher energy than the other two walls at the onset of first bar ruptured.

5.4 Comparison of the current tests with previous tests in different research programs

A detailed comparative study is performed to assess the trend of shear wall behavior in different research programs with different geometric parameters, reinforcement distribution and different loading conditions. The main objective of the

comparative study is to investigate the role of confinement in affecting the strength, ductility and the failure modes of reinforced concrete shear walls. Four research programs are selected in this study including the current research work. A review of each research program, including the test objectives, specimen's description, test type, test results and the tests conclusions, is already presented in Chapter 2 but a brief introduction of each program is presented in the next section. The information provided in these research programs is reported through either journal publications or engineering reports provided by the institutes. The description of the test specimens, loading conditions, geometric and material properties including reinforcement configuration and distribution are tabulated in Table 5.1. It is important to mention here that some of the comparison parameters are not mentioned numerically in the published reports and these are thus calculated manually with the help of detailed drawings or figures provided in these reports or journal publications. The manually computed parameters include gross cross-sectional area (A_g), aspect ratio of walls (h/w), percentage of flexural steel reinforcement (ρ_f), percentage of horizontal shear reinforcement (ρ_h), volumetric ratio of the transverse confinement reinforcement in the boundary elements (ρ_s) and displacement ductility ratio (μ_Δ, which is calculated from the lateral load versus tip displacement response of the test specimens). It is also important to mention here that the maximum moment noted for any test in Table 5.1 does not include P-Δ effect. Flexural, axial and shear capacities are also calculated by using methods and equations mentioned in Section 5.2 and are presented in Table 5.1.

Coreley, W. G., Fiarto, A. E.,Oesterle, R. G., (1980)

Corley, et al. (1980) tested a total of 16 reinforced concrete shear walls, under a research program conducted by Engineering Development Division, Portland Cement Association, supported by the National Science Foundation, Skokie. Out of the 16, two are rectangular section shear walls, twelve are barbell sections, two are flanged and two are rectangular section. Refer to Chapter 2 for the review of test parameters, test results and conclusions. For the current comparative study, only the barbell sections are selected, since the flanged-section walls are not suited for the current comparison and the

rectangular section are also not included as their detailed drawings and the test results are not available in the referenced documents available.

Within the twelve barbell-section walls, nine walls (B1 to B9) are selected for the comparison while the remaining walls are dropped out because of not having similar test objectives. Of the nine wall specimens, one specimen (B9) was loaded with modified reversing load cycles and one specimen (B4) was loaded with monotonic loading, while the remaining seven specimens were loaded with reversing load cycles. Details of the loading procedure are not available in the research publication including the number of cycles at each load or displacement level and also about the test controlling method (load control or displacement control). However the test results show that three cycles were performed at every load (or displacement) level. All other related information and data are summarized in Table 5.1.

Dazio, A., Wenk, T., and Bachmann, H. (1999)

Dazio, et al.(1999) tested six concrete shear walls (WSH1 to WSH6) at the Laboratories of the Institute of Structural Engineering (IBK), Swiss Federal Institute of Technology (ETH), Zurich. The walls were rectangular cross-sectioned and were tested under fully reversible quasi-static cyclic loading. Refer to Chapter No. 2, Section 2.4.1 for the summary of the testing program, specimen's description and review of the test results. For the comparative study here, geometric and material properties of test specimens, loading procedures and test results are presented in table 5.1. Nominal flexural, axial and shear capacities are also calculated by using the detailed sketches provided in the research report by the methods described in Section 5.2 These are also summarized in table 5.1.

Cardenas, A. E. and Magura, D. D. (1973)

Cardenas, A.E and Magura, D.D (1973) carried out tests on six rectangular cross-sectioned, reinforced concrete shear walls (SW-1 to SW-6) at the Structural development

laboratory of Portland Cement association. The tests were carried out monotonically with main parameters being the amount and distribution of the flexural reinforcement. The related research publication presents the description of the specimens and the reinforcement distribution in a tabular form showing only the percentage of horizontal and vertical reinforcement (ρ_f and ρ_h) without any detailed drawing for the reinforcement layout, so, for computing the nominal strength parameters, the distribution and type of reinforcement is best approximated here in order to meet the vertical and horizontal reinforcement steel ratios mentioned in the available document. Similarly, the vertical flexural steel reinforcement is assumed to be provided in a single row because of the small wall thickness (3 inches) and is also obvious from the photograph shown in the corresponding referenced paper (Figure A-1) showing the photograph of a steel cage prior to concreting. All the provided and computed parameters are summarized in Table 5.1. Based on the information provided in the available publication and the computed parameters discussed above, nominal flexural, axial and shear capacities are calculated by using the methods described in Section 5.2. These are also summarized in table 5.1. The available research paper provides only the Moment-curvature response of the tested specimens including the information of the yield and ultimate curvatures (ϕ_y and ϕ_u). Curvature ductility ratios (μ_ϕ) are also tabulated in the published paper which is defined as the ratio of ultimate to the yield curvature (ϕ_u / ϕ_y). To achieve the displacement ductility ratio (μ_Δ), which is required for the comparative study, Figure 5.33 (Paulay and Priestley, 1992) is used which is provided in Section 5.4.3, Paulay and Priestley (1992) which gives a graphical relation between μ_ϕ and μ_Δ with variation in h/w ratio for structural walls.

5.4.1 Analysis of results of the comparative study

Variation of desirable parameters has been studied with the intention of focusing on "the confinement in boundary elements" as the key parameter and all other strength and ductility parameters are studied with reference to the key parameter. The results of the comparative study, as tabulated in Table 5.1, are studied and plotted graphically and will be discussed in detail in two major categories. First category presents the results of

the comparative study performed on the strength affecting parameters like flexure, shear or axial capacities, while the other category presents the results of the comparison performed on the ductility affecting parameters like the displacement ductility ratio (μ_Δ), or the number of inelastic cycles etc.

5.4.2 Discussion of the results involving the Strength parameters

The strength parameters in the present study include bending moment, shear force and axial load. Axial load is not a variable parameter in the shear wall tests and it is usually applied as a constant quantity representing some fraction of the compressive strength of concrete. The intention again here is to highlight the confinement affect on different strength parameters.

Effect of confinement on flexure capacity

Figure 5.20, shows the effect of variation in volumetric ratio of confinement on the flexural capacities of different walls normalized with their nominal moment capacities (M_n). It is obvious from the figure that in most of the tests the effect of increase in the confinement volumetric ratio results in increase in the flexural capacity of walls, provided that axial load ratio is not high. Walls having 0 % confinement (Cardenas, 1973) achieved $M_{max} / M_n = 1.27$, while wall having maximum 2.64 % confinement (B9 Corley, 1980) achieved M_{max} / M_n of 1.54, which is 21 % higher than the wall with 0 % confinement. It appears from this comparison that the flexural capacity has increased by the increase in confinement volumetric ratio but there are also some other factors like axial load (P_{max} / P_n) ratio and wall cross-section type, which are also affecting the above comparison. The effect of axial load ratio on M_{max} / M_n versus confinement amount relation could be assessed by comparing the behavior of B5 and B7 (Corley, 1980). Both walls have the same cross-section, vertical steel reinforcement and confinement steel ratio; B5 has 0.0 % axial load ratio while B7 has 9.3 % axial load ratio; but the gain in M_{max} / M_n in B7 is 5 % only. B9 appears to be the wall with highest M_{max} / M_n ratio of 1.54, it might be because of the loading procedure of B9 that was more or less a

monotonic loading. Walls B8 and B6 also noted to have high M_{max} / M_n ratios, B8 achieved only 2 % higher M_{max} / M_n than B6 due to an enhancing effect of increase in confinement reinforcement by 64 % but at the same time a degrading effect of increase of axial load ratio (P_{max} / P_n) on B6 by 25 %.

A useful comparison can be made between walls having high and close P_{max} / P_n ratio. Figure 5.21 shows this comparison between B6 (Corley, 1980) and W-1, W-2, W-3 of this thesis. The three walls of this thesis have nearly identical confinement volumetric ratio of approximately 1.9 % which is higher than B6 confinement amount by 18 % approximately, but, M_{max} / M_n appeared to be decreased by 4 % to 6 % in W-1, W-2 and W-3, instead of increasing although P_{max} / P_n is little higher in all the three walls of this thesis. Two reasons become obvious in this comparison, first is the **shape effect** of the B6 cross section (barbell shape) and the other reason is 2.3 times higher flexural reinforcement ratio (ρ_f) in the boundary elements of B6 compared to the (ρ_f) in the boundary elements of W-1, W-2 and W-3. Barbell shape attract more lateral shear than its anticipated nominal capacity due to strong dowel action provided by the boundary elements which in turn increases the maximum moment (M_{max}). Comparing two walls of Dazio et al. (1999), WSH6 has 33 % more confinement ratio than WSH5 but the gain in M_{max} / M_n is only 5 %, the main reason being the P_{max} / P_n ratio which is 22 % higher in WSH5 and which increases the maximum moment in WSH5 even after a lower confinement content.

The comparison also includes walls loaded monotonically (Cardens etal, 1973), SW-1 to SW-6. It is important to note that although all six walls have 0 % confinement reinforcement, but still SW-6 achieved highest M_{max} / M_n ratio of 1.27 (within these six walls), which is 16 % higher than the SW-3 M_{max} / M_n ratio of 1.098 (lowest among these six walls). The main reason appeared to be the concentration of 30 % flexural reinforcement at the wall extremes in SW-6 compared to evenly distributed flexural reinforcement in SW-3.

Effect of Confinement on Shear capacity

In cantilever shear walls, maximum moment applied on the wall is also a function of shear force acting on the wall for a particular height of wall, keeping the applied shear below the nominal shear capacity of the wall. It is also obvious from Figure 5.22 that those walls achieved higher values of V_{max} / V_n ratio which have already found to be having higher M_{max} / M_n ratios in figure 5.20, except those walls in which the nominal shear strength (V_n) provided is high such as B8 (Corley et al.,1980). B8 achieved 30 % lower V_{max} / V_n ratio because of having 82 % high nominal shear strength (V_n) compared to B5. Axial load has the same enhancing effect on V_{max} / V_n as it has on M_{max} / M_n as obvious from comparing B5 and B7. B7 has V_{max} / V_n ratio 27 % more than B5 which is basically because of presence of 9.3 % P_{max} / P_n ratio compared to 0.0 % in B5.

B6 achieved 6.6 % less V_{max} / V_n than B7 although it has 43 % higher axial load ratio (P_{max} / P_n) which might have resulted in higher V_{max} / V_n ratio but because of 40 % higher confinement content in B7 the enhance effect of axial load ratio in B6 degraded and that is why the final result is a negligible enhancement in V_{max} / V_n ratio.

A globally experienced result can be viewed and verified here by examining the behavior of SW4 and SW5 (Cardenas, 1973) with reference to V_{max} / V_n. These are the only walls within the six walls of this testing program in which V_{max} / V_n exceeded 1.0, not only it exceeded 1.0 but appears to be highest in the present comparative study. The main reason lies in their low h/w ratio (less than 2.0), which made them shear dominating walls and hence their V_{max} / V_n is high. Another good conclusion can be drawn by viewing the SW6 behavior, whose V_{max} / V_n lies close to one. The main reason is the concentration of 33 % flexural reinforcement in the wall extremities, which enhances the shear applied to the wall and hence increases both V_{max} / V_n and M_{max} / M_n ratios. Similarly SW1 lies in the lowest regions showing very low V_{max} / V_n ratio, which could be understood by comparing it with SW2 above it. SW1 and SW2 both has uniformly

distributed vertical reinforcement but SW1 has 70 % lower total reinforcement ratio (ρ_t) than SW2 which results in decreasing the V_{max} / V_n by 37 %. A similar comparison between SW2 and SW3 shows that a decrease in ρ_t by 66 % in SW2 compared to SW1 results in the 38 % decrease in V_{max} / V_n.

Role of confinement also becomes obvious by comparing WSH5 and WSH6 of Dazio etal, (1999). WSH6 achieved 31 % more V_{max} / V_n than WSH5 although it has 18 % less P_{max} / P_n value of 1.0, the main reason being more confinement content in the boundary elements of WSH6 which is 33 % more than WSH5. Although the nominal shear strength (V_n) of WSH5 is 4 % higher than WSH6 but it is negligible for comparison.

Walls W1, W2 and W3 of this thesis show the least V_{max} / V_n ratio compared to the other walls. The main reason is the higher shear reinforcement ratio (ρ_h), which increases the nominal shear strength (V_n) of the three walls.

Concluding remarks about the effect Variation of V_{max} / V_n

V_{max} / V_n resembles the maximum shear attracted or achieved during tests by any specimen relative to its nominal shear capacity according to the ACI 318-95 Section 5.2. From Figure 5.22 it is obvious that walls from two testing programs exceeded the V_{max} / V_n value of 1.0; namely, Corley, (1980) and Cardenas (1973). The obvious reason for the two walls of Cardenas (1980) exceeding V_{max} / V_n value of 1.0 is their h/w ratio being less than 2.0 while the reasons behind the Corley, (1980) walls exceeding V_{max} / V_n value of 1.0 appears to be high P_{max} / P_n ratio and also their **barbell cross-section shape.** The shape effect can be understood by analyzing the equation used for computing V_n as it considers A_{cv} as the concrete area resisting the shear force and which only considers the area of boundary elements obtained by the extension of the web into these boundary elements, but, in reality the two big boundary elements also acting as strong columns in increasing the shear capacity (and ultimately the nominal moment capacity) of these walls through dowel action (Corley et al.,1980). The role of confinement is important in

keeping the integrity of the boundary elements and thus in turn it enhances the shear and moment capacities.

5.4.3 Role of confinement in affecting displacement ductility (μ_Δ)

Role of confinement in increasing ductility capacity has been discussed in detail in Chapter 2 and it will be studied in the present comparative study by analyzing the lateral load versus tip displacement relationship of the test specimens of the selected testing programs. The displacement ductility ratio μ_Δ was worked out from the lateral load versus tip displacement relationship of all the walls selected in the study by computing the ratio of ultimate to yield tip displacements (Δ_u / Δ_y). Refer to Table 5.1 for the computed values of μ_Δ. The displacement ductility ratio μ_Δ is plotted for all tested walls against volumetric ratio of confinement ρ_s in the boundary elements in Figure 5.23. The trend of the points in the Figure shows an increase in μ_Δ with the increase in ρ_s but there are various wall results that deviated from the general trend that reflects the degrading or enhancing effects of some factors. The dominating factors that appeared to be affecting ductility of walls are axial load ratio (P_{max} / P_n) and shear ratio (V_{max} / V_n) in addition to the confinement volumetric ratio and these are the factors that make the deviation of certain walls from the general trend in Figure 5.23. These factors will be discussed separately in detail afterwards but they are just mentioned here with reference to the Figure 5.23. B5, B6, B7, B8, B9 (Corley et al., 1980) have either high (P_{max} / P_n) or (V_{max} / V_n) ratio that is why these walls are less ductile, although most of them have high confinement reinforcement ratio (ρ_s). Similarly WSH6 has highest V_{max} / V_n ratio within its group walls along with high P_{max} / P_n. Walls, SW-1 to SW-6, belong to Cardenas et al. (1973), are all monotonically loaded tests and they have no confined boundary elements because of single layer of flexural reinforcement except that wall SW-5 and SW-6 have concentrated flexural reinforcement at their extremities.

Effect of axial load ratio (P_{max} / P_n) on displacement ductility (μ_Δ)

Variation of displacement ductility ratio (μ_Δ) with axial load ratio (P_{max} / P_n) is plotted in figure 5.24. The figure does not show a linear trend of the variation of P_{max} / P_n with μ_Δ because of the effect of several other factors or combination of other factors like V_{max} / V_n ratio and ρ_s that critically affect the ductility ratio and those are not obvious in Figure 5.24. Walls having 0 % axial load ratio like B1 and B3 (Corley et al., 1980), show high ductility ratios as they are not affected by high V_{max} / V_n ratio. Similarly ductility reduces by 54 % while comparing B5 and B6 due to 13.3 % P_{max} / P_n applied in B6 compared to 0 % in B5. Although this ductility reduction may also be caused partly by the increase in V_{max} / V_n ratio by 19 % and decrease in ρ_s by 39 % . Refer to Figure 5.25 for a clear view of axial load effect on walls with identical cross-section configuration. The ductility ratio increased by 100 % between B6 and B7 as P_{max} / P_n reduced by 30%, although there is an increase in ρ_s 64 % in B7 which will also be effecting the increase in ductility ratio. Similarly the reason of B5 appearing 10 % more ductile than B7 is the existence of P_{max} / P_n in B7 as 9.3 % as compared to 0 % in B5, although there is an increase of 27 % in V_{max} / V_n in B7 which may also be effecting ductility ratio.

Axial load effect is also obvious while comparing W3 and W1. Effect of confinement configuration in W-3 may also be affecting this comparison. W3 was reinforced with double head studs with the same volumetric ratio ρ_s as the cross ties in W1. The decrease in the ductility ratio in W1 is 18 % while the increase in P_{max} / P_n in W1 is 13 % compared to W3.

Effect of confinement content (ρ_s) on displacement ductility (μ_Δ)

The effect of confinement content on the ductility can be best studied within the walls having approximately identical values of P_{max} / P_n, identical cross-section and approximately identical values of V_{max} / V_n. Figure 5.26 shows a comparison between walls WSH3, WSH4 and WSH5 (Dazio etal, 1999) in which the effect of confinement content on increasing the ductility is highlighted. WSH5 was loaded with 132 % higher

P_{max} / P_n ratio compared to WSH3 and from the previous section it can be assumed that WSH5 would achieve low ductility but actually the ductility ratio increased by 67 % which may be due to 59 % higher ρ_s compared to WSH3. Similar conclusions can be drawn by comparing the increase in the ductility ratio by 20 % between WSH4 and WSH3, which is also because of increase in ρ_s in WSH3 by 29 % in spite of the increase in P_{max} / P_n in WSH3 compared to WSH4 by 8.5 %. The role of confinement is now become obvious in the above comparison that higher confinement content in the boundary elements results in higher ductility ratio if the effect of axial load and shear force is negligible.

Similarly comparing B1 and B3 (Corley et al., 1980), the effect of confinement also found to be enhancing the displacement ductility ratio μ_Δ. B1 and B3 carried 0 % P_{max} / P_n and the μ_Δ increases by 47 % in B3 just because of increase in the boundary element confinement by approximately 10 times compared to B1 as there is a negligible difference in the V_{max} / V_n ratio.

Another comparison that highlights the effect of confinement configuration is shown in Figure 5.23, made between W3 of this thesis and B3 of Corley et al., (1980). The ductility ratio (μ_Δ) is decreased by a small amount in W3 although there is much difference in the two walls regarding P_{max} / P_n ratio. The reduction in the μ_Δ is 12 % only while the P_{max} / P_n ratio increased from 0 in B3 to 16.2 % in W3, so, by observing the small reduction in μ_Δ in spite of a very significant increase in P_{max} / P_n it could be assumed that the studs might be providing lateral resistance to the bulging of concrete in W3 because of their geometric configuration.

Effect of shear force ratio (V_{max} / V_n) on displacement ductility (μ_Δ)

The effect of shear force ratio V_{max} / V_n is same as the axial load ratio P_{max} / P_n on the displacement ductility ratio μ_Δ. The increase in shear force ratio decreases the

ductility ratio if axial load ratio and the confinement content (ρ_s) in the boundary element are not significantly changed.

Refer to Table 5.1, comparison of B2 and B3 (Corley et al., 1980) with respect to the V_{max} / V_n shows that the increase in the V_{max} / V_n in B2 by 63 % results in decreasing the ductility ratio by 42 % in B2, although the ρ_s is 57 % higher in B2 compared to B3. It is important to note here that both wall has 0 % P_{max} / P_n and the ρ_s is more in B2 which usually increases the ductility, so, the only thing that make the wall B2 less ductile will be the only factor V_{max} / V_n which is significantly increased in B2. Figure 5.27 also shows a comparison between walls B7, B8 and B9, with high P_{max} / P_n ratios but with less difference with each other. The increase in V_{max} / V_n in B7 compared to B8 or B9 is 80 % which reduces the ductility ratio by 17 % in B7 and by 11 % in B9 compared to B8. The three walls have same ρ_s and it is also important to note that the axial load ratio is increased in B8 compared to B7 by 14 % whose tendency is to reduce the ductility ratio but due to reduction in V_{max} / V_n by 45 % in B8 overcome the axial load effect and finally increases the ductility ratio in B8. Although B9 was tested with modified reversing cycles close to monotonically loading but it is included in the comparison for the reference.

Effect of number of inelastic cycles on the displacement ductility ratio (μ_Δ)

The number of inelastic cycles may affect the ductility of walls if the failure is dominated by fracture of flexural reinforcement. Flexural reinforcement continuously undergoes repeated inelastic cycles and in each cycle it goes through tension and compression yielding causing a low-cycle-fatigue type failure. The total number of inelastic cycles that a wall has completed before failure is also studied in this comparative study. The number of cycles is computed from the test results provided in the respective referenced journal paper or publication. Figure 5.28 shows the variation of displacement ductility ratio (μ_Δ) with the number of inelastic cycles. A general observation from the figure is that both variables are proportional. W3 of this thesis achieved maximum number of inelastic cycles, which is approximately 10 % more than B3 (Corley, et al., 1980) achieved but the displacement ductility ratio of B3 is 14 % higher than W3,

although W3 did not reach complete failure. W1 and W2 of this thesis also achieved higher number of cycles, W2 achieved 5 % more inelastic cycles than B3 while W1 and B3 achieved same number of inelastic cycles. The displacement ductility ratio is 41 % more in B3 compared to both W1 and W2 which is because of the cross-section shape effect, higher P_{max} / P_n ratio in W1 and W2 compared to B3. W1 and W2 achieved only 5 % higher displacement ductility ratio than B1, which is insignificant, but the number of inelastic cycles achieved in W-2 and W1 are 47 % and 30 % respectively more than B1. B6 completed least number of inelastic cycles within Corley; et al. (1980) test series Comparison of B6 and B3 shows 66 % reduction in inelastic cycles and 81 % reduction in displacement ductility ratio.

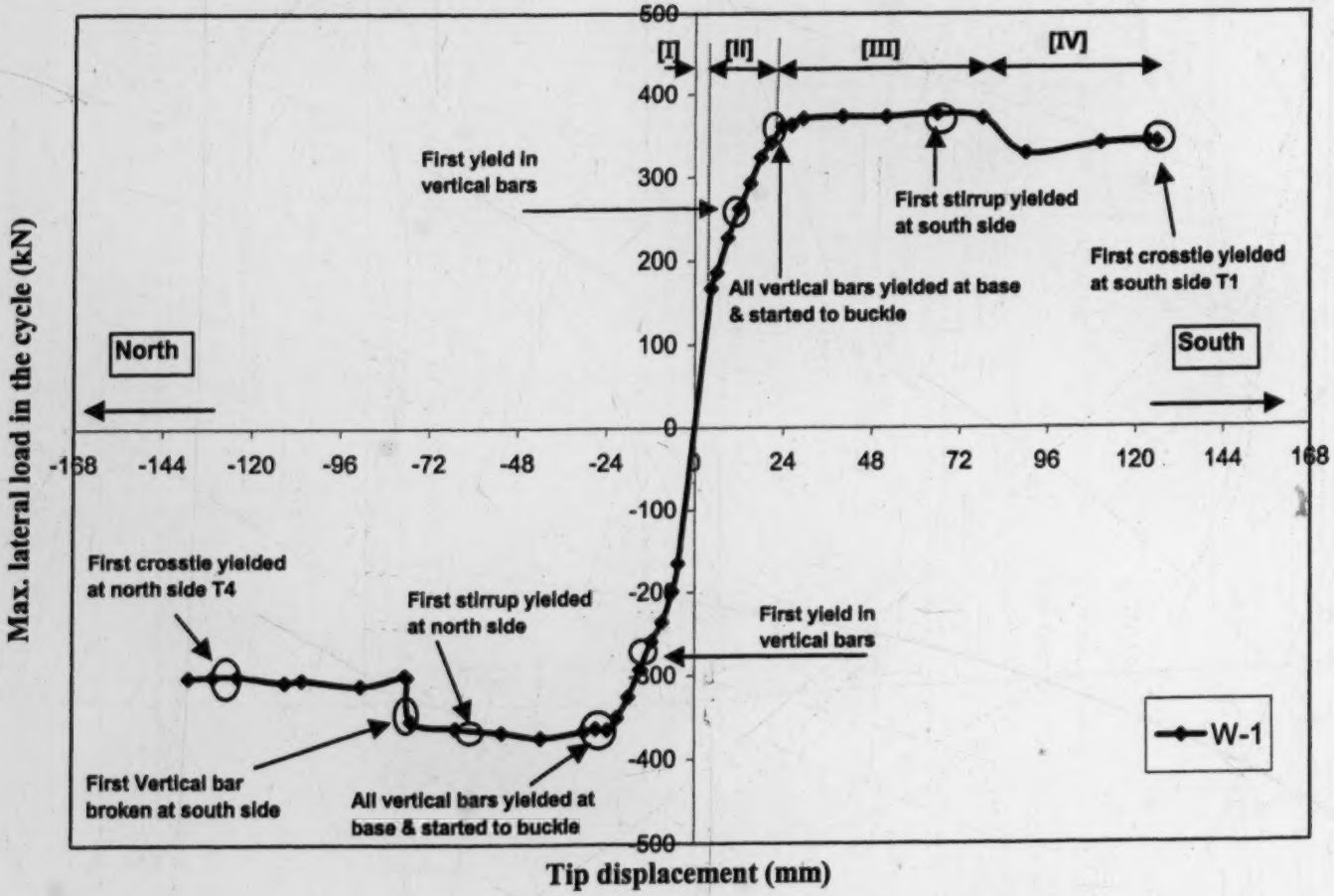

Figure 5.1 W-1 Four stages of response with summary of events occurred during test

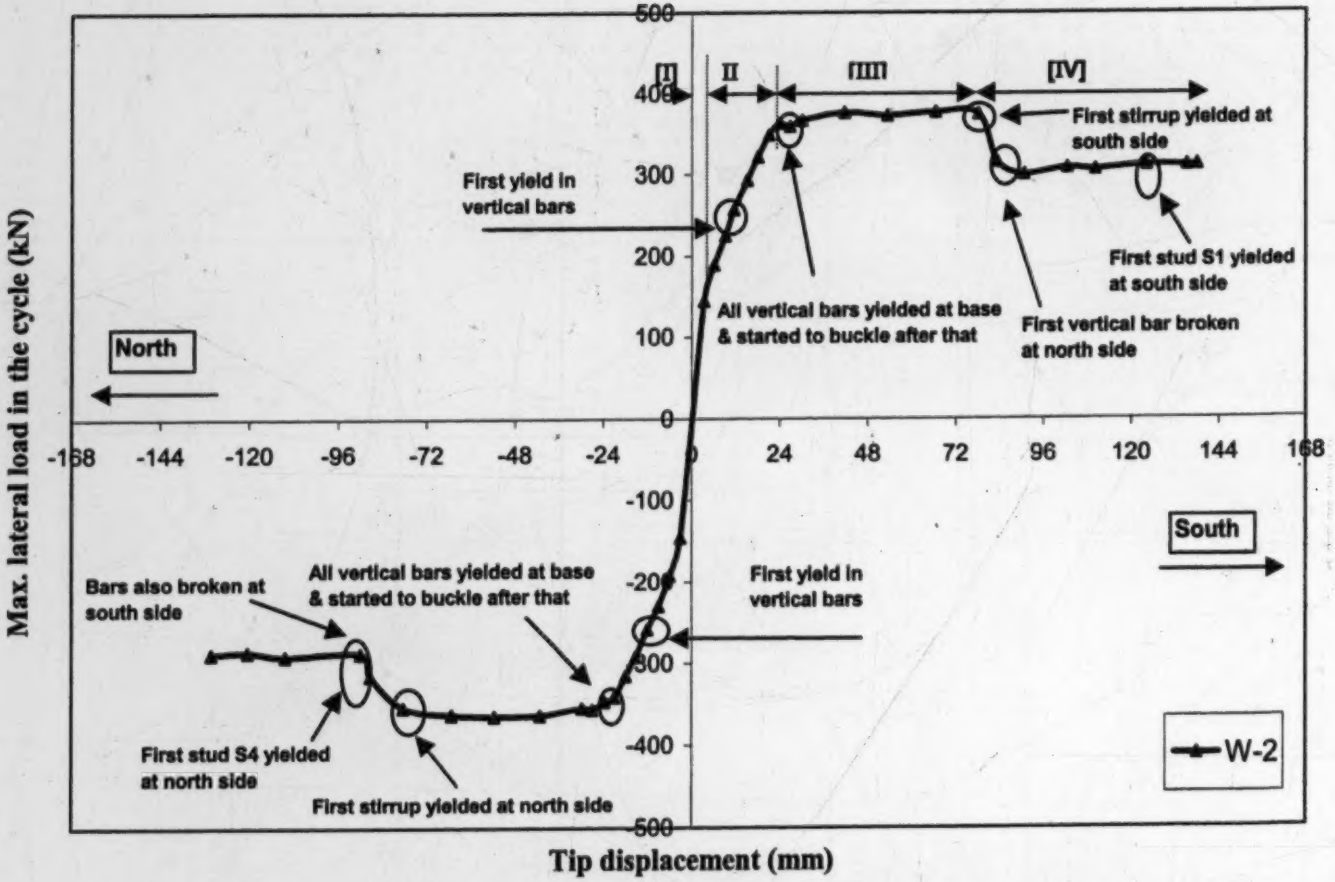

Figure 5.2 W-2 Four stages of response with summary of events occurred during test

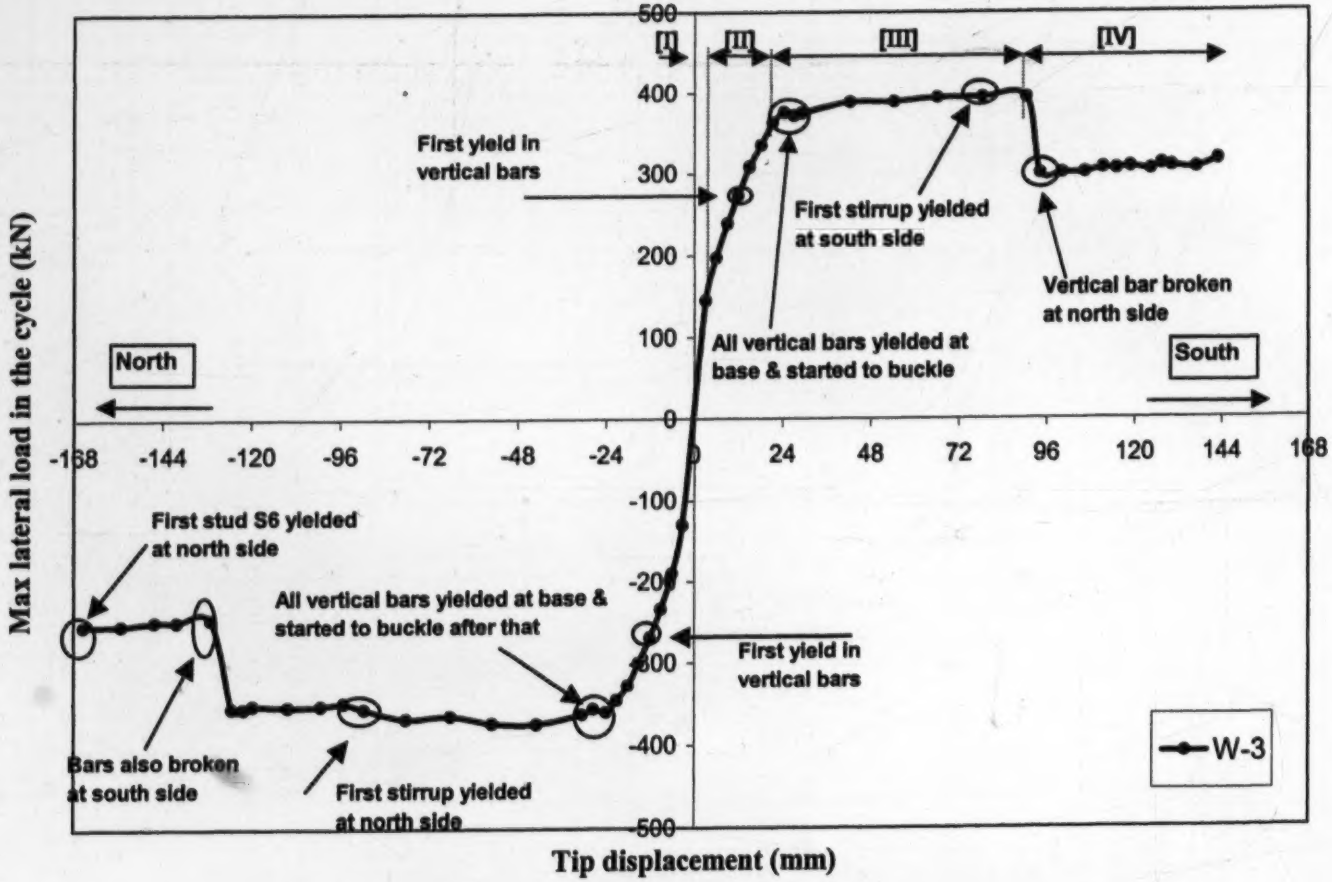

Figure 5.3 W-3 Four stages of response with summary of events during test

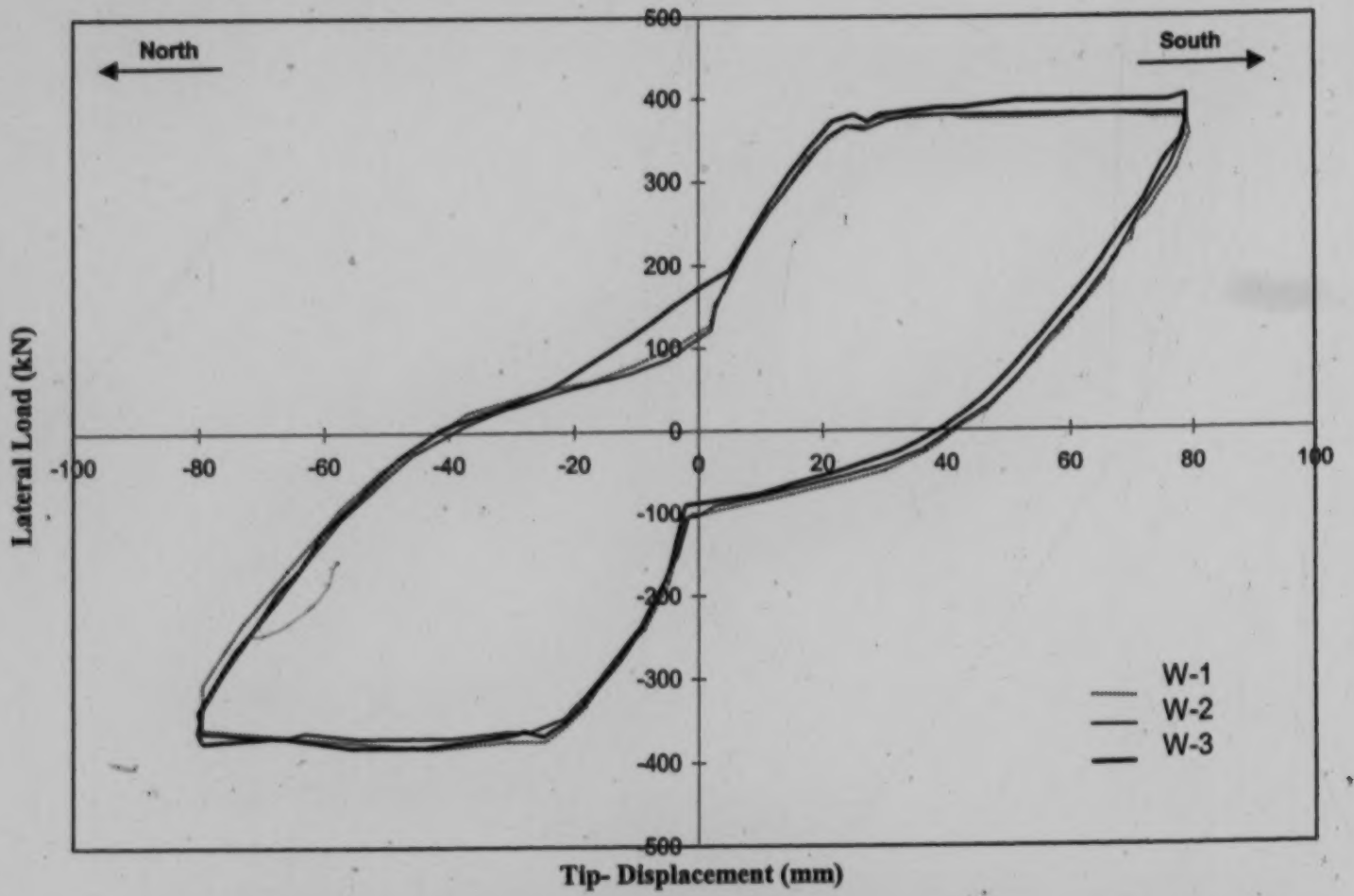

Figure 5.4 Load-tip displacement envelops of three wall specimens (Up to 78 mm tip displacement)

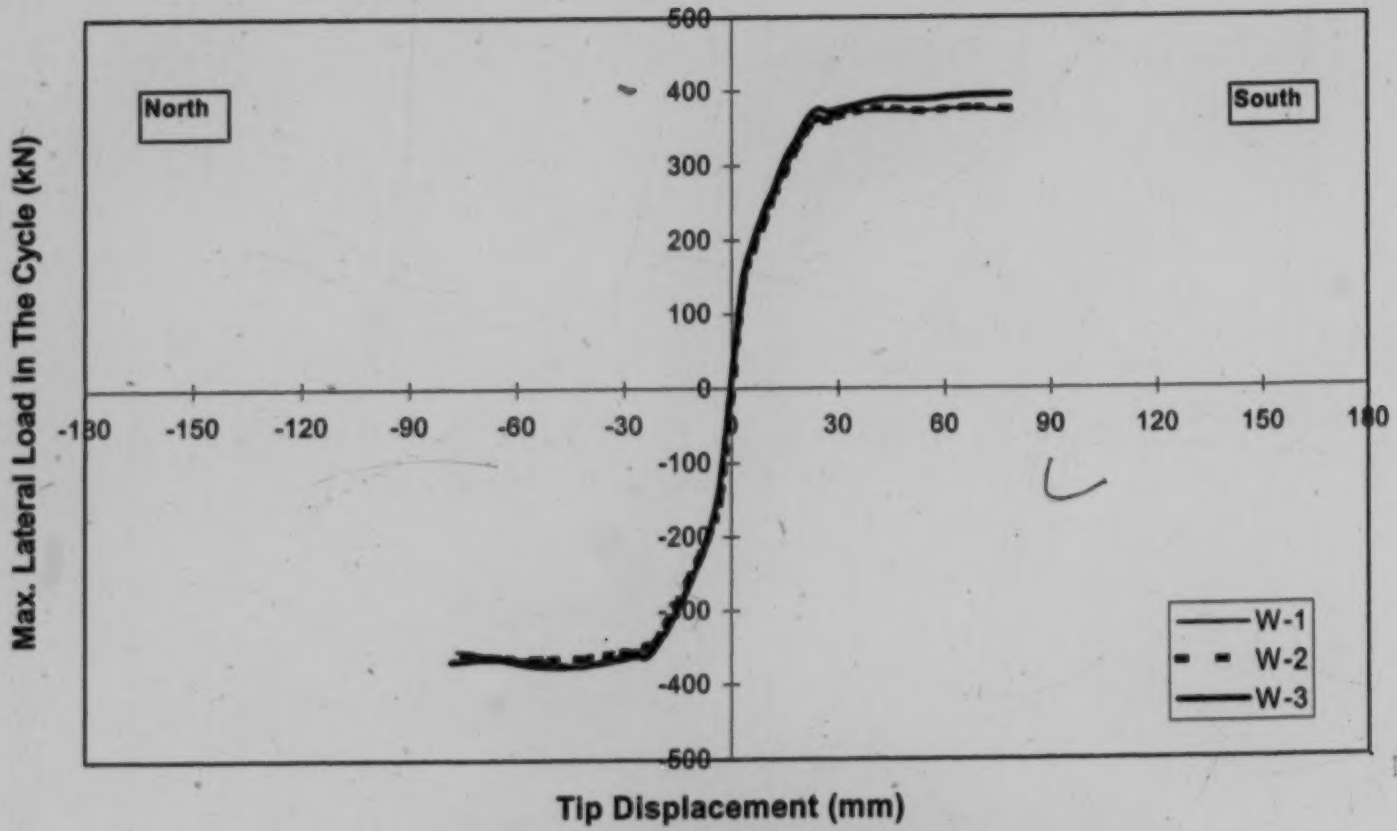

Figure 5.5 Load-displacement response of three walls (Up to 78mm tip deflection)

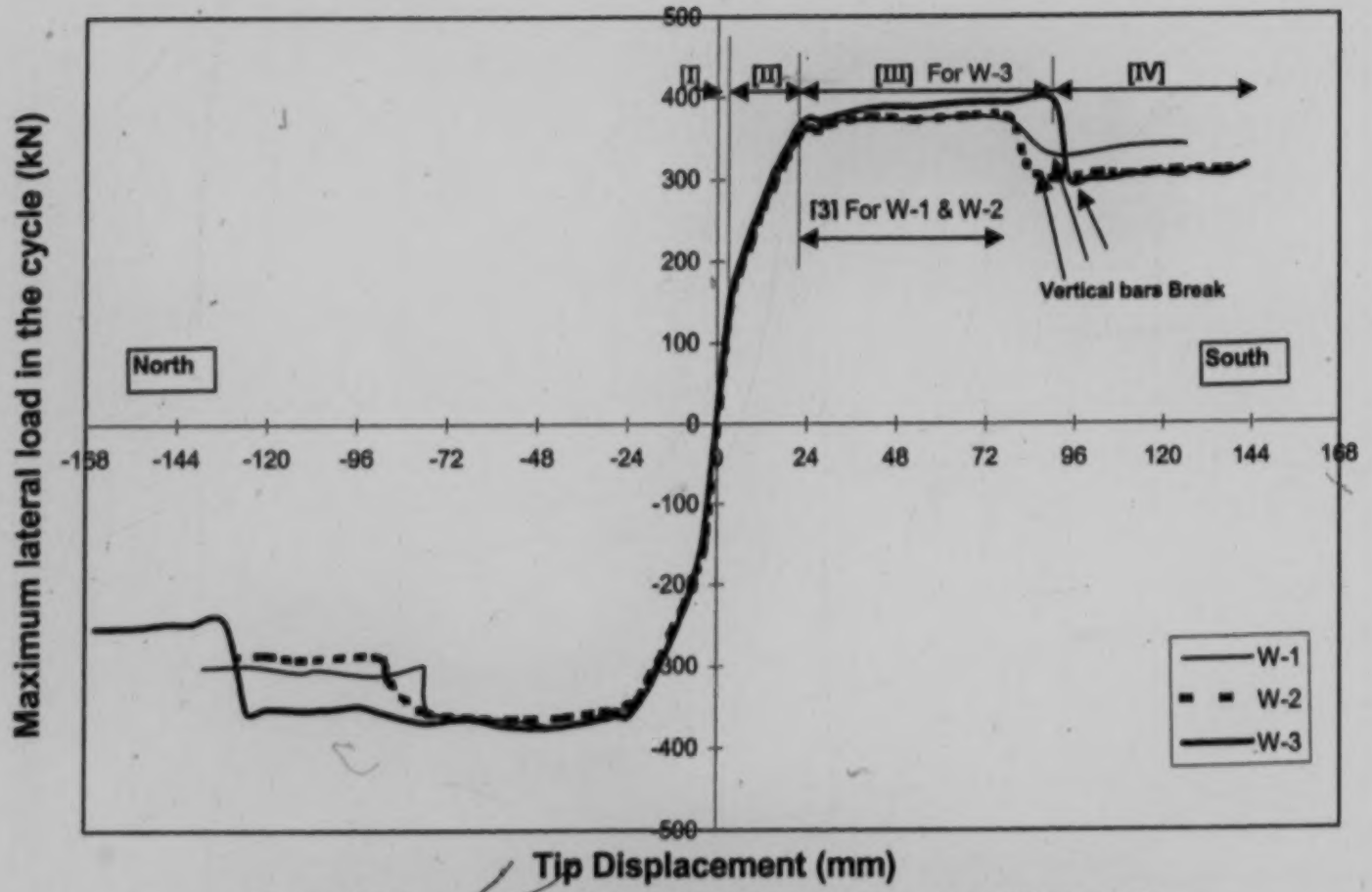

Figure 5.6 Four stages of load-displacement response of three walls

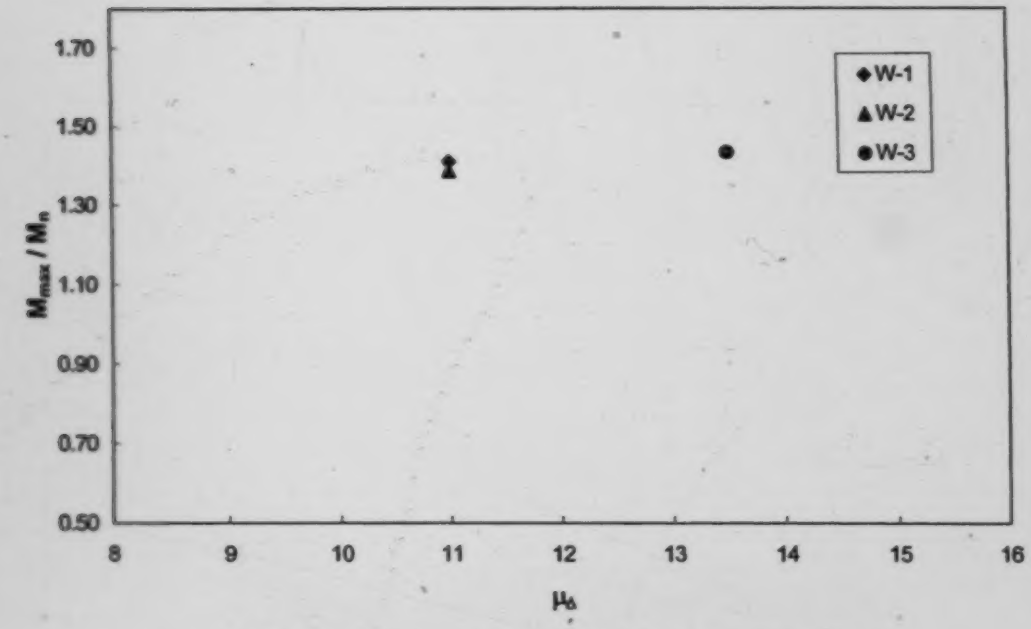

Figure 5.7 Moment ratio Vs displacement ductility

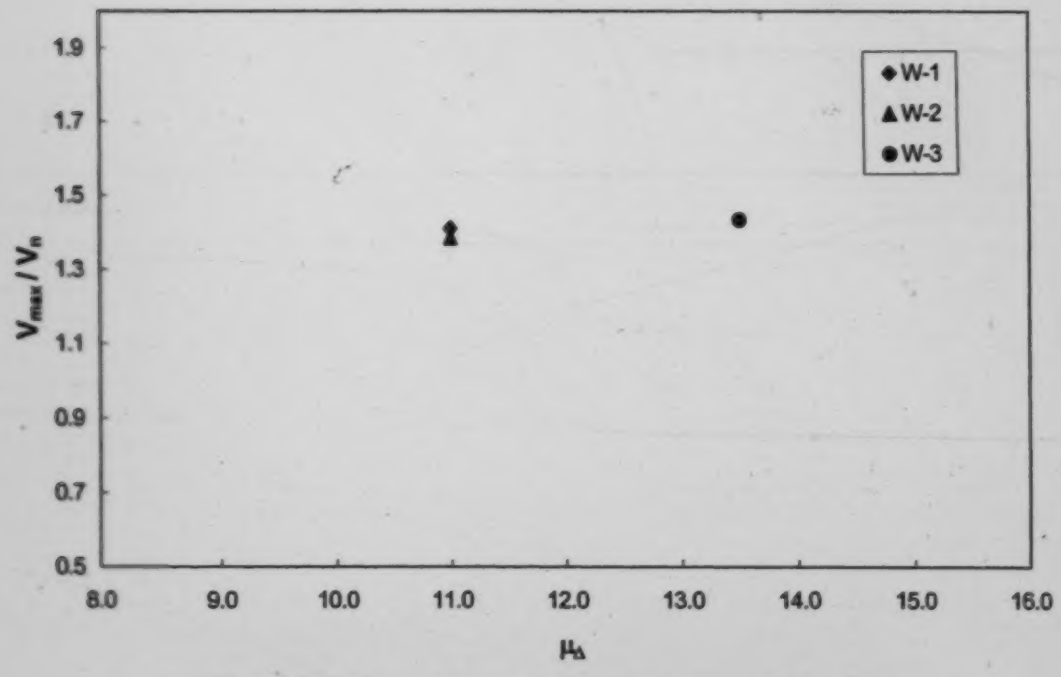

Figure 5.8 Shear force ratio Vs displacement ductility

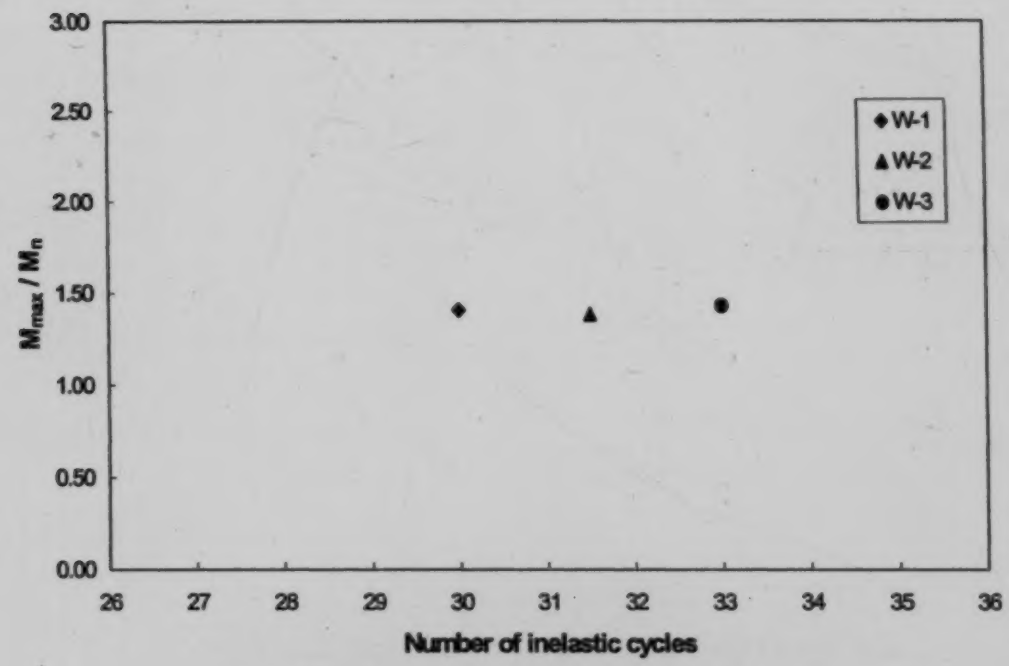

Figure 5.9 Moment ratio Vs number of inelastic cycles

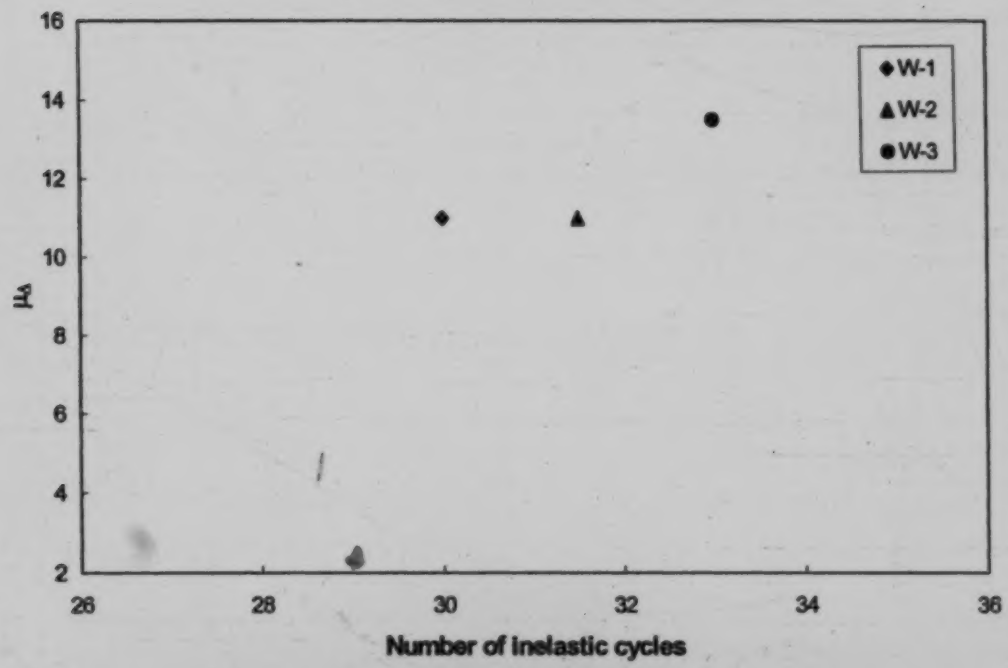

Figure 5.10 Displacement ductility ratio Vs number of inelastic cycles

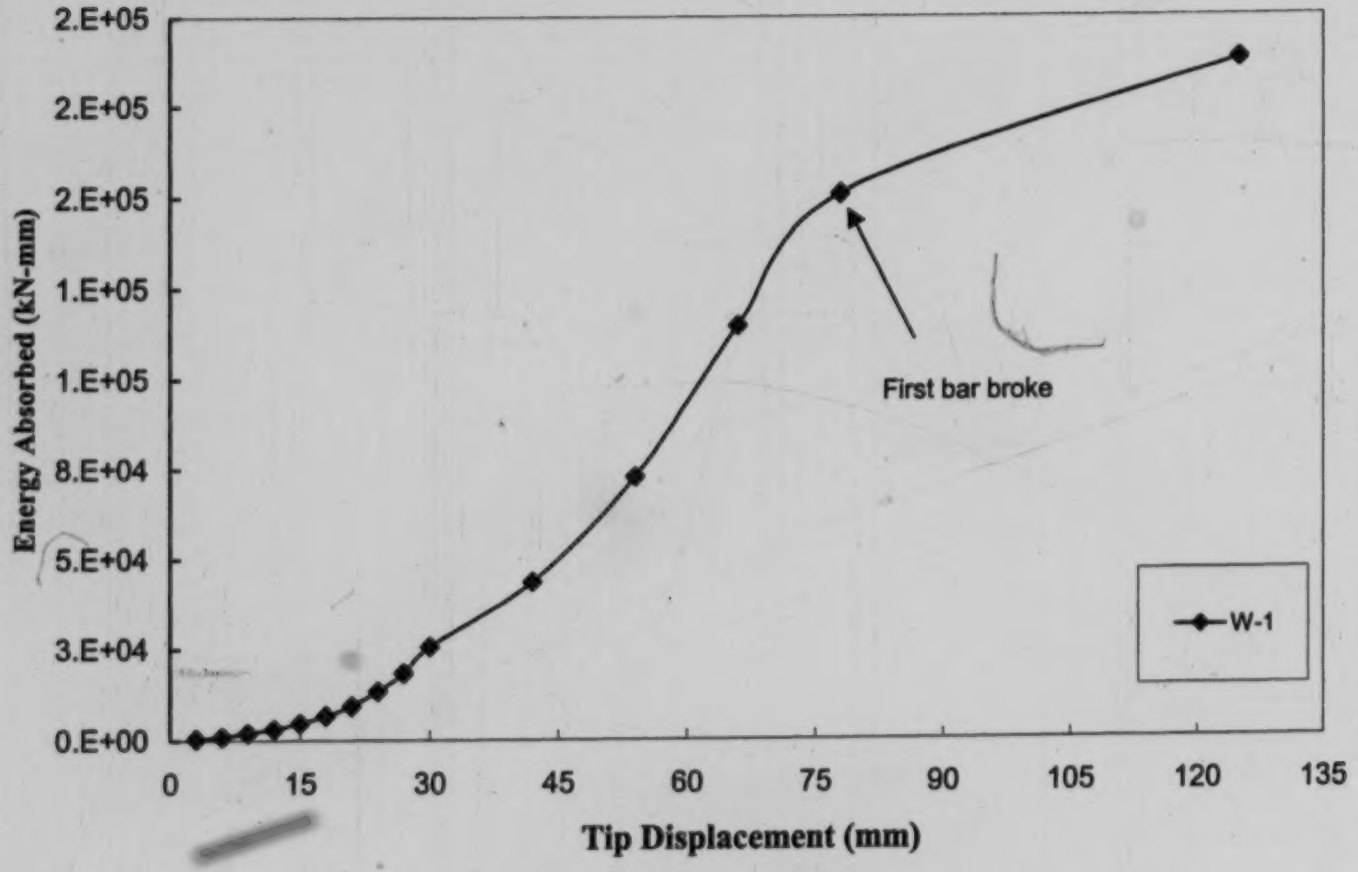

Figure 5.11 W1-Energy absorbed Vs tip displacement (Total response-south)

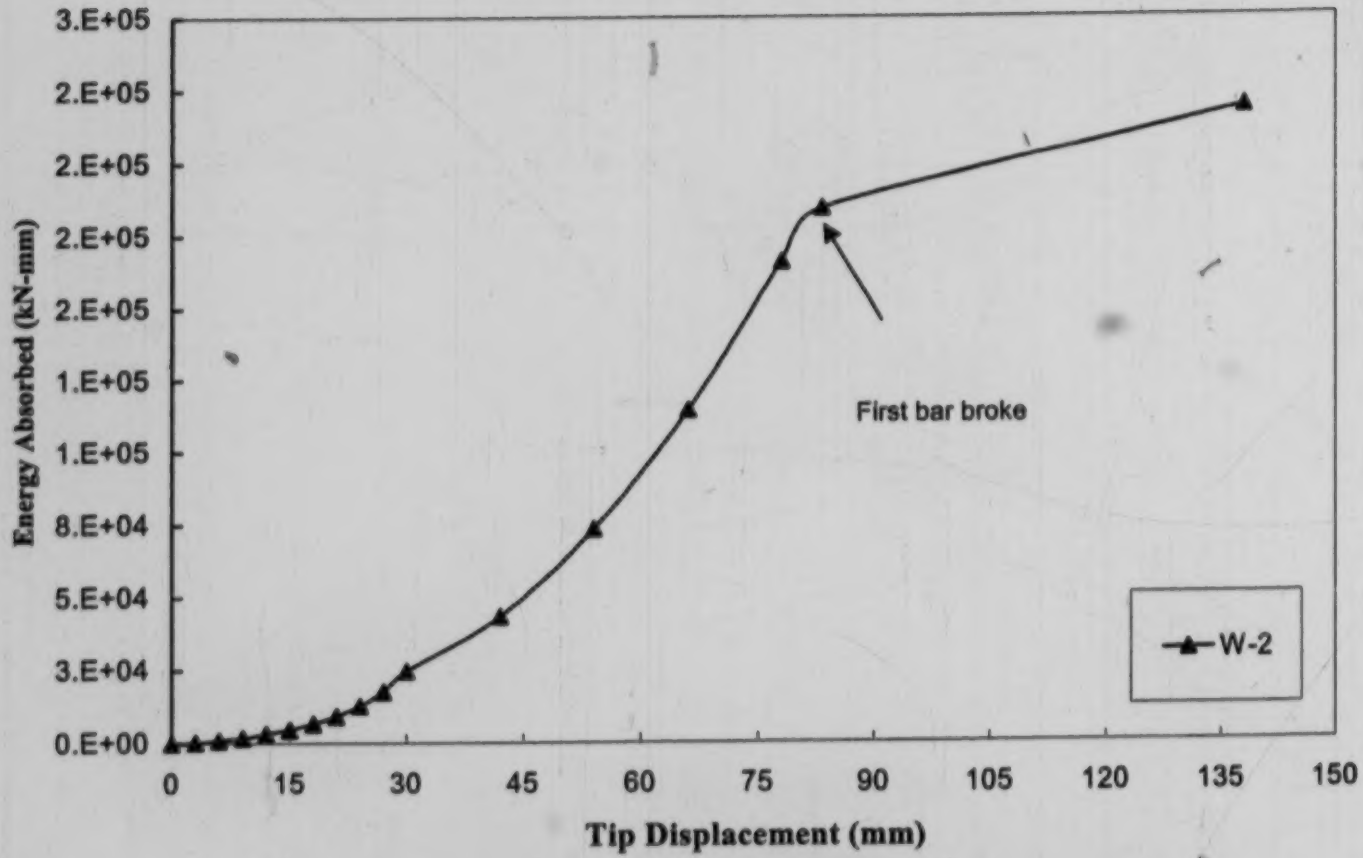

Figure 5.12 W2-Energy absorbed Vs tip displacement (Total Response–South)

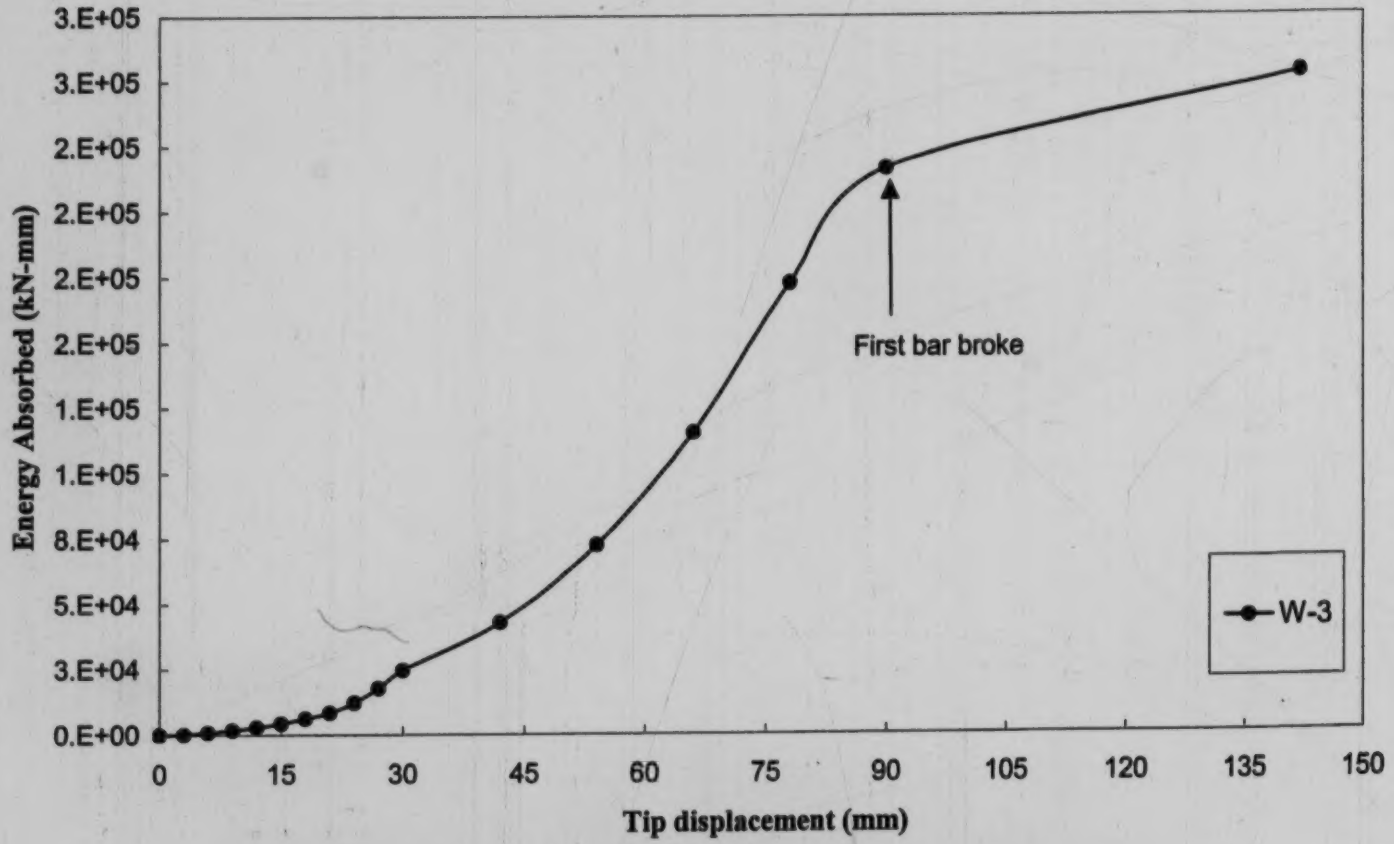

Figure 5.13 W3-Energy absorbed Vs tip displacement (Total Response –south)

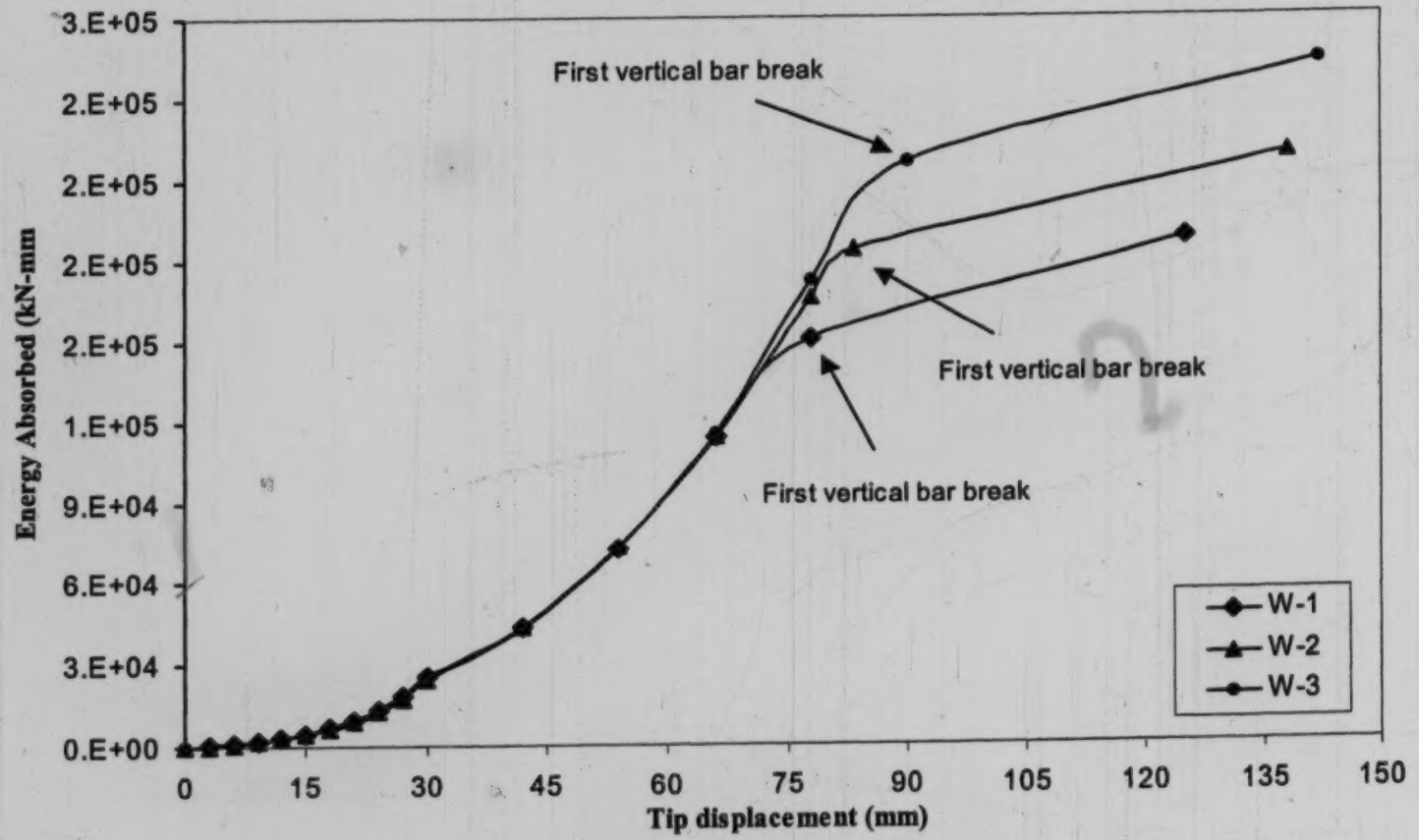

Figure 5.14 Energy absorbed Vs tip displacement (Total Response–South)

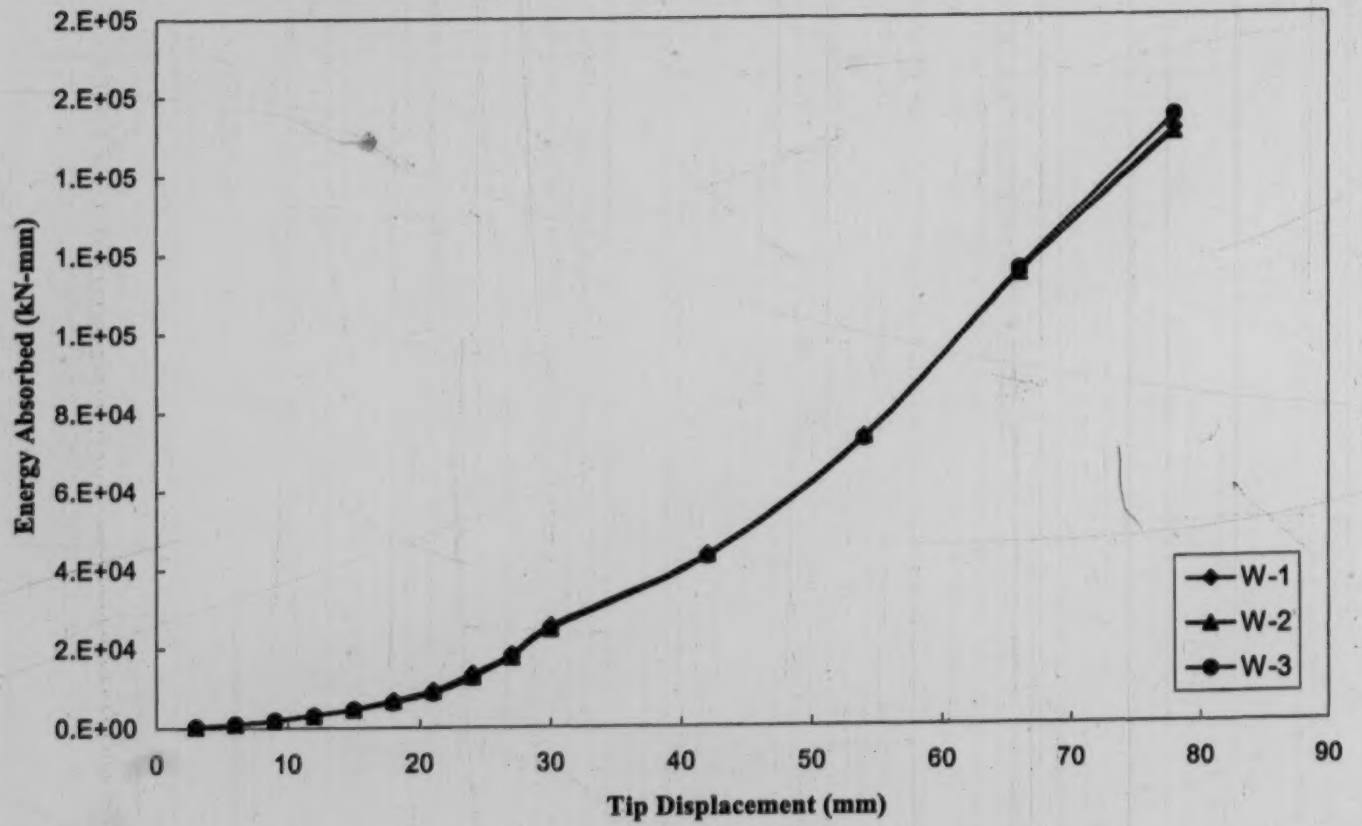

Figure 5.15 Energy absorbed Vs tip displacement (Up to 78mm tip displacement–South)

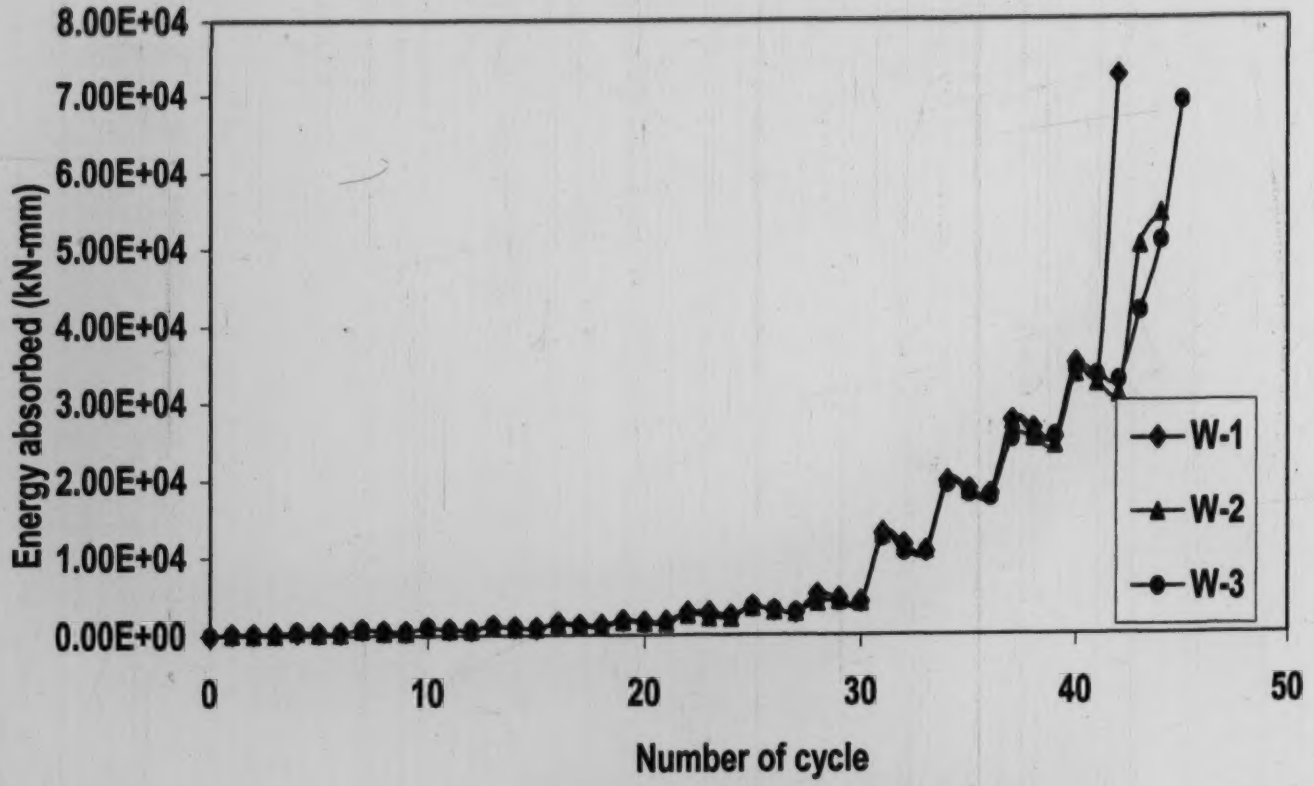

Figure 5.16 Energy absorbed in each cycle

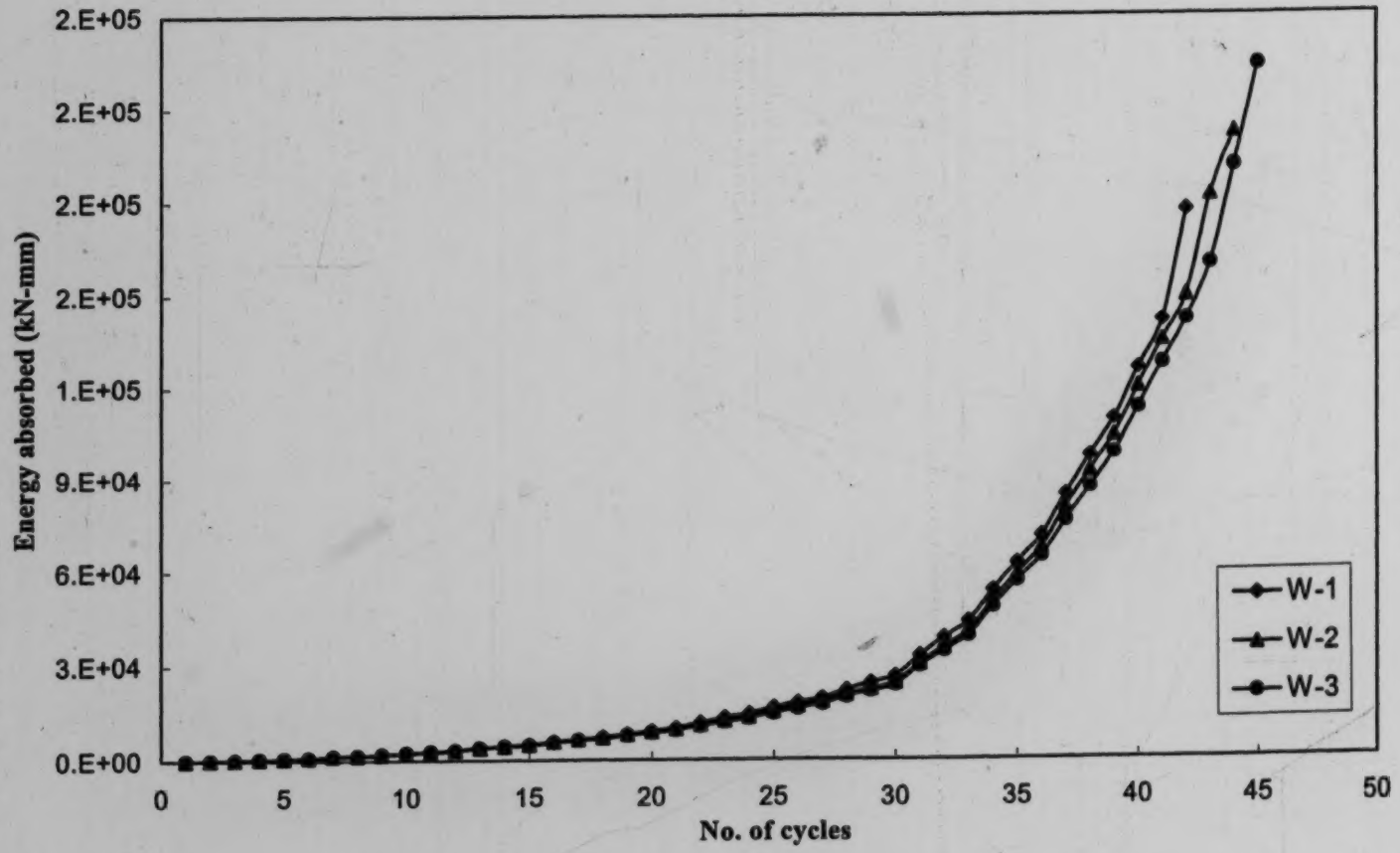

Figure 5.17 Energy absorbed with number of cycles

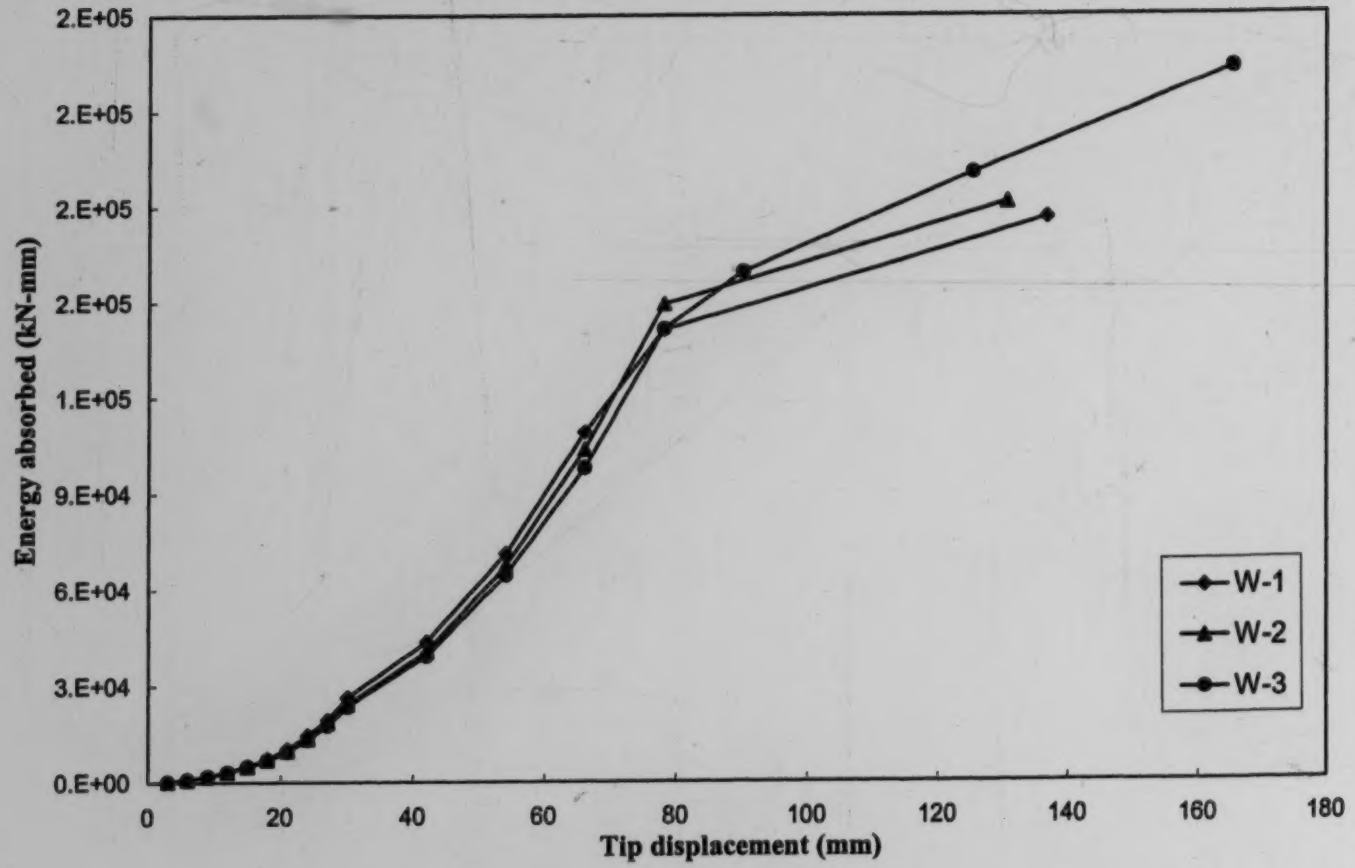

Figure 5.18 Energy absorbed Vs tip displacement (Total response-North)

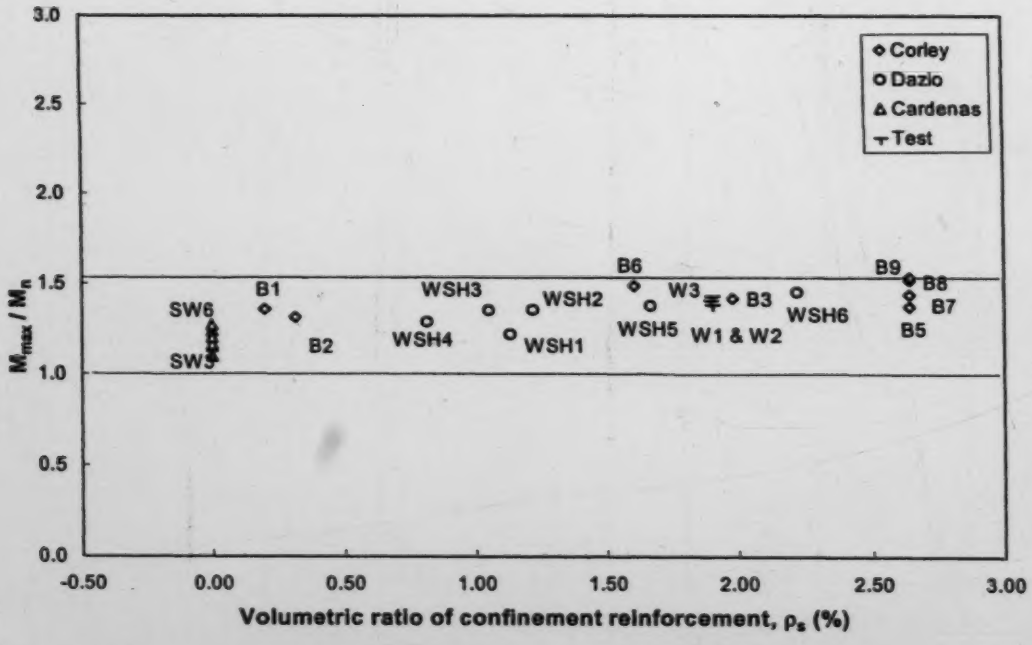

Figure 5.19 Variation of moment ratio with confinement reinforcement

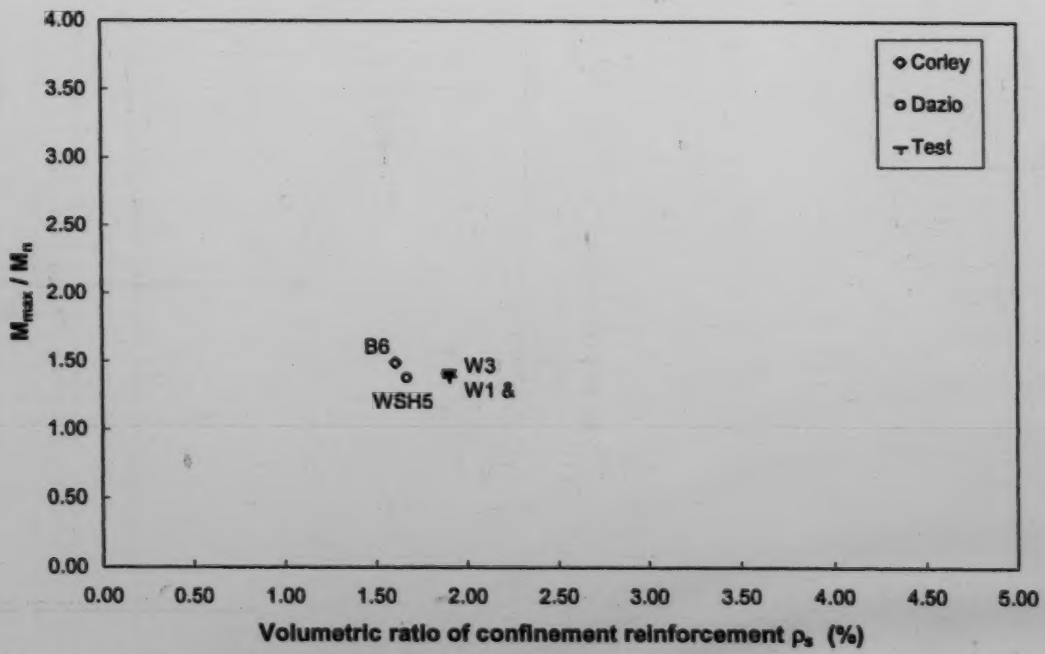

Figure 5.20 Moment ratio VS confinement ratio

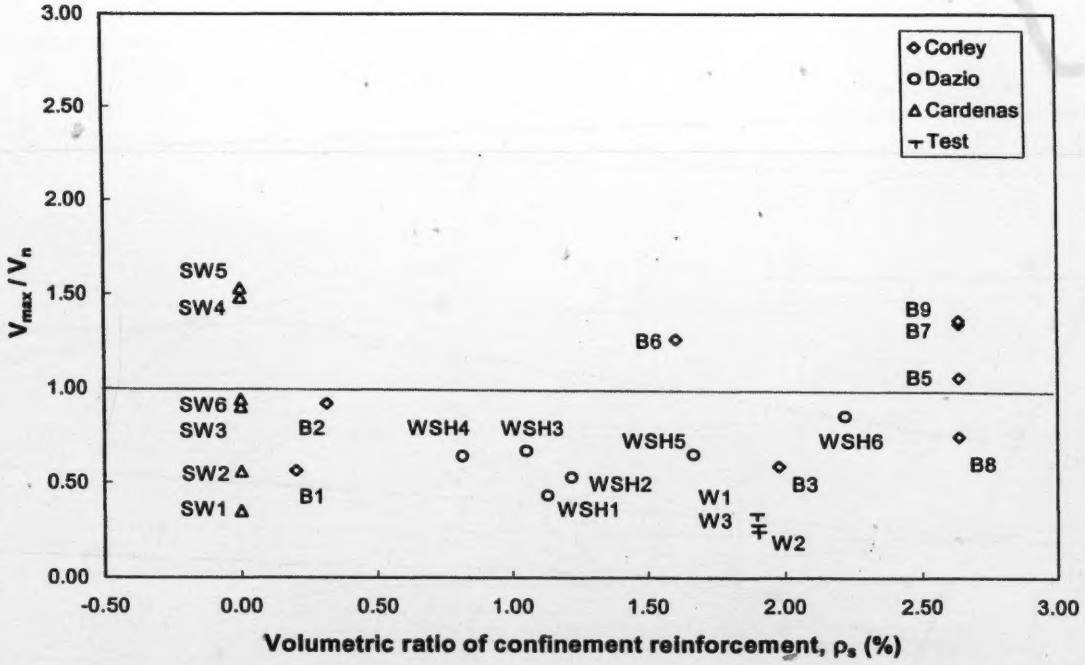

Figure 5.21 Variation of shear ratio with confinement reinforcement content

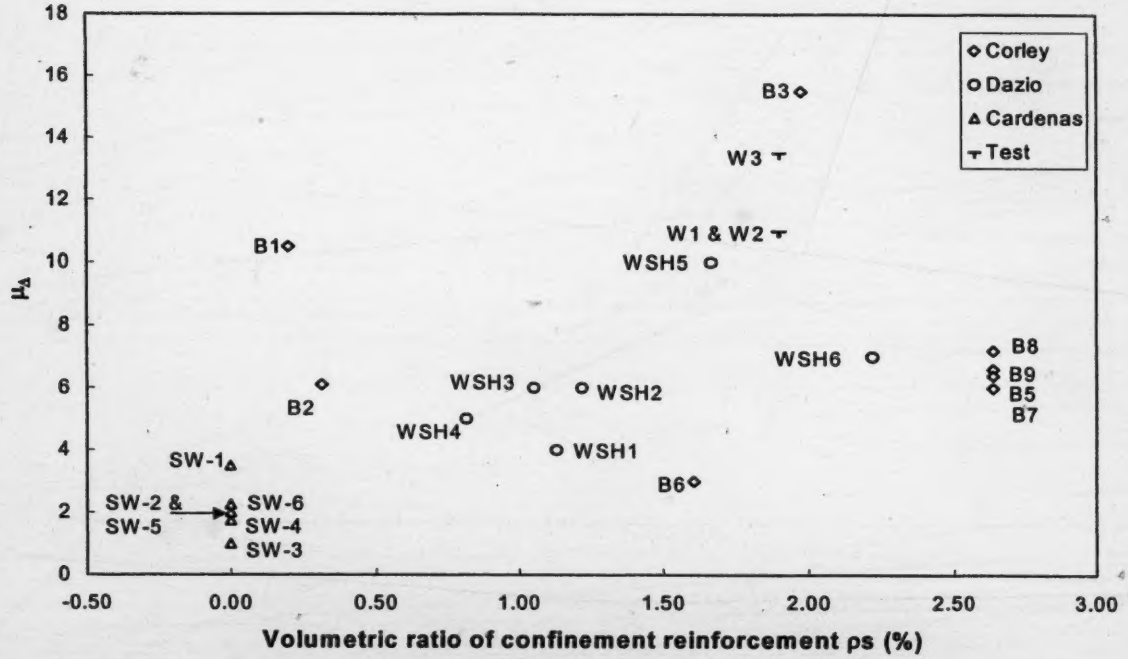

Figure 5.22 Variation of displacement ductility ratio with confinement

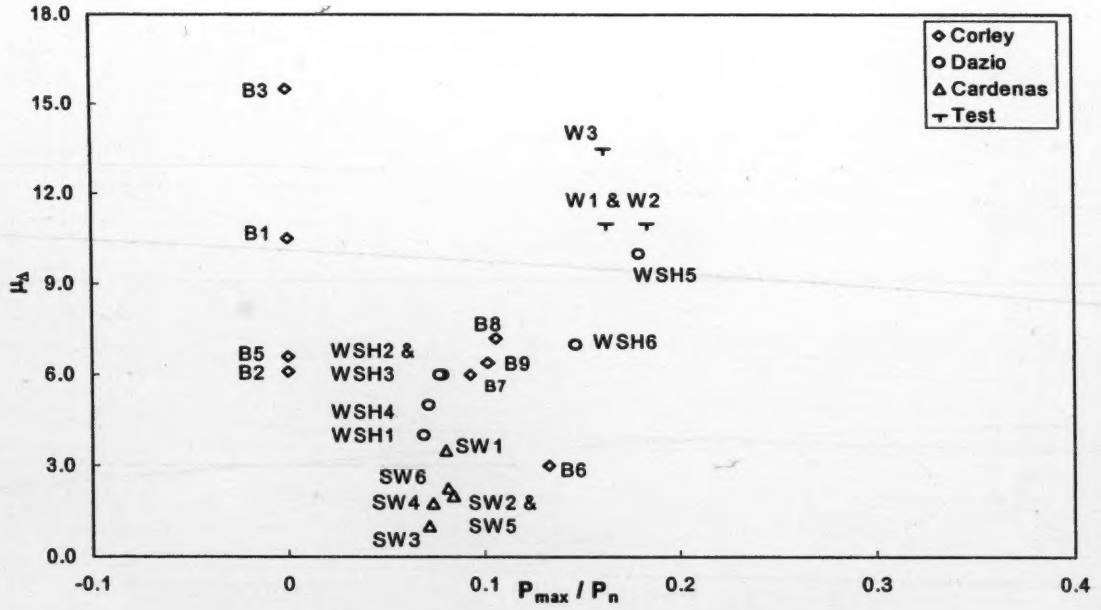

Figure 5.23 Effect of axial load on displacement ductility ratio

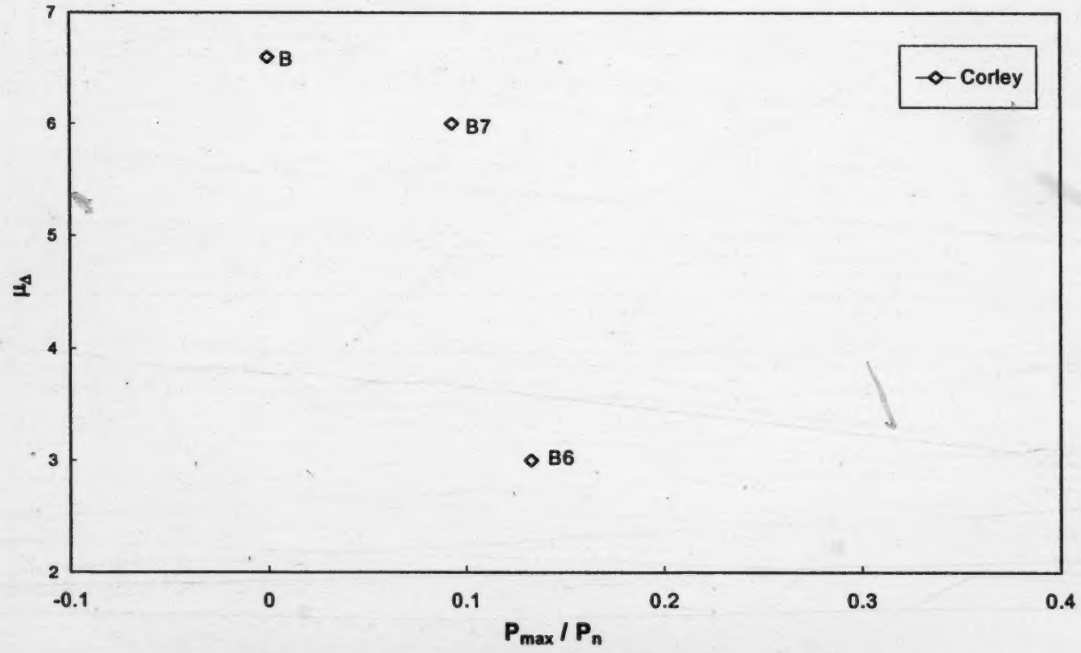

Figure 5.24 Effect of axial load on ductility between selected walls

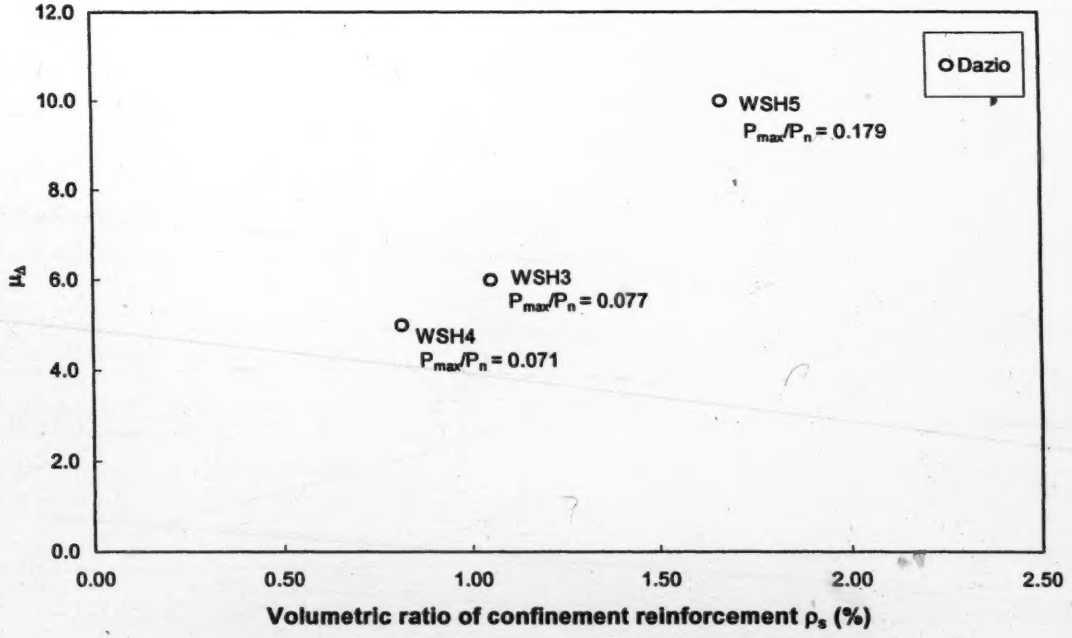

Figure 5.25 Effect of confinement on displacement ductility ratio

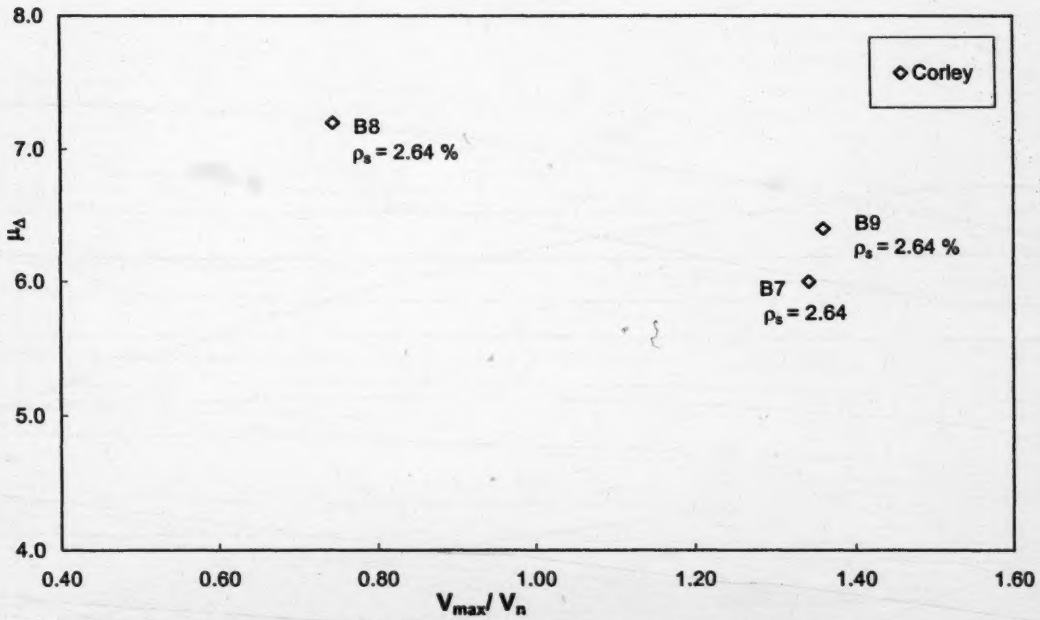

Figure 5.26 Effect of shear ratio on displacement ductility ratio

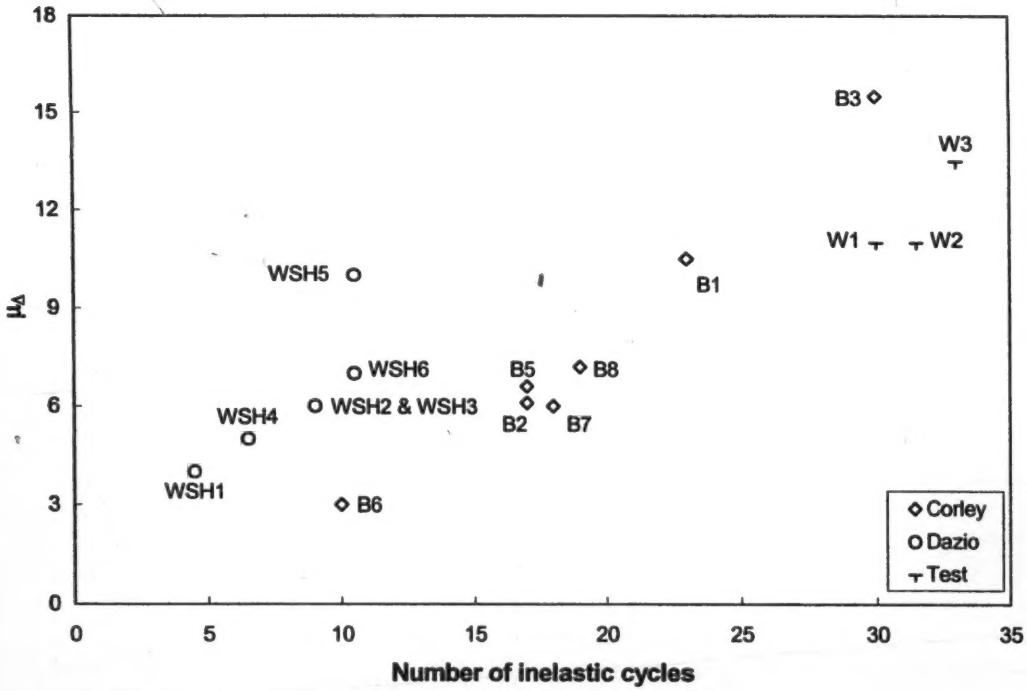

Figure 5.27 Effect of number of in elastic cycles on displacement ductility ratio

Table 5.1 (a) Test details

Designation	Test Type	*NC	*NSC	*NIC	X-Sec Shape	Concentrated Vertical r/f in end zones	End zone laterally confined	Confinement configuration
Corley et al.								
B1	*Cyc	36	28	23	Barbell	YES	YES	Hoop + X-ties
B2	Cyc	30	28	17	Barbell	YES	YES	Hoop + *Int. hoops
B3	Cyc	43	38	30	Barbell	YES	YES	Hoop + X-ties
B4	*Mono.	-	-	-	Barbell	YES	YES	Hoop + X-ties
B5	Cyc	30	29	17	Barbell	YES	YES	Hoop + X-ties
B6	Cyc	26	25	10	Barbell	YES	YES	Hoop + X-ties
B7	Cyc	31	30	18	Barbell	YES	YES	Hoop + X-ties
B8	Cyc	32	30	19	Barbell	YES	YES	Hoop + X-ties
B9	*M Cyc	5	3	-	Barbell	YES	YES	Hoop + X-ties
Dazio et al.								
WSH1	Cyc	7.5	5	4.5	*Rect	YES	YES	Hoop + X-ties
WSH2	Cyc	12.5	9	9	Rect	YES	YES	Hoop + X-ties
WSH3	Cyc	11.5	11	9	Rect	YES	YES	Hoop + X-ties
WSH4	Cyc	8.5	8	6.5	Rect	YES	Partially	U-shaped ties
WSH5	Cyc	13.5	12	10.5	Rect	YES	YES	Hoop + Int. hoops
WSH6	Cyc	12.5	12	10.5	Rect	YES	YES	Hoop + Int. hoops
Cardenas et al.								
SW-1	Mono.	-	-	-	Rect	NO	NO	-
SW-2	Mono.	-	-	-	Rect	NO	NO	-
SW-3	Mono.	-	-	-	Rect	NO	NO	-
SW-4	Mono.	-	-	-	Rect	NO	NO	-
SW-5	Mono.	-	-	-	Rect	YES	NO	-
SW-6	Mono.	-	-	-	Rect	YES	NO	-
This Thesis								
W-1	Cyc	42	40	30	Barbelled	YES	YES	Hoop + X-ties
W-2	Cyc	43.5	42	31.5	Barbelled	YES	YES	Hoop + Stud
W-3	Cyc	45	43	33	Barbelled	YES	YES	Hoop + Stud

* Refer list of notations

Table: 5.1 (b) Concrete dimensions

Designation	Web Thick. in.	Height (h) ft	Width (w) in.	h / w	*A_g sq in.	*$A_{end\ zone}$ / A_g
Corley et al.						
B1	4	15	75	2.4	492	0.584
B2	4	15	75	2.4	492	0.584
B3	4	15	75	2.4	492	0.584
B4	4	15	75	2.4	492	0.584
B5	4	15	75	2.4	492	0.584
B6	4	15	75	2.4	492	0.584
B7	4	15	75	2.4	492	0.584
B8	4	15	75	2.4	492	0.584
B9	4	15	75	2.4	492	0.584
Dazio et al.						
WSH1	5.91	15	78.74	2.3	465	0.2032
WSH2	5.91	15	78.74	2.3	465	0.2032
WSH3	5.91	15	78.74	2.3	465	0.2592
WSH4	5.91	15	78.74	2.3	465	0.2592
WSH5	5.91	15	78.74	2.3	465	0.2572
WSH6	5.91	15	78.74	2.3	465	0.382
Cardenas et al.						
SW-1	3	21	75	3.36	225	0
SW-2	3	21	75	3.36	225	0
SW-3	3	21	75	3.36	225	0
SW-4	3	12	75	1.92	225	0
SW-5	3	12	75	1.92	225	0.2
SW-6	3	21	75	3.36	225	0.2
This thesis						
W-1	7.87	11.8	47.24	3	436	0.711
W-2	7.87	11.8	47.24	3	436	0.711
W-3	7.87	11.8	47.24	3	436	0.711

* Refer list of notations

Table: 5.1 (c) Reinforcement ratios

Designation	A_{cv}	ρ_t	ρ_f	ρ_n	ρ_h	ρ_s	$\rho_{s(hoops)}$	$\rho_{s(ties)}$
	in2	%	%	%	%	%	%	%
Corley et al.								
B1	300	0.77	1.11	0.29	0.31	0.200	0.133	0.066
B2	300	2.27	3.67	0.29	0.63	0.314	0.131	0.180
B3	300	0.77	1.11	0.29	0.31	1.980	1.322	0.661
B4	300	0.77	1.11	0.29	0.31	1.980	1.322	0.661
B5	300	2.27	3.67	0.29	0.63	2.640	1.322	1.322
B6	300	2.27	3.67	0.29	0.63	1.607	0.804	0.804
B7	300	2.27	3.67	0.29	0.63	2.640	1.322	1.322
B8	300	2.27	3.67	0.29	1.38	2.640	1.322	1.322
B9	300	2.27	3.67	0.29	0.63	2.640	1.322	1.322
Dazio et al.								
WSH1	465	0.54	1.5	0.284	0.25	1.131	1.060	0.071
WSH2	465	0.54	1.5	0.284	0.25	1.220	1.060	0.161
WSH3	465	0.82	1.7	0.497	0.25	1.052	0.974	0.078
WSH4	465	0.82	1.7	0.482	0.25	0.816	0.816	-
WSH5	465	0.39	0.782	0.254	0.25	1.670	0.732	0.935
WSH6	465	0.82	1.358	0.488	0.25	2.220	1.300	0.920
Cardenas et al.								
SW-1	225	0.29	-	0.29	0.27	0.00	-	-
SW-2	225	0.98	-	0.98	0.27	0.00	-	-
SW-3	225	2.93	-	2.93	0.27	0.00	-	-
SW-4	225	2.93	-	2.93	0.27	0.00	-	-
SW-5	225	2.4	7.8	1	0.27	0.00	-	-
SW-6	225	2.4	7.8	1	0.27	0.00	-	-
This thesis								
W-1	372	1.35	1.6	0.74	1	1.900	1.395	0.501
W-2	372	1.35	1.6	0.74	1.1	1.906	1.550	0.356
W-3	372	1.35	1.6	0.74	1.14	1.904	1.595	0.360

Table: 5.1 (d) Applied load and capacity

Desig.	P_n Kip	P_{max} Kip	V_n Kip	V_{max} Kip	M_n Kip-ft	M_{max} Kip-ft	μ_Δ	P_{max}/P_n	V_{max}/V_n	M_{max}/M_n
Corley et al.										
B1	2734.80	0	108.42	61.0	674.0	915.0	10.50	0	0.563	1.358
B2	3079.87	0	166.32	152.80	1743.30	2292.00	6.10	0	0.919	1.315
B3	2459.25	0	105.50	62.00	655.20	930.00	15.50	0	0.588	1.419
B4	2671.17	0	104.29	75.30	672.40	1129.50	16.67	0	0.722	1.680
B5	2684.25	0	162.03	171.30	1868.80	2569.50	6.60	0	1.057	1.375
B6	1572.56	209.1	147.18	185.50	1867.50	2782.50	3.00	0.133	1.260	1.490
B7	2877.16	268.1	164.17	220.40	2293.10	3306.00	6.00	0.093	1.343	1.442
B8	2527.30	268.1	295.22	219.80	2168.70	3297.00	7.20	0.106	0.745	1.520
B9	2628.66	268.1	161.40	219.60	2142.40	3294.00	6.40	0.102	1.361	1.538
Dazio et al.										
WSH1	2245.48	154.67	174.14	75.54	926.17	1130.00	4.00	0.069	0.434	1.220
WSH2	1959.37	154.67	152.77	80.71	1207.50	1637.00	6.00	0.079	0.528	1.356
WSH3	2007.29	154.67	152.37	102.07	1128.65	1526.83	6.00	0.077	0.670	1.353
WSH4	2164.09	154.67	155.38	99.59	1155.50	1490.00	5.00	0.071	0.641	1.289
WSH5	1858.84	333.63	151.51	98.69	1069.50	1476.00	10.00	0.179	0.651	1.380
WSH6	2268.52	333.63	157.32	134.22	1367.35	1990.00	7.00	0.147	0.853	1.455
Cardenas et al.										
SW-1	1163.97	93.4	76.00	26.50	353.00	406.00	3.50	0.080	0.349	1.150
SW-2	1149.93	96.75	74.38	41.40	545.60	675.00	2.00	0.084	0.557	1.237
SW-3	1323.39	94.5	73.50	66.00	977.20	1073.00	1.00	0.071	0.898	1.098
SW-4	1317.45	96.75	73.39	108.60	925.90	1077.00	1.75	0.073	1.480	1.163
SW-5	1140.24	95.63	71.02	108.60	897.10	1078.00	2.00	0.084	1.529	1.202
SW-6	1190.90	96.75	77.24	72.50	928.00	1179.00	2.25	0.081	0.939	1.270
This thesis										
W-1	1283.21	236	251.37	84.50	645.70	910.20	11.00	0.184	0.336	1.410
W-2	1361.00	236	273.76	84.70	658.00	912.20	11.00	0.163	0.243	1.386
W-3	1416.57	236	283.20	88.70	666.40	955.08	13.50	0.162	0.277	1.433

Table: 5.1 (e) Material properties

Designation	f'_c	$f_{y\ ver.}$	$f_{y\ hor.}$	$f_{y\ trans.}$
	Ksi	Ksi	Ksi	Ksi
Corley et al.				
B1	7.69	65.2	60.0	NA
B2	7.78	59.5	60.0	NA
B3	6.86	63.5	60.0	NA
B4	6.53	65.3	60.0	NA
B5	6.57	64.4	60.0	NA
B6	3.17	63.9	60.0	NA
B7	7.16	66.4	60.0	NA
B8	6.09	64.9	60.0	NA
B9	6.4	62.3	60.0	NA
Dazio et al.				
WSH1	6.59	79.6	84.7	84.70
WSH2	5.78	83.8	70.5	70.49
WSH3	5.72	83.8	70.5	70.49
WSH4	6.22	84.56	70.5	70.49
WSH5	5.58	76.14	70.5	70.49
WSH6	6.55	77.60	70.5	70.49
Cardenas et al.				
SW-1	7.42	60.20	61.3	NA
SW-2	6.88	65.40	61.0	NA
SW-3	6.78	66.00	60.0	NA
SW-4	6.74	60.00	60.0	NA
SW-5	5.90	60.00	60.0	NA
SW-6	5.95	63.00	70.0	NA
This thesis				
W-1	3.49	57.30	55.8	55.80
W-2	3.76	57.30	55.8	73.97
W-3	3.95	57.30	55.8	64.40

CHAPTER 6

SUMMARY, CONCLUSIONS AND FUTURE RECOMMENDATIONS

6.1 Summary

The primary objective of the current testing program is the study of confinement behavior in the boundary elements of reinforced concrete shear walls. Specifically, the behavior of walls confined with double head studs is compared with the behavior of walls confined with conventional crossties. The secondary objective is to reduce reinforcement congestion due to hooks and bends of conventional crossties, causing additional allowance in concrete dimensions and free floor space.

Three full-scale concrete shear walls, with confined boundary elements, have been tested at the University of Alberta under fully reversible quasi-static cyclic action.

W-1, which also acts as the reference wall, was confined with conventional crossties with a 135 degree hook at one end and a 90 degree hook at its other end (as permitted by the ACI 318-2002). W-2 and W-3 were confined with double head studs in place of the conventional cross ties. Volumetric ratio of the confinement was identical in the three walls. W-2 was confined with 9.5 mm Ø studs with 30.1 mm Ø circular heads placed in pairs in each boundary element at each level while W-3 was confined with 12.7 mm Ø studs with 40.2 mm Ø circular head such that only one stud was provided in each boundary element at each level instead of two as in W-2.

The three walls have approximately identical designed geometric, material and strength properties. Actual measured concrete strength (f'_c) of W-3 is 12 % and 8 % higher than W-1 and W-2 respectively.

The three walls were tested in a displacement control mode under approximately identical compressive axial load. The behavior of walls during the tests was quite similar regarding their lateral load versus tip displacement response, cracking pattern and stiffness degradation modes except some differences that are discussed below.

Closed stirrups in W-1 yielded prior to W-2 and W-3. In W-1 the yielding in stirrups occurred at μ_Δ of 4.5, which corresponds to 54 mm tip displacement while in W-2 and W-3 the yielding of stirrups occurred at μ_Δ of 6.5, which corresponds to the tip displacement of 78 mm. Vertical flexural reinforcement in the three walls yielded at approximately identical tip displacement (also referred to as yield displacement).

The yield displacement (Δ_y) in the three walls is approximately identical and is equal to the tip displacement of 12 mm.

The drop in lateral load carrying capacity of all walls was initiated by the fracture of the vertical reinforcements in the boundary elements.

The difference in the lateral load carrying capacity or in the strength of the walls W-1 and W-2 is insignificant while W-3 showed a little higher strength compared to the other two walls, which is approximately 5 % higher than W-1 or W-2.

W-3, which was confined with larger diameter double head studs, achieved 22 % higher displacement ductility ratio (μ_Δ) compared to W-1 and W-2.

W-3 achieved maximum number of inelastic cycles compared to W-2 and W-1 before rupture of any vertical reinforcement and also before the end of tests. At the onset of first bar-rupture, W-1 was in the second cycle of $\mu_\Delta = 6.5$, W-2 was in the first cycle of $\mu_\Delta = 7.5$ (but its bar was ruptured on reaching 85 % of the total tip displacement of the current ductility ratio) and W-3 was in the second cycle of $\mu_\Delta = 7.5$.

At the end of tests, W-3 achieved 5 % more inelastic cycles compared to W-2 and 10 % more than W-1 while W-2 achieved 5 % more inelastic cycles compared to W-1.

Energy absorption of the three walls was similar up to μ_Δ = 6.5, which corresponds to the tip displacement of 78 mm after which the vertical bars started to rupture in W-1 and hence it absorbed less energy till the end of test compared to the other two walls. W-2 completed one cycle more than W-1 before the first bar-rupture, so it absorbed slightly higher energy than W-1. W-3 achieved the maximum number of cycles before the initiation of bar-rupture so it absorbed comparatively more energy than W-1 and W-2. Vertical bars in W-3 started to rupture at $\mu_\Delta = 7.5$, which corresponds to the tip displacement of 90 mm.

Comparison of the current test with previous shear wall tests in other research programs showed a good consistency of test results regarding strength and ductility under the effect of various parameters.

The comparison showed that the effect of increase in confinement reinforcement content (ρ_s) in the boundary elements increases the strength less significantly as compared to the increase in ductility. The comparison also showed that both the axial load ratio and shear force ratio detrimentally affect the displacement ductility ratio (μ_Δ).

Keeping the other factors constant such as axial load ratio, shear force ratio and the cross-section shape, the displacement ductility ratio (μ_Δ) increases with the increase in confinement reinforcement ratio (ρ_s). In some tests it is found to be increasing even in the presence of significant axial load and shear force ratios.

Overall comparison shows that W-3, which has half the number of studs but with larger diameter heads, achieved maximum number of inelastic cycles than any other wall. W-3 achieved 5 % more inelastic cycles compared to W-2, which appears to be the next wall in the comparison that achieved more inelastic cycles after W-3.

Comparison of W-3 with similar walls tested by other shows a 10 % increase in the number of inelastic cycles achieved in W-3. Also W-3 did not experience a significant drop in the displacement ductility ratio (12 % drop) even after a significant increase in the axial load ratio.

6.2 Conclusions

Effective and higher confinement content in the boundary elements of shear wall can significantly increase ductility of the wall but its effect on strength gain is comparatively small.

Walls confined with double head studs in their boundary elements, behave similar to walls confined with conventional crossties regarding strength and ductility. Walls confined with larger diameter studs behave better than walls with cross ties and walls with smaller studs, even when half the number of studs are used, hence causing less reinforcement congestion.

Effectiveness of larger double head studs in wall W-3 is obvious in restraining the lateral bulging of concrete compared to the smaller studs in wall W-2. The effective head area and the total cross-sectional area of studs at any particular level in wall W-3 is 12 % lesser then the studs in wall W-2.

Reinforcement congestion is seemed to be least in W-3 because of having reduced number of double head studs and also their effective head area.

Energy absorbed in wall W-3 significantly increased compared to the other two walls. At the onset of first vertical bar-rupture, the energy absorbed in W-3 is 43 % higher than the energy absorbed in W-1, which was confined with conventional crossties. The energy absorption in W-2, which was confined with relatively smaller studs, also increased by 22 % compared to the W-1, at the onset of first bar-rupture.

6.3 Future recommendations

This thesis reports on walls loaded cyclically with a low axial force ratio and high lateral (shear) force ratio. The author understands that a parallel series of test is being conducted elsewhere, where long columns are loaded with higher axial force ratios and very low lateral loads.

The tests carried out in the present research work were based upon constant confinement content in all the test specimens, which includes closed stirrups and double head studs contents lumped together. It is recommended to test the walls or columns confined with higher content of double head studs and a smaller content of closed stirrups.

Only two types of stud's head configurations were used in the present research, 9.5 mm diameter stem stud with 30.1 mm diameter head and 12.7 mm diameter stem stud with 40.2 mm diameter head. Keeping in view the improvement in behavior of wall confined with larger studs, it is recommended to perform tests by using larger studs.

It is recommended to study the number of inelastic cycles required at each displacement ductility level that simulates actual number of cycles a real structure might undergo during any seismic event as both steel reinforcement and concrete experience detrimental effect of more inelastic cycles. Vertical reinforcement started to rupture due to low cycle fatigue and concrete also undergo cyclic degradation due to loss of concrete particles between the confinement reinforcement as the load reversed, so the number of inelastic cycles seemed to effect the desired behavior during the test.

If the study shows that the number of cycles required are more or less same as performed in the present tests then the rebars seems to be deficient and hence needed to be more ductile to bear that large number of inelastic cycles. On the other hand, if the study shows that the number of cycles required in a test is less than that performed in the present test then it is recommended to perform less number of inelastic cycles to avoid rupture of vertical bars.

In the present tests only narrow and elongated boundary elements are provided at the wall extremities due to which the intermediate confinement was provided only along the short direction of the cross-section. It is recommended to study the behavior of walls provided with square boundary elements and confined with double head studs in the bi-axial directions.

LIST OF REFERENCES

ACI Committee 318, 1995. Building code requirements for structural reinforced concrete. American Concrete Institute, Detroit, MI.

Cardenas, A.E. and Magura, D.D., (1973) "Strength of High-Rise Shear Walls-Rectangular Cross Section", *Response of Multi-story Concrete Structures to Lateral Forces,* SP-36, American Concrete Institute, Detroit, 1973, pp. 119-150

Corley, W. G., Fiarto, A. E., and Oesterle, R. G., (1981), "Structural Walls", Paper No. 4, Significant Developments in Engineering Practice and Research, ACI Publication SP-72, 1981, pp. 77-130

Dazio, A., Wenk, T., and Bachmann, H., (1999), " Test on RC Structural Walls under Cyclic-Static Action", Report No. 239, Institute of Structural Engineering (IBK), Swiss Federal Institute of Technology (ETH), Zurich.

Dilger W. H., and Ghali, A., (1997), "Double-Head Studs as Ties in Concrete", Concrete International, Vol. 19, No. 6, June 1997, pp. 59-66

Moehle, J. P., Cavanagh, T., (1985) "Confinement Effectiveness of Crossties in RC", Journal of Structural Engineering, ASCE, Vol. 111, No. 10, October 1985, pp. 2105-2120

Naeim, F., (1989), "The Seismic Design Handbook", Structural Engineering Series, *VAN NOSTRAND REINHOLD*, New York, 1989

Oesterle, R. G., Fiarato, A. E. and Corley W. G., (1980), "Reinforcement Details for Earthquake-Resistant Structural Walls", Concrete International, Vol. 2, No. 12, December 1980, pp. 55-66

Ozcebe, G., and Saatcioglu, M., (1987), "Confinement of Concrete Columns for Seismic Loading", ACI Structural Journal, Vol. 84, No. 4, July-August 1987, pp. 308-315

Paulay, T., Priestley, M. J. N., (1992), "Seismic Design of Reinforced Concrete and Masonary Buildings", John Wiley & Sons, Newyork, 1992

Sheikh, S. A., Uzmeri, S. M., (1980), " Strength and Ductility of Tied Concrete Columns", Journal of the Structural Division, Proceedings of ASCE, Vol. 106, ST5, May 1980, pp. 1079-1102

Uniform Building Code-UBC-97, Chapter-16.